

國立臺灣大學生物資源暨農學院園藝暨景觀學系

碩士論文

Department of Horticulture and Landscape Architecture

College of Bioresources and Agriculture

National Taiwan University

Master Thesis

以高通量定序方式分析蝴蝶蘭感染齒舌蘭輪斑病毒及

蕙蘭嵌紋病毒後小型核糖核酸組成之變化

Genome Wide Analysis of Small RNAs from

Odontoglossum ringspot virus and

Cymbidium mosaic virus Infected *Phalaenopsis*

by Deep Sequencing

白暄

Hsuan Pai

指導教授：張耀乾 博士、林納生 博士

Advisor: Dr. Yao-Chien Alex Chang and Dr. Na-Sheng Lin

中華民國 102 年 1 月

January 2013

Contents

Contents.....	I
Contents of Tables	V
Contents of Figures.....	VII
Abstract.....	1
Introduction	3
Literature Review	6
1. The incidence of virus diseases in orchids.....	6
1.1. <i>Cymbidium mosaic virus</i> (CymMV).....	6
1.2. <i>Odontoglossum ringspot virus</i> (ORSV).....	7
1.3. Symptoms and pathogenesis of CymMV and ORSV in orchids	8
1.4. Molecular mechanisms of the synergism between CymMV and ORSV	10
2. The role of RNA silencing in plant-virus interactions.....	12
2.1. RNA silencing pathways in plants	12
2.2. Profiling characteristics of virus-derived small interfering RNAs (vsRNAs)	14
2.2.1. Functions of DCL proteins and size distribution of vsRNAs.....	15
2.2.2. Preference of 5' terminal nucleotide of vsRNAs.....	16
2.2.3. Strand polarity and hotspot distribution of vsRNAs along the virus genome.....	17
2.3. Interactions between virus-modulated RNA silencing and the pathogenesis of viruses in plants.....	18
2.3.1. Roles of viral suppressors of RNA silencing (VSRs) in symptom induction	18
2.3.2. Symptom induction through vsRNA-mediated host gene regulation	19
2.3.3. Infection induced dysregulation of miRNA expression and its association in plant-virus interactions	20
Materials and Methods	22
1. Maintenance of CymMV- and ORSV-free plants	22
1.1. Plant materials and growing conditions	22
1.2. Detecting virus infection in newly purchased plants	22
1.2.1. Extracting total RNA from leaf tissues.....	22

1.2.2. Reverse transcription-polymerase chain reaction (RT-PCR).....	23
2. Detection of CymMV and ORSV spread in <i>P. amabilis</i>	24
2.1. Experimental locations.....	24
2.2. Virus source.....	24
2.3. Virus inoculation and sequential sampling.....	25
2.4. Tissue blotting and hybridization assay for detecting virus	26
2.4.1. Tissue blotting	26
2.4.2. Preparation of digoxigenin (DIG)-labeled probes.....	27
2.4.3. Hybridization and chemiluminescent detection	28
3. Genome wide analysis of small RNAs from ORSV-infected <i>P. amabilis</i> by deep sequencing	29
3.1. ORSV inoculation assay and RNA sample preparation.....	29
3.2. Analyzing viral RNA and siRNA accumulation.....	29
3.2.1. Analyzing viral RNA accumulation by Northern blot.....	29
3.2.2. Analyzing viral siRNA accumulation by small RNA Northern blot	30
3.3. Small RNA deep-sequencing and annotation.....	31
3.3.1. cDNA library construction and sequencing.....	31
3.3.2. Sequencing data trimming and annotation	32
3.3.3. Target prediction for vsRNAs and miRNAs.....	33
3.3.3.1. Analyzing differential expressions of miRNAs.....	33
3.3.3.2. Prediction of putative miRNA target genes	33
3.3.3.3. Prediction of putative vsRNA target genes.....	34
3.4. Experimental validation of small RNAs	35
3.4.1. Validating miRNA expression by stem-loop quantitative RT-PCR (qRT-PCR)	35
3.4.2. VsRNA co-transfection assay in <i>Oncidium</i> protoplasts	36
3.4.2.1. Protoplast isolation	36
3.4.2.2. Co-transfection by electroporation method	37
3.4.2.3. RNA purification and Northern blot analysis	37
4. Genome wide analysis of small RNAs from CymMV and double infected <i>P.</i> <i>amabilis</i> by deep sequencing.....	38
4.1. CymMV and mixed inoculation assays.....	38

4.2. Analyzing viral RNA and siRNA accumulation.....	38
4.3. Construction of small RNA libraries from CymMV and double infected <i>P. amabilis</i> and bioinformatic analysis	39
Results	40
1. Preliminary time course assay of CymMV and ORSV infection in <i>P. amabilis</i>	40
1.1. ORSV infection in inoculated leaves 2 to 11 dpi	40
1.2. ORSV infection spreaded to non-inoculated tissues after 10 dpi.....	40
1.3. Accelerated spreading of CymMV infection in mixed inoculated leaves.....	41
2. Analysis of small RNAs from ORSV-infected <i>P. amabilis</i> by deep sequencing	42
2.1. Analysis of ORSV infection.....	42
2.2. Deep sequencing of small RNAs from ORSV-infected <i>P. amabilis</i>	43
2.3. Characteristics of ORSV viral siRNAs (vsRNAs).....	45
2.3.1. ORSV vsRNA populations in inoculated (Oi) and non-inoculated (Oc) tissues.....	45
2.3.2. Size distribution, strand polarity, and 5'-end nucleotide preference of ORSV vsRNAs	45
2.3.3. Genome mapping, coverage and hotspots of ORSV vsRNAs	46
2.3.4. Specific vsRNA hotspot in ORSV 3'-UTR.....	47
2.3.5. Functional analysis of ORSV 3'-UTR hotspot vsRNA.....	48
2.4. Identification and analysis of conserved miRNAs.....	49
2.4.1. miRNA populations.....	49
2.4.2. Differential expressions of miRNAs in response to ORSV infection	50
2.4.3. Target prediction and possible roles of ORSV-infection responsive miRNAs	51
3. Analyses of small RNAs from CymMV and mixed infected <i>P. amabilis</i> by deep sequencing	53
3.1. Analysis of CymMV and mixed infection.....	53
3.2. Deep sequencing of small RNAs from CymMV and mixed infected <i>P. amabilis</i>	55
3.3. Characteristics of vsRNAs in CymMV and doubly infected tissues	56
3.3.1 VsRNA populations in singly and doubly infected tissues	56
3.3.2. Characteristics of vsRNAs in CymMV and double infected tissues.....	57

3.3.3. Genome mapping and coverage of CymMV vsRNAs	58
3.3.4. Specific ORSV vsRNA hotspots occurred in mixed infected tissues.....	59
3.3.5. Prediction of potential <i>P. amabilis</i> target transcripts of vsRNAs	59
3.4. Identification and analysis of conserved miRNAs in CymMV and mixed	
infected <i>Phalaenopsis amabilis</i>	61
3.4.1. miRNA populations	61
3.4.2. Differential expressions and predicted targets of CymMV and double	
infection responsive miRNAs.....	62
Discussion.....	64
1. Synergistic enhancement of CymMV infection by ORSV co-inoculation in	
<i>Phalaenopsis amabilis</i>	64
2. The leading roles of DCL4 and DCL2 in <i>P. amabilis</i>	66
3. Asymmetrical strand polarity and 5'-end nucleotide identity of CymMV and	
ORSV vsRNAs	66
4. Differential distribution of CymMV and ORSV vsRNA along viral genomes	68
5. VsRNA-mediated host gene silencing may underly the mechanism of symptom	
formation	70
6. Roles of infection responsive miRNAs in <i>Phalaenopsis</i> -virus interactions.....	71
7. The involvement of novel miRNAs and other small RNAs in response to viral	
stresses.....	74
Conclusion and Future Directions	76
References	78

Contents of Tables

Table 1. Summary of total reads in small RNA libraries constructed from mock- and ORSV-inoculated tissues.....	98
Table 2. Summary of unique reads in small RNA libraries constructed from mock- and ORSV-inoculated tissues.....	99
Table 3. The major sequences and total reads of abundant miRNAs in small RNA libraries constructed from mock- and ORSV-inoculated tissues.....	100
Table 4. Expression fold-changes of some abundant miRNAs in small RNA libraries constructed from mock- and ORSV-inoculated tissues.....	105
Table 5. Putative target genes of ORSV infection responsive miRNAs.....	106
Table 6. Summary of total reads in small RNA libraries constructed from mock-, CymMV-, and CymMV and ORSV mixedly-inoculated tissues.....	108
Table 7. Summary of total unique reads in small RNA libraries constructed from mock-, CymMV-, and CymMV and ORSV mixedly-inoculated tissues.....	109
Table 8. Potential ORSV vsRNA targeting <i>Phalaenopsis</i> genes.....	110
Table 9. Potential Di library-specific ORSV vsRNA targeting <i>Phalaenopsis</i> genes.....	114
Table 10. Potential CymMV vsRNA targeting <i>Phalaenopsis</i> genes.....	116
Table 11. Potential CymMV vsRNA targeting <i>Phalaenopsis</i> genes.....	117
Table 12. Potential Di library-specific CymMV vsRNA targeting <i>Phalaenopsis</i> genes. (continued).....	121
Table 13. The major sequences and total reads of abundant miRNAs in small RNA libraries constructed from mock-, CymMV-, and CymMV and ORSV mixedly-inoculated tissues.....	128
Table 14. Expression fold-changes of some abundant miRNAs in mock-, CymMV-, or mixedly-infected tissues.....	137
Table 15. Putative target genes of virus infection-responsive miRNAs.....	138
Table S1. Primers used in RT-PCR and stem-loop qRT-PCR.....	140
Table S2. Information about the super-abundant miR166 (ID:3004100) tag small RNA libraries constructed from mock- and ORSV-infected tissues.....	143
Table S3. The non-redundant list of the top 50 abundant CymMV vsRNAs in Ci, Di and	

Dc libraries.	144
Table S4. The non-redundant list of the top 50 abundant ORSV vsRNAs in Oi and Di libraries.	146
Table S5. List of ORSV vsRNAs specifically sequenced in Di library.....	149
Table S6. List of CymMV vsRNAs specifically sequenced in Di library.	150
Table S7. The super-abundant miR166 (ID:3004100) tag in small RNA libraries of mock-, CymMV-, and mixedly-inoculated tissues.	151



Contents of Figures

Fig. 1. Diagrams of leaf tip-inoculation and tissue-blotting methods used in the infection time-course assays.	152
Fig. 2. Time-course detection of ORSV infection in ORSV-inoculated <i>Phalaenopsis</i>	153
Fig. 3. Time-course detection of ORSV infection in one month period in ORSV-inoculated <i>Phalaenopsis</i>	154
Fig. 4. Time-course detection of virus infection in ORSV or CymMV singly inoculated <i>Phalaenopsis</i>	155
Fig. 5. Time-course detection of virus infection in mixedly-inoculated <i>Phalaenopsis</i>	156
Fig. 6. Diagrams of leaf tip-inoculation and tissue-blotting methods used in the inoculation assays.	157
Fig. 7. Virus infection of ORSV-inoculated <i>Phalaenopsis</i> at 10 days post inoculation.	158
Fig. 8. Accumulation of ORSV viral RNA and virus-specific siRNA in <i>Phalaenopsis</i>	159
Fig. 9. Size distribution of small RNAs in mock- or ORSV-inoculated <i>Phalaenopsis</i>	160
Fig. 10. Annotation procedures of deep sequencing data.	161
Fig. 11. Abundance and size distribution of ORSV vsRNAs in ORSV-infected <i>Phalaenopsis</i>	162
Fig. 12. Nucleotide composition of ORSV vsRNAs in ORSV-infected <i>Phalaenopsis</i>	163
Fig. 13. Distribution of vsRNAs along ORSV genome corresponding to reads from Oi and Oc libraries.	164
Fig. 14. Alignment of tobamovirus 3'-untranslated region (3'-UTR) conserved sequence. Identical bases among 22 viruses are highlighted in grey.	165
Fig. 15. Location and frequency of abundant 3'-UTR-originating ORSV positive stranded vsRNAs.	166
Fig. 16. ORSV viral RNA accumulation in ORSV and synthetic siRNAs co-transfected protoplasts.	167
Fig. 17. The abundance of miRNA families in Mi, Mc, Oi, and Oc libraries. The percentage was calculated from sum of Mi, Mc, Oi, and Oc libraries.	168
Fig. 18. Expression levels of some ORSV-infection responsive miRNAs validated by stem-loop qRT-PCR.	169
Fig. 19. Expression of some miRNAs in ORSV- or mock-inoculated tissues validated by stem-loop qRT-PCR.	170

Fig. 20. Virus infection of CymMV- and doubly-inoculated <i>Phalaenopsis</i> at 10 days post inoculation (DPI).	172
Fig. 21. Accumulation of CymMV and ORSV viral RNA and virus-specific siRNA in <i>Phalaenopsis</i>	173
Fig. 22. Size distribution of small RNAs in mock-, CymMV-, or CymMV and ORSV mixedly-inoculated <i>Phalaenopsis</i>	174
Fig. 23. Abundance and size distribution of CymMV vsRNAs in CymMV, or CymMV and ORSV mixedly-inoculated <i>Phalaenopsis</i>	175
Fig. 24. Abundance and size distribution of ORSV vsRNAs in CymMV and ORSV mixedly-inoculated <i>Phalaenopsis</i>	176
Fig. 25. Nucleotide composition of 5'-end of CymMV vsRNAs in CymMV, or CymMV and ORSV mixedly-inoculated <i>Phalaenopsis</i>	177
Fig. 26. Nucleotide composition of 5'-end of ORSV vsRNAs in CymMV and ORSV mixedly-inoculated <i>Phalaenopsis</i>	178
Fig. 27. Distribution of vsRNAs along CymMV genome corresponding to reads from Ci, Cc, Di, Dc and Dsc libraries.	179
Fig. 28. Distribution of vsRNAs along ORSV genome corresponding to reads from Di, Dc, and Dsc libraries.	180
Fig. 29. The abundance of miRNA families in Mi-2, Mc-2, Ci, Cc, Di, Dc, and Dsc libraries.	181
Fig. 30. Fold changes of expression levels of some virus infection-responsive miRNAs in mock-, CymMV-, or CymMV and ORSV mixedly-inoculated <i>Phalaenopsis</i> validated by stem-loop qRT-PCR.	182
Fig. 31. Fold changes of expression levels of some miRNAs in mock-, CymMV-, or CymMV and ORSV mixedly-inoculated <i>Phalaenopsis</i> validated by stem-loop qRT-PCR.	183
Fig. S1. Plasmids used for generating ORSV- or CymMV-specific RNA probes for detecting virus infection.	184
Fig. S2. Plasmids used for generating ORSV- or CymMV-specific RNA probes for detecting vsRNA accumulation.	185
Fig. S3. Percentages of CymMV and ORSV vsRNAs of total clean reads in small RNA	

libraries.	186
Fig. S4. Distribution of 21- and 22-nt viral siRNAs along ORSV genome corresponding to reads from Oi library.	187
Fig. S5. Validation of miR166 abundance.	188
Fig. S6. Size distribution of small RNAs modified with the removal of the super-abundant miR166 tag.	189
Fig. S7. Modified relative abundance of miRNA families after removal of the super-abundant miR166 tag.	190
Fig. S8. The redundancy of top 50 abundant vsRNA tags in Oi, Ci, Di, and Dc libraries.	191



Abstract

Cymbidium mosaic virus (CymMV) and *Odontoglossum ringspot virus* (ORSV) are the most prevalent viruses infecting orchids and causing economic losses worldwide. Upon virus infection, small RNA mediated antiviral RNA silencing response is activated. Such biotic stress may affect virus-specific interfering RNAs (vsRNAs) or microRNA (miRNA) regulated host gene expression. To advance our understanding of the offense-defense interactions between CymMV, ORSV and orchids, this study employed deep sequencing to analyze small RNAs from virus infected *Phalaenopsis*. The leaf tip-inoculation method first distinguished early and late stages of infection in non-inoculated and inoculated tissues at ten days post inoculation (dpi). Small RNA Solexa sequencing generated 11 libraries with more than five million reads each from CymMV and ORSV singly and doubly inoculated leaves and from mock-inoculated leaves. Generally, CymMV and ORSV vsRNAs were predominantly 21 and 22 nucleotides (nt), with excess positive polarity accumulating in single inoculations. While most CymMV vsRNAs were derived from RNA-dependent RNA polymerase (RdRp) coding regions, ORSV vsRNAs encompassed the coat protein coding gene and 3'-untranslated region, with a specific hotspot residing in the pseudoknot upstream to the 3'-terminal tRNA-like structure. These results suggest Dicer-like (DCL) 4 and DCL2 homologs play a leading role in mediating antiviral RNA silencing in *P. amabilis* using single-stranded RNA derived secondary structure as templates. Biased distribution of 5' terminal adenosine (A), uridine (U), cytosine (C) and underrepresented 5'-guanine (G) indicate vsRNAs could be recruited into multiple Argonaute (AGO) complexes. Under mixed infection, chlorotic necrosis symptoms appeared specifically in inoculated tissues at 10 dpi, and accelerated spreading and

enhanced viral titer of CymMV also occurred. The proportion of CymMV vsRNAs in total small RNAs ranged from 5.83% in singly infected tissues to 27.9% in doubly infected tissues, providing evidence of the enhancement of CymMV titer. While most vsRNA features remained unchanged in double inoculations, three additional prominent ORSV vsRNA hotspot peaks were observed. *In silico* prediction revealed *Phalaenopsis* transcript hotspots that are potential targets for vsRNA are also likely to be involved in symptom formation. The virus infection also modulated miRNA expression—for example, miR156, miR168, miR894 were up regulated and miR398, miR408, miR528 were down regulated after CymMV or ORSV infection. These infection responsive miRNAs participate in a broad spectrum of cellular processes like hormone and metabolite assimilation, signal transduction, and oxidative stress calibration. Taken together, the deep sequencing provided a global profile of vsRNAs and miRNAs in *Phalaenopsis* under CymMV and ORSV infection. Further research should provide valuable insights into small RNA-mediated virus-plant interactions.

Introduction

The Orchidaceae is an immense family composed of more than 800 genera, about 25,000 native species and over 110,000 cultivars (Sheehan, 2003). Ornamental orchids commonly seen in the market include *Cattleya*, *Cymbidium*, *Dendrobium*, *Oncidium*, *Paphiopedilum*, and especially *Phalaenopsis* (the moth orchid). People have long appreciated the fascinating array of colors, elegant flower shapes, ease of growing moth orchids indoors, as well as the long duration of their inflorescence. *Phalaenopsis* are native throughout Sri Lanka, southern India, New Guinea, northern Australia, China, Vietnam, the Philippines and other tropical and subtropical mountain areas. Taiwan is the habitat of two native *Phalaenopsis* species, including *P. aphrodite* and *P. equestris* (李, 2005). Taking advantage of the optimal climate for growing *Phalaenopsis*, and aided by fine cultivation protocols, Taiwan is well situated as a major exporter. The Council of Agriculture has chosen the *Phalaenopsis* as one of the top four important export commodities in 2004, and which has become third in wholesale value of exported agricultural products since 2008 (楊, 2010). However, Taiwan *Phalaenopsis* exports are now facing competition with other countries such as China, America, and especially the Netherlands. A major challenge is virus infection, since virus indexing techniques have not been routinely applied at the early stage of orchid industry development in Taiwan (張, 2006).

Of numerous orchid pests and diseases, viruses are the most troublesome and no efficient measures can be used to control virus diseases. Virus infections can result in retarded and weakened growth of orchid plants, even though the plants appear symptomless. In addition, the hidden risk of latent infection after shipment also poses a

thorny problem (張, 2007). Since large-scale cultivation via tissue culture has become the trend in orchid production, virus infections through mechanical transmission have become a major threat (鄭等, 2008). Of more than 50 orchid-infecting viruses, *Cymbidium mosaic virus* (CymMV) and *Odontoglossum ringspot virus* (ORSV) are the most prevalent worldwide. Isolation of CymMV and ORSV was first reported in the 1950s (Jensen, 1950 ; Jensen and Gold, 1951). Co-infection with these two viruses is commonly observed in orchid nurseries, and synergistic effects between CymMV and ORSV have long been reported (Ajjikuttira et al., 2005). Several studies have recorded the characteristics of virus particles and their induced symptoms, and also decoded the complete genome sequences (Ryu and Park, 1995 ; Wong et al., 1997). However, most studies aimed to establish rapid virus diagnosis techniques (Chen et al., 2010; Chia et al., 1992; Eun and Wong, 1999; Hu and Wong, 1998; Lee et al., 2011; Lee and Chang, 2010; Ryu et al., 1995; Seoh et al., 1998; Tanaka et al., 1997), few have probed the molecular determinants of CymMV and ORSV pathogenesis (Ajjikuttira et al., 2005 ; Hu et al., 1998 ; Lu et al., 2009) and the mechanism of infection remains largely unknown.

Recently, pathogen derived resistance is one of the interesting areas in biotechnological research on *Phalaenopsis*. Investigating the interaction between CymMV or ORSV and host plants will provide useful knowledge for establishing a foundation of virus-proofing techniques and generating virus-resistant plants. Sequence-specific RNA silencing has been revealed as one of a number of general antiviral mechanisms in plants (Angell and Baulcombe, 1997; Dougherty, 1994; Ruiz et al., 1998; and reviewed in Llave, 2010). RNA silencing is triggered by double-stranded

or self-folding RNAs that are processed into small and functioning fragments by RNase III-type DICER enzymes. The small RNAs are mainly categorized in plants into small interfering RNAs (siRNAs) or microRNAs (miRNAs) according to their origin and biogenesis pathways (reviewd in Naqvi et al. 2009 and Vazquez et al., 2010). Virus-derived small interfering RNAs (vsRNAs) usually accumulate at high levels in infected plant tissues. VsRNAs are further recruited into RNA-induced silencing complex (RISC) and guiding sequence-specific viral RNA cleavage. Furthermore, recent studies have provided evidence that RNA silencing may in turn play an important role in disease induction, since plant endogenous miRNAs may be dysregulated upon virus infection, and vsRNAs are also potentially targeted to plant mRNAs rather than viral RNAs (Moissiard and Voinnet, 2006; Qi et al., 2009; and reviewd in Wang et al., 2012).

This study investigated the profile of small RNAs in *P. amabilis* plants with ORSV and CymMV single- or mixed-infection and focused on 1) analyzing the characteristics of CymMV and ORSV vsRNAs, such as abundance, size classes, strand polarities, and hotspot distribution along the viral genome, and 2) the expression levels of several conserved miRNAs which respond to virus infection. Possible roles of these small RNAs in defense and counter-defense interactions are also explored by predicting potential *Phalaenopsis* mRNA targets of miRNAs and vsRNAs. Furthermore, the study also addresses the synergistic effect between CymMV and ORSV.

Literature Review

1. The incidence of virus diseases in orchids

Virus diseases have long been a serious problem in orchid cultivation. Plant viruses are infectious obligate parasitic nanoparticles constituted by an RNA or DNA genome encapsidated inside its coat protein (CP) shells. More than 50 viruses are reported to infect orchids and about 30 of them have been described in detail (Ajjikuttira and Wong, 2009). Six of those 30 viruses have been observed in Taiwan, including *Capsicum chlorosis virus* (CaCV), *Carnation mottle virus* (CarMV), CymMV, *Cucumber mosaic virus* (CMV), ORSV, and *Phalaenopsis chlorotic spot virus* (PhCSV). Of these, CymMV and ORSV are the most prevalent and cause serious economic loss (鄭等, 2008; Zettler et al., 1990).

1.1. *Cymbidium mosaic virus* (CymMV)

CymMV belongs to the family Alphaflexiviridae, genus Potexvirus. It has a positive-sense single-stranded RNA [(+)-ssRNA] monopartite genome with five open reading frames (ORFs) encoding a 160-kilo Dalton (kDa) RNA-dependent RNA polymerase (RdRp), three triple-gene-block proteins (TGBps), and a 24-kDa CP. The TGBps have been recognized as movement proteins (MP). The genomic RNA is 5'-capped and about 6200 nucleotides (nt) in length (e.g. GenBank accession no. AB197937, AF016914, AM055720, AY571289, EF125178, EF125179, EF125180, EU314803, HQ681906, NC_001812), excluding the 3'-poly(A) tail (Ajjikuttira and Wong, 2009; Wong et al., 1997). The non-enveloped, flexuous and filamentous virions

with a length of ~480 nm and a width of ~13 to 18 nm are constituted by 5.6% RNA and 94% protein. The axial canal is indistinct. The thermo inactivation point (TIP) is about 60 to 70°C and the longevity *in vitro* (LIV) is reported to be around 25 days. It is easily transmitted through mechanical wounds, since the virions are quite stable, but no known vectors have been reported to date (Ajjikuttira and Wong, 2009; Frowd and Tremaine, 1977; Jenson and Gold, 1955; Murakishi, 1958). CymMV was first found in *Cymbidium* orchids (Jenson, 1950), and its natural hosts include several orchid families such as *Phalaenopsis*, *Cymbidium*, *Cattleya*, *Epidendrum*, *Laelia*, *Laeliocattleya*, *Oncidium*, *Vanda*, *Vanilla* and *Zygopetalum*. Local lesions or patches are formed in CymMV-inoculated leaves of *Cassia occidentalis* and *Chenopodium quinoa*, thus these plants are commonly used as indicators. In addition, *Nicotiana benthamiana* are systemic hosts of CymMV and are often used as experimental hosts for inoculation assays and virion propagation (Ajjikuttira and Wong, 2009; Faccioli and Marani, 1979; Hiruki et al., 1980; Jenson and Gold, 1955; Kado and Jenson, 1964; Murashiki, 1958).

1.2. *Odontoglossum ringspot virus* (ORSV)

ORSV belongs to the Tobamovirus group and had previously been regarded as *Tobacco mosaic virus* orchid strain (TMV-O). ORSV was reclassified as a separate species after nucleotide sequence analysis and other phylogenetic evidence accumulated (Edwardson and Zettler, 1988). It has a (+)-ssRNA monopartite genome with three ORFs. ORF1 encodes 126- and 183-kDa RdRp proteins, the latter expressed by read-through strategy. Other ORFs encode 34-kDa MP and 18-kDa CP (Ajjikuttira and Wong, 2009; Ryu and Park, 1995). The genomic RNA of ORSV is about 6600 nt in length (e.g. GenBank accession no. AY571290, DQ139262, NC_001728, ORU3458),

with a 5'-capped structure but lacking the 3'-poly(A) tail. Instead, its 3'-untranslated region (3'-UTR) is comprised of a tRNA-like structure (TLS) in the terminus and three upstream consecutive homologous regions, forming a pseudoknot (PK) chain (Chng et al., 1996). The virus particles are rigidly rod-shaped, with a length of ~300 nm and a width of ~18 nm and comprised of ~5% RNA. ORSV is inactivated at about 90°C and is mechanically transmitted, without recognized vectors (Ajjikuttira and Wong, 2009; Corbett, 1967; Edwardson and Zettler, 1986; Jenson and Gold, 1951; Kado et al., 1986; Paul et al., 1965). Previous study has shown ORSV virions can retain infectivity for more than ten years (Inouye, 1983). ORSV was first reported infecting *Odontoglossum grande* (Jensen and Gold, 1951). Other natural hosts include *Odontoglossum*, *Cymbidium*, *Cattleya*, *Dendrobium*, *Epidendrum*, and *Zygopetalum*. For biological diagnosis of ORSV infection, *Gomphrena globosa* and *C. quinoa* can be used as indicators by forming local lesions on the inoculated leaves. *N. benthamiana* is one of the systemic hosts of ORSV, showing mild mosaic and distorted emerging leaves after infection and is commonly used as an experimental host (Ajjikuttira and Wong, 2009; Navalinskienė et al., 2005; Wisler et al., 1979).

1.3. Symptoms and pathogenesis of CymMV and ORSV in orchids

Variable symptoms of CymMV and ORSV have been observed in orchids and are variable by cultivars, growing stages, and environmental factors, such as seasonal changes. Despite this variation, classical symptoms showed chlorotic spots formed on leaves of CymMV singly infected *Phalaenopsis*; the spots were 0.2-0.5 cm in diameter at first, then gradually enlarged or became necrotic at later stages (陳等, 2006). Common symptoms of CymMV in orchids include chlorosis streak or stripe, necrosis

spots or line patterns on leaves and stems. In addition, the necrotic type symptoms in florescence are specific to CymMV (張, 2006; 陳等, 2006). The most prevalent symptoms caused by ORSV infection include irregular chlorotic patches, ringspots, mosaic, mottle, streak, color breaking, and necrosis in orchids, with mosaic and streak. However, the incidence of symptom formation with single infection by ORSV is much lower than when infected with CymMV alone. In particular, ORSV symptoms were minimal in juvenile *Phalaenopsis* and *Oncidium* before the plants grew up and flowered (張, 2006).

Co-infection with both CymMV and ORSV has been frequently observed in orchid nurseries, and synergism exists between the two viruses (張, 2006; Hadley et al., 1987). Latent virus infection could result in retarded growth and reduced flower quality, even though infected plants are sometimes symptomless. An increase of 65% and 21% in inflorescence size and photosynthetic capacity, respectively, were obtained in virus-eradicated *Oncidium* Gower Ramsey, demonstrating the impact of virus infection on plant growth (Chia and He, 1999).

Infection with CymMV was detected in rub-inoculated leaves of *Dendrobium* × Jaquelyn Thomas 'Uniwai Supreme' and 'Uniwai Prince' nine days post inoculation (dpi) on average. Systemically movement of CymMV was first detected in the root (about 17 dpi) and then in leaves (about 20 dpi). Slash (13/15) and cut (13/22) inoculation was less efficient than rub inoculation (41/41) for CymMV (Hu et al., 1994). ORSV was inoculated only through rub-inoculation method and systemic movement was not detected in the dendrobiums, indicating CymMV is more easily spread through cultivation practices than ORSV (Hu et al., 1994). Wong et al. (1994) conducted a

survey of CymMV and ORSV incidence in Singapore and found 54.6% plants in orchid farms infected with CymMV, 4.0% with ORSV and 14.2% with both viruses. On the other hand, in the Singapore Botanical Garden, 34.5% of orchids were detected to have CymMV, 0.3% with ORSV and 8.3% had mixed infection. These studies indicate higher incidence of CymMV which might suggest a greater susceptibility to CymMV than to ORSV in orchids. Furthermore, frequent flower cutting in farms increased the risk of mechanical transmission (Wong et al., 1994).

1.4. Molecular mechanisms of the synergism between CymMV and ORSV

Infection with multiple viruses from different groups often shows synergetic interaction, and results in intensified symptoms and higher amounts of virus accumulation. Synergism has also been noticed in double infections of potexvirus and tobamovirus (Goodman and Ross, 1974; Taliensky et al., 1982). Severe necrosis and sunken patches more frequently occur in CymMV and ORSV mixedly infected orchids than singly infected ones (鄭等, 2008). The synergism between CymMV and ORSV has also been observed in transfected protoplasts (Hu et al., 1998). In protoplasts isolated from *Dendrobium* 'Sonia' petals, CymMV genomic viral RNA was detectable six hours after electroporation and reached a maximum accumulation at 18 hours. ORSV genomic RNA was also detected beginning six hours after electroporation but reached a maximum accumulation later at 24 hours. Accelerated ORSV viral RNA accumulation in co-infected protoplasts was observed, taking only half the time (12 h) to reach the maximum accumulation. The accumulation of both sense and antisense strands of CymMV and ORSV viral RNA was increased in mixed infections. The positive and negative strands of ORSV showed approximately 6- and 12-fold accumulation

compared to single infected protoplasts, respectively. The negative strands of CymMV also increased 5-fold in co-infected protoplasts compared to singly infected ones, indicating increased replication of both CymMV and ORSV during co-infection (Hu et al., 1998).

Viral MP and CP are often required for the virus movement through plants. Several studies demonstrate taxonomically distinct viruses display reciprocal transport functions. For example, TMV MP can complement the defective cell-to-cell movement of CMV, *Barley stripe mosaic virus* (BSMV), *Potato virus X* (PVX) and other unrelated viruses (Cooper et al., 1996; Morozov et al., 1997; Solovyev et al., 1996). The cell-to-cell movement of an MP-deficient CymMV was restored in ORSV MP-expressing transgenic *N. benthamiana*. Similarly, cell-to-cell movement of a MP-deficient ORSV was rescued in CymMV TGBp1-expressing plants, suggesting reciprocal functions between CymMV TGBps and ORSV MP. On the other hand, systemic movement of CP-deficient CymMV was supported by ORSV CP. However, CymMV CP did not support the long-distance movement of CP-deficient ORSV (Ajjikuttira et al., 2005).

In summary, more pronounced disease symptoms are often observed in double infections and may be related to increased accumulation of either or both viruses. (Hu et al., 1998; Ajjikuttira et al., 2005). Functional complementation of MPs and CPs of CymMV and ORSV facilitates virus movement and may enhance the susceptibility to the other virus after infection with either one (Ajjikuttira et al., 2005). However, though it is generally agreed that intensified symptom formation occurs during co-infection as a consequence of the synergism between CymMV and ORSV, the molecular details of virus accumulation and symptom formation in double infections have not been determined.

2. The role of RNA silencing in plant-virus interactions

2.1. RNA silencing pathways in plants

The central dogma of molecular biology describes the cascade of transferring sequential genetic information through transcription of DNA to RNA, and translation of RNA to protein. However, researchers have identified several regulatory non-coding RNAs which are not translated into proteins. Non-coding RNAs, such as transfer RNA (tRNA) and ribosomal RNA (rRNA), were first characterized in the 1960s and 1980s, respectively, whereas small RNAs were not noticed and studied intensively until the 1990s (Fire et al., 1998; Napoli et al., 1990; Romano and Macino, 1992; van der Krol et al., 1990a and 1990b). Small RNAs are 20 to 40 nt-long molecules present in most eukaryotes that regulate gene expression in a sequence-specific manner. Various small RNA classes, such as micro RNA (miRNA), small-interfering RNA (siRNA), and piwi-interacting RNA (piRNA) have been identified and categorized on the basis of their biogenesis and precursor structure. In plants, the best described classes are siRNA and miRNA (e.g. Bazzini et al., 2007; for recent reviews, see Naqvi et al., 2009).

Biogenesis of siRNAs and miRNAs relies on the overlapping requirement of dsRNA, as precursor and conserved protein families are involved. The major difference is that miRNAs are derived from imperfectly base-paired hairpin-loop transcripts of miRNA genes generated by RNA polymerase II, whereas siRNAs are generated from longer double-stranded RNA precursors, both endogenously or exogenously (Elbashir et al., 2001; Vazquez et al., 2010). After the short duplexes are processed from precursors by RNase-III DICER-LIKE (DCL) enzymes, and methylated by HEN1 methyltransferase, they are unwound by ARGONAUTE (AGO) effectors, then

assembled into RNA-induced silencing complex (RISC) to provide sequence-specific targeting (Schauer et al., 2002; Papp et al., 2003; Tang et al., 2003; Bernstein et al., 2001; Hamilton and Baulcombe, 1999; Hammond et al., 2000). They then mediate either transcriptional regulation such as DNA methylation and histone modification, or post-transcriptional regulation through mRNA cleavage or translational inhibition (Aukerman and Sakai, 2003; Chen, 2004; Doench et al., 2003; Hammond et al., 2001; Hutvagner and Zamore, 2002). The consequently repressed expressions of miRNA/siRNA-targeted genes are thus subject to the name “gene silencing,” “RNA silencing” or “RNA interference (RNAi)” (Jones-Rhoades et al., 2006; Mallory and Vaucheret, 2010; Molnar et al., 2011; Naqvi et al., 2009; Voinnet, 2009; Zamore et al., 2000).

SiRNA-mediated antiviral RNA silencing plays a critical role in plant-virus interactions. Double-stranded viral RNAs, such as replication intermediates or self-annealing hairpin structures, can serve as templates for DCL processing. The virus-derived siRNAs (vsRNAs) are recruited by RISC and guide RISC to cleave single-stranded viral RNAs. In addition, plant endogenous RNA-dependent RNA polymerases (RDRs) are also involved in synthesizing dsRNAs from single-stranded viral RNAs. The dsRNAs again serve as substrates for the DCL-dependent formation of secondary vsRNAs, and thus amplify the antiviral cascade (Angell and Baulcombe, 1997; Dougherty, 1994; Ruiz et al., 1998; Blevins et al., 2006; Llave, 2010). Furthermore, several studies have revealed siRNAs are mobile molecules and spread throughout the plant via vascular bundles (Palauqui et al., 1997; Jorgensen et al., 1998; Voinnet et al., 1998; Vance and Vaucheret, 2001), suggesting vsRNAs may act as signal molecules and confer systemic antiviral silencing throughout the plants.

In addition, numerous plant viruses have evolved viral suppressors of RNA silencing (VSRs) as a counter-defense strategy, and even vsRNAs are mediators of viral diseases (Burgyán and Havelda, 2011; Lu et al., 2008). Moreover, VSRs may interfere with the host miRNA pathway and dysregulate normal plant development, whereas vsRNAs highly complementary to a host sequence could also induce silencing of the host genes (Dunoyer and Voinnet, 2005; Wang et al., 2004; Wang et al., 2012; Qi et al., 2009). Collectively, the RNA silencing machinery plays an important role in regulating plant growth and also constitutes a complex layer of defense and counter-defense interactions between plants and viral pathogens.

2.2. Profiling characteristics of virus-derived small interfering RNAs (vsRNAs)

High accumulation of vsRNAs is frequently observed in virus-infected plants and is recognized as a hallmark of antiviral RNA silencing machinery. Several proteins are involved in the antiviral silencing mechanism. Thoroughly studied in *Arabidopsis thaliana*, vsRNAs are mainly 21-nt and 22-nt through processing of DCL4 and DCL2, respectively (Blevins et al., 2006). Different AGOs associate with vsRNAs based on the 5'-terminal nucleotide classes and guide different modes of silencing pathways. For example, AGO1- and AGO10-containing RISC complexes often mediate mRNA cleavage or translational inhibition, while AGO4 mainly directs transcriptional silencing through DNA methylation (Hutvagner and Simard, 2008; Mi et al., 2008; Yan et al., 2010). Consequently, characteristics such as size, strand polarity, hotspots of DCLs processing and 5'-nucleotide preference of vsRNAs are associated with these proteins. High throughput sequencing techniques provide an efficient way to analyze small RNAs and have been used to profile vsRNAs. Some features of vsRNAs produced from

diverse groups of viruses in different hosts are described below.

2.2.1. Functions of DCL proteins and size distribution of vsRNAs

Specific size classes of small RNAs are produced via different DCLs. DCL1 and DCL4 generate 21-nt small RNAs. DCL2 and DCL3 process 22-nt and 24-nt small RNAs respectively (Blevins et al., 2006; Vaucheret, 2006). Viral RNAs are differentially processed by multiple DCL proteins. Since DNA viruses tend to multiply in the nucleus but RNA viruses normally replicate in the cytoplasm, the major DCLs mediating vsRNA production from DNA or RNA viruses are different (Blevins et al., 2006; Wang et al., 2012). As shown in *A. thaliana* mutants, all four types of DCLs target DNA viruses such as *Cabbage leaf curl virus* (CaLCuV) and *Cauliflower mosaic virus* (CaMV), whereas DCL4 and DCL2 mainly affect RNA viruses such as CMV, *Tobacco rattle virus* (TRV), and *Oilseed rape mosaic virus* (ORMV) (Blevins et al., 2006; Bouché et al., 2006; Deleris et al., 2006).

High throughput sequencing has revealed similar profiles of vsRNA size class distribution. In most cases, vsRNAs from RNA viruses are mainly 21-nt, followed by 22-nt class. For instance, a number of viruses have been reported as generating more 21-nt vsRNAs, including TMV, TRV and CMV in *Arabidopsis*, *Bamboo mosaic virus* (BaMV), *Tunip mosaic virus* (TuMV), *Pepper mild mottle virus* (PMMoV) and PVX in *N. benthamiana*, *Watermelon mosaic virus* (WMV) and *Melon necrotic spot virus* (MNSV) in *Cucumis melo*, *Tomato yellow leaf curl virus* (TYLCV) in *Solanum lycopersicum* and several grape viruses such as *Grapevine rupestris stem-pitting associated virus* (GRSPaV), *Grapevine fleck virus* (GFkV), *Grapevine red globe virus* (GRGV), *Grapevine asteroid mosaic-associated virus* (GAMaV) and *Grapevine*

rupestris vein feathering virus (GRVfV) in *Vitis vinifera* Pinot Noir (Donaire et al., 2009; Lin et al., 2010; Pantaleo et al., 2010; Qi et al., 2009). Furthermore, the patterns of vsRNA size distribution of BaMV and *Rice stripe virus* (RSV) did not differ according to host plant species (Lin et al., 2010; Xu et al., 2012; Yan et al., 2010). The only exception was *Cymbidium ringspot virus* (CymRSV), with more 22-nt vsRNAs over 21-nt found in infected *N. benthamiana*, which is possibly related to the activity of silencing suppressor P19 of CymRSV to sequester 21-nt sRNAs (Donaire et al., 2009).

2.2.2. Preference of 5' terminal nucleotide of vsRNAs

Since the 5' nucleotide identity dictates the loading of vsRNAs into a particular AGO effector (Czech and Hannon, 2011; Kim, 2008), the base composition of vsRNAs 5' termini may infer different downstream pathways involved in RISC-mediated silencing mechanisms. Most viruses studied revealed preference for 5'-uridine (U) or 5'-adenosine (A). The sense-stranded vsRNAs with a 5'-U were more abundant for CMV, CymRSV, MNSV, PMMoV, RSV, TRV and TYCV, while 5'-U or A were observed equally for WMV, TMV, TuMV and PVX sense-stranded vsRNAs (Donaire et al., 2009). When it comes to antisense-stranded vsRNAs, 5'-U, A, or 5'-cytosine (C) were similarly represented for most viruses (Donaire et al., 2009; Qi et al., 2009). In particular, grape viruses such as GRSPaV, GFkV, GRGV, GAMaV and GRVfV were observed to favor 5'-C (Pantaleo et al., 2010). Nonetheless, a clear tendency to avoid 5'-guanidine (G) was observed in the cases above. The diverse categories of 5'-nucleotide of vsRNAs also suggest that vsRNAs may potentially be recruited into multiple AGO-containing complexes (Donaire et al., 2009).

2.2.3. Strand polarity and hotspot distribution of vsRNAs along the virus genome

Double-stranded viral RNA formed by direct hybridization between (+)- and (-)-strand replication intermediates or synthesized by host RDR from single-stranded viral RNA can serve as substrates of DCL enzymes (Blevins et al., 2006; Ding, 2010; Wang et al., 2012). VsRNA pools with near equal abundance of both sense- and antisense-polarities have been profiled in TuMV- and PVX-infected *N. benthamiana*, WMV- and MNSV-infected melons, and TYLCV-infected tomato plants (Donaire et al., 2009). Furthermore, other evidence suggests hairpin structures formed by self-annealing within single-stranded viral RNA can also serve as DCL processing templates (Dunoyer and Voinnet, 2005; Molnár et al., 2005). In fact, biased strand polarity and asymmetrical distribution of vsRNAs along virus genomes are often observed. Profiles of TMV, TRV and CMV in *Arabidopsis*, GRSPaV in grapevine, also CymRSV and PMMoV in *N. benthamiana* presented more (+)-stranded vsRNAs (Donaire et al., 2009; Pantaleo et al., 2010; Qi et al., 2009), while GFkV, GRGV and GAMaV vsRNAs were mostly (-)-stranded in co-infected grapevine (Pantaleo et al., 2010).

Furthermore, differential distribution of vsRNAs has been observed with the same virus in different hosts. Negative-strand predominance of BaMV vsRNAs has been found in *N. benthamiana*, whereas slightly higher sense-polarity presented in *A. thaliana*. In addition, while most vsRNAs mapped to the CP and 3'-UTR regions in infected *N. benthamiana*, vsRNAs profiled in *A. thaliana* were largely generated from the RdRp region of the 5' half of the BaMV genome (Lin et al., 2010). Although RSV vsRNAs generally possessed (+)-polarity in both *Oryza sativa* and *N. benthamiana* plants, most vsRNAs identified in rice were generated from RSV RNA 3 and 4, whereas RNA 4 is the major source of vsRNAs in tobacco (Xu et al., 2012).

2.3. Interactions between virus-modulated RNA silencing and the pathogenesis of viruses in plants

2.3.1. Roles of viral suppressors of RNA silencing (VSRs) in symptom induction

As a counter-defense strategy, many viruses evolved VSRs during evolution. A number of studies have shown multiple steps of disrupting RNA silencing pathways of certain VSRs. For example, tombusvirus P19 sequesters double-stranded siRNAs, potyvirus Hc-Pro and P38 interfere with RISC assembly, and cucumovirus 2b inhibits the slicing activity of AGO1 (reviewed in Burguán and Havelda, 2011). Silencing suppressors can contribute to viral symptoms via indirectly helping virus accumulation or directly modifying endogenous small RNA-regulated pathways (Silhavy and Burguán 2004). Diminished virus accumulation has been found in the dark-green zones of the mosaic patterns compared to the light-green zones of infected leaves of *Tamarillo mosaic virus* (TaMV) and *Tomato mosaic virus* (ToMV) (Moore et al. 2001; Hirai et al. 2008). The mottling seed coat patterns in CMV-infected *Glycine max* 'Jack' seeds has been shown to result from suppression of chalcone synthase (*CHS*) gene silencing by the suppressor protein 2b (Senda et al., 2004). CMV infection dysregulated the star-type color pattern of *Petunia hybrida* 'Red Star' flowers mediated by natural RNA silencing of *CHS* in the white sectors, significantly increasing the *CHS* mRNA and turning all the white patterns red (Koseki et al., 2005). Viral symptom-like phenotypes are often observed in transgenic plants that express VSR. For instance, transgenic *Arabidopsis* expressing *Tomato bushy stunt virus* (TBSV) P19, TuMV P1/Hc-Pro or *Turnip crinckle virus* (TCV) CP exhibited serrated rosette leaves (Chapman et al., 2004). Dymorphogenic and sterile male inflorescences with narrow sepals and protruding

internal whorls also displayed on P19 and HcPro expressing plants (Dunoyer et al., 2004; Mallory et al., 2002).

2.3.2. Symptom induction through vsRNA-mediated host gene regulation

In contrast to the viral RNA clearance activity of plant RNA silencing pathways, studies have also demonstrated that mRNA of host genes are conversely targeted by virus- or subviral agent-derived siRNA-guided RISC complexes, if high sequence complementarity exists between pathogen and host mRNA (Llave, 2004; Wang et al., 2004). Several studies have proven that some viroids and satellites direct RNA silencing against physiologically important host genes, thus causing disease symptoms. For example, viroid symptoms were observed in transgenic tomato plants expressing *Potato spindle tuber viroid* sequence hairpin RNA (Wang et al., 2004). The symptom determinant sequence of CMV Y satellite RNA (Y-sat) was complementary to a 22-nt region of a chlorophyll biosynthetic gene *ChlI* in tobacco, thus inducing bright yellowing symptoms via indirect repression of chlorophyll accumulation (Shimura et al. 2011; Smith et al. 2011). A severe chlorotic symptom called peach-calico resulted from retarded expression of a chloroplastic heat-shock protein 90 via *Peach latent mosaic viroid* (PLMVd)-derived siRNA-mediated RNA silencing (Navarro et al., 2012). Moreover, several CaMV vsRNAs have near-perfect sequence complementarity to *Arabidopsis* mRNAs and therefore, may direct silencing of these genes (Moissiard and Voinnet 2006). Qi et al. have predicted potential target genes of TMV crucifer strain (TMV-Cg) and the cleavage of two host genes, the cleavage and polyadenylation specificity factor (CPSF30) and the translocon-associated protein α (TRAP α), have been verified by 5' rapid amplification of cDNA ends (5'-RACE) assays (Qi et al. 2009).

2.3.3. Infection induced dysregulation of miRNA expression and its association in plant-virus interactions

Plant endogenous miRNAs are broadly involved in plant development, signal transduction, protein degradation, and biotic or abiotic stress responses. Since miRNAs and siRNAs share many common features, it has been proposed that the miRNA-mediated gene regulation pathways may also be perturbed by virus infection (Lu et al., 2008; Silhavy and Burguán, 2004). Bazzini and colleagues used beta-glucuronidase (GUS) reporter vectors to reveal elevated activity of miR164a promoter upon *Oilseed rape mosaic virus* (ORMV) and TMV infection, and up regulation of miR164 was verified by RT-PCR in virus infected *Arabidopsis* (Bazzini et al., 2009). Bazzini likewise observed disease-like phenotypes in TMV CP and MP co-expressing transgenic *N. tabacum* along with up regulated expression of miR156, miR164, miR165 and miR167, resembling TMV-infected plants and leading to the hypothesis that a complex formed between MP and CP may dysregulate miRNA expression and result in disease symptoms (Bazzini et al., 2007). An array of miRNAs, including miR319 and miR172 in tomato 'Pusa Ruby', were responsive to *Tomato leaf curl new delhi virus* (ToLCNDV) infection and may be involved in the formation of leaf curl symptoms (Naqvi et al., 2010). Reduced levels of miR159, miR165/166 and miR171 were found in cassava and *N. benthamiana* infected with geminivirus *African cassava mosaic virus* Cameroon Strain (ACMV) with severe symptoms, whereas the reduction was absent in plants infected with another geminivirus, *East African cassava mosaic Cameroon virus* (EACMCV), which induced only mild symptoms (Chellapan et al., 2005). In *Brassica rapa*, miR1885 was identified as a novel miRNA and was

specifically induced upon TuMV infection, mediating cleavage of TIR–NBS–LRR class *R* gene transcripts thus breaking the host’s disease resistance (He et al., 2008). It has also been shown that the phytoalexin transcript targeting miR408 was specifically down regulated at late stage of TMV infection in tobacco, and the repressed expression may impact several metabolites involved in respiratory pathways (Bazzini et al., 2011). Induction of miR168 expression has been recognized as a common response to virus infection (Lang et al., 2011; Várallyay et al., 2010). CymRSV viral RNA and increased miR168 accumulation displayed an overlapping distribution, and this up-regulation of miR168 was absent in suppressor P19-deficient CymRSV-infected *Arabidopsis*. In contrast, Várallyay and colleagues observed increased accumulation of AGO1 mRNA in plants infected with either wild-type or P19-mutated CymRSV, suggesting *AGO1* gene expression was elevated as an antiviral mechanism. In contrast, virus-induced up-regulation of miR168 was due to VSR activity (Várallyay et al., 2010).

In conclusion, these studies indicate that virus infection affects expressions of host genes through vsRNA-mediated RNA silencing or dysregulated miRNA pathways, and is thus involved in pathogenesis and development of plant diseases.

Materials and Methods

1. Maintenance of CymMV- and ORSV-free plants

1.1. Plant materials and growing conditions

Mature mericlone *P. amabilis* plants in 7.5-cm pots were purchased from I-hsin Biotechnology Inc. (Chia-yi, Taiwan). CymMV and ORSV-free plants were examined by reverse transcription-polymerase chain reaction (RT-PCR) and grown in natural sunlight phytotron at the Genome Research Center, Academia Sinica. Growth conditions were day/night temperature of 25/20° C with shade cloths used to maintain maximum light intensity of 300 $\mu\text{mol}\cdot\text{m}^{-2}\cdot\text{s}^{-1}$ photosynthetic photon flux density (PPFD). Plants were fertigated with 15N-2.2P-12.5K (Peters 15-5-15 Ca Mg, Scotts Co., Marysville, Ohio, USA) and leached using distilled water as needed.

1.2. Detecting virus infection in newly purchased plants

For detecting CymMV and ORSV infection by RT-PCR, total RNA was purified from 0.1 g lower-positioned leaves of each plant. Disposable razor blades and gloves were used to cut off the sampled tissues to prevent contamination if some plants were virus-infected.

1.2.1. Extracting total RNA from leaf tissues

A CTAB method modified from the pine tree method (Chang et al., 1993) was used to purify total RNA from *Phalaenopsis* leaves. About 0.1 g fresh or frozen leaf tissues were gounded into fine powder with liquid nitrogen, mixed vigorously with 1 mL grinding buffer [0.55 mM CTAB, 0.1 M Tris (pH7.5), 0.2 M EDTA, 20 mM NaCl, 0.03

mM PVP40, and 2% β -mercaptoethanol] and incubated it at 65° C for 15 min. The mixture was centrifuged at 3000 xg for 10 min at room temperature, the supernatant was then mixed with an equal volume of CI (chloroform : isoamylalcohol = 24 : 1), then centrifuged at room temperature again at 12000 xg for 10 min. Total RNA were precipitated by adding one third volume of 8M LiCl into the supernatant and chilling it at -20 °C overnight. The RNA pellet was obtained by centrifuging it at 12000 xg, 4° C for 30 min, then washing it with pre-chilled 70% ethanol and dissolving it in RNase-free water. The concentration of total RNA was determined by NanoDrop 1000 Spectrophotometer (Thermo Fisher Scientific, Waltham, MA, USA).

1.2.2. Reverse transcription-polymerase chain reaction (RT-PCR)

RT-PCR was performed using primer pairs specific for CymMV/ORSV coat protein (CP) genes or RNA-dependent RNA polymerase (RdRp) genes. Details of the primers are listed in Table S1. For the RT reaction, 500 ng total RNA was mixed with 1 μ L of 10 μ M reverse primer and 2 μ L of 10 mM dNTP, and RNase-free water was added to bring up the volume to 12 μ L. The mixture was incubated at 70° C for 5 mins then quenched at least 5 mins on ice. 4 μ L 5X first strand buffer, 2 μ L 0.1M DTT, 0.5 μ L RNasin[®] (40 U· μ L⁻¹, Promega, Madison, WI, USA), 0.5 μ L Super-Script[™] III Reverse Transcriptase (200 U· μ L⁻¹, Invitrogen, Carlsbad, CA, USA), and 1 μ L RNase-free water were added to the solution to produce a final volume of 20 μ L. After incubating at 42° C for 1 hour, the cDNA can be used as template for amplification in PCR.

PCR amplification was performed in a 25 μ L reaction mix containing 2 μ L RT product, 0.5 μ L of each 10 μ M forward and reverse primers, 12.5 μ L *Taq* 2X Master Mix (GeneMark, Taichung, Taiwan) and 9.5 μ L RNase-free water. The Tpersonal

Thermocycler (Biometra, Göttingen, Germany) was set to the following program: 1) 42° C, 45 min, 2) 95° C, 5 min, 3) 95° C, 30 sec, 4) 55° C, 30 sec, 5) 72° C, 30 sec, 6) repeat step 3 to 5 for 34 cycles (total 35 cycles), 7) 72° C, 7 min, 8) 4° C, pause. The PCR products was then analyzed by 1% agarose gel electrophoresis with 1 Kb Plus DNA Ladder (Invitrogen, Carlsbad, CA, USA) as size markers.

2. Detection of CymMV and ORSV spread in *P. amabilis*

2.1. Experimental locations

When conducting inoculation assays, plants were moved from the phytotron to a growth room in the basement of the Institute of Plant and Microbial Biology Building, Academia Sinica. Growth conditions were set to a constant temperature of 28° C, 70% relative humidity, and the light period from 0600_{AM} to 0800_{PM} with a light intensity of 100 $\mu\text{mol}\cdot\text{m}^{-2}\cdot\text{s}^{-1}$ PPF_D supplied by fluorescent lights.

2.2. Virus source

The purified virion and viral RNA were used in inoculation assays. CymMV and ORSV isolates were obtained through three successive single lesion passages on *C. quinoa* (Lin et al., unpublished). After propagating in *N. benthamiana*, virus particles were purified using a method described previously (Lin and Chen, 1991; Lin et al., 1992). Infected leaves were ground in 4 volume of borate buffer (0.5 M boric acid, 1 mM EDTA, and 0.5% β -mercaptoethanol, pH 9.0) and filtrated through microcloth (Calbiochem, Billerica, MA, USA). The filtrate was centrifuged at 8,800 rpm for 22 min in a JA-10 rotor (Beckman Coulter, Brea, CA, USA). K_2HPO_4 and CaCl_2 were then added to the supernatant to reach a final concentration of 40 mM. The mixture was

stirred well for 30 min at 4° C and was then centrifuged at 8,800 rpm for 22 min. PEG 6000 was added to the supernatant to a final concentration of 6% and stirred for 60 min at 4° C. The pellet was obtained after centrifuging at 8,800 rpm for 18 min, and resuspended in 0.05 M borate buffer (0.05 M boric acid and 1 mM EDTA, pH 8.0). Triton X-100 was added to a final concentration of 2% and the mixture was stirred for 20 min at 4° C. After centrifuging at 6,000 rpm for 5 min, the supernatant was layered under a 5-ml cushion of 20% sucrose. Ultrahigh speed centrifugation of 43,000 rpm for 1 hr 40 min was carried out by a RP70T rotor (Hitachi, Tokyo, Japan). The pellet was then dissolved in 5 ml 0.05 M borate buffer at 4° C overnight and yield of purified virions was determined by ultraviolet absorption, assuming the extinction coefficient (ϵ) = 3 for CymMV and ORSV at 260 nm (Choi et al., 2002; Frowd and Tremarine, 1977).

Viral RNA was isolated from purified virions as previously described (Lin and Chen, 1991; Lin et al., 1992). Virions were disrupted by adding one-fourth volume of 4X disruption buffer [100 mM Na₂HPO₄, 50 mM NaH₂PO₄, 5 mM EDTA, 500 mg/ml bentonite (Sigma), 5% SDS, 1 μ L RNasin[®] (40 U· μ L⁻¹, Promega, Madison, WI, USA) and 5% β -mercaptoethanol] and incubated at 60° C for 5 min. Proteins were removed by extracting twice with PCI (phenol:chloroform:isoamyl alcohol = 25:24:1, pH 8.0). The RNA was precipitated by NaOAc and ethanol and finally dissolved in RNase-free water. The concentration of viral RNA was measured by the NanoDrop 1000 Spectrophotometer (Thermo Fisher Scientific, Waltham, MA, USA). Virions and viral RNA were stored at -70° C for further use.

2.3. Virus inoculation and sequential sampling

To observe cell-to-cell and systemic movements of CymMV and ORSV in *P.*

amabilis inoculated leaves, preliminary tests were conducted from 18 Mar 2011 to 29 Mar 2011 and 5 July 2011 to 4 Aug 2011. The fully expanded second leaf from the top was used as the inoculated leaf. The inoculums were as follows:

- 1) 1.5 µg ORSV viral RNA dissolved in 20 µL inoculation buffer [5mM Tris-HCl (pH 8.0), 1mM EDTA (pH 8.0), 5mM phosphate buffer (pH 8.0), and 1 g·L⁻¹ bentonite.]
- 2) 1.5 µg CymMV viral RNA dissolved in 20 µL inoculation buffer
- 3) 0.75 µg of each ORSV and CymMV viral RNA mixed in 20 µL inoculation buffer
- 4) Mock-inoculation with buffer only

Three plants were subjected to each treatment. Assuming the virus would spread along parallel veins, plants were mechanically inoculated with carborundum and cotton swabs at the tip side of about 30% of the area of the leaf. Four areas were marked parallel to veins for sequential sampling at 2, 4, 7, and 11 days post inoculation (dpi) or 4, 11, 16, and 22 dpi to determine the timing of virus movement (Fig. 1). And a longer test period with ORSV inoculation treatment only was conducted starting from 16 Aug 2011 and sampling at 5, 10, 20, 30 dpi. Virus infection and distribution were detected by tissue blotting.

2.4. Tissue blotting and hybridization assay for detecting virus

2.4.1. Tissue blotting

The study employed tissue blotting to reveal virus infection and distribution in inoculated leaves (Lin et al., 1990). Sampling areas were cut off with disposable razor blades and sliced perpendicular to the veins from base to tip sides sequentially with about 3 mm spacing. Each single plane cut surface was pressed on Hybond™-N⁺ (GE Healthcare Life Sciences, Little Chalfont, UK) nylon membranes for about two seconds.

Pressed leaf strips were collected in 15 mL Falcon tubes and frozen in liquid nitrogen, stored at -70°C for further experiments. Positive and negative controls and serial diluted (1 ng to 0.1 pg) viral RNA samples were dotted on the membranes to measure probe specificity and sensitivity. The blots were air-dried, UV cross-linked with 3-minute exposure to $1,200\ \mu\text{W}\cdot\text{cm}^{-2}$ UV light using the HL-2000 Hybrilinker UV crosslinker (UVP, Cambridge, UK) and kept in a dry box for following hybridization assays.

2.4.2. Preparation of digoxigenin (DIG)-labeled probes

The plasmid pGOCP2 and pGCCP (Fig. S1) were constructed for synthesis of ORSV CP and CymMV CP probes, respectively. ORSV and CymMV CP gene fragments were amplified from virus infected *Phalaenopsis* using RT-PCR with ORSV-3, ORSV-6 and CymMV CP-F1, CymMV CP-R1 primer pairs. Detailed information about the primers is listed in Table S1 and the RT-PCR reaction was performed as described in Section 1.2. Desired products were cleaned up using Gel/PCR DNA fragments Extraction Kit (Geneaid Biotech Ltd., New Taipei City, Taiwan), cloned to pGEM[®]-T Easy vector (Promega, Madison, WI, USA) and transformed into Fast-Trans[™] *Escherichia coli* DH5 α competent cells (Protech Technology Enterprise Co., Ltd., Taipei, Taiwan) following the manufacturer's protocol. After selection, the plasmids were purified from cultures of positive clones by NucleoBond[®] PC 500 Maxi-Prep kit (MACHEREY-NAGEL GmbH & Co. KG, Düren, Deutschland) and stored them at -20°C for further assays.

Non-radioactive DIG-labeling RNA probes were generated by *in vitro* transcription from pGOCP2 and pGCCP plasmids. The RNA probes were complementary to (+)-strand viral RNAs and recognized the CP region of CymMV and ORSV,

respectively. Plasmids were first linearized with restriction enzyme *NdeI* (New England Biolabs Inc., Beverly, MA, USA). The 1 μg linearized plasmid in 2 μL DIG-labeling Mix (Roche Applied Science, Penzberg, Germany) was mixed with 0.5 μL RNasin[®] (40 $\text{U}\cdot\mu\text{L}^{-1}$, Promega, Madison, WI, USA), 2 μL 10X polymerase reaction buffer and 2 μL T7 polymerase (50 $\text{U}\cdot\mu\text{L}^{-1}$, New England Biolabs Inc., Beverly, MA, USA) and brought the final volume to 20 μL with RNase-free water. After incubating 2 hrs at 37[°]C, 2 μL RQ1 RNase-Free DNase (1 $\text{U}\cdot\mu\text{L}^{-1}$, Promega, Madison, WI, USA) was added and incubated at 37[°]C for another 30 mins to digest the DNA template. Enzyme reaction was terminated by adding 2 μL 0.2 M EDTA. RNA transcripts were precipitated with 3 M NaOAc and 100% ethanol after refrigeration at -70[°]C for 1 hr. Centrifuged and dried RNA pellet was resuspended with RNase-free water to a final concentration about 400 $\text{ng}\cdot\mu\text{L}^{-1}$ and stored at -70[°]C for further use.

2.4.3. Hybridization and chemiluminescent detection

Tissue blots were hybridized with ~1 μg DIG-labeling probes for about 200 cm^2 membranes. The following detection was performed using DIG detection kit (Roche Applied Science, Penzberg, Germany) according to the manufacturer's protocol. After adding probes and overnight-incubation at 65[°]C with a hybridization buffer [50% formamide, 50 mM PO_4 , 0.8M NaCl, 1mM EDTA, 0.5% SDS, 10X Denhardt's reagent, 250 $\mu\text{g}\cdot\text{L}^{-1}$ D-1626 Sodium salt Type 3 salmon sperm DNA (Sigma-Aldrich Corporation, St. Louis, MO, USA), and 500 $\mu\text{g}\cdot\text{L}^{-1}$ s R-6750 Type 6 baker's yeast ribosomal RNA (Sigma-Aldrich Corporation, St. Louis, MO, USA)], unhybridized probes were washed off with high stringency buffer (0.1X SSC containing 0.1% SDS) and low stringency buffer (2X SSC containing 0.1% SDS) at 65[°]C and 25[°]C, respectively. Membranes

were incubated with blocking solution to reduce non-specific binding, then hybridized with 2 μL Anti-digoxigenin-AP Fab fragments ($1.5 \text{ U}\cdot\mu\text{L}^{-1}$, Roche Applied Science, Penzberg, Germany). CDP-*Star* (Roche Applied Science, Penzberg, Germany) was used as chemiluminescent substrate and light emission was recorded on X-ray films.

3. Genome wide analysis of small RNAs from ORSV-infected *P. amabilis* by deep sequencing

3.1. ORSV inoculation assay and RNA sample preparation

To construct small RNA libraries from ORSV-infected *P. amabilis*, 1 μg of purified ORSV virion per leaf was inoculated on the first and second fully expanded leaf of each plant at the tip side as performed in preliminary tests. Plants mock-inoculated with 20 μL inoculation buffer were used as controls. The inoculated area (i) and non-inoculated area (c) of ORSV-inoculated (O) leaves were designated as Oi and Oc, respectively. Corresponding non-infected tissues from the mock (M) plants were designated as Mi and Mc (Fig. 6). At 10 dpi, Oi, Oc, Mi, and Mc tissues were collected separately and frozen-stored at -70°C . After confirming virus infection by tissue blotting, tissues from three leaves were pooled for total RNA purification using the CTAB method. In addition, we performed RT-PCR to detect virus infection at a higher level of sensitivity. Protocol for tissue blotting, RNA extraction and RT-PCR reaction were the same as previously described.

3.2. Analyzing viral RNA and siRNA accumulation

3.2.1. Analyzing viral RNA accumulation by Northern blot

Northern blot assays were conducted to analyze viral genomic and subgenomic

RNA accumulation. Two μg of total RNA was denatured with glyoxal and separated on 1% agarose gel as previously described (Lin et al., 1996). RNA was transferred to HybondTM-N⁺ (GE Healthcare Life Sciences, Little Chalfont, UK) nylon membranes by the capillary method with 3 M NaCl and 0.01 N NaOH and immobilized with UV cross-link non-radioactive probes. Hybridization methods used for northern blot were the same as those used for tissue blotting as described in Section 2.4.

3.2.2. Analyzing viral siRNA accumulation by small RNA Northern blot

To detect viral siRNA accumulation, twenty-five μg total RNA was mixed with equal volume of 50% deionized formamide with bromophenol blue, boiled for 5 mins then placed on ice until loaded into the gel. MicroRNA Marker (New England Biolabs Inc., Beverly, MA, USA) containing a set of 17, 21 and 25-nt synthetic single-stranded RNA oligonucleotides was used as size markers. After separation in the 15% acrylamide/7M urea gel, RNA were transferred to HybondTM-N⁺ (GE Healthcare Life Sciences, Little Chalfont, UK) nylon membranes by Trans-Blot® SD Semi-Dry Transfer Cell (BioRad Laboratories, Hercules, CA, USA) and immobilized by UV cross-link.

The following hybridization assay was performed with radioactive ³²P-labeled probes. To detect a pool of siRNAs generated from ORSV RdRp or ORSV CP to 3'-UTR regions, viral gene fragments were cloned with ORSV RdRp-F/R and ORCP3UTR-F/R primer pairs (Table S1) from infected *Phalaenopsis* using RT-PCR, and ligated into pGEM[®]-T Easy (Promega, Madison, WI, USA) vectors according to the same method as described for the DIG-labeled probes. The consequent plasmids pGORd and pGOC3U (Fig. S2) were first linearized with restriction enzyme *NcoI*, and then used for SP6 polymerase-driven preparation of *in vitro* transcribed [α -³²P]CTP

labeled probes as described previously (Lin et al., 1993; Lin et al., 1996). To increase the efficiency of small RNA detection, probes were chemically hydrolyzed to reduce their size with alkaline carbonate buffer (containing 8.5 mM Na₂CO₃ and 1 mM NaHCO₃, pH10.2) at 60° C for 1 hr 30 min before hybridization. Alternatively, when detecting a specific viral siRNA, corresponding anti-sense synthetic single-stranded DNA oligonucleotide was used as probe and labeled with [γ -³²P]ATP by T4 Polynucleotide Kinase (New England Biolabs Inc., Beverly, MA, USA) at the 5'-end. A 21-nt DNA oligonucleotide complementary to the microRNA Marker was also labeled by 5'-end labeling and used to hybridize with the size marker.

The membranes for small RNA northern blot were incubated with ULTRAhyb®-Oligo hybridization solution (Ambion, Carlsbad, California, USA) at 42° C for 1 hr for pre-hybridization. Radioactive probes were added into roller bottles and incubated overnight at 42° C. After two post-hybridization washes with wash solution (2X SSC and 0.1% SDS), radioactive signals were recorded by reusable phosphorimager screens and scanned by Typhoon® FLA7000 Biomolecular Imager (GE Healthcare Life Sciences, Little Chalfont, UK).

3.3. Small RNA deep-sequencing and annotation

3.3.1. cDNA library construction and sequencing

Small RNAs from inoculated (Oi and Mi) and non-inoculated (Oc and Mc) tissues of ORSV- or mock-inoculated plants were subjected to deep sequencing on 28 Nov 2011. The integrity of the RNA was checked by Agilent 2100 Bioanalyzer (Agilent Technologies, Santa Clara, CA, USA). For each library, 10 μ g of total RNA was size fractionated on 15% tris-borate-EDTA urea polyacrylamide gel. Small RNAs were

recovered from the bands of gel corresponding to 18-30 nts of the marker. Construction of cDNA libraries were performed according to TruSeq™ Small RNA Sample Preparation protocol (Illumina, San Diego, CA, USA). In brief, 3' (RA3, TGGAATTCTCGGGTGCCAAGG) adapter and 5' adapter (RA5, GTTCAGAGTTCTACAGTCCGACGATC) were ligated to small RNAs with T4 RNA ligase. The RT-PCR was performed to create and amplify cDNA constructs using primers annealed to the adapters. Multiplexing indexes were incorporated at the amplification step following reverse transcription. The cDNA constructs were then gel-purified, validated on an Agilent 2100 Bioanalyzer using an Agilent DNA-1000 Chip (Agilent Technologies, Santa Clara, CA, USA). Bar-coded libraries were pooled and loaded in a single channel of the flow cell. High-throughput sequencing was carried out on an Illumina HiSeq 2000 (Illumina, San Diego, CA, USA).

3.3.2. Sequencing data trimming and annotation

After the platform generated sequencing images, raw image analysis, base calling, and demultiplexing were done using CASAVA (Illumina, San Diego, CA, USA) and the results were exported as individual libraries in FASTQ file format. Further processing of the sequencing data was performed by customized Perl script. Raw sequences were first trimmed to obtain clean reads in the following steps: 1) reads with sequences exactly matched to size markers (AATGATACGGCGACCACCGA and GATCGGAAGAGCGGTTCAGCAGGAATGCCGAG) were discarded as contaminants. 2) using adapter sequences as probes, 5' and 3' adapter and non-input bases in each read were removed, and reads without adapters were discarded. 3) The poly-A/T/C/G reads and 4) reads with N (null) callings were then discarded. Clean reads were further

grouped to unique reads (tags) according to sequence identity. Low frequency tags (i.e. tags with only one read in a single library that were not detected in any other libraries) and tags with sizes < 15-nt or > 27-nt were filtered out from the analysis that followed. CymMV and ORSV specific siRNAs and plant conserved miRNAs were identified through alignment against virus genome sequences and miRBase v18.0 (<http://www.mirbase.org>, Griffiths-Jones et al., 2008) conducted by stand-alone BLAST suites (<http://blast.ncbi.nlm.nih.gov/>, Altschul et al., 1990). *P. aphrodite* transcriptome database (Orchidstra, <http://orchidstra.abrc.sinica.edu.tw/>, Su et al., 2011), Rfam v10.1 (<http://rfam.sanger.ac.uk/>, Gardner et al., 2009) and other local BLAST databases were also involved in the annotation pipeline, with the hierarchy and criteria as indicated in Fig. 10.

3.3.3. Target prediction for vsRNAs and miRNAs

3.3.3.1. Analyzing differential expressions of miRNAs

For comparing relative abundances between libraries of a specific miRNA family, the expression level of miRNA tags was converted into tags per million (TPM, which stands for the frequency of a specific tag among a million redundant reads) to normalize differences in library size. Thus, each miRNA read count was divided by total miRNA reads of the corresponding library and multiplied by 10^6 . After normalization, pair-wise comparisons between libraries generated a fold-change index representing differential expression levels of a miRNA family.

3.3.3.2. Prediction of putative miRNA target genes

Potential miRNA target genes in *Phalaenopsis* were predicted based on BLAST programs through two approaches. First, through a direct BLASTN search against *P.*

aphrodite mRNA sequences, complementary pairs matching the following criteria were kept as candidates: 1) Taking into consideration that plant miRNA:mRNA pairings typically encompass the 2-13rd 5'-end bases (known as the “seed region,” and the second base of a mature miRNA sequence in miRBase was designated as a “relation site”) of the miRNA (Fahlgren and Carrington, 2010). Tags that did not include the relation sites were ignored in the prediction program. 2) Sixteen or more nucleotides should be aligned in the pairing, but up to three mismatches were allowed. Another approach involved searching *P. aphrodite* homologs of known miRNA targeted genes in *Arabidopsis* (as deposited in the *Arabidopsis* Small RNA Project (ASRP) database, <http://asrp.cgrb.oregonstate.edu/>) using a TBLASTN algorithm, and the e-value was set lower than 1e-30. The annotation of putative target genes was downloaded from Orchidstra database (<http://orchidstra.abrc.sinica.edu.tw/>).

3.3.3.3. Prediction of putative vsRNA target genes

To search for transcripts that could be targeted by viral siRNA, vsRNA sequences were used as queries to search through *P. aphrodite* transcriptome database (Orchidstra, <http://orchidstra.abrc.sinica.edu.tw/>) by BLAST. Permissive alignment settings were first applied to ensure that all possible vsRNA:mRNA pairings were captured. Next, taking into consideration that the RISC mediated mRNA cleavage requires a high degree of base pairing, the study adopted a position-dependent scoring matrix described by Fahlgren and Carrington (2010). In brief, mismatches and single-nucleotide bulges or gaps were scored as 1, G:U pairs was scored as 0.5. Penalty scores were doubled when mismatches, gaps, bulges, and G:U pairs resided in the core region (position 2 to 13 according to the 5' end of vsRNA). Generally, a maximum score cut-off of 3.5

maintains reliable sensitivity and specificity as studied in *A. thaliana* (Fahlgren and Carrington, 2010). The annotation and GO terms of putative target genes were downloaded from Orchidstra database (<http://orchidstra.abrc.sinica.edu.tw/>). GO enrichment analysis was performed on GeneSpring software (Agilent Technologies, Santa Clara, CA, USA).

3.4. Experimental validation of small RNAs

3.4.1. Validating miRNA expression by stem-loop quantitative RT-PCR (qRT-PCR)

The differential expressions of some miRNAs were validated by stem-loop qRT-PCR using the SYBR green method. Stem-loop reverse primers for reverse-transcribed specific miRNAs were designed according to the method provided by Varkonyi-Gasic and Hellens (2010), and the following RT reaction was mainly based on the described protocol with a slight modification. Sequences of the primers are listed in Table S1. For reverse transcription, 0.5 μL of 1 μM stem-loop reverse primer was mixed with 1 μL of 10 mM dNTP and 3.9 μL RNase-free water and incubated at 65 $^{\circ}\text{C}$ for 5 mins, then quenched on ice to de-associate the stem pairing of the primer. The concentration of total RNA of each sample was adjusted to 10 $\text{ng}\cdot\mu\text{L}^{-1}$ and 1 μL total RNA of each sample was used for synthesizing the cDNA. The primer solution and total RNA were mixed with 2 μL 5X first strand buffer, 1 μL 0.1 M DTT, 0.1 μL RNaseOUTTM (40 $\text{U}\cdot\mu\text{L}^{-1}$, Invitrogen, Carlsbad, CA, USA), 0.3 μL Super-ScriptTM III Reverse Transcriptase (200 $\text{U}\cdot\mu\text{L}^{-1}$, Invitrogen, Carlsbad, CA, USA), and the final volume was brought to 10 μL with 0.2 μL RNase-free water. The solution was incubated at 16 $^{\circ}\text{C}$ for 30 min, followed by 50 $^{\circ}\text{C}$ for 1 hr and the reaction was terminated with incubation at 85 $^{\circ}\text{C}$ for 5 min. The cDNA was 3-fold diluted (adding 20 μL RNase-free

water to the 10 μ L solution) and stored at -20° C if PCR was not conducted immediately following the RT reaction.

For PCR amplification, 10 μ L reaction was performed using a 384-well plate. Each well contained 2 μ L diluted cDNA, 1 μ L of 5 μ M forward primer, 1 μ L of 5 μ M universal-reverse primer (which was annealed to the conserved stem sequence amplified from the stem-loop reverse primers), and 5 μ L 2X FastStart Universal SYBR Green Master (Rox) (Roche Applied Science, Penzberg, Upper Bavaria, Germany). The PCR program was set as follows and carried out using ABI QuantStudio 12K Flex system (Applied Biosystems, Inc., Foster City, CA, USA): 1) 50° C, 2 min, 2) 95° C, 10 min, 3) 95° C, 15 sec, 4) 60° C, 1 min, 5) repeat step 3-4 for 40 cycles, 6) 95° C, 15 sec.

The relative quantity of miRNA expression was calculated using a comparative C_T ($\Delta\Delta C_T$) algorithm (Livak and Schmittgen, 2001) with miR399 as a reference. A web-based tool, BootstRatio (<http://regstattools.net/br>, Cléries et al., 2012), was used to tackle the statistical significance of the relative expression through resampling methods.

3.4.2. VsRNA co-transfection assay in *Oncidium* protoplasts

To verify whether ORSV hotspot siRNA could confer interference of virus replication, hotspot siRNA and ORSV co-transfection assay was performed.

3.4.2.1. Protoplast isolation

Protoplasts were isolated from *Oncidium* Gower Ramsey suspension-cultured cells. Take 3 g of mesh-filtered cells in a Petri dish containing 20 ml enzyme mixture of 0.44% MS salt (Sigma-Aldrich Corporation, St. Louis, MO, USA), 2.5% Cellulysin (Merck KGaA, Darmstadt, Germany), 0.4% Driselase (Sigma-Aldrich Corporation, St. Louis, MO, USA), 0.6% Pectinase (Merck KGaA, Darmstadt, Germany), 1% BSA and

0.4 M sucrose (pH 5.6), then incubated for 7 h at 25 °C in the dark on a rotatory shaker at 50 rpm. Gently filtered the suspension through a 100 µm nylon sieve and collected the filtrate in a 40 ml sterile centrifuge tube. Following centrifugation at 1000 rpm for 6 min, collected the suspended protoplasts and gently added into electroporation buffer (0.42 M mannitol, 80 mM KCl, 6.6 mM CaCl₂, and 10 mM HEPES, pH 5.6) with a dropper. Centrifuged the solution at 1000 rpm for 6 min, removed the supernatant and left about 0.5 mL protoplast solution then count the yield with a hemocytometer.

3.4.2.2. Co-transfection by electroporation method

For each inoculation, 0.5 ml of electroporation buffer containing 10⁵ protoplasts was electroporated with 1 µg ORSV viral RNA individually or combined with either 1 µg, 2.5 µg, or 6.25 µg synthetic hotspot vsRNA, coldspot vsRNA, or green fluorescence protein (GFP) siRNA duplexes (Integrated DNA Technologies, Coralville, IA, USA) with BTX ECM 600 Electroporation system (Biotechnologies & Experimental Research, Inc., Sandiago, CA, USA) at 250 HV, 200 Ω and 50 µF. The electroporated protoplasts were incubated in the dark for 24 h for virus replication.

3.4.2.3. RNA purification and Northern blot analysis

An amount of 200 µl extraction buffer (0.33 M glycine, pH 9.5, 0.33 M NaCl, 33 mM EDTA, 3.3% SDS, 8.3 mg/ml bentonite) was added into 500 µl infected protoplasts to lyse the cells. Proteins were extracted with 500 µl PCI, and the RNA was precipitated with 2-propanol. After the RNA was washed with 70% EtOH, the pellet was dissolved in 30 µl DEPC-H₂O. Northern blot analysis of viral RNA accumulation was performed with 5 µl purified RNA and the method was the same as described in Section 3.2.1.

4. Genome wide analysis of small RNAs from CymMV and double infected *P. amabilis* by deep sequencing

4.1. CymMV and mixed inoculation assays

To construct small RNA libraries from CymMV- and CymMV plus ORSV double-infected *P. amabilis*, 1 µg of CymMV or 0.5 µg of each CymMV and ORSV virion per leaf was inoculated on the first and second fully expanded leaf of a single plant. The inoculation method was the same as that performed for ORSV single inoculation, and mock-inoculated plants were included as controls. At 10 dpi, tissues were collected separately and subjected to virus detection and RNA purification as described previously. The inoculated areas (i) of CymMV- (C), double- (D), and mock- (M) inoculated leaves were designated as Ci, Di, and Mi-2, respectively, and the non-inoculated areas (c) were designated as Cc, Dc, and Mc-2 (Figs. 6 and 20). Basically, CymMV was systemically moved to non-inoculated (Dc) tissues at 10 dpi, but restricted infection of CymMV was also observed in a few doubly inoculated leaves. Thus the inoculated and non-inoculated tissues of mildly infected leaves were specifically designated as Dsi and Dsc, respectively.

4.2. Analyzing viral RNA and siRNA accumulation

Northern blot assays were also conducted to reveal viral genomic RNA, subgenomic RNAs and siRNA accumulation as previously described, with the probes used for CymMV siRNA detection. Probes recognizing partial CymMV RdRp region were *in vitro* transcribed from restriction enzyme *ApaI*-linearized pGCRd plasmid (Fig. S2) which is harboring CymMV RdRp sequence cloned with CymRdRp1319 F/R primer pairs. The sequence of the primers is listed in Table S1.

4.3. Construction of small RNA libraries from CymMV and double infected *P.*

***amabilis* and bioinformatic analysis**

Small RNA libraries from CymMV-infected (Ci, Cc), doubly infected (Di, Dc, and Dsc), and mock-inoculated (Mi-2 and Mc-2) tissues were constructed on 25 July 2012. cDNA library construction, small RNA deep-sequencing, data trimming and annotation, and bioinformatic analysis such as target prediction were carried out as described for the preparation of small RNA libraries from the ORSV-infected tissues.



Results

1. Preliminary time course assay of CymMV and ORSV infection in *P. amabilis*

ORSV and CymMV commonly infect orchids. Although several studies have detected the virus infection in systemically infected leaves over two to eight weeks post inoculation (楊, 2008; 劉, 2000; Chan et al., 2005; Liao et al., 2004; Lu et al., 2007; Lu et al., 2009), the time course of ORSV and CymMV infection in inoculated leaves remains unclear. To determine ORSV and CymMV time course distribution within a period of < 1 month in inoculated leaves of *P. amabilis*, virus-free plants were mechanically inoculated with virions and virus infection was detected by tissue-blotting at different time points. Three batches of tests were carried out with different sampling schedules.

1.1. ORSV infection in inoculated leaves 2 to 11 dpi

To determine the spread of the virus along the vein, *P. amabilis* plants were leaf-tip inoculated and sampled one-fourth parallel areas at 2, 4, 7, and 11 dpi by tissue-blotting as shown in Fig. 1B. In the three inoculated plants, restrained virus accumulation in inoculated areas was detected at 7 and 11 dpi after a single inoculation with ORSV (Fig. 2). Dangling signals were detected at earlier time points (2 and 4 dpi), these were confined in adaxial epidermis and could not be clearly distinguished from background signals (Fig. 2).

1.2. ORSV infection spreaded to non-inoculated tissues after 10 dpi

Following the first test, a similar assay was performed to determine the course of ORSV infection over a longer duration. Plants were inoculated with ORSV and sampled

at 5, 10, 20, and 30 dpi. Of the ten inoculated leaves, virus infection was detected in 60% starting at 5 dpi, and virus infection was detected in another 30% starting later at 10 dpi. At 20 dpi, ORSV infection was detected in all ten leaves and in 70%, infection had spread to non-inoculated areas. During the 30-day period, virus infection gradually spread from the tip to the base in nine out of ten inoculated leaves (Fig. 3).

1.3. Accelerated spreading of CymMV infection in mixed inoculated leaves

To determine if ORSV and CymMV co-inoculation had a synergistic effect, mixed-inoculation and inoculation with ORSV or CymMV alone were assayed. The sampling time points were 4, 11, 16, and 20 dpi. For single infection with ORSV, virus infection was localized in the inoculated area up to 16 dpi, and with a confined spreading in the non-inoculated regions at 20 dpi, similar to previous results (Fig. 4A). The detection for CymMV single infection were uncertain, since the virus infection was unevenly distributed and could only be detected at 4 and 11 dpi in one out of four inoculated plants (Fig. 4B and data not shown). Interestingly, when inoculated with CymMV and ORSV together, the spread of CymMV was greatly accelerated. CymMV infection was detected throughout the leaf strip at 11, 16, and 20 dpi (Fig. 5B), whereas ORSV remained localized accumulation in the inoculated areas at least until 16 dpi and was detected in neighboring non-inoculated tissues at 20 dpi (Fig. 5A), similar to the ORSV single infection.

These results suggest that ORSV accumulated locally in the inoculated area around 7-15 dpi and spreaded to the non-inoculated area afterwards. The time-course of CymMV infection was unclear and could not be observed well from the weak infection.

However, enhanced CymMV infection aided by synergism with ORSV was observed, but in contrast, the ORSV infection pattern remained similar to that observed in single ORSV infection. In conclusion, 10 dpi was considered the time point by which ORSV accumulated in inoculated areas. Assuming CymMV single infection may spread through a similar time course pattern, inoculated leaves were collected at 10 dpi for the following inoculation assays.

2. Analysis of small RNAs from ORSV-infected *P. amabilis* by deep sequencing

RNA silencing is widely involved in plant developmental processes and stress responses, and also plays important roles in defense mechanisms (Blevins et al., 2006; Llave, 2010; Molnar et al., 2011). This study employed high-throughput sequencing technology to reveal vsRNAs generated by antiviral DCL processing and altered expression levels of several conserved miRNAs under virus infection. Potential *Phalaenopsis* mRNA targets were predicted to tackle the possible role of infection responsive small RNAs in the plant defense and counter-defense interactions.

Based on the preliminary tests, ORSV infection was confined to inoculated areas at 10 dpi. In order to analyze the difference in small RNA profiles from tissues at different stages of infection, small RNAs in inoculated and non-inoculated tissues were profiled separately.

2.1. Analysis of ORSV infection

As described above, virus-free *P. amabilis* were tip-inoculated with ORSV virions to detect the accumulation of ORSV and their derived small RNAs. As shown in Fig. 6B, tissues from inoculated and non-inoculated areas of ORSV-inoculated leaves were

collected separately for RNA extraction. Inoculated (i) and non-inoculated (c) tissues of the ORSV-inoculated (O) leaves were designated as Oi and Oc, respectively. Corresponding mock (M) tissues with (i) or without (c) buffer inoculation were designated as Mi and Mc, respectively.

At 10 dpi, no clear symptoms were observed and the phenotype of ORSV inoculated leaves was indistinguishable from that of mock-inoculated plants (Fig. 7A). In accordance with previous results, ORSV infection was confined to the inoculated area in most inoculations, as revealed by tissue blotting at 10 dpi (Fig. 7A and data not shown). ORSV infection was detected in non-inoculated tissues in some leaves (16 out of 70 leaves), but these leaves were excluded from further analysis (data not shown).

RT-PCR assay detected ORSV RNA in Oc when performed with higher sensitivity assay (Fig. 7B). RT-PCR also confirmed ORSV single infection in inoculated plants, and mock-infected plants were virus-free (Fig. 7B). Northern blot analysis showed CP-expressing subgenomic RNAs (sgRNAs) were largely accumulated in Oi tissues, but were much less in Oc tissues (Fig. 8). Similarly, small RNA Northern blot revealed a 21-nt vsRNA accumulation in Oi tissues. However, vsRNA was undetectable in Oc tissues, probably due to the low accumulation of ORSV (Fig. 8). Thus the level of vsRNAs was strongly associated with ORSV accumulation in infected tissues. These results also show that two different stages of ORSV infection, early and late, could be distinguishable in the Oc and Oi tissues, respectively.

2.2. Deep sequencing of small RNAs from ORSV-infected *P. amabilis*

To profile the small RNAs in ORSV-infected *Phalaenopsis*, this study subjected gel-purified small RNA pools which were prepared from Oi, Oc, Mi, and Mc samples as

described above to Solexa sequencing. The small RNA molecules were ligated with bar-coded adapters and sequenced in the same lane, generating 34,518,220 total raw reads. After demultiplexing, small RNA reads were separated into four libraries. About 89% to 95% of reads had recognizable adapter sequences and were further filtered to exclude poly-A/T/C/G tags and reads containing poor-quality N (null) base-calling. Considering that known functioning small RNAs are usually 15-27 nt species (Ruiz-Ferrer, 2009; Vaucheret, 2006), only tags with sizes in this range were retained. Ultimately the experiment obtained 10,374,208 (Oi), 4,759,861 (Oc), 8,044,535 (Mi), and 8,385,985 (Mc) clean reads (Table 1) from 2,270,835 (Oi), 984,602 (Oc), 3,012,462 (Mi), and 2,999,050 (Mc) unique reads (tags) (Table 2), respectively. The size distribution of tags was similar among libraries, with 24-nt classes as the most abundant and contributing to over 50% of total unique reads (Fig. 9A). For the redundant reads, approximately 45% to 72% of small RNAs were between 21 to 24-nt sizes, but these distributed differently between ORSV-infected and mock-infected tissues. With 24-nt accounting for the highest and 21-nt the second most abundant in the Mi and Mc libraries, 21-nt became the most prevalent size among the Oi. For the Oc library, both the 21 and 24-nt small RNAs were reduced in abundance compared to mock-inoculated tissues (Fig. 9B). To simplify the sequencing data, identical tags among the four libraries were grouped, and low frequency tags (with only one read count among libraries) were removed from further analysis. The tags were subjected to BLAST-based annotation following the hierarchy of virus > *Phalaenopsis* transcripts > Rfam > miRNA, as diagrammed in Fig. 10.

2.3. Characteristics of ORSV viral siRNAs (vsRNAs)

2.3.1. ORSV vsRNA populations in inoculated (Oi) and non-inoculated (Oc) tissues

Small RNA reads were first searched against a local microorganism database to remove possible environmental contaminant inputs, then matched with the ORSV genome (DQ139262). About 29.6% (2,454,779 reads) and 0.07% (2,458 reads) of total annotated reads in the Oi and Oc libraries, respectively, were perfectly matched to the ORSV genome (Table 1 and Fig. S3). The small percentage of vsRNAs in Oc indicated an initial stage of infection in non-inoculated tissues. To examine infection with other viruses, reads matched to genomes of other prevalent orchid viruses (CaCV, CarMV, CMV, CymMV, INSV, OFV, PhCSV, and TSWV) were also searched. As shown in Table 1, very few matches were generated. These matches were likely a consequence of sequence homology with plant endogenous nucleotides.

2.3.2. Size distribution, strand polarity, and 5'-end nucleotide preference of ORSV vsRNAs

Within the ORSV-specific vsRNA population, the size distribution, strand polarity, and 5'-end nucleotide preference were analyzed. Size class of 21-nt (57.3% and 74.1% of total vsRNAs in Oi and Oc, respectively) was the most dominant, followed by 22-nt species (16.2% and 15.8% of total vsRNAs in Oi and Oc, respectively). Together, these constituted 73.5% (Oi) and 89.9% (Oc) of total vsRNAs, respectively, indicating that antiviral RNA silencing in *P. amabilis* may be mediated mainly by DCL4 and DCL2 homologous proteins. Asymmetrical distribution of vsRNAs in strand polarity with prevalence of sense strands was observed in Oi, accounting for 70.6% of the total reads (Fig. 11A). In the Oc library, vsRNAs derived almost equally from both polarities, and

possessed only a modest enrichment (53.7%) of (+)-stranded reads (Fig. 11B).

When grouped by the 5'-end nucleotide (A, C, G, and U), 21 to 24-nt vsRNAs with 5'-A, (25.2 to 35.4% in Oi and 26.9 to 32.3% in Oc) or 5'-U (30.9-34.7% in Oi and 28.3-38.5% in Oc) were frequently observed, together constituting 59 to 66% and 43 to 67% of the Oi and Oc libraries, respectively (Fig. 12). In contrast, vsRNAs that 5' terminated with a guanine (G) (7.7 to 14.6% in Oi and 8.0 to 19.6% in Oc) were underrepresented (Fig. 12). Avoidance of Gs in the 5'-end position was clearly demonstrated, since the base composition of ORSV genomic RNA is U (30.76%) > A (29.81%) > G (21.64%) > C (17.79%). No preferential vsRNA size class was associated with strand polarity and 5' nucleotide preference, indicating the bias was not introduced by different DCL processing. The 5' nucleotide bias may have a stronger relation with AGO recruitment, as numerous studies have suggested 5' nucleotide identity plays a role in strand selection and AGO sorting (Czech and Hannon, 2011; Kim, 2008). AGO proteins have been reported with preferred binding affinities for small RNAs having 5' terminal U (AGO1), A (AGO2, 4), and C (AGO5) (Hu et al., 2011). Based on the 5'-U and 5'-A preference, ORSV vsRNAs may potentially be loaded into AGO1, AGO2, and AGO4.

2.3.3. Genome mapping, coverage and hotspots of ORSV vsRNAs

In order to study the vsRNA distribution across the entire ORSV genome, vsRNAs were spotted according to their 5'-end sites along both positive and negative strands of the ORSV genome (DQ139262) and the coverage of vsRNAs on each base was also analyzed. Plotting with both polarities and all sizes, the vsRNAs encompassed about 85.9 to 99.3% of the ORSV genome, reflecting broad covering but heterogeneous

deposition, with some genomic regions showing higher densities of vsRNA reads. VsRNAs exhibited similar patterns in Oi and Oc (Fig. 13). Abundant ORSV vsRNAs were located within the CP-coding region and 3' UTR (Fig. 13); these results were confirmed with hybridization analysis using probes of the nt 5762 to 6608 CP to the 3' UTR region, whereas vsRNAs were hardly detected using probes from nt 2410 to 3269 RdRp region (Fig. 8). The genome distribution of 21 nt and 22 nt vsRNAs were similar, showing most prominent peaks of vsRNA of 21 nt were localized within the same genomic regions as the 22 nt vsRNA peaks (Fig. S2). These distribution patterns seemed to indicate the resemblance of targeting affinities toward the same regions between different DCL proteins in ORSV genome.

2.3.4. Specific vsRNA hotspot in ORSV 3'-UTR

The vsRNA mapping also identified several vsRNA-generating hotspots comprised by clustering of multiple overlapping vsRNA species within a narrow region, and a specific hotspot located in 3' UTR was observed (Fig. 13). Most strikingly, the sharp peak here was contributed by only one (+)-stranded tag and accounted for 1.15% (28,143 reads) and 1.75% (43 reads) of total ORSV-specific siRNAs in Oi and Oc, respectively. Further analysis revealed the hotspot vsRNA tag (5'-UCCACUAAAUCGAAGGGUUG-3') had a conserved sequence among tobamovirus 3'-UTRs (Fig. 14). The tobamovirus 3'-UTR lacks a poly(A) tail but instead contains a highly structured pseudoknot chain and ends with a tRNA-like structure (Zeenko et al., 2002). Whilst most tobamoviruses have only 3 PKs in the conserved domain, ORSV 3'-UTR was about 412 nt long, comprised of three consecutive homologous regions and found with 11 PKs (Fig. 15) (Ajjikuttira and Wong,

2009; Chng et al., 1996; Gulyaev et al., 1994). The two duplicated sequences also contain the hotspot sequence but with one base variation, substituting a G into a U at the 3'-end (5'-UCCACUAAAUCGAAGGGUUU-3'). VsRNAs generated from the other duplicated sequences were found, however, the reads were much lower, with 830 and 1 reads in Oi and Oc libraries, respectively.

2.3.5. Functional analysis of ORSV 3'-UTR hotspot vsRNA

Co-transfection assay was performed to verify whether the abundance of the 3'-UTR hotspot vsRNA could confer efficient elimination of viral RNAs. Due to poor yield of protoplast isolation resulting from the high abundance of calcium oxalate crystals in *Phalaenopsis* leaves (data not shown), protoplasts from *Oncidium* Sweet Sugar suspension cells were isolated instead (Fig. 16A-B). Besides the hotspot vsRNA, one of the vsRNA tags (5'-UCACCUUCACUCAAGUGACA-3') residing in the ORSV RdRp-coding region with only five reads in Oi was chosen as coldspot vsRNA, and together with another sequence-unrelated GFP siRNA as control. Viral RNA and different amounts of synthetic siRNAs were electro-transfected into protoplasts and total RNA was extracted after 24 h post transfection.

Northern blot analysis revealed ORSV accumulation increased in a siRNA dose-dependent manner no matter whether plants were co-inoculated with hotspot, coldspot, or GFP siRNAs (Fig. 16C). The dose-dependent increment was most prominent in co-transfection with hotspot siRNA duplexes. Compared to protoplasts transfected with viral RNA only, ORSV viral RNA accumulated to 5.3-, 7.2-, and 12.2-fold, respectively, after co-transfecting 1, 2.5, and 6.25 μ g hotspot siRNAs (Fig. 16C). Thus the co-transfection assay failed to provide evidence that 3'-UTR hotspot

vsRNA functions to interfere with ORSV accumulation.

2.4. Identification and analysis of conserved miRNAs

2.4.1. miRNA populations

In addition to profiling ORSV vsRNAs, *P. amabilis* endogenous non-coding RNAs were also analyzed. Non-viral sequences were further used as queries to search against conserve miRNAs and other non-coding RNAs using BLASTN algorithm. Tags perfectly matched to annotated *P. aphrodite* coding gene transcripts were removed prior to searching against the Rfam and miRBase, as these sequences might be fragments from degraded mRNAs. After searching against miRBase v18.0 with a tolerance of three mismatches, 104,797 unique miRNA sequences corresponding to 154 families were identified. The number of members in each family varied widely, ranging from a single member to over hundreds of species, and miR166, with 313 members, was the largest family (Table 3). Diverse members indicated isoforms existed within the same family, though some tags had only one or two reads and the possibility that the variation resulted from sequencing errors could not be excluded. Nonetheless, these data suggest a diverse and complex miRNA pool in *P. amabilis*.

Unexpectedly, the analysis profiled a super-abundant tag of miR166 (5'-TCGGACCAGGCTTCATTCCCC-3', perfect match to osa-miR166e-3p). With 933,712 (Mi), 663,895 (Mc), 451,972 (Oi), and 268,708 (Oc) reads, the single tag proportioned to 68 to 79% of total miRNAs (Fig. 17) and 6 to 15% of total clean reads in each library (Table S2). After discarding the tag, the percentage of total miRNAs in total clean reads was dropped from about 9 to 19% to about 3 to 4% (Table S2). However, the super-abundance of miR166 revealed in deep sequencing data could not

be validated by stem-loop qRT-PCR (Fig. S5A) and small RNA northern blot (Fig. S5B). Thus the super-abundance of miR166 is assumed to be an artifact.

2.4.2. Differential expressions of miRNAs in response to ORSV infection

To search for miRNAs responsive to virus infection, the abundance of various miRNA families were compared between different libraries. The read counts were first normalized with total miRNA reads within a corresponding library and converted to tags per million (TPM) values for further comparison. Fold changes (FC) calculated from comparing the Oi/Mi and Oc/Mc libraries revealed some miRNAs were regulated after ORSV infection. As shown in Table 4, with a threshold of 1.5-fold, the infection response of some abundant miRNAs (TPM ≥ 10 in at least one library) was demonstrated between mock-infected and ORSV-infected tissues (Table 4). Stem-loop qRT-PCR further validated the expression levels of miR156, miR159, miR162, miR165, miR168, miR169, miR171, miR172, miR319, miR393, miR394, miR396, miR398, miR408, miR5139, miR528, miR535, and miR894 (Figs. 18-19). However, the expression patterns showed differences between the qRT-PCR and deep sequencing data. At a threshold of 1.5-fold change, miR156, miR171 and miR394 were up-regulated in both Oi and Oc tissues compared to Mi and Mc tissues. The expression levels of miR396 and miR5139 were specifically increased in Oc, while miR168 was up-regulated only in Oi. MiR528 was down-regulated in Oi but up-regulated in Oc (Fig. 18). Significant variations were confirmed in miR168, miR528, and miR535 according to statistical analysis ($P \leq 0.05$). The expression levels of other validated miRNAs were similar to mock-infected tissues (Fig. 19).

2.4.3. Target prediction and possible roles of ORSV-infection responsive miRNAs

Target prediction of the infection responsive miRNAs was performed to infer the possible roles of these miRNAs in response to virus invasion in *P. amabilis* (Table 5). BLASTN hits with fewer than three mismatches against the reverse complementary sequence of 233,924 assembly transcripts (Orchidstra, <http://orchidstra.abrc.sinica.edu.tw>) were obtained as candidates. After the search, 22 potential targets were predicted for miR535, 20 for miR156, 7 for miR171, 4 for miR5139, 2 for miR528, and miR168 and miR394 each with only one match (Table 5).

Evidence showed miR156 primarily regulated SQUAMOSA PROMOTER BINDING PROTEIN LIKE (SPL) genes and was involved in the transition from the vegetative phase to flowering (Gou et al., 2011; Poethig, 2009; Rhoades et al., 2002; Xing et al., 2010). Several SPL genes were also predicted as putative targets of miR156 in *Phalaenopsis*. Other matches included some transcription factors [PHD-finger homeodomain protein], molecules involved in protein biosynthesis, metabolism and phosphorylation [*UB-LIKE PROTEASE 1D* (ULP1D), Peptidase M20/M25/M40 family proteins, *EMBRYO DEFECTIVE 1873* (EMB1873), Sister chromatid cohesion 1, *GASSHO1* (GSO1)], cellular components [Tetratricopeptide repeat (TPR)-like superfamily protein, kinesin-like protein (PAK)] and other coding genes of hypothetical proteins (Table 5).

It has been proven miR168 and AGO1 were transcriptionally co-regulated (Vaucheret et al. 2006), and the role of AGO1 mediating the RNA silencing pathway has been extensively studied (Baumberger and Baulcombe 2005; Morel et al. 2002; Qu et al. 2008). The putative *Phalaenopsis* AGO1 mRNA was also predicted as an miR168 target gene. Putative targets of miR171 included *HAIRY MERISTEM 3* (HAM3) and other

GRAS family transcription factors involved in meristem differentiation (Stuurman et al., 2002), a protein phosphorylation kinase and an unknown transcript. MiR 394 was predicted targeting *LEAF CURLING RESPONSIVENESS* (LCR), which participated in vascular tissue formation and the auxin mediated signaling pathway (Song et al., 2012) (Table 5).

MiR5139, miR528 and miR535 were less conserved and have been identified in few species. MiR5139 was first identified in *Rehmannia glutinosa* (Yang et al., 2011) and has not been reported in other plant species to date. One of the potential target genes of miR5139, membrane-associated progesterone binding protein 2 (MAPR2), was predicted to have oxidation reduction activity. Studies have reported some putative target genes of the monocot-specific miR528 function in transport, mitosis, or RNA editing in rice and *Arabidopsis* (Cheng et al., 2003; del Pozo et al., 2010; Li et al., 2010.), including HUA1 (Cheng et al., 2003) and histone H2A (Deal et al., 2007) which are involved in flower development pathways. Another study on *P. aphrodite* also predicted miR528 may target to HUA1 genes based on searching a local database (An and Chan, 2012). However, a chloroplast localized tubulin-folding cofactor E was the only target predicted for miR528 in this study (Table 5).

Of the seven ORSV infection responsive miRNAs, miR535 has the largest number of predicted targets. The roles of these target genes could be categorized into signaling or stress response [Glutathione S-transferase family protein, SPX domain-containing zinc finger protein, *SORTING NEXIN 2B* (SNX2B)], protein phosphorylation [protein kinase, plastid-lipid associated PAP/fibrillin family protein], metabolic processes [Ferredoxin 1 (FD1), NagB/RpiA/CoA transferase-like superfamily protein, *MYO-INOSITOL POLYPHOSPHATE 5-PHOSPHATASE 1* (IP5P1)], cellular

development [*IRREGULAR XYLEM 9 HOMOLOG* (I9H), pentatricopeptide repeat (PPR-like) superfamily protein, *UREIDE PERMEASE 2* (UPS2), NAC domain containing protein 47 (NAC047)], and other unassigned genes (Table 5).

3. Analyses of small RNAs from CymMV and mixed infected *P. amabilis* by deep sequencing

In addition to ORSV, CymMV is the other important *Phalaenopsis*-infecting virus. Moreover, synergistic effects between ORSV and CymMV have been reported in double infections (Ajjikuttira et al., 2005; Hu et al., 1998). To analyze the differences between vsRNA profiles from taxonomically distinct CymMV and ORSV, and the impact of synergism over small RNA profiles, small RNAs in CymMV and doubly infected tissues were then subjected to deep sequencing. Similar to the previous method used for ORSV inoculation assay, *P. amabilis* plants were tip-inoculated, and inoculated and non-inoculated tissues were designed to be harvested separately for RNA purification.

3.1. Analysis of CymMV and mixed infection

Similar to ORSV inoculation, no clear symptom was observed on leaves singly infected with CymMV at 10 dpi in Cc and Ci tissues (Fig. 20A). Tissue blotting revealed about half of inoculations (32 out of 60 leaves) resulted in CymMV accumulation confined to the inoculated area only at 10 dpi (Fig. 20A-Ci/Cc and data not shown), while the other half of the inoculation caused the CymMV infection to move into the non-inoculated area (data not shown). As shown in Fig. 20A, only the former tissues were then harvested from inoculated and non-inoculated areas for RNA purification, and designated as Ci and Cc, respectively. Leaves with CymMV infection

spreading to non-inoculated areas were excluded from further study.

While singly infected leaves were symptomless, chlorotic lesions and ringspots appeared in mixedly infected leaves but these were restrained in inoculated areas (Fig. 20A-Di/Dc). As revealed by tissue blotting, ORSV infection in mixed inoculated leaves was only detected in inoculated areas of all 60 inoculated leaves (Fig. 20A-Di/Dc and Dsi/Dsc), similar to ORSV single infection (Fig. 7). In contrast, enhanced CymMV spreading was observed in mixed infected leaves, CymMV infection was detectable by tissue-blotting in non-inoculated areas of 54 out of 60 leaves. These leaves were harvested and designated as Di and Dc indicating tissues from its inoculated and non-inoculated areas, respectively (Fig. 20A-Di/Dc). For the other six mixed inoculated leaves with CymMV infection confined to the inoculated area, the inoculated and non-inoculated tissues were harvested and designated as Dsi and Dsc, respectively (Fig. 20A-Dsi/Dsc).

As shown in Fig. 21, northern blot revealed much higher CymMV viral RNA accumulation in Di than in Ci, suggesting enhanced CymMV titer during co-infection with ORSV (Fig. 21). Although CP sgRNAs were produced during CymMV infection, more genomic RNAs (gRNA) accumulated than sgRNAs (Fig. 21A), consistent with previous studies by Lu et al (2007 and 2009). Accordingly, higher amounts of CymMV vsRNAs were detected by small RNA northern blot in Di than in Dc or Ci tissues, indicating levels of vsRNAs were associated with virus accumulation in infected tissues (Fig. 21A). RT-PCR assay further revealed virus infection was also detected in Cc and Dsc (Fig. 20B), which had been undetectable using tissue-blotting and northern blot, indicating the viruses had started invading these tissues at the initial stage of infection.

However, there was no significant difference in ORSV accumulation with high

levels of CP-sgRNA expression in doubly infected tissues compared to ORSV single inoculations. Like CymMV vsRNA, higher ORSV vsRNA was detected in Di than in Dc (Fig. 21B). RT-PCR also revealed ORSV infection in Dc and Dsc (Fig. 20B), which had been undetectable by hybridization blots. Thus, in doubly infected leaves, early and late stages of CymMV and ORSV mixed infections could be distinguished in Dsc and Di tissues, whereas Dc represented a common phenomena in which tissues accumulated high titer of CymMV while ORSV infection remained only at the initial stage.

3.2. Deep sequencing of small RNAs from CymMV and mixed infected *P. amabilis*

Small RNA libraries of Mi-2, Mc-2, Ci, Cc, Di, Dc, and Dsc tissues were constructed by multiplexed Solexa sequencing as described. Separating a total 37,216,683 reads into seven libraries, about 94.7% to 97.3% were usable reads with recognizable adapter sequences. After filtering poly-A/T/C/G tags, poor-quality N (null) base-calling containing reads, and selecting sizes within the range of 15 to 27 nt, 4,853,176 (Ci), 5,471,939 (Cc), 5,183,147 (Di), 5,126,864 (Dc), 4,960,095 (Dsc), 5,093,963 (Mi-2), and 4,964,619 (Mc-2) clean reads (Table 6) representing 1,369,862 (Ci), 1,449,080 (Cc), 1,090,673 (Di), 1,139,151 (Dc), 1,315,318 (Dsc), 1,243,341 (Mi-2), and 1,122,813 (Mc-2) unique reads (tags) were retrieved (Table 7). Overall, the most prevalent tags were 24 nt in length and proportioned to over 50% of total unique reads (Fig. 22A). For the redundant reads, 21 nt sequences were predominant in all libraries, followed by the 24 nt sequences (Fig. 22B). However, the predominance of the 21 nt class was biased from a super-abundant miR166 tag (as later described in Section 3.4.1.). Nonetheless, the percentage of 24 nt reads was overwhelmingly lowered due to the much lower number of 24 nt tags in the Di library (Fig. 22A). After filtering low

frequency tags (with only one read count among libraries), reads were further annotated as described and categorized into microorganism contaminants, vsRNAs, mRNA fragments, non-coding structure RNAs, miRNAs, and others (Tables 6-7).

3.3. Characteristics of vsRNAs in CymMV and doubly infected tissues

3.3.1 VsRNA populations in singly and doubly infected tissues

CymMV and ORSV vsRNAs were identified after searching against the viral genome of both viruses. About 5.83% (190,786 reads) and 0.02% (858 reads) total annotated reads in the Ci and Cc libraries, respectively, were perfectly matched to the CymMV genome, corresponding to different stages of infections in these tissues (Table 6 and Fig. S3).

Compared to singly infected tissues, CymMV vsRNAs accumulated to reach a higher amount in doubly infected tissues, with 27.90% (1,082,211 reads) and 7.82% (283,087 reads) of total annotated reads in Di and Dc, respectively. ORSV vsRNAs were proportioned to 13.27% (514,758 reads), exhibiting about a 2-fold lower amount compared to CymMV vsRNAs in the Di library. An even larger gap between proportions of CymMV and ORSV vsRNAs was evident in Dc tissues, since only 0.01% (294 reads) of total annotated reads were identified as ORSV vsRNAs. The enrichment of CymMV vsRNAs again demonstrated synergistic enhancement of CymMV replication. For Dsc tissues in which virus infections were undetectable by tissue-blotting and northern blot assays, the ORSV and CymMV vsRNAs contributed only to <0.01% of total annotated reads (Table 6 and Fig. S3).

3.3.2. Characteristics of vsRNAs in CymMV and double infected tissues

The size distribution, strand polarity, and 5'-end nucleotide preference of CymMV and ORSV vsRNAs were then analyzed. In the Ci and Cc libraries, which represented CymMV singly infected tissues, CymMV vsRNA of 21 nt (~61.2 to 63.5%) was predominant, followed by the 22 nt class (~18.3 to 22.3%) (Fig. 23-Ci/Cc). Size distribution of CymMV and ORSV vsRNAs in doubly infected tissues (Di, Dc, and Dsc) displayed similar patterns, with 21 nt as the predominant size class (~56.7 to 62.3% for CymMV vsRNAs and ~50.4 to 53.9% for ORSV vsRNAs) and 22 nt as the second most abundant (~13.3 to 22.3% for CymMV vsRNAs and ~12.2 to 15.6% for ORSV vsRNAs) (Figs. 23-24, Di/Dc/Dsi).

In regard to strand polarity, sense-stranded CymMV vsRNA proportioned to 70.3% and 73.4% in the Ci and Cc libraries, respectively (Fig. 23-Ci/Cc). Similar ratios of (+)-stranded vsRNAs were observed in the Di, Dc, and Dsc libraries, accounting for about 71.4 to 73.4% of total CymMV vsRNAs (Fig. 23-Di/Dc/Dsi), and about 57.9-64.8% of total ORSV vsRNAs (Fig. 24-Di/Dc/Dsi).

After grouping by 5' end nucleotide identity (A, C, G, and U), differential nucleotide preference among 21 to 24 nt vsRNAs was observed. Generally, C- and U-terminated vsRNAs were dominant in the 21 and 22 nt classes, and specifically in the 24 nt class, the proportion of 5'-A vsRNAs was elevated and became dominant (Fig. 25). This pattern was likewise observed in the Ci, Cc, Di, and Dc libraries, and regardless of CymMV or ORSV origins in the Di and Dc libraries. With the exception of the Dsc library, a more drastic nucleotide preference was observed, however, it seemed biased from low vsRNA reads (Figs. 25-Dsc and 26-Dsc). Moreover, this pattern was inconsistent with ORSV singly infected tissues (Oi and Oc) in which ORSV vsRNAs

possessed an even distribution of 5'-A, C, and U in the 21 to 24 nt classes (Fig. 12). Nonetheless, CymMV and ORSV vsRNAs were always less frequently 5'-G, regardless of size classes in all libraries (Figs. 25-26).

Collectively, the prevalence of 21 and 22 nt size classes and (+)-stranded polarity was found for both CymMV and ORSV vsRNAs in all libraries, indicating these features differed little between the two viruses, and were also not much affected under mixed infection. In double infections, the 5'-end nucleotide preference remained unchanged for CymMV vsRNAs, but not for ORSV vsRNAs.

3.3.3. Genome mapping and coverage of CymMV vsRNAs

To study the distribution of vsRNA origins along virus genomes, vsRNAs were mapped along each polarity of the CymMV and ORSV genome according to the 5'-end sites. Including both sense- and anti-sense stranded and all sizes of vsRNAs, the genome coverage was up to 91.04% and 98.81% for CymMV and ORSV vsRNAs in the Di library, respectively, suggesting widespread targeting of DCL enzymes. The CymMV vsRNA distribution along the CymMV genome extensively encompassed the RdRp-coding region, and obviously was seldom located in the TGBp- and CP-coding regions (Fig. 27). The distribution of CymMV vsRNA origins was less affected by co-infection with ORSV. Northern blot hybridization confirmed the accumulation of nt 2404 to 3703 RdRp region-originated CymMV vsRNAs in Ci, Di, and Dc tissues (Fig. 21A). The enrichment of the near 5' region vsRNAs possibly reflected that more CymMV genomic RNA accumulated in these tissues, as northern blot revealed (Fig. 21A).

3.3.4. Specific ORSV vsRNA hotspots occurred in mixed infected tissues

While CymMV vsRNA hotspot distribution displayed resemblance to singly infected CymMV tissues and co-infected CymMV with ORSV tissues (Fig. 27), a sharp difference in ORSV vsRNA hotspots was observed in the Di and Dc libraries (Fig. 28) compared to ORSV singly infected tissues (Oi and Oc, as previously described) (Fig. 13). ORSV vsRNAs originated around (-)-strand nt 2640 to 2680, 2240 to 2280, and 4150 to 4180(9680) RdRp regions, comprising three prominent peaks (Fig. 28). The major vsRNA tags of these peaks were proportioned to 0.99% (5118 reads), 1.43% (7377 reads) and 1.88% (9680 reads) total ORSV vsRNA pool in the Di library, respectively. Similar peaks were also observed in the Dc library (Fig. 28). Interestingly, the hotspot tags were also sequenced in the ORSV singly inoculated (Oi) library, but contributed to a much lower percentage than in doubly infected tissues, specifically, 0.01% (158 reads), 0.10% (2542 reads), and 0.12% (2865 reads) for the three topmost tags, respectively. The enrichment of these tags in the Di and Dc libraries indicating DCL accessibility to ORSV viral RNA may be affected under co-infection with CymMV.

3.3.5. Prediction of potential *P. amabilis* target transcripts of vsRNAs

Based on the sequence homology, previous research has suggested vsRNA induced symptoms form through RNA silencing mediating host mRNA degradation (Navarro et al., 2012; Shimura et al., 2011). To search transcripts that could be targeted by CymMV or ORSV vsRNAs, some vsRNA tags were aligned to the reverse complementary of *P. aphrodite* EST sequences. Assuming tags with prevalent reads may have a higher chance of impacting expressions of target genes, the search was focused on the 50 most

abundant reads in the Oi, Ci, Di, and Dc libraries (Tables S3-S4). Moreover, since the necrotic symptoms only appeared in the Di tissues at 10 dpi, tags with over 50 reads and those only sequenced in the Di library were also subjected to target prediction (Tables S5-S6).

After the permissive alignment search, a position-dependent scoring matrix and MFE ratio criteria were applied to candidate vsRNA:mRNA duplexes following the method described by Allen et al., 2005. The search resulted in 78 and 48 potential targets for the 50 most abundant CymMV and ORSV vsRNAs, respectively. Of these, 49 of the CymMV and 42 of the ORSV vsRNA targets were genes predicting coding annotated proteins. Regarding the Di specific vsRNAs, 125 (88 were annotated contigs) transcripts were matched to CymMV and 22 (14 were annotated contigs) transcripts were matched to ORSV vsRNAs. The functional annotations of potential targets of Di specific CymMV vsRNAs were found to be significantly enriched ($P < 0.001$) in annotations of protochlorophyllide oxidoreductase activity, and endopeptidase activity, and chlorophyll biosynthetic process. The annotations of molecular functions of ORSV vsRNA targets were significantly enriched ($P < 0.001$) in ligase activity and substrate-specific transporter activity, and also enriched in biological functions such as sexual reproduction, multicellular organism reproduction, and response to biotic stimulus.

The matches of ORSV vsRNAs include ureide permease 2, ribosomal L38e protein, eukaryotic translation initiation factor (eIF) 2 beta subunit, putative cellular apoptosis susceptibility protein, UDP-glycosyltransferase superfamily protein, flavin-dependent monooxygenases (FMO) and other oxidoreductases or kinases. (Tables 8-9). CymMV vsRNAs were perfectly matched to geranyl diphosphate synthase, aspartokinase, and the

26S ribosomal RNA gene. Other potential targets included RNase III-like enzyme, chloroplastic glutaminyl-tRNA synthase, xyloglucan galactosyltransferase, abscisic acid response protein, serine/threonine kinase, light-dependent NADPH:protochlorophyllide oxidoreductase and other enzymes. (Tables 10-12).

3.4. Identification and analysis of conserved miRNAs in CymMV and mixed infected *Phalaenopsis amabilis*

3.4.1. miRNA populations

Known miRNAs were annotated using BLASTN search against miRBase with a tolerance of up to three mismatches. Again, the super-abundant miR166 tag was sequenced and contributed to an even higher proportion. This time, the super-abundant tag contributed to over 80% total miRNA reads and was proportioned to about 17 to 31% of total clean reads among the seven libraries (Table S7). The overwhelming preponderance of this miR166 tag was again inconsistent with qRT-PCR validation (data not shown). With the miR166 tag, conserved miRNAs were proportioned to about 21 to 36% of total clean reads within each library (Tables 6 and S7). The percentage dropped to about 4 to 6% after the miR166 tag was removed (Table S7). Nonetheless, 104,797 unique miRNA sequences corresponding to 154 families were identified in the seven libraries. The number of members within each family ranged from one to hundreds of species. The largest family was miR166, with 392 members identified (Table 13). Regardless of whether it was a single or mixed infection, the categories of miRNA families and members within each family remained similar in the different libraries (Table 7).

3.4.2. Differential expressions and predicted targets of CymMV and double infection responsive miRNAs

The expression levels of miRNA families between libraries as described were compared. In brief, read counts were normalized with miRNA pool sizes and converted to TPM for calculating the FC index between inoculated (Ci, Di), non-inoculated (Cc, Dc, Dsc) and mock-inoculated (Mi, Mc) tissues (Table 14). With a threshold of 1.5-fold, stem-loop qRT-PCR results and statistical analysis supported the up regulation of miR156, miR168, miR319 and miR5139 in inoculated tissues. MiR156 and miR168 were induced in Ci, Di, and Dsi tissues, whereas the induction of miR319 and miR5139 expression was only observed in the Di library (Table 14 and Fig. 30). Repressed expressions were observed in miR398, miR408, miR528 and miR535. The down regulation of miR398, miR408, and miR528 reached a greater extent, especially in Dsc and Dsi tissues (Table 14 and Fig. 30).

Target prediction was next performed with the focus on validated infection responsive miRNAs as described. The prediction for miR156, miR168, miR5139, miR528 and miR535 was shown in Section 2.4.3. After searching against *P. aphrodite* contigs, 18 potential targets were predicted for miR396, 11 for miR319, 5 for miR408, 2 for miR393, 1 for miR394, and miR162, miR169, miR398 each with three matches (Table 15). Moreover, none of the *Phalaenopsis* transcript was matched to miR894 sequences, thus the target remained unknown. Integrating the prediction results, the potential target genes can be grouped into two major categories based on the functional annotations. First, several targets were involved in ABA, GA, and auxin mediated pathways and other signaling cascades, such as *NUCLEAR FACTOR Y A5* (NFYA5), *CYCLOIDEA AND PCF TRANSCRIPTION FACTOR* (TCP) and MYB domain protein,

TRANSPORT INHIBITOR RESPONSE 1 (TIR1), *LEAF CURLING RESPONSIVENESS* (LCR), and Phox-associated domain protein. Second, *SUPPRESSOR OF VARIATION 3* (SVR3) and ABA 8'-hydroxylase targeted by miR396, *COPPER/ZINC SUPEROXIDE DISMUTASE 2* (CSD2) targeted by miR398, and *LACCASE 3* (LAC3) targeted by miR408 were involved in oxidation processes and other metabolic pathways (Bueno et al., 1995; Yu et al., 2008). Other targets including genes functioning in developmental regulation such as plantacyanin (targeted by miR408) and PAUSED (PSD) karyopherin (targeted by miR396) played roles in vegetative and reproductive phase transition (Dong et al., 2005; Li and Chen, 2003; Ranocha et al., 2002) (Table 15). Of the predicted targets, CSD2 has been proven to be an important antioxidant enzyme that can scavenge reactive oxygen species (ROS) in *A. thaliana* (Jones-Rhoades and Bartel, 2004; Sunkar et al., 2006). The plantacyanins were associated with programmed cell death and callose deposition processes in pollen development (Dong et al., 2005), and have also been designated as stress-related proteins mediating lignin polymerization, which are thus involved in plant defense responses (Hampton et al., 2004; Nersissian et al., 1998). The target prediction revealed a broad spectrum of cellular processes potentially involved in the plant responses to virus infection.

Discussion

This study aimed to profile the small RNAs from CymMV and ORSV singly or doubly infected orchid tissues by Solexa deep sequencing. Using the leaf tip-inoculation method, two stages of infection, early and late, were distinguishable in non-inoculated and inoculated tissues. The characteristics of vsRNAs and their expressions under viral stress were further analyzed by bioinformatics. Target prediction provided information about possible roles of infection responsive small RNAs in plant-virus defense and counter-defense interactions.

1. Synergistic enhancement of CymMV infection by ORSV co-inoculation in *Phalaenopsis amabilis*

In double inoculation assays, synergistic effects were observed between CymMV and ORSV. First, chlorotic lesions and ringspots were noticed around 7 dpi and continued enlarging afterwards in mixed inoculated tissues (Fig. 20 and data not shown), consistent with previous studies reporting synergism between CymMV and ORSV and intensified symptoms in doubly infected plants (Hadley et al., 1987; Lawson and Brannigan, 1986; Pearson and Cole, 1991). Second, northern blot analysis revealed enhanced CymMV titer (Fig. 21A) as well as about 5-fold accumulation of CymMV vsRNAs in doubly inoculated tissues (Di) compared to singly inoculated tissues (Ci). In contrast, the viral titer of ORSV did not increase in Di tissues by CymMV co-infection and was non-detectable with northern blot in Dc tissues (Fig. 21B). The lower ORSV titer in Di than in Oi (Fig. 21B) may be due to lower amount of virions as inoculum (1 μg for the single inoculation and 0.5 μg each in the double inoculation). Previously, Hu

et al. reported that accumulation of both CymMV and ORSV progeny RNA were increased in *Dendrobium* protoplasts, and, in particular, the accumulation of ORSV viral RNA reached a peak earlier in double infections than when infected with ORSV alone (Hu et al., 1998). Likewise, the acceleration of ORSV genomic RNA accumulation was observed in mixed-infected *N. benthamiana* (Ajjikuttira and Wong, 2009). The results in this study was contradict to both reports. This discrepancy may be due to different host species, virus strains or the experimental systems used in individual studies. Different adaptability of CymMV and ORSV in *P. amabilis* should also be taken into consideration when interpreting these results.

Finally, accelerated spreading of CymMV in doubly infected tissues was found in this study. In contrast, spreading of ORSV was less affected by co-inoculation. Thus enhanced viral titer may facilitate the faster spreading of CymMV. In addition, the molecular interactions between CymMV and ORSV may also aid in viral movement. Ajjikuttira et al. (2005) proved the MPs and CPs were functionally interchangeable between CymMV and ORSV, facilitating movement of these viruses in plants, with the exception of long-distance movement of ORSV RNA by CymMV CP. CymMV CP may play a dominant role in determining the host range as suggested by Lu et al. (2009) since a CymMV strain that infected *Phalaenopsis* but failed to accomplish systemic infection in *N. benthamiana*. In this study, the CymMV strain used for inoculation assays could not systemically infect *N. benthamiana* (data not shown). Perhaps the movement of ORSV was not greatly facilitated under double inoculation with this CymMV strain, and consequently, CymMV benefitted more than ORSV from the synergistic interactions.

2. The leading roles of DCL4 and DCL2 in *P. amabilis*

Characteristics of vsRNAs analyzed through deep sequencing profiles could contribute to deciphering the host defense mechanism. The size distribution of vsRNAs is an indicator of activities of multiple DCL proteins. Most of vsRNAs are 21- and 22-nt through processing of DCL4 and DCL2, respectively, as well established in *A. thaliana* (Blevins et al., 2006). The previous studies as well as the present results support this finding. RNA viruses from different families, such as TMV (Qi et al., 2009), CMV, MNSV, PMMoV, PVX, TRV, TuMV, TYLCV, WMV (Donaire et al., 2009), generated more 21 nt vsRNAs. In *P. amabilis*, ORSV and CymMV vsRNAs were mainly 21 nt, followed by 22 nt class (Figs 11, 23, and 24), mirroring the conserved roles of DCL4 and DCL2 homologs in *P. amabilis* antiviral RNA silencing, as in many other plants. In addition, our results showed similar size distribution patterns between inoculated and non-inoculated tissues, and these also remained unchanged in singly and doubly infected tissues. These data indicate the leading role of DCL4 homologs in *P. amabilis* was activated in the early stage of infection and was not much affected under conditions of mixed-infection.

3. Asymmetrical strand polarity and 5'-end nucleotide identity of CymMV and ORSV vsRNAs

Previous studies suggested vsRNAs were generated from sense and antisense annealed replicative intermediates and long dsRNA synthesized through host RDR activities using viral ssRNA templates (Ding, 2010; Ruiz-Ferrer and Voinnet, 2009; Voinnet, 2005), thus vsRNAs derived equally from positive and negative strands, as observed in *Cucumber yellow virus* (Yoo et al., 2004). However, asymmetrical polarity

of vsRNAs has been reported in several studies and was also profiled in this one. In *P. amabilis*, CymMV and ORSV vsRNAs mainly derived from sense strands of viral genomes and presented consistent asymmetry in strand polarity, both between single and double infections, and also regardless of late or early stages of infection (Figs 11, 23, and 24). For other viruses, more positive stranded vsRNAs were cloned in plants infected with TuMV (Ho et al., 2007), TCV (Ho et al., 2006), TMV (Qi et al., 2009), PVX, CymRSV (Molnar et al., 2005), or *Cotton leafroll dwarf virus* (Silva et al., 2011). In contrast, vsRNAs of several grape viruses such as GFkV, GRGV, and GAMaV have been profiled revealing a predominance of antisense polarity (Pantaleo et al., 2010). Collectively, these data imply vsRNAs may not solely be processed from long dsRNA templates, consistent with studies suggesting self-annealing hairpin structures formed from complementary sequences within viral ssRNA served as templates for vsRNA biogenesis (Moissiard and Voinnet, 2006; Molnár et al., 2005).

While the size distribution and strand polarity were similar for CymMV and ORSV vsRNAs, one major difference between the vsRNA of these two viruses was found in the 5'-end nucleotide composition. ORSV vsRNA generally showed a modest preference for 5'-A and 5'-U among 21 to 24 nt classes in single infections (Fig. 12), similar to vsRNAs of CMV, CymRSV, MNSV, PMMoV, PVX, TRV, TuMV and WMV (Donaire et al., 2009). In contrast, CymMV vsRNA had a strong tendency to be terminated with 5'-C or 5'-U among 21 to 23 nt species (Fig. 25), resembling GRSPaV (Pantaleo et al., 2010) and *Citrus tristeza virus* (CTV) (Ruiz-Ruiz et al., 2011). Nonetheless, this study observed a common feature of underrepresented 5'-G in both CymMV and ORSV as well as many other viruses reported (Donaire et al., 2009; Pantaleo et al., 2010; Ruiz-Ruiz et al., 2011). Since the 5'-end nucleotide identity is a

key determinant for sorting vsRNAs to associate with distinct AGO proteins (Mi et al., 2008), which have different affinities for binding small RNAs with 5'- U (AGO1), A (AGO2 and AGO4), and C (AGO5) (Mi et al., 2008; Montgomery et al., 2008; Takeda et al., 2008), thus the 5'-A and U preferred ORSV vsRNA may be recruited into AGO1, AGO2, and AGO4, whereas CymMV vsRNAs may preferentially bind to AGO1 and AGO5. Furthermore, the absence of known 5'-G preferred AGO species may explain the avoidance of 5'-G vsRNAs (Donaire et al., 2009).

The nucleotide preference did not solely represent the base composition of viral genomes [U(30.76%)>A(29.81%)>G(21.64%)>C(17.79%) for ORSV and C(29.16%)>A(26.44%)>T(24.67%)>G(19.73%) for CymMV]. The different preferences of 5'-terminal nucleotide among different size classes observed in CymMV vsRNAs was a special feature, compared to other plant viruses. In addition, the proportion of 5'-A was also elevated in the 24 nt class of ORSV vsRNAs in mixedly infected tissues (Fig. 26). In this case, unknown factors specific to CymMV may be involved in the enrichment of 5'-A in the 24 nt class, and possibly affect ORSV vsRNA generation or stabilization in the mixed infections. Moreover, the 5'-A preference of 24 nt vsRNAs seemed to coincide with features of plant endogenous small RNAs which are involved in RNA-dependent DNA methylation (RdDM) pathways (Molnar et al., 2010). Since CymMV is a cytoplasmic replicated RNA virus, further analysis is needed to determine how the 24-nt vsRNA was generated and whether these vsRNAs could be incorporated into AGO4 and act in the mode of RdDM machinery.

4. Differential distribution of CymMV and ORSV vsRNA along viral genomes

One substantial difference between the characteristics of CymMV and ORSV

vsRNAs was the vsRNA origin along viral genomes. In singly infected tissues, more hotspots resided in the RdRp coding region of CymMV and the CP to 3'-UTR region of the ORSV genome, respectively (Figs. 13, 27, and 28). This discrepancy may be due to higher accumulation of ORSV CP-expressed subgenomic RNA and of more abundant CymMV gRNAs in the infected *P. amabilis* tissues as shown in northern blot (Figs. 8 and 21A). This may be a possible explanation as to why more vsRNAs originated from different genome sites for CymMV and ORSV.

In ORSV singly infected tissues (Oi and Oc), a specific hotspot located in 3'-UTR of the ORSV genome was found With some interesting features. First, it was constituted by one specific tag and mainly from sense strands. Second, though three consecutive homologous regions reside in the PK chain of ORSV 3'-UTR, the hotspot only peaked at the lattermost repeat, but not at the other two upstream homologous sequences. Last, modelling of the 3'-UTR secondary structure by Gultyaev et al. (1994) revealed the hotspot vsRNA resided in the first PK structure upstream to the TLS (Fig. 15), which was not a typical double stranded structure expected to be preferentially cleaved by DCL enzymes. These features suggested that the accessibility of DCL enzyme dicing at the hotspot was not merely based on the primary sequence or secondary structures, and may involve other determinant factors although the abundant hotspot vsRNAs were generated within the positive strand. Furthermore, it has been demonstrated that the highly structured PK chain and TLS ends are critical for tobamovirus replication and protein translation (Zeenko et al., 2002). However, overexpression of the hotspot vsRNA failed to interfere with ORSV replication in the co-transfection assay. Similarly, mutations in *Zucchini yellow mosaic virus* (ZYMV) at the loci of hotspots did not break the resistance in hotspot vsRNA expressing transgenic plants (Leibman et al., 2011).

Thus whether hotspot vsRNAs could confer efficient targeting and clearing of viral RNAs remains unknown.

While the genomic distribution of CymMV vsRNA hotspots in single and double infections resembled each other, in contrast, three prominent hotspot peaks resided in the negative polarity of the ORSV genome specifically in doubly infected tissues. The presence of unique ORSV vsRNA hotspots after co-infection with CymMV may be due to changes in the ORSV viral RNA folding structure, or other factors affecting DCL accessibility in interaction with CymMV.

5. VsRNA-mediated host gene silencing may underly the mechanism of symptom formation

Since viral symptoms appeared only in Di tissues, combined with presence of unique ORSV vsRNA hotspots under double infection, it raises the possibility that the disease phenotypes are associated with vsRNA-mediated RNA silencing of host genes. Navarro et al. (2012) have shown that targeting of a chloroplastic heat shock protein coding gene by viroid-derived siRNAs resulted in chloroplast malformation and finally induced albino patches on the leaves. Similarly, silencing based interference with a chlorophyll synthesis gene was the underlying mechanism of yellowing symptoms induced by co-infection of Y satellite with CMV (Shimura et al., 2011). Our study predicted some potential *Phalaenopsis* targeting genes of ORSV and CymMV vsRNAs. Among the predicted targeting genes, eukaryotic translation initiation factors (eIFs), pectin methyltransferase 1 (PME1), serine/threonine kinase, protochlorophyllide oxidoreductase and several others were specifically noted (Tables. 8-12). For example, eIFs participate in assembling ribosomal subunits which are competent for protein

synthesis (Browning, 2004). Of these, eIF1 was induced upon salt stress and conferred tolerance to salinity via regulating redox status (Diédhiou et al. 2008; Sun and Hong, 2012). Serine/threonine kinase is a large family characterized by protein phosphorylation activity (Hardie, 1999) and several members are reported to be involved in defense responses (Afzal et al., 2008; Rodriguez et al., 2010). Cytochrome P450 and UDP-glucuronosyltransferase are involved in calibrating xenobiotics and secondary metabolites (Osami et al., 2008; Sawada et al., 2005). Depressed cytochrome p450 expression has been observed in iron deficient soybeans and may be related to the chlorotic phenotype (O'Rourke et al., 2008). Collectively, targeting of these genes may interfere with the metabolism pathway and possibly contribute to symptom formation. It will be interesting to investigate whether these targets can indeed be dysregulated by vsRNAs.

6. Roles of infection responsive miRNAs in *Phalaenopsis*-virus interactions

In addition to vsRNAs, there were some miRNAs involved in priming responses to CymMV and ORSV infections. Twelve miRNA families, namely miR156, miR162, miR168, miR169, miR171, miR319, miR393, miR394, miR396, miR398, miR408, miR5139, miR528, miR535 and miR894, were validated in response to virus infection in *P. amabilis* (Figs. 18, 19, 30, and 31). These miRNAs are conserved among several plant species and have been reported to respond to viral stresses in other plants. Among these, increased expression of miR168 was generally observed in plants infected with viruses belonging to diverse families, such as CymRSV (Várallyay et al. 2010), *Oilseed rape mosaic virus* (ORMV)(Hu et al., 2011), PVX (Lang et al., 2011), *Sun-hemp mosaic virus* (shMV), TMV (Bazzini et al., 2011), *Tomato aspermy virus* (TAV) (Feng et al.,

2009), and different strains of CMV (Cillo et al., 2009; Feng et al., 2009). In the present datasets, miR168 was also up regulated in inoculated tissues (Oi, Ci, Di, Dsi), however, not in Dc tissues, which were also detected with high accumulation of CymMV (Table 6 and Fig S3). In this case, the elevated expression of miR168 might be a late response, thus observed only in inoculated tissues and not merely correlated to viral titers.

Besides miR168, other arrays of miRNAs showed diverse expression patterns. Previous studies also profiled different trends of expression of these miRNAs under infections of different viruses, or even in different stages of infection. For instance, while miR162 and miR396 were up regulated and miR169 down regulated upon *Watermelon mosaic virus* (WMV) or *Melon necrotic spot virus* (MNSV) infections (Gonzalez-Ibeas et al., 2011), a reverse expression pattern of these miRNAs in PVX or CMV infected plants (Lang et al., 2011). Bazzini et al. reported a dynamic variation of miRNA expression in different stages of TMV infection, and suggested several miRNAs might undergo biphasic changes. Among them, miR156, miR168, miR171, miR398, and miR535 were down-regulated first at 5 dpi then up-regulated at 15 and 22 dpi. In contrast, the expression of miR408 was enhanced in the initial stage, but turned out to be repressed at later stages (Bazzini et al., 2011). These infection responsive miRNAs participate in multiple aspects and processes, such as the involvement in hormone and metabolite assimilation of miR393 and miR408 (Bazzini et al., 2011; Lang et al., 2011), the involvement of miR172 in signal transduction (Lang et al., 2011), and the involvement of miR169, miR398, and miR528 in calibrating ROS stress (Jagadeeswaran et al., 2009; Li et al., 2010). MiR156 and miR319 play regulatory roles through their impact on several transcription factors or promoters (Bazzini et al., 2007, Bazzini et al., 2009; Lang et al., 2011), and may consequently mediate symptom

formation (Bazzini et al., 2007; Naqvi et al., 2010).

In this study, though some miRNAs showed in response to CymMV and ORSV infection, as indicated by deep sequencing analysis and later validated with qRT-PCR, fold changes were not great in most tissues. Higher variations were observed in Dsi and Dsc tissues which represented relatively early infections with CymMV and ORSV (Table 14 and Figs. 30 and 31). However, the qRT-PCR data for Dsi and Dsc tissues presented large standard variations and should be further confirmed. It is possible that the infections in inoculated tissues had not reached the severe stage at 10 dpi though viral RNAs and vsRNAs did accumulate. Perhaps the miRNAs were not directly involved in virus replication, thus their expression was largely unaffected. Also, the array of conserved miRNAs mainly participate in developmental processes, drastic dysregulation of these miRNAs was often observed in plants possessing severe symptoms in other studies, but not in the symptomless *P. amabilis* infection in this study. With severe infections, the changes in developmental miRNA regulation may occur in signaling cascades and repair systems after cellular damage. The role of these miRNAs in priming defense responses at an early stage of infection remain obscure. In addition, conserved miRNAs may regulate expression of novel targets in different plant species. For instance, *in silico* analysis revealed that a NBS-LRR protein encoding gene may be targeted by miR156 in flax (Barozai, 2012). This study also predicted several potential target transcripts specifically residing in *Phalaenopsis* (Tables 5 and 15), and their expression under CymMV and ORSV infection remains to be analyzed. Furthermore, VSR activities often result in interference of miRNA pathways (Kasschau et al., 2003). Though the 126-kDa replicase of tobamoviruses (Kurihara et al., 2007; Vogler et al., 2007) and the movement protein of potexviruses (Chiu et al., 2010; Voinnett et al., 2000)

have been described as VSRs, the molecular features of VSRs of CymMV and ORSV have not yet been analyzed and their impact on miRNA accumulation is still unknown.

7. The involvement of novel miRNAs and other small RNAs in response to viral stresses

In addition to conserved miRNAs, potential unidentified novel miRNAs or other classes of small RNAs involved in the interactions between *Phalaenopsis* and viruses could not be excluded. Novel miRNAs have been identified in various plant species (Gonzalez-Ibeas et al., 2011; He et al., 2008; Sanan-Mishra et al., 2009; Yao et al., 2007). Since different plants are armed with various anti-virus mechanisms, specific controlling modes residing within diverse species is expected. For example, miR1885 was identified as a novel miRNA in *Brassica rapa* and mediated *R* gene based resistance to TuMV infection (He et al., 2008). The tolerance of *Phalaenopsis* to CymMV and ORSV infections may possibly be mediated by unidentified novel miRNAs.

Besides miRNAs, other plant endogenous small RNAs also play important roles in regulation of plant development and morphogenesis, such as trans-acting siRNAs (ta-siRNAs). Recent studies revealed several abnormal phenotypes in ta-siRNA mutants resemble viral symptoms, and viral infections indeed interfered with ta-siRNA pathways. For example, misregulation of ta-siRNAs and its target gene AUXIN RESPONSE FACTOR3 (ARF3) and ARF4 programmed shoestring leaf syndrome in tomato mutants (Yifhar et al., 2012). Rescued ta-siRNA pathways in Potyviral VSRs Hc-Pro deficient *Zucchini yellow mosaic virus* (ZYMV) infected plants exhibited a recovery phenotype, thus demonstrating interference with ta-siRNA functioning was involved in symptom

development and pathogenicity in natural infections (Wu et al., 2010). Furthermore, 24-nt siRNAs mediating RdDM machinery were also reported to be affected under virus invasion (Góngora-Castillo et al., 2012; Matzke et al., 2009). For instance, a dramatic decrease of 24-nt small RNA was observed in peanut witches-broom (PnWB) phytoplasma infected periwinkle, and resulted in chloroplast development in the phyllody of diseased floral organs by reactivating some methylated genes (曾, 2011). The drastic reduction of 24 nt small RNAs in lesion-formed doubly infected tissues (Di) was observed in this study (Fig. 22), possibly underlying 24-nt siRNA mediated symptom formation mechanisms.



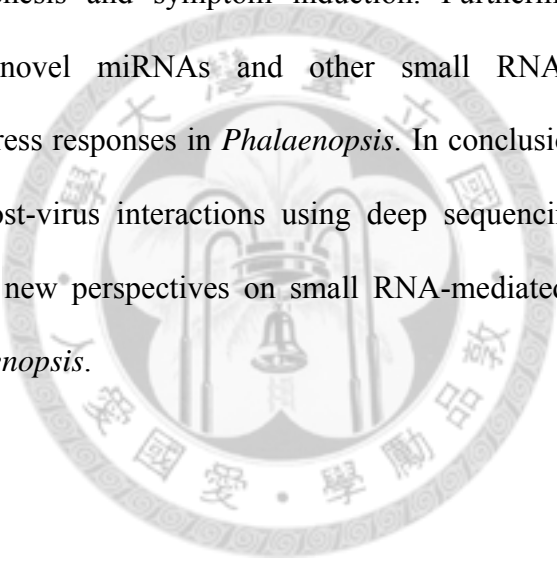
Conclusion and Future Directions

This study used Solexa-based deep sequencing to profile the small RNA pools in CymMV and ORSV infected *P. amabilis*. The purpose of this study is to elucidate the underlying mechanism of antiviral RNA silencing in *Phalaenopsis*, and to quantitatively compare small RNAs under conditions of CymMV and ORSV single and double infection. In addition, early and late stages of infection were determined in order to search for infection responsive small RNAs in the initial stage of infection. Overall, intensified symptoms and accelerated CymMV spreading were observed in double inoculations, along with higher viral titer, reflecting a synergistic effect between CymMV and ORSV. The elevated proportions of CymMV vsRNAs in mixed-infected tissues likewise indicated synergism. From the sequencing data, most vsRNA characteristics were less affected by double infection, except for ORSV hotspot vsRNA origins. The 21 and 22 nt dominance of ORSV and CymMV vsRNAs suggest the antiviral RNA silencing mechanisms were mainly mediated by DCL4 and DCL2 homologs in *P. amabilis*, as conserved in many other plants. Asymmetrical strand polarity suggested the vsRNAs were processed from highly structured viral RNAs instead of a long double-stranded precursor. Different 5'-end nucleotide preferences of CymMV and ORSV vsRNAs indicate vsRNAs from different viruses and size classes may be selectively loaded into diverse AGO-containing RISC complexes.

In addition to profiling vsRNAs, the common set of conserved miRNAs reported in response to other viral invasions, such as miR156, miR168, miR319, miR398, miR408, miR5139, miR528, and miR535, was also responsive to CymMV and ORSV infections. The up and down regulation of various miRNAs governed multiple cellular processes

and signaling pathways, and comprised a complicated network of responses to virus infection. Target prediction of infection responsive miRNAs and hotspot vsRNAs provides insight into possible roles of these small RNAs in defense and counter-defense interactions between CymMV, ORSV and *P. amabilis*.

Subjects for further study include the question of whether *P. amabilis* DCLs and AGOs have the same properties as the homologous proteins in *Arabidopsis*, and whether the infection-responsive miRNAs play a leading role in defense mechanisms. It is also worth investigating the possible role of vsRNA-mediated host gene silencing at the heart of pathogenesis and symptom induction. Furthermore, identification of infection-responsive novel miRNAs and other small RNAs will also aid in understanding viral stress responses in *Phalaenopsis*. In conclusion, our study provides initial insight into host-virus interactions using deep sequencing technique. Further analysis will provide new perspectives on small RNA-mediated defense and disease mechanisms in *Phalaenopsis*.



References

- 李岍. 2005. 蝴蝶蘭. p.899-902. 刊於：黃美華等編著. 台灣農家要覽-農作篇(二). 行政院農業委員會. 台北.
- 張清安 2006. 蘭花病毒之診斷、鑑定與偵測. 植物重要防疫檢疫病害診斷鑑定技術研習會專刊(五). 行政院農業委員會動植物防疫檢疫局及國立中興大學植物病理系編印. p.103-118.
- 張清安. 2007. 蘭花種苗病毒檢測與相關產業發展趨勢. 農業生技產業季刊. 9:42-48.
- 陳慶忠、陳煜焜、柯文華、葉士財. 2006. 齒舌蘭輪斑病毒及蕙蘭嵌紋病毒感染蝴蝶蘭之病徵學及細胞病理學探討. 臺中區農業改良場研究彙報 93:15-27.
- 曾欣怡. 2011. 利用高通量定序分析日日春感染植物菌質體其 RNA 及 small RNA 之差異性. 臺灣大學植物病理與微生物學研究所碩士論文.
- 楊玉婷. 2010. 全球蘭花發展現況與未來展望—兼論我國蝴蝶蘭與文心蘭發展策略. 台灣經濟研究月刊. 33:36-41.
- 鄭尤琇、陳慶忠、詹富智. 2008. 台灣蝴蝶蘭之新興病毒病害. 植物重要防疫檢疫病害診斷鑑定技術研習會專刊(七). 行政院農業委員會動植物防疫檢疫局及國立中興大學植物病理系編印. p67-82.
- Afzal, A.J., A.J. Wood, and D.A. Lightfoot. 2008. Plant receptor-like serine threonine kinases: roles in signaling and plant defense. *Mol. Plant Microbe Interact.* 21:507-517.
- Ajjikuttira, P., and S.M. Wong. 2009. Molecular biology of two orchid infecting viruses: *Cymbidium mosaic potexvirus* and *Odontoglossum ringspot tobamovirus*. p.251-277. In: T. Kull, J. Arditti and S.M. Wong (eds.). *Orchid biology: Reviews and perspectives*, X. Springer, Netherlands.
- Ajjikuttira, P., C.S. Loh, and S.M. Wong. 2005. Reciprocal function of movement proteins and complementation of long distance movement of *Cymbidium mosaic virus* RNA by *Odontoglossum ringspot virus* coat protein. *J. Gen. Virol.* 86:1543-1553.
- Altschul S.F., W. Gish, W. Miller, E.W. Myers, and D.J. Lipman. 1990. Basic local

- alignment search tool. *Mol. Biol.* 215:403–410.
- An, F.M. and M.T. Chan. 2012. Transcriptome-wide characterization of miRNA-directed and non-miRNA-directed endonucleolytic cleavage using degradome analysis under low ambient temperature in *Phalaenopsis aphrodite* subsp. *formosana*. *Plant Cell Phys.* 53:1737-1750.
- An, F.M., S.R. Hsiao, and M.T. Chan. 2011. Sequencing-based approaches reveal low ambient temperature-responsive and tissue-specific microRNAs in *Phalaenopsis* orchid. *PLoS One* 6:e18937.
- Angell, S.M. and D.C. Baulcombe. 1997. Consistent gene silencing in transgenic plants expressing a replicating *Potato virus X* RNA. *EMBO J.* 16:3675–3684.
- Aukerman, M.J., and H. Sakai. 2003. Regulation of flowering time and floral organ identity by a microRNA and its *APETALA2*-like target genes. *Plant Cell* 15:2730–2741.
- Barozai, M.Y.K. 2012. *In silico* identification of microRNAs and their targets in fiber and oil producing plant flax (*Linum usitatissimum* L.). *Pak. J. Bot.* 44:1357-1362.
- Baumberger, N. and D.C. Baulcombe. 2005. Arabidopsis ARGONAUTE1 is an RNA slicer that selectively recruits microRNAs and short interfering RNAs. *Proc. Natl. Acad. Sci. USA* 102:11928–11933.
- Bazzini, A.A., H.E. Hopp, R.N. Beachy, and S. Asurmendi. 2007. Infection and coaccumulation of *Tobacco mosaic virus* proteins alter microRNA levels, correlating with symptom and plant development. *Proc. Nat. Aca. Sci.* 104:12157-12162.
- Bazzini, A.A., N.I. Almasia, C.A. Manacorda, V.C. Mongelli, G. Conti, G.A. Maroniche, M.C. Rodriguez, A.J. Distefano, H.E. Hopp, M. del Vas, and S. Asurmendi. 2009. Virus infection elevates transcriptional activity of miR164a promoter in plants. *BMC Plant Biol.* 9:152-163.
- Bazzini, A.A., C.A. Manacorda, T. Tohge, G. Conti, M.C. Rodriguez, A. Nunes-Nesi, S. Villanueva, A.R. Fernie, F. Carrari, and S. Asurmendi. 2011. Metabolic and miRNA profiling of TMV infected plants reveals biphasic temporal changes. *PLoS One* 6:e28466.
- Bernstein, E., A.A. Caudy, S.M. Hammond, and G.J. Hannon. 2001. Role for a bidentate ribonuclease in the initiation step of RNA interference. *Nature* 409:363–366.

- Blevins, T., R. Rajeswaran, P.V. Shivaprasad, D. Beknazariants, A. Si-Ammour, H.S. Park, F. Vazquez, D. Robertson, F. Meins Jr, T. Hohn, and M.M. Pooggin. 2006. Four plant Dicers mediate viral small RNA biogenesis and DNA virus induced silencing. *Nucl. Acid. Res.* 34:6233-6246.
- Bouché, N., D. Laressergues, V. Gasciolli, and H. Vaucheret. 2006. An antagonistic function for *Arabidopsis* DCL2 in development and a new function for DCL4 in generating viral siRNAs. *EMBO J.* 25:3347–3356.
- Browning, K.S. 2004. Plant translation initiation factors: it is not easy to be green. *Biochem. Soc. Trans.* 32:589–591.
- Bueno, P., J. Varela, G. Gimenez-Gallego, and L. del Rio. 1995. Peroxisomal copper,zinc superoxide dismutase. *Plant Physiol.* 108:1151-1160.
- Burgyan, J. and Z. Havelda. 2011. Viral suppressors of RNA silencing. *Trend. Plant Sci.* 16:265-272.
- Chang, S., J. Puryear, and J. Cairney. 1993. A simple and efficient method for isolating RNA from pine trees. *Plant Mol. Biol. Rep.* 11: 113-116.
- Chapman, E.J., A.L. Prokhnevsky, K. Gopinath, V.D. Valerian, and J.C. Carrington. 2004. Viral RNA silencing suppressors inhibit the microRNA pathway at an intermediate step. *Genes Dev.* 18:1179-1186.
- Chellappan, P., R. Vanitharani, and C.M. Fauquet. 2005. MicroRNA-binding viral protein interfere with *Arabidopsis* development. *Proc. Natl. Acad. Sci. USA* 102:10381-10386.
- Chen, X. 2004. A *MICRORNA* as a translational repressor of *APETALA2* in *Arabidopsis* flower development. *Science* 303:2022–2025.
- Chen, Y.S., Y.C. Huang, J.C. Chiou, H.L. Wang, H.S. Huang, L.C. Huang, and G.S. Huang. 2010. Ultrasensitive detection of *Cymbidium mosaic potexvirus* using a single-wall carbon nanotube-functionalized quartz crystal microbalance. *Jpn. J. Appl. Phys.* 49:105103.
- Cheng, Y., N. Kato, W. Wang, J. Li, and X. Chen. 2003. Two RNA binding proteins, HEN4 and HUA1, act in the processing of *AGAMOUS* pre-mRNA in *Aabidopsis thaliana*. *Dev. Cell* 4:53-66.
- Chia, T.F., and J. He. 1999. Photosynthetic capacity in *Oncidium* (Orchidaceae) plants after virus eradication. *Environ. Expt. Bot.* 42:11-16.

- Chia, T.F., Y.S. Chan, and N.H. Chua. 1992. Detection and localization of viruses in orchids by tissue-print hybridization. *Plant Pathol.* 41:355-361.
- Chiu, M.H., I.H. Chen, D.C. Baulcombe, and C.H. Tsai. 2010. The silencing suppressor P25 of *Potato virus X* interacts with Argonaute1 and mediates its degradation through the proteasome pathway. *Mol. Plant. Pathol.* 11:641-649.
- Chng, C.G., S.M. Wong, P.H. Mahtani, C.S. Loh, C.J. Goh, M.C.C. Kao, M.C.M. Chung, and Y. Watanabe. 1996. The complete sequence of a Singapore isolate of *Odontoglossum ringspot virus* and comparison with other tobamoviruses. *Gene* 171: 155–161.
- Choi, S.K., S.H. Choi, K.H. Ryu, C.W. Choi, J.K. Choi, and W.M. Park. 2002. Identification and characterization of a ringspot isolate of *Odontoglossum ringspot virus* from *Cymbidium* var. 'Grace Kelly'. *Plant Pathol. J.* 18:317-322.
- Cillo, F., T. Mascia, M.M. Pasciuto, and D. Gallitelli. 2009. Differential effects of mild and severe *Cucumber mosaic virus* strains in the perturbation of microRNA-regulated gene expression in tomato map to the 3' sequence of RNA 2. *Mol. Plant Microbe Interact.* 22:1239-1249.
- Cleries, R., J. Galvez, M. Espino, J. Ribes, V. Nunes, and M.L. de Heredia. 2012. BootstRatio: A web-based statistical analysis of fold-change in qPCR and RT-qPCR data using resampling methods. *Comp. Biol. Med.* 42:438-445.
- Cooper, B., I. Schmitz, A.L.N. Rao, R.N. Beachy, and A.J. Dodds. 1996. Cell-to-cell transport of movement-defective cucumber mosaic and tobacco mosaic viruses in transgenic plants expressing heterologous movement protein genes. *Virology* 216:208-213.
- Corbett, M.K. 1967. Some distinguishing characteristics of the orchid strain of tobacco mosaic virus. *Phytopathology* 57:164-172.
- Czech, B., and G.J. Hannon. 2011. Small RNA sorting: matchmaking for Argonautes. *Nat. Rev. Genet.* 12:19-31.
- de Fatima Rosas-Cardenas, F., N. Duran-Figueroa, J.P. Vielle-Calzada, A. Cruz-Hernandez, N. Marsch-Martinez, and S. de Folter. 2011. A simple and efficient method for isolating small RNAs from different plant species. *Plant Methods* 7:4-10.
- Deal, R.B., C.N. Topp, E.C. McKinney, and R.B. Meagher. 2007. Repression of

- flowering in *Arabidopsis* requires activation of *FLOWERING LOCUS C* expression by the histone variant H2A.Z. *Plant Cell* 19:74-83.
- del Pozo, T., V. Cambiazo, and M. Gonzalez. 2012. Gene expression profiling analysis of copper homeostasis in *Arabidopsis thaliana*. *Biochem. Biophys. Res. Commun.* 393:248-252.
- Deleris, A., J. Gallego-Bartolome, J. Bao, K.D. Kasschau, J.C. Carrington, and O. Voinnet. 2006. Hierarchical action and inhibition of plant Dicer-like proteins in antiviral defense. *Science* 313:68–71.
- Diedhiou, C.J., O.V. Popova, K.J. Dietz, and D. Golldack. 2008. The SUI-homologous translation initiation factor eIF-1 is involved in regulation of iron homeostasis in rice. *Plant Biol.* 10:298–309.
- Ding, S.W. 2010. RNA-based antiviral immunity. *Nat. Rev. Immunol.* 10:632-644.
- Doench, J.G., C.P. Petersen, and P.A. Sharp. 2003. siRNAs can function as miRNAs. *Genes Dev.* 17:438–442.
- Donaire, L., Y. Wang, D. Gonzalez-Ibeas, K.F. Mayer, M.A. Aranda, and C. Llave. 2009. Deep-sequencing of plant viral small RNAs reveals effective and widespread targeting of viral genomes. *Virology* 392:203-214.
- Dong, J., S.T. Kim, and E.M. Lord. 2005. Plantacyanin plays a role in reproduction in *Arabidopsis*. *Plant Physiol.* 138:778–89.
- Dougherty, W.G. 1994. RNA-mediated virus resistance in transgenic plants: exploitation of a cellular pathway possibly involved in RNA degradation. *Mol. Plant Microbe Interact.* 7:544–552.
- Dunoyer, P., and O. Voinnet. 2005. The complex interplay between plant viruses and host RNA-silencing pathways. *Curr. Opin. Plant Biol.* 8:415-423.
- Dunoyer, P., C.H. Lecellier, E.A. Parizotto, C. Himber, and O. Voinnet. 2004. Probing the microRNA and small interfering RNA pathways with virus-encoded suppressors of RNA silencing. *Plant Cell* 16: 1235–1250.
- Edwardson, J.R. and F.W. Zettler. 1988. Odontoglossum ringspot virus. In: *The plant viruses*. Vol. 2. van Regenmortel, M.H.V. and Fraenkel-Conrat, H. (eds.). Plenum Publishing Corporation, New York, USA. p.233-247.
- Elbashir, S.M., J. Harborth, K. Weber, and T. Tuschl. 2002. Analysis of gene function in somatic mammalian cells using small interfering RNAs. *Methods* 26:199–213.

- Elbashir, S.M., W. Lendeckel, and T. Tuschl. 2001. RNA interference is mediated by 21- and 22-nucleotide RNAs. *Genes Dev.* 15:188–200.
- Eun, A.J.C. and S.M. Wong. 1999. Detection of *Cymbidium mosaic potexvirus* and *Odontoglossum ringspot tobamovirus* using immuno-capillary zone electrophoresis. *Phytopathology* 89:522-528.
- Faccioli, G. and F. Marani. 1979. Cymbidium mosaic virus associated with flower necrosis in *Cattleya* orchids. *Phytopathol. Medit.* 18:21-25.
- Fahlgren, N., and J.C. Carrington. 2010. miRNA target prediction in plants. *Methods Mol. Biol.* 592:51-57.
- Feng, J., K. Wang, X. Liu, S. Chen, and J. Chen. 2009. The quantification of tomato microRNAs response to viral infection by stem-loop real-time RT-PCR. *Gene* 437:14-21.
- Fire, A., S. Xu, M.K. Montgomery, S.A. Kostas, S.E. Driver, and C.C. Mello. 1998. Potent and specific genetic interference by double-stranded RNA in *Caenorhabditis elegans*. *Nature* 391:806–811.
- Frowd, J.A. and J.H. Termaine. 1977. Physical, chemical, and serological properties of *Cymbidium mosaic virus*. *Etiology* 67: 43-49.
- Gardner, P.P., J.Daub, J.G. Tate, E.P. Nawroki, D.L. Kolbe, S. Lindgreen, A.C. Wilkinson, R.D. Finn, S. Griffiths-Jones, S.R. Eddy, and A. Bateman. 2009. Rfam: updates to the RNA families database. *Nucl. Acid. Res.* 37:D136-D140.
- Gongora-Castillo, E., E. Ibarra-Laclette, D. Trejo-Saavedra, and R.F. Rivera-Bustamante. 2012. Transcriptome analysis of symptomatic and recovered leaves of geminivirus-infected pepper (*Capsicum annuum*). *Virol. J.* 9:295.
- Gonzalez-Ibeas, D., J. Blanca, L. Donaire, M. Saladie, A. Mascarell-Creus, A. Cano-Delgado, J. Garcia-Mas, C. Llave, and M.A. Aranda. Analysis of the melon (*Cucumis melo*) small RNAome by high-throughput pyrosequencing. 2011. *BMC Genom.* 12:393.
- Goodman, R.M. and A.F. Ross. 1974. Enhancement by *Potato virus Y* of *Potato virus X* synthesis in doubly infected tobacco depends on the timing of invasion by the viruses. *Virology* 58: 263–271.
- Gou, J.Y., F.F. Felippes, C.J. Liu, D. Weigel, and J.W. Wang. 2011. Negative regulation of anthocyanin biosynthesis in *Arabidopsis* by a miR156-targeted SPL

- transcription factor. *Plant Cell* 23:1512–1522.
- Griffiths-Jones, S., H.K. Saini, S. van Dongen, and A.J. Enright. 2008. miRBase: tools for microRNA genomics. *Nucl. Acid. Res.* 36:D154-158.
- Haag, J. R. and C.S. Pikaard. 2011. Multisubunit RNA polymerases IV and V: purveyors of non-coding RNA for plant gene silencing. *Nat. Rev. Mol. Cell Biol.* 12:483-492.
- Hadley, G., M. Arditti, and J. Arditti. 1987. Orchids diseases-a compedium. In: J. Arditti (ed.), *Orchid Biology, Reviews and Perspectives IV*. Cornell University Press, Ithaca, pp. 263–322.
- Hamilton, A.J. and D.C. Baulcombe. 1999. A species of small antisense RNA in posttranscriptional gene silencing in plants. *Science* 286:950–952.
- Hammond, S.M., E. Bernstein, D. Beach, and G.J. Hannon. 2000. An RNA-directed nuclease mediates post-transcriptional gene silencing in *Drosophila* cells. *Nature* 404:293–296.
- Hammond, S.M., A.A. Caudy, A.A., and G.J. Hannon. 2001. Post-transcriptional gene silencing by double-stranded RNA. *Nat. Rev. Genet.* 2:110–119.
- Hampton, C.R., H.C. Bowen, M.R. Broadley, J.P. Hammond, A. Mead, K.A. Payne, J. Pritchard, and P.J. White. 2004. Cesium toxicity in *Arabidopsis*. *Plant Physiol.* 136:3824–37.
- Hardie, D.G. 1999. Plant protein serine/threonine kinases: classification and functions. *Ann. Rev. Plant Physiol. Plant Mol. Biol.* 50:97-131.
- He, X.F., Y.Y. Fang, L. Feng, and H.S. Guo. 2008. Characterization of conserved and novel microRNAs and their targets, including a TuMV-induced *TIR-NBS-LRR* class *R* gene-derived novel miRNA in *Brassica*. *FEBS Lett.* 582:2445-2452.
- Hirai, K., K. Kubota, T. Mochizuki, S. Tsuda, and T. Meshi. 2008. Antiviral RNA silencing is restricted to the marginal region of the dark green tissue in the mosaic leaves of *Tomato mosaic virus*-infected tobacco plants. *J. Virol.* 82:3250-3260.
- Hiruki, C., M.H. Chen, and D.V. Rao. 1980. Ultrastructure of *Cattleya* leaf cells infected with cymbidium mosaic virus. *Acta. Hort.* 110:273-279.
- Ho, T., D. Pallett, R. Rushholme, T. Dalmay, and H. Wang. 2006. A simplified method for cloning of short interfering RNAs from *Brassica juncea* infected with *Turnip mosaic potyvirus* and *Turnip crinckle carmovirus*. *J. Virol. Method.* 136:217-223.

- Ho, T., H. Wang, D. Pallett, and T. Dalmay. 2007. Evidence for targeting common siRNA hotspots and GC preference by plant Dicer-like proteins. *FEBS Lett.* 581:3267-3272.
- Homma, M.K. and Y. Homma. 2005. Regulatory role of CK2 during the progression of cell cycle. *Mol. Cell Biochem.* 274:47-52.
- Hu, J.S., S. Ferreira, M.Q. Xu, M. Lu, M. Iha, E. Phlum, and M. Wang. 1994. Transmission, movement, and inactivation of cymbidium mosaic and odontoglossum ringspot viruses. *Plant Dis.* 78:633-636.
- Hu, Q.N., J. Hollunder, A. Niehl, C.J. Korner, D. Gerige, D. Windels, A. Arnold, M. Kuiper, F. Vazquez, M. Pooggin, and M. Heinlein. 2011. Specific impact of Tobamovirus infection on the *Arabidopsis* small RNA profile. *PLoS One* 6:e19549.
- Hu, W.W. and S.M. Wong. 1998. The use of DIG-labelled cRNA probes for the detection of *Cymbidium mosaic potexvirus* (CymMV) and *Odontoglossum ringspot tobamovirus* (ORSV) in orchids. *J. Virol. Methods* 70:193-199.
- Hu, W.W., S.M. Wong, C.S. Loh, and C.J. Goh. 1998. Synergism in replication of *Cymbidium mosaic virus* (CymMV) and *Odontoglossum ringspot virus* (ORSV) RNA in orchid protoplasts. *Arch. Virol.* 143:1265-1275.
- Hutvagner, G., J. McLachlan, A.E. Pasquinelli, E. Balint, T. Tuschl, and P.D. Zamore. 2001. A cellular function for the RNA-interference enzyme Dicer in the maturation of the *let-7* small temporal RNA. *Science* 293:834-838.
- Hutvagner, G., and M.J. Simard. 2008. Argonaute proteins: key players in RNA silencing. *Nat. Rev. Mol. Cell Biol.* 9:22-32.
- Hutvagner, G. and P.D. Zamore. 2002. RNAi: nature abhors a double-strand. *Curr. Opin. Genet. Dev.* 12:225-232.
- Inouye, N. 1983. Host range and properties of a strain of *Odontoglossum ringspot virus* in Japan. *Nogaku Kenkyu* 60:53-67.
- Jagadeeswaran, G., A. Saini, and R. Sunkar. 2009. Biotic and abiotic stress down-regulate miR398 expression in *Arabidopsis*. *Planta* 229:1009-1014.
- Jay, F., Y. Wang, A. Yu, L. Tacconnat, S. Pelletier, V. Colot, J.P. Renou, and O. Voinnet, 2011. Misregulation of *AUXIN RESPONSE FACTOR 8* underlies the developmental abnormalities caused by three distinct viral silencing suppressors in *Arabidopsis*. *PLoS Pathog.* 7:e1002035.

- Jensen, D.D. 1950. Mosaic of *Cymbidium* orchids. *Phytopathology* 40:966-967.
- Jensen, D.D. 1951. Mosaic or black streak disease of *Cymbidium* orchids. *Phytopathology* 41:401-414.
- Jensen, D.D., and H.A. Gold. 1951. A virus ring spot of *Odontoglossum* orchid : symptoms, transmission and electron microscopy. *Phytopathology* 41 : 648-653.
- Jensen, D.D. and A.H. Gold. 1955. Hosts, transmission and electron microscopy of cymbidium mosaic virus with special reference to *Cattleya* leaf necrosis. *Phytopathology* 45:327-334.
- Jones-Rhoades, M.W., and D.P. Bartel. 2004. Computational identification of plant microRNAs and their targets, including a stress-induced miRNA. *Mol. Cell* 14:787–99.
- Jones-Rhoades, M.W., D.P. Bartel, and B. Bartel. 2006. MicroRNAs and their regulatory roles in plants. *Annu. Rev. Plant Biol.* 57:19-53.
- Jorgensen, R.A., R.G. Atkinson, R.L.S. Forster, and W.J. Lucas. 1998. An RNA-based information superhighway in plants. *Science* 279:1486–1487.
- Kado, C.I. and D.D. Jensen. 1964. *Cymbidium mosaic virus* in *Phalaenopsis*. *Phytopathology* 54:974-977.
- Kado, C.I., M.H.V. van Regenmortel, and C.A. Knight. Studies on some strains of tobacco mosaic virus in orchids. I. Biological, chemical, and serological studies. *Virology* 34:17-24.
- Kasschau, K.D., Z. Xie, E. Allen, C. Llave, E.J. Chapman, K.A. Krizan, and J.C. Carrington. 2003. P1/HC-Pro, a viral suppressor of RNA silencing, interferes with *Arabidopsis* development and miRNA uncton. *Dev. Cell* 4:205-217.
- Kim, V.N., 2008. Sorting out small RNAs. *Cell* 133:25–26.
- Khvorova, A., A. Reynolds, and S.D. Jayasena. 2003. Functional siRNAs and miRNAs exhibit strand bias. *Cell* 115:209–216.
- Koseki, M., K. Goto, C. Masuta, A. and Kanazawa. 2005. The star-type color pattern in *Petunia hybrida* ‘Red Star’ flowers is induced by sequence-specific degradation of chalcone synthase RNA. *Plant Cell Physiol.* 46:1879-1883.
- Kurihara, Y., N. Inaba, N. Kutsuna, A. Takeda, Y. Tagami, and Y. Watanabe. 2007. Binding of tobamovirus replication protein with small RNA duplexes. *J. Gen. Virol.* 88:2347-2352.

- Lang, Q., C. Jin, L. Lai, J. Feng, S. Chen, and J. Chen. 2011. Tobacco microRNAs prediction and their expression infected with *Cucumber mosaic virus* and *Potato virus X*. *Mol. Biol. Rep.* 38:1523-1531.
- Lawson, R. H. and M. Brannigan. 1986. Virus diseases of orchids. In: Handbook of orchid pests and diseases. American Orchid Society, West Palm Beach, FL.
- Lee, M.S., M.J. Yang, Y.C. Hseu, G.H. Lai, W.T. Chang, Y.H. Hsu, and M.K. Lin. 2011. One-step reverse transcription loop-mediated isothermal amplification assay for rapid detection of *Cymbidium mosaic virus*. *J. Virol. Methods* 173:43-48.
- Lee, S.C. and Y.C. Chang. 2006. Multiplex RT-PCR detection of two orchid viruses with an internal control of plant *nad5* mRNA. *Plant Pathol. Bullet.* 15:187-196.
- Lee, S.C., and Y.C. Chang. 2010. Performances and application of antisera produced by recombinant capsid proteins of *Cymbidium mosaic virus* and *Odontoglossum ringspot virus*. *Eur. J. Plant Pathol.* 122:297-306.
- Leibman, D., D. Wolf, V. Saharan, A. Zelcer, T. Arazi, S. Yoel, V. Gaba, and A. Gal-On. 2011. A high level of transgenic viral small RNA is associated with broad potyvirus resistance in *Curcubits*. *Mol. Plant Microbe Interact.* 24:1220-1238.
- Leisner, S.M., and Turgeon, R. 1993. Movement of virus and photoassimilates in the phloem: A comparative analysis. *Bioassays* 15:741-748.
- Li, J. and X. Chen. 2003. *PAUSED*, a putative exportin-t, acts pleiotropically in *Arabidopsis* development but is dispensable for viability. *Plant Physiol.* 132:1913-1924.
- Li, T., H. Li, Y.X. Zhang, and J.Y. Liu. 2010. Identification and analysis of seven H₂O₂-responsive miRNAs and 32 new miRNAs in the seedlings of rice (*Oryza sativa* L. ssp. *indica*). *Nucl. Acid. Res.* 39:2821-2833.
- Li, Y.F., Y. Zhen, C. Addo-Quaye, L. Zhang, A. Saini, G. Jagadeeswaran, M.J. Axtell, W. Zhang, and R. Sunkar. 2010. Transcriptome-wide identification of microRNA targets in rice. *Plant J.* 62:742-759.
- Lin, K.Y., C.P. Cheng, B.C.H. Chang, W.C. Wang, Y.W. Huang, Y.S. Lee, H.D. Huang, Y.H. Hsu, and N.S. Lin. 2010. Global analyses of small interfering RNAs derived from *Bamboo mosaic virus* and its associated satellite RNAs in different plants. *PLoS One* 5:e11928.
- Lin, N.S., Y.J. Chai, T.Y. Huang, T.Y. Chang, and Y.H. Hsu. 1993. Incidence of bamboo

- mosaic potexvirus in Taiwan. *Plant Dis.* 77:448-450.
- Lin, N.S., and C.C. Chen., 1991. Association of *Bamboo mosaic virus* (BaMV) and BaMV-specific electron-dense crystalline bodies with chloroplasts. *Phytopathology* 81, 1551-1555.
- Lin, N.S., Y.S. Lee, B.Y. Lin, C.W. Lee, and Y.H. Hsu. 1996. The open reading frame of bamboo mosaic potexvirus satellite RNA is not essential for its replication and can be replaced with a bacterial gene. *Proc. Nat. Acad. Sci.* 93:3138-3142.
- Lin, N.S., Y.H. Hsu and H.T. Hsu. 1990. Immunological detection of plant viruses and a mycoplasma-like organism by direct tissue blotting on nitrocellulose membranes. *Phytopathology* 80:824–828.
- Lin, N.S., T.Z Huang., and Y.H. Hsu., 1992. Infection of barely protoplasts with bamboo mosaic virus RNA. *Bot. Bull. Acad. Sin.* 33, 271-275.
- Lin, N.S., Y.J.Chai, T.Y. Huang, and Hsu, Y.H. 1993. Incidence of bamboo potexvirus in Taiwan. *Plant Dis.* 77:448-450.
- Lin, N.S., Y.S. Lee, B.Y. Lin, C.W. Lee, and Y.H. Hsu. 1996. The open reading frame of bamboo mosaic virus satellite RNA is not essential for its replication and can be replicated with a bacterial gene. *Proc. Natl. Acad. Sci. U.S.A.* 93: 3138-3142.
- Livak, K.J. and T.D. Schmittgen. 2001. Analysis of relative gene expression using RealTime quantitative PCR and the $2^{-\Delta\Delta C_T}$ method. *Methods* 25:402-408.
- Llave, C. 2010. Virus-derived small interfering RNAs at the core of plant–virus interactions. *Trend. Plant. Sci.* 15:701-707.
- Llave, C., K.D. Kasschau, M.A. Rector, and J.C. Carrington. 2002a. Endogenous and silencing-associated small RNAs in plants. *Plant Cell* 14:1605–1619.
- Llave, C., Z.X. Xie, K.D. Kasschau, and J.C. Carrington. 2002b. Cleavage of Scarecrow-like mRNA targets directed by a class of *Arabidopsis* miRNA. *Science* 297:2053–2056.
- Lu, H.C., C.E. Chen, M.H. Tsai, H.I. Wang, H.J. Su, and H.H. Yeh. 2009. *Cymbidium mosaic potexvirus* isolate-dependent host movement systems reveal two movement control determinants and the coat protein is the dominant. *Virology* 388:147-159.
- Lu, H.C., H.H. Chen, W.C. Tsai, W.H. Chen, H.J. Su, D.C.N. Chang, and H.H. Yeh. 2007. Strategies for functional validation of genes involved in reproductive stages of orchids. *Plant Physiol.* 143:558-569.

- Lu, S., Y.H. Sun, H. Amerson, and V.L. Chiang. 2007. MicroRNAs in loblolly pine (*Pinus taeda* L.) and their association with fusiform rust gall development. *Plant J.* 51:1077-1098.
- Lu, Y.D., Q.H. Gan, X.Y. Chi, and S. Qin. 2008. Roles of microRNA in plant defense and virus offense interaction. *Plant Cell Rep.* 27:1571-1579.
- Mallory, A.C. and H. Vaucheret. 2010. Form, function, and regulation of ARGONAUTE proteins. *Plant Cell* 22:3879-3889.
- Mallory, A.C., B.J. Reinhart, D. Bartel, V.B. Vance, and L.H. Bowman. 2002. A viral suppressor of RNA silencing differentially regulates the accumulation of short interfering RNAs and micro-RNAs in tobacco. *Proc. Natl. Acad. Sci. U.S.A.* 99:15228–15233.
- Mallory, A.C., B.J. Reinhart, M.W. Jones-Rhoades, G. Tang, P.D. Zamore, M.K. Barton, and D.P. Bartel. 2004. MicroRNA control of *PHABULOSA* in leaf development: importance of pairing to the microRNA 5' region. *EMBO J.* 23:3356–3364.
- Matzke, M., T. Kanno, L. Daxinger, B. Huettel, and A.J.M. Matzke. 2009. RNA-mediated chromatin-based silencing in plants. *Curr. Opin. Cell Biol.* 21:367-376.
- Mi, S., T. Cai, Y. Hu, Y. Chen, E. Hodges, F. Ni, L. Wu, S. Li, H. Zhou, C. Long, S. Chen, G.J. Hannon, and Y. Qi. 2008. Sorting of small RNAs into *Arabidopsis* argonaute complexes is directed by the 5' terminal nucleotide. *Cell* 133:116-127.
- Moissiard, G. and O. Voinnet. 2006. RNA silencing of host transcripts by cauliflower mosaic virus requires coordinated action of the four *Arabidopsis* Dicer-like proteins. *Proc. Nat. Amer. Sci.* 103:19593-19598.
- Molnar, A., C. Melnyk, and D.C. Baulcombe. 2011. Silencing signals in plants: a long journey for small RNAs. *Genome Biol.* 12:215.
- Molnar, A., C.W. Melnyk, A. Basseett, T.J. Hardcastle, R. Dunn, and D.C. Baulcomb. 2010. Small silencing RNAs in plants are mobile and direct epigenetic modification in recipient cells. *Science* 328:872-875.
- Molnar, A., T. Csorba, L. Lakatos, E. Varallyaya, C. Lacomme, and J. Burgyan. 2005. Plant virus-derived small interfering RNAs originate predominantly from highly structured single-stranded viral RNAs. *J. Virol.* 79:7812-7818.
- Montgomery, T.A., M.D. Howell, J.T. Cuperus, D. Li, J.E. Hansen, A.L. Alexander, E.J.

- Chapman, N. Fahlgren, E. Allen, and J.C. Carrington. 2008. Specificity of ARGONAUTE7-miR390 interaction and dual functionality in *TAS3* trans-acting siRNA formation. *Cell* 133:128-141.
- Moore, C. J., P.W. Sutherland, R.L. Forster, R.C. Gardner, and R.M. MacDiarmid. 2001. Dark green islands in plant virus infection are the result of posttranscriptional gene silencing. *Mol. Plant-Microbe Interact.* 14:939-946.
- Morel, J.B., C. Godon, P. Mourrain, C. Beclin, S. Boutet, F. Feuerbach, F. Proux, and H. Vaucheret. 2002. Fertile hypomorphic ARGONAUTE (*ago1*) mutants impaired in posttranscriptional gene silencing and virus resistance. *Plant Cell* 14:629–639.
- Morozov, S.Y., O.N. Fedorkin, G. Juttner, J. Schiemann, D.C. Baulcombe, and J.G. Atabekov. 1997. Complementation of a potato virus X mutant mediated by bombardment of plant tissues with cloned viral movement protein genes. *J. Gen. Virol.* 78:2077-2083.
- Murakishi, H.H. 1958. Host range, symptomatology, physical properties, and cross-protection studies of orchid virus isolates. *Phytopathology* 48:132-137.
- Napoli, C., C. Lemieux, and R. orgensen. 1990. Introduction of a chimeric chalcone synthase gene into petunia results in reversible co-suppression of homologous genes in trans. *Plant Cell* 2:279–289.
- Naqvi, A.R., M.N. Islam, N.R. Choudhury, and Q.M.R. Haq. 2009. The fascinating world of RNA interference. *Int. J. Biol. Sci.* 5:97-117.
- Naqvi, A.R., Q.M. Haq, and S.K. Mukherjee. 2010. MicroRNA profiling of *Tomato leaf curl new delhi virus* (ToLCNDV) infected tomato leaves indicates that degradation of miR159/319 and miR172 might be linked with leaf curl disease. *Virol. J.* 7:281-296.
- Navalinskienė, M., J. Raugalas, and M. Samuitiene. 2005. Viral diseases of flower plants. 16. Identification of viruses affecting orchids. *Biologija* 2:29-34.
- Navarro, B., A. Gisel, M.E. Rodio, S. Delgado, R. Flores, and F. Di Serio. 2012. Small RNAs containing the pathogenic determinant of a chloroplast-replicating viroid guide the degradation of a host mRNA as predicted by RNA silencing. *Plant J.* 70:991-1003.
- Nersissian A.M., C. Immoos, M.G. Hill, P.J. Hart, G. Williams, R.G. Herrmann, and J.S. Valentine. 1998. Uclacyanins, stellacyanins, and plantacyanins are distinct

- subfamilies of phytoeyanins: plant-specific mononuclear blue copper proteins. *Protein Sci.* 7:1915–29.
- Olsen, P.H. and Ambros, V. 1999. The (*lin-4*) regulatory RNA controls developmental timing in *Caenorhabditis elegans* by blocking LIN-14 protein synthesis after the initiation of translation. *Dev. Biol.* 216:671–680.
- O'Rourke, J.A., R.T. Nelson, D. Grant, J. Schmutz, J. Grimwood, S. Cannon, C.P. Vance, M.A. Graham, and R.C. Shoemaker. 2008. Integrating microarray analysis and the soybean genome to understand the soybeans iron deficiency response. In: A genomic study of soybean iron deficiency chlorosis. O'Rourke, J.A. (eds.) Iowa State University. Ames, Iowa.
- Osami, S.A., S. Bak, A. Imberty, C.E. Olsen, and B.L. Moller. 2008. Catalytic key amino acids and UDP-sugar donor specificity of a plant glucuronosyltransferase, UGT94B1: molecular modeling substantiated by site-specific mutagenesis and biochemical analysis. *Plant Physiol.* 148:1295-1308.
- Palauqui, J.C., T. Elmayer, J.M. Pollien, and H. Vaucheret. 1997. Systemic acquired silencing: Transgene-specific post-transcriptional silencing is transmitted by grafting from silenced stocks to non-silenced scions. *EMBO J.* 16:4738–4745.
- Pantaleo, V., P. Saldarelli, L. Miozzi, A. Giampetruzzi, A. Gisel, S. Moxon, T. Dalmay, G. Bisztray, and J. Burgyan. 2010. Deep sequencing analysis of viral short RNAs from an infected Pinot Noir grapevine. *Virology* 408:49-56.
- Papp, I., M.F. Mette, W. Aufsatz, L. Daxinger, S.E. Schauer, A. Ray, J. van der Winden, M. Matzke, M., and A.J.M. Matzke. 2003. Evidence for nuclear processing of plant micro RNA and short interfering RNA precursors. *Plant Physiol.* 132:1382–1390.
- Paul, H.L., Wetter, K., Wittmann, H.G. and J. Brandes, 1965. Untersuchungen am *Odontoglossum ringspot virus*, einem verwandten des Tabakmosaik-virus. *Z. VererbLehre* 97:186-203.
- Pearson, M. N. and J. S. Cole. 1991. Further observations on the effects of *Cymbidium mosaic virus* and *Odontoglossum ringspot virus* on the growth of *Cymbidium* orchids. *J. Pathol.* 131:193–198.
- Poethig, R.S. 2009. Small RNAs and developmental timing in plants. *Curr. Opin. Genet. Dev.* 19:374–378.
- Qi, X., F.S. Bao, and Z. Xie. 2009. Small RNA deep sequencing reveals role for

- Arabidopsis thaliana* RNA-dependent RNA polymerase in viral siRNA biogenesis. PLoS One 4:e4971.
- Qu, F., X. Ye, and T.J. Morris. 2008. *Arabidopsis* DRB4, AGO1, AGO7, and RDR6 participate in a DCL4-initiated antiviral RNA silencing pathway negatively regulated by DCL1. Proc. Natl. Acad. Sci. USA 105:14732–14737.
- Ranocha, P., M. Chabannes, S. Chamayou, S. Danoun, A. Jauneau, A.M. Boudet, and D. Goffner. 2002. Laccase down-regulation causes alterations in phenolic metabolism and cell wall structure in poplar. Plant Physiol. 129:145-155.
- Rhoades, M.W., B.J., Reinhart, L.P. Lim, C.B. Burge, B. Bartel, and D.P. Bartel. 2002. Prediction of plant MicroRNA targets. Cell 110:513–520.
- Rodriguez, M.C.S., M. Petersen, and J. Mundy. 2010. Mitogen-activated protein kinase signaling in plants. Ann. Rev. Plant Biol. 61:621-649.
- Romano, N. and G. Macino. 1992. Quelling: transient inactivation of gene expression in *Neurospora crassa* by transformation with homologous sequences. Mol. Microbiol. 6:3343–3353.
- Ruiz, M.T., O. Voinnet, and D.C. Baulcombe. 1998. Initiation and maintenance of virus-induced gene silencing. Plant Cell 10:937–946.
- Ruiz-Ferrer, V. and O. Voinnet. 2009. Role of plant small RNAs in biotic stress responses. Annu. Rev. Plant Biol. 60:485-510.
- Ruiz-Ruiz, S., B. Navarro, A. Gisel, L. Pena, L. Navarro, P. Moreno, F. Di Serio, and R. Flores. 2011. *Citrus tristeza virus* infection induces the accumulation of viral small RNAs (21-24-nt) mapping preferentially at the 3'-terminal region of the genomic RNA and affects the host small RNA profile. Plant Mol. Biol. 75:607-619.
- Ryu, K.H. and W.M. Park. 1995. The complete nucleotide sequence and genome organization of odontoglossum ringspot tobamovirus RNA. Arch. Virol. 140:1577-1587.
- Ryu, K.H., K.E. Yoon, and W.M. Park. 1995. Detection by RT-PCR of cymbidium mosaic virus in orchids. J. Phytopathol. 143:643-646.
- Samuel, G. 1934. The movement of tobacco mosaic virus within the plant. Ann. Appl. Biol. 21:90-111.
- Sanan-Mishra, N., V. Kumar, S.K. Sopory, and S.K. Mukherjee. 2009. Cloning and validation of novel miRNA from basmati rice indicates cross talk between abiotic

- and biotic stresses. *Mol. Genet. Genom.* 282:463-474.
- Sawada, S., H. Suzuki, F. Ichimaida, M.A. Yamaguchi, T. Iwashita, Y. Fukui, H. Hemmi, T. Nishini, and T. Nakayama. 2005. UDP-glucuronic acid: anthocyanin glucuronosyltransferase from red daisy (*Bellis perennis*) flowers: enzymology and phylogenetics of a novel glucuronosyltransferase involved in flower pigment biosynthesis. *J. Biol. Chem.* 280:899–906.
- Schauer, S.E., S.E. Jacobsen, D.W. Meinke, and A. Ray. 2002. DICER-LIKE1: Blind men and elephants in *Arabidopsis* development. *Trends Plant Sci.* 7:487–491.
- Senda, M., C. Masuta, S. Ohnishi, K. Goto, A. Kasai, T. Sano, J.S. Hong, and S. MacFarlane. 2004. Patterning of virus-infected *Glycine max* seed coat is associated with suppression of endogenous silencing of chalcone synthase genes. *Plant Cell* 16:807-818.
- Seoh, M.L., S.M. Wong, and L. Zhang. 1998. Simultaneous TD/RT-PCR detection of *Cymbidium mosaic potexvirus* and *Odontoglossum ringspot tobamovirus* with a single pair of primers. *J. Virol. Methods* 72:197-204.
- Sheehan, T.J. 2003. What is an orchid? Characteristics unite more than 25,000 species and 110,000 hybrids into a family of amazing diversity. *Orchids.* (April):274-283.
- Shimura, H., V. Pantaleo, T. Ishihara, N. Myojo, J. Inaba, K. Sueda, J. Burgyan, and C. Masuta. 2011. A viral satellite RNA induces yellow symptoms on tobacco by targeting a gene involved in chlorophyll biosynthesis using the RNA silencing machinery. *PLoS Pathog.* 7:e1002021.
- Silhavy, D., J. Burgyan. 2004. Effects and side-effects of viral RNA silencing suppressors on short RNAs. *Trends Plant Sci.* 9:76–83.
- Smith, N.A., A.L. Eamens, and M.B. Wang. 2011. Viral small interfering RNAs target host genes to mediate disease symptoms in plants. *PLoS Pathog.* 7:e1002022.
- Solovyev, A.G., D.A. Zelenina, E.I. Savenkov, V.Z. Grdzlishvili, S.Y. Morozov, D.E. Lesemann, E. Maiss, R. Casper, and J.G. Atabekov. 1996. Movement of *Barley stripe mosaic virus* chimera with a *Tobacco mosaic virus* movement protein. *Virology.* 217:435-441.
- Song, J.B., S.Q. Huang, T. Dalmay, and Z.M. Yang. 2012. Regulation of leaf morphology by microRNA 394 and its target *LEAF CURLING RESPONSIVENESS*. *Plant Cell Physiol.* 53:1669.

- Stuurman, J., F. Jaggi, and C. Kuhlemeier. 2002. Shoot meristem maintenance is controlled by a *GRAS*-gene mediated signal from differentiating cells. *Genes Dev.* 16:2213–2218.
- Su, C.L., Y.T. Chao, Y.C.A. Chang, W.C. Chen, C.Y. Chen, A.Y. Lee, K.T. Hwa and M.C. Shih. 2011. De novo assembly of expressed transcripts and global analysis of the *Phalaenopsis aphrodite* transcriptome. *Plant Cell Physiol.* 52:1501-1514.
- Sun, Y.L. and S.K. Hong. 2012. Sensitivity of translation initiation factor eIF1 as a molecular target of salt toxicity to sodic-alkaline stress in the halophytic grass *Leymus chinensis*. *Biochem. Genet.*
- Sunkar, R., A. Kapoor, and J.K. Zhu. 2006. Posttranscriptional induction of two Cu/Zn superoxide dismutase genes in *Arabidopsis* is mediated by downregulation of miR398 and important for oxidative stress tolerance. *Plant Cell* 18:2051–2065.
- Szittyá, G., S. Moxon, V. Pantaleo, G. Toth, R.L.R. Pilcher, V. Moulton, J. Burgyan, and T. Dalmay. 2010. Structural and functional analysis of viral siRNAs. *Plos Pathog.* 6: e1000838.
- Takeda, A., S. Iwasaki, T. Watanabe, M. Utsumi, and Y. Watanabe. 2008. The mechanism selecting the guide strand from small RNA duplexes is different among argonaute proteins. *Plant Cell Physiol.* 49:493-500.
- Taliansky, M.E., T.I. Atabekova, I.B. Kaplan, S. Yu, S.I. Malysenko, and J.G. Atabekov. 1982. A study of TMV *ts* mutant Ni2519. I. Complementation experiments. *Virology* 118:301–308.
- Tanaka, S., H. Nishii, M. Kameyalwaki, and P. Sommaria. 1997. Detection of *Cymbidium mosaic potexvirus* and *Odontoglossum ringspot tobamovirus* from Thai orchids by rapid immunofilter paper assay. *Plant Dis.* 81:167-170.
- Tang, G.L., B.J. Reinhart, D.P. Bartel, and P.D. Zamore. 2003. A biochemical framework for RNA silencing in plants. *Genes Dev.* 17:49–63.
- van der Krol, A.R., L.A. Mur, M. Beld, J.N. Mol, and A.R. Stuitje. 1990a. Flavonoid genes in petunia: addition of a limited number of gene copies may lead to a suppression of gene expression. *Plant Cell* 2:291–299.
- van der Krol, A.R., L.A. Mur, P. de Lange, J.N. Mol, and A.R. Stuitje. 1990b. Inhibition of flower pigmentation by antisense CHS genes: promoter and minimal sequence requirements for the antisense effect. *Plant Mol. Biol.* 14:457–466.

- Vance, V. and H. Vaucheret. 2001. RNA silencing in plants—Defense and counterdefense. *Science* 292:2277–2280.
- Várallyay, E., A. Valoczi, A. Agyi, J. Burgyan, and Z. Havelda. 2010. Plant virus-mediated induction of miR168 is associated with repression of *ARGONAUTE1* accumulation. *EMBO J.* 29:3507-3519.
- Varkonyi-Gasic, E. and R.P. Hellens. 2010. qRT-PCR of small RNAs. *Methods Mol. Biol.* 631:109-122.
- Vaucheret, H., A.C. Mallory, and D.P. Bartel. 2006. AGO1 homeostasis entails coexpression of miR168 and AGO1 and preferential stabilization of miR168 by AGO1. *Mol. Cell* 22:129–136.
- Vazquez, F., S. Legrand, and D. Windels. 2010. The biosynthetic pathways and biological scopes of plant small RNAs. *Trend. Plant Sci.* 15:337-345.
- Vogler, H., R. Akbergenov, P.V. Shivaprasad, V. Dang, M. Fasler, M.O. Kwon, S. Zhanybekova, T. Hohn, and M. Heinlein. 2007. Modification of small RNAs associated with suppression of RNA silencing by tobamovirus replicase protein. *J. Virol.* 81:10379-10388.
- Voinnet, O. 2005. Induction and suppression of RNA silencing: Insights from viral infections. *Nat. Rev. Genet.* 6:206-220.
- Voinnet, O. 2009. Origin, biogenesis, and activity of plant microRNAs. *Cell* 136:669-687.
- Voinnet, O., C. Lederer, and D.C. Baulcombe. 2000. A viral movement protein prevents spread of the gene silencing signal in *Nicotiana benthamiana*. *Cell* 103:157–167.
- Voinnet, O., P. Vain, S. Angell, and D.C. Baulcombe. 1998. Systemic spread of sequence-specific transgene RNA degradation in plants is initiated by localized introduction of ectopic promoterless DNA. *Cell* 95:177–187.
- Wang, M.B., C. Masuta, N.A. Smith, and H. Shimura. 2012. RNA silencing and plant viral diseases. *Mol. Plant Microbe Interact.* 25:1275-1285.
- Wang, M.B., X.Y. Bian, L.M. Wu, L.X. Liu, N.A. Smith, D. Isenegger, R.M. Wu, C. Masuta, V.B. Vance, J.M. Watson, A. Rezaian, E.S. Dennis, and P.M. Waterhouse. 2004. On the role of RNA silencing in the pathogenicity and evolution of viroids and viral satellites. *Proc. Nat. Acad. Sci.* 101: 3275-3280.
- Wisler, G.C., F.W. Zettler, and T.J. Sheehan. 1979. Relative incidence of cymbidium

- mosaic virus and odontoglossum ringspot virus in several genera of wild and cultivated orchids. Proc. Fla. State Hort. Soc. 92:339-340.
- Wong, S.M., C.G. Chng, Y.H. Lee, K. Tan, and F.W. Zettler. 1994. Incidence of cymbidium mosaic and odontoglossum ringspot viruses and their significance in orchid cultivation in Singapore. Crop Protec. 13:235-239.
- Wong, S.M., P.H. Mahtani, K.C. Lee, H.H. Yu, Y. Tan, K.K. Neo, Y. Chan, M. Wu, and C.G. Chng. 1997. Cymbidium mosaic potexvirus RNA: complete nucleotide sequence and phylogenetic analysis. Arch. Virol. 142:383-391.
- Wu, H.W., S.S. Lin, K.C. Chen, S.D. Yeh, and N.H. Chua. 2010. Discriminating mutations of HC-Pro of *Zucchini yellow mosaic virus* with differential effects on small RNA pathways involved in viral pathogenicity and symptom development. Mol. Plant Microbe Interact. 23:17-28.
- Xin, M.M., Y. Wang, Y.Y. Yao, C.J. Xie, H.R. Peng, Z.F. Ni, and Q.X. Sun. 2010. Diverse set of microRNAs are responsive to powdery mildew infection and heat stress in wheat (*Triticum aestivum* L.). BMC Plant Biol. 10:123.
- Xing, S., M. Salinas, S. Hohmann, R. Berndtgen, and P. Huijser. 2010. miR156-targeted and nontargeted SBP-Box transcription factors act in concert to secure male fertility in *Arabidopsis*. Plant Cell 22:3935–3950.
- Yan, F., H. Zhang, M.J. Adams, J. Yang, J. Peng, J.F. Antoniow, Y. Zhou, and J. Chen. 2010. Characterization of siRNAs derived from *Rice stripe virus* in infected rice plants by deep sequencing. Arch. Virol. 155:935-940.
- Yang, Y., X. Chen, J. Chen, H. Xu, J. Li, and Z. Zhang. 2011. Differential miRNA expression in *Rehmannia glutinosa* plants subjected to continuous cropping. BMC Plant Biol. 11:53.
- Yao, Y.Y., G.G. Guo, Z.F. Ni, R. Sunkar, J.K. Du, J.K. Zhu, and Q.X. Xun. 2007. Cloning and characterization of microRNAs from wheat (*Triticum aestivum* L.). Genome Biol. 8:R96.
- Yifhar, T., I. Pekker, D. Peled, G. Friedlander, A. Pistunov, M. Sabban, G. Wachsman, J.P. Alvarez, Z. Amsellem, and Y. Eshed. 2012. Failure of the tomato *trans*-acting short interfering RNA program to regulate AUXIN RESPONSE FACTOR3 and ARF4 underlies the wiry leaf syndrome. Plant Cell 24:3575-3589.
- Yoo, B.C., F. Kragler, E. Varkonyi-Gasic, V. Haywood, S. Archer-Evans, Y.M. Lee, T.J.

- Lough, and W.J. Lucas. 2004. A systemic small RNA signaling system in plants. *Plant Cell* 16:1979-2000.
- Yu, F., X. Liu, M. Alsheikh, S. Park, and S. Rodermel. 2008. Mutations in *SUPPRESSOR OF VARIATION1*, a factor required for normal chloroplast translation, suppress *var2*-mediated leaf variegation in Arabidopsis. *Plant Cell* 20:1786-1804.
- Zamore, P.D., T. Tuschl, P.A. Sharp, D.P. Bartel. 2000. RNAi: double-stranded RNA directs the ATP-dependent cleavage of mRNA at 21–23 nucleotide intervals. *Cell* 101:25–33



Table 1. Summary of total reads in small RNA libraries constructed from mock- and ORSV-inoculated tissues.

	Mi ^a	Mc	Oi	Oc
raw data input				
Total reads	8,637,816	9,350,999	11,447,603	5,081,802
Poor quality reads filtered ^b	8,044,535	8,385,985	10,374,208	4,759,861
15-27 nt	7,868,534	8,305,831	9,640,182	5,600,371
low frequency reads filtered ^c	5,995,466	6,435,986	8,298,644	4,995,552
sRNAs from microbes				
Contaminants ^d	4,383	4,383	4,575	3,373
ORSV ^e	174	360	2,454,779 (29.58%)	2,458 (0.07%)
CymMV	2	10	3	1
CMV ^f	1	0	1	2
TSWV	2	1	1	0
sRNAs from <i>Phalaenopsis</i>				
clean reads ^g	5,990,907	6,428,789	5,839,287	3,489,671
<i>P. aphrodite</i> ESTs	2,595,412	2,614,270	2,314,618	1,563,949
structure RNA (Rfam)	801,306	1,029,125	1,566,394	798,597
<i>P. aphrodite</i> chloroplast	555,849	716,630	316,649	206,394
miRNA ^h	1,134,103 (18.93%)	901,940 (14.03%)	608,497 (10.42%)	325,957 (9.34%)

^a Mi: mock-inoculated, inoculated tissues; Mc: mock-inoculated, non-inoculated tissues;

Oi: ORSV-inoculated, inoculated tissues, Oc: ORSV-inoculated, non-inoculated tissues

^b Adapter trimming and removal of poly-A/T/C/G or N (null)-calling bases containing tas.

^c Reads with only 1 counts is defined as low frequency reads and filtered before further analysis.

^d Reads matched to *Escherichia coli* and other microbes.

^e The numbers in grey stand for the percentage of ORSV viral siRNAs in low frequency reads -filtered total small RNAs.

^f Besides *Cymbidium mosaic virus* (CymMV) and *Odontoglossum ringspot virus* (ORSV), matching reads to genomes of some prevalent orchid viruses [*Capsicum chlorotic virus* (CaCV), *Carnation mosaic virus* (CarMV), *Cucumber mosaic virus* (CMV), *Impatiens necrotic spot virus* (INSV), *Orchid fleck virus* (OFV), *Phalaenopsis chlorotic spot virus* (PhCSV), and *Tomato spotted wilt virus* (TSWV)] was performed and only perfect matched reads are shown.

^g Contaminants and viral siRNAs excluded reads.

^h The numbers in grey stand for the percentage of miRNAs in total clean reads.

Table 2. Summary of unique reads in small RNA libraries constructed from mock- and ORSV-inoculated tissues.

	Mi ^a	Mc	Oi	Oc
raw data input				
Total unique reads (tags)	3,417,716	3,491,584	2,949,397	1,290,004
Poor quality filtered tags ^b	3,012,462	2,999,050	2,270,835	984,602
15-27 nt	2,980,879	2,982,172	2,204,548	904,344
low frequency tags filtered ^c	1,107,811	1,112,327	863,010	402,573
sRNA tags from microbes				
Contaminants ^d	959	1180	851	397
ORSV	169	346	59,496	1,645
CymMV	2	11	3	5
CMV ^e	1	0	1	2
TSWV	2	1	1	0
sRNA tags from <i>Phalaenopsis</i>				
clean tags ^f	1,106,681	1,110,790	802,660	400,526
<i>P. aphrodite</i> ESTs	222,395	224,654	178,955	85,762
structure RNA (Rfam)	48,258	51,431	47,108	40,218
<i>P. aphrodite</i> chloroplast	28,699	30,171	28,220	17,623
miRNA (tag counts)	2,125	2,046	1,863	1,627
miRNA (family categories)	85	80	75	55

^a Mi: mock-inoculated, inoculated area; Mc: mock-inoculated, non-inoculated area;

Oi: ORSV-inoculated, inoculated area, Oc: ORSV-inoculated, non-inoculated area

^b Adapter trimming and removal of poly-A/T/C/G or N (null)-calling bases containing tags.

^c Reads with only 1 counts is defined as low frequency reads and filtered before further analysis.

^d Reads matched to *Escherichia coli* and other microbes.

^e Besides *Cymbidium mosaic virus* (CymMV) and *Odontoglossum ringspot virus* (ORSV), matching reads to genomes of some prevalent orchid viruses [*Capsicum chlorotic virus* (CaCV), *Carnation mosaic virus* (CarMV), *Cucumber mosaic virus* (CMV), *Impatiens necrotic spot virus* (INSV), *Orchid fleck virus* (OFV), *Phalaenopsis chlorotic spot virus* (PhCSV), and *Tomato spotted wilt virus* (TSWV)] was performed and only perfect matched reads are shown.

^f Contaminants and viral siRNAs excluded tags

Table 3. The major sequences and total reads of abundant miRNAs in small RNA libraries constructed from mock- and ORSV-inoculated tissues.

ID	Family	Size	Sequence	Reads ^a			
				Mi	Mc	Oi	Oc
4565061	miR156	21	CUGACAGAAGAUAGAGAGCAC	163	229	174	80
4228356	miR156	20	UGACAGAAGAGAGUGAGCAC	176	251	161	102
	miR156		total^b	392	553	371	229
6789462	miR159	21	UUUGGAUUGAAGGGAGCUCUU	116	175	72	39
3587752	miR159	20	UUGGAUUGAAGGGAGCUCUG	101	190	110	20
8628938	miR159	18	UUUGGAUUGAAGGGAGCU	99	190	128	55
4920752	miR159	21	UUGGAUUGAAGGGAGCUCUGC	897	1,322	957	331
5173640	miR159	19	UUUGGAUUGAAGGGAGCUC	1,033	1,487	720	281
5852294	miR159	20	UUUGGAUUGAAGGGAGCUCU	7,619	10,009	3,831	1,421
2344141	miR159	21	UUUGGAUUGAAGGGAGCUCUG	13,198	14,812	11,821	2,184
867925	miR159	21	UUUGGAUUGAAGGGAGCUCUA	33,886	48,653	20,133	7,423
	miR159		total	58,326	78,829	38,773	12,751
5410504	miR162	21	UCGAUAAACCUCUGCAUACGG	0	0	0	202
4061480	miR162	21	UCGAUAAACCUCUGCAUGC GG	0	3	0	222
1307734	miR162	18	UCGAUAAACCUCUGCAUC	114	145	53	34
2768096	miR162	22	UCGAUAAACCUCUGCAUCCGGU	1,105	1,007	588	345
9227853	miR162	21	UCGAUAAACCUCUGCAUCCGG	9,877	12,325	4,861	3,422
	miR162		total	11,490	13,906	5,717	4,517
3025792	miR165	21	UCGGACCAGGCUUCAUCCCCC	283	192	117	40
	miR165		total	393	285	169	168
6067802	miR166	21	UCGGACCAGGCUUCAUUGGCC	1	0	0	115
14697744	miR166	21	UCGGACCAGGCUUCAUAGCC	0	0	0	131
1131391	miR166	21	UCGGACCAGGCUUCAUCCCA	102	64	60	21
6441303	miR166	21	UCGGACCAGGCUUCUUCCCC	108	74	41	30
7570448	miR166	21	UCGGACCAGGCUUGAUUCCCC	100	67	39	65
849600	miR166	21	UCGGACCAAGCUUCAUUCCCC	112	67	57	53
9275462	miR166	21	UCGGACUAGGCUUCAUUCCCC	114	92	66	19
13705989	miR166	21	UUCGGACCAGGCUUCAUGCCC	0	0	0	307
7877325	miR166	21	UCGGACCAGGCUUCAUUCGCC	66	49	24	197
1626117	miR166	21	ACGGACCAGGCUUCAUUCCCC	136	93	89	37
3411178	miR166	21	UCGGACCAGGCUUCAUCCUC	151	155	42	24

^a Sequences with the more than 100 reads or being the tag with the highest read within the family was designated as abundant miRNAs.

^b Sub-totaled reads within a single miRNA family
(continued)

Table 3. The major sequences and total reads of abundant miRNAs in small RNA libraries constructed from mock- and ORSV-inoculated tissues. (continued)

ID	Family	Size	Sequence	Reads ^a			
				Mi	Mc	Oi	Oc
9033509	miR166	21	UCGGGCCAGGCUUCAUUC	152	101	78	63
274081	miR166	21	UCGGACCAGGCUCCAUUC	167	125	79	25
2770477	miR166	21	UCGGACCAGACUUCAUUC	167	82	83	77
9769609	miR166	21	UCGGACCAGGCUUCACUC	182	130	73	25
7087901	miR166	22	UCGGACCAGGCUUCAUUC	158	97	112	48
6175229	miR166	21	UUUCGGACCAGGCUUCAU	134	190	84	26
9044926	miR166	21	UCGGACCGGGCUUCAUUC	176	140	76	60
2811658	miR166	21	UCGGAUCAGGCUUCAUUC	220	138	94	23
3030416	miR166	21	CCGGACCAGGCUUCAUUC	216	124	121	37
4804583	miR166	21	UCGGACCAGGCUUCGUUC	228	153	103	78
3554030	miR166	21	UCGGACCAGGCUUAAUUC	156	181	104	129
7416352	miR166	21	UCGGACCAGGCCUCAUUC	247	182	114	38
4033576	miR166	21	UCGGACCAGGCUUCAUUC	258	166	101	73
7491037	miR166	21	UCGGACCAGGUUCAUUC	298	206	145	46
7003658	miR166	21	UUGGACCAGGCUUCAUUC	321	237	136	26
1639010	miR166	19	UCGGACCAGGCUUCAUUC	257	286	169	53
4253006	miR166	22	UCUCGGACCAGGCUUCAU	343	223	176	77
9371738	miR166	21	UCAGACCAGGCUUCAUUC	352	214	183	120
220884	miR166	21	UCGGACCAGGCUUCCUUC	567	162	152	65
6380141	miR166	21	UCUCGGACCAGGCUUCAU	451	407	89	42
1537655	miR166	20	CGGACCAGGCUUCAUUC	638	355	357	27
8517396	miR166	22	CUCGGACCAGGCUUCAUUC	614	429	273	98
5105791	miR166	19	GGACCAGGCUUCAUUC	646	469	323	17
8880687	miR166	20	UCGGACCAGGCUUCAUUC	649	555	488	121
4014606	miR166	21	UCGGACCAGGCUUUAUUC	959	1,140	514	99
7688138	miR166	21	UCGGACCAGGCUUCAUUC	698	491	322	6,073
6100862	miR166	21	CUCGGACCAGGCUUCAUUC	5,143	3,499	3,245	753
6763642	miR166	21	UCGGACCAGGCUUCAUUA	86	73	40	12,967
3758512	miR166	21	UCGGACCAGGCUUCAUUG	101	63	57	15,555
5650228	miR166	21	UUCGGACCAGGCUUCAUUC	11,744	15,440	8,681	4,625
3004100	miR166	21	UCGGACCAGGCUUCAUUC	904,248	635,301	433,744	224,357
	miR166		total^b	933,712	663,895	451,972	268,708

^a Sequences with the more than 100 reads or being the tag with the highest read within the family was designated as abundant miRNAs.

^b Sub-totaled reads within a single miRNA family

(continued)

Table 3. The major sequences and total reads of abundant miRNAs in small RNA libraries constructed from mock- and ORSV-inoculated tissues. (continued)

ID	Family	Size	Sequence	Reads ^a			
				Mi	Mc	Oi	Oc
5236125	miR167	22	UGAAGCUGCCAGCAUGAACUGA	1	0	1	160
4566293	miR167	22	UGAAGCUGCCAGCAUGAGCUGA	0	0	0	222
4686497	miR167	21	UGAAGCUGCCAGCUUGAUCUG	85	148	80	23
1093010	miR167	19	UGAAGCUGCCAGCAUGAUC	149	131	132	33
6578147	miR167	22	UGAAGCUGCCAGCAUGAUCUGG	235	171	63	65
4422450	miR167	21	UGAAGCUGCCAGCAUGAUCUG	985	989	1,074	408
8116347	miR167	22	UGAAGCUGCCAGCAUGAUCUGA	12,690	10,326	9,073	3,335
9798196	miR167	22	UGAAGCUGCCAGCAUGAUCUGU	38,612	37,834	23,906	12,298
	miR167		total^b	53,627	50,378	34,975	17,134
6370317	miR168	22	UCGCUUGGUGCAGGUCGGGACC	40	33	132	7
8616779	miR168	22	UCGCUUGGUGCAGGUCGGGAAA	86	114	56	20
10034897	miR168	22	UCGCUUGGUGCAGGUCGGGAAU	115	103	76	26
1165472	miR168	20	CGCUUGGUGCAGGUCGGGAA	111	125	62	24
10684205	miR168	21	UUCGCUUGGUGCAGGUCGGGA	132	102	87	41
9455314	miR168	20	UCGCUUGGUGCAGGUCGGGA	1,906	2,950	1,390	818
5143698	miR168	21	CGCUUGGUGCAGGUCGGGAAU	2,419	2,742	1,792	587
4108757	miR168	21	UCGCUUGGUGCAGGUCGGGAA	4,278	4,062	2,303	984
5435433	miR168	21	UCGCUUGGUGCAGGUCGGGAU	2,543	2,046	8,940	678
9237120	miR168	21	UCGCUUGGUGCAGGUCGGGAC	2,612	2,053	18,749	500
	miR168		total	14,935	15,089	34,700	4,252
92645	miR169	20	UAGCCAAGGAUGACUUGCCU	449	628	371	157
	miR169		total	492	663	398	179
6992510	miR171	21	UUGAGCCGUGCCAAUAUCGCG	80	137	188	27
901181	miR171	21	UUGAGCCGCGUCAAUUUCUCC	391	509	380	92
	miR171		total	615	877	706	151
5678076	miR172	21	GCUGCAUCAUCAAGAUUCACG	17	23	161	3
8576633	miR172	21	CGAAUCUUGAUGAUGCUGCAU	109	92	64	26
	miR172		total	170	154	284	31
5145149	miR2950	21	UCCAUCUCUUGCACACUGGA	799	847	391	102
	miR2950		total	838	887	421	132
3648109	miR319	23	CUUGGACUGAAGGGAGCUCCCUU	116	187	75	29
3429010	miR319	21	CUUGGACUGAAGGGAGCUCC	181	322	223	55

^a Sequences with the more than 100 reads or being the tag with the highest read within the family was designated as abundant miRNAs. ^b Sub-totaled reads within a single miRNA family (continued)

Table 3. The major sequences and total reads of abundant miRNAs in small RNA libraries constructed from mock- and ORSV-inoculated tissues. (continued)

ID	Family	Size	Sequence	Reads ^a			
				Mi	Mc	Oi	Oc
2288091	miR319	22	UUGGACUGAAGGGAGCUCCCUU	549	952	209	111
9593653	miR319	20	UUGGACUGAAGGGAGCUCCC	1,293	2,290	765	220
2485503	miR319	22	CUUGGACUGAAGGGAGCUCCCU	2,659	5,307	3,962	913
6920538	miR319	21	UUGGACUGAAGGGAGCUCCCU	4,691	9,499	3,147	699
	miR319		total^b	9,750	18,963	8,571	2,372
1365095	miR393	22	UCCAAAGGGAUCGCAUUGAUCU	12,448	15,742	9,182	1,651
	miR393		total	12,868	16,260	9,423	1,878
1879254	miR394	20	UUGGCAUUCUGUCCACCUCC	92	88	69	7
	miR394		total	104	98	92	7
3930814	miR396	21	UUCCACACCUUUCUUGAACUG	53	102	22	6
6948306	miR396	21	UUUCACAGCUUUCUUGAACUG	52	102	29	19
1688761	miR396	19	CCACAGCUUUCUUGAACUG	103	59	40	17
3519222	miR396	21	UUCCAUAGCUUUCUUGAACUG	81	120	38	24
7607118	miR396	21	UUCCACAGCUUUCUUGAGCUG	3	0	3	258
4381227	miR396	22	UUCCACAGCUUUCUUGAACUGC	140	167	64	36
2351483	miR396	21	UUCCACAUCUUCUUGAACUG	144	293	40	42
5534103	miR396	21	UUCCACAGCUUUCUUGAACUC	229	274	74	83
4197730	miR396	19	UUCCACAGCUUUCUUGAAC	387	506	185	130
5944696	miR396	18	CACAGCUUUCUUGAACUG	342	504	170	479
10189858	miR396	21	UUCCACAGCUUUCUUGAACUU	619	727	228	230
6824584	miR396	20	UUCCACAGCUUUCUUGAACU	704	897	527	243
10285039	miR396	21	UUCCACAGCUUUCUUGAACUG	15,500	19,587	5,073	3,896
	miR396		total	19,242	24,366	6,823	6,009
3618747	miR398	21	UAUGUUCUCAGGUCGCCCCUG	54	74	13	6
	miR398		total	102	131	52	134
1359557	miR399	21	UGCCAAAGGAGAGUUGCCCCUG	75	109	54	30
	miR399		total	79	123	64	36
7920685	miR408	22	UGCACUGCCUCUUCCCUGGCUU	730	904	709	275
	miR408		total	820	1,020	801	317
3643220	miR5139	20	GUAACCUGGCUCUGAUACCA	116	39	45	7
9266145	miR5139	23	AUCGGAACCUGGCUCUGAUACCA	175	79	92	24
2057251	miR5139	22	UCGGAACCUGGCUCUGAUACCA	182	93	105	34

^a Sequences with the more than 100 reads or being the tag with the highest read within the family was designated as abundant miRNAs. ^b Sub-totaled reads within a single miRNA family (continued)

Table 3. The major sequences and total reads of abundant miRNAs in small RNA libraries constructed from mock- and ORSV-inoculated tissues. (continued)

ID	Family	Size	Sequence	Reads ^a			
				Mi	Mc	Oi	Oc
5843306	miR5139	18	AACCUGUCUCUGAUACCA	124	172	108	73
601994	miR5139	19	GAACCUGGCUCUGAUACCA	285	158	132	108
3989836	miR5139	22	UCGUAACCUGGCUCUGAUACCA	379	155	218	68
4853865	miR5139	23	AUCGUAACCUGGCUCUGAUACCA	384	168	211	59
6273896	miR5139	21	CGGAACCUGGCUCUGAUACCA	495	169	232	62
4869602	miR5139	23	AUCGAAACCUGGCUCUGAUACCA	404	281	422	124
9098106	miR5139	22	UCGAAACCUGGCUCUGAUACCA	408	354	377	140
357536	miR5139	21	CGUAACCUGGCUCUGAUACCA	920	359	412	103
3515492	miR5139	19	UAACCUGGCUCUGAUACCA	854	455	485	343
8279168	miR5139	18	AACCUGGCUCUGAUACCA	3,970	4,223	2,982	1,282
	miR5139		total^b	9,502	7,252	6,370	2,886
8668768	miR528	21	UGUAAGGGGCAUGCAGAGGAG	8	3	4	7
	miR528		total	18	15	16	28
1824587	miR535	21	UGACAACGAGAGAGAGCACGC	142	121	153	81
3728764	miR535	21	UUGACAAAGAGAGAGAGCACG	171	337	190	77
	miR535		total	352	504	385	185
74087	miR5368	21	AGGGACAGUCUCAGGUAGACC	58	121	32	10
	miR5368		total	181	326	126	58
1874983	miR894	19	UUUCACGUCGGGGUCACCA	75	140	83	13
4649088	miR894	20	GAUUCACGUCGGGUUCACCA	106	167	111	48
5227291	miR894	24	GUUCGUUUCACGUCGGGUUCACCA	216	208	175	59
8533642	miR894	22	UCGUUUCACGUCGGGUUCACCA	229	288	175	82
7118193	miR894	23	UUCGUUUCACGUCGGGUUCACCA	592	572	440	189
6938561	miR894	21	CGUUUCACGUCGGGUUCACCA	579	699	456	200
2584993	miR894	20	GUUUCACGUCGGGUUCACCA	1,013	1,296	762	370
5444280	miR894	19	UUUCACGUCGGGUUCACCA	1,315	2,024	1,379	1,057
	miR894		total	4,627	5,950	3,992	2,423

^a Sequences with the more than 100 reads or being the tag with the highest read within the family was designated as abundant miRNAs.

^b Sub-totaled reads within a single miRNA family

Table 4. Expression fold-changes of some abundant miRNAs in small RNA libraries constructed from mock- and ORSV-inoculated tissues.

miRNA Family	TPM (Tags per million) ^a				FC (miR%) ^b			FC (qRT-PCR) ^c		
	Mi	Mc	Oi	Oc	Mc/Mi	Oi/Mi	Oc/Mc	Mc	Oi	Oc
miR156	392	553	371	229	1.22	1.24	0.99	1.3	3.2	1.9
miR159	58326	78829	38773	12751	1.17	0.87	1.02	1.2	1	1.2
miR162	11490	13906	5717	4517	1.04	0.65	0.73	1.1	1.1	1.1
miR165	393	285	169	168	0.63	0.57	1.18	0.9	1.1	1
miR166	933712	663895	451972	268708	0.61	0.64	0.65	0.9	1	1
miR167	53627	50378	34975	17134	0.81	0.86	1.03	0.8	1.2	1.3
miR168	14935	15089	34700	4252	0.87	3.06	1.01	1.1	2.1 ^d	1.3
miR169	492	663	398	179	1.16	1.06	1.33	1	1	0.7
miR171	615	877	706	151	1.23	1.51	1.08	1	1.5	1.5
miR172	170	154	284	31	0.78	2.20	1.14	0.9	1.2	1
miR319	9750	18963	8571	2372	1.68	1.16	0.84	1.1	1	1.1
miR393	12869	16261	9423	1878	1.09	0.96	1.10	0.9	1	0.9
miR394	104	98	92	7	0.81	1.16	1.42	0.8	1.6	1.6
miR396	19242	24366	6823	6009	1.09	0.47	0.55	1.3	1.2	2.9
miR398	102	131	52	134	1.11	0.67	0.21	0.9	1	0.8
miR408	820	1020	801	317	1.07	1.28	0.94	0.9	1	1
miR5139	9502	7252	6370	2886	0.66	0.88	3.19	0.9	1.1	1.5
miR528	18	15	16	28	0.72	1.17	2.26	0.9	0.5	3.2
miR535	352	504	385	185	1.23	1.44	0.97	1.1	0.9	1
miR894	4627	5950	3992	2423	1.11	1.13	1.65	0.9	1.9	1.5
miR1318	57	78	57	13	1.18	1.32	1.61	- ^e	-	-
miR1511	73	76	36	6	0.90	0.65	0.85	-	-	-
miR158	37	15	4	0	0.35	0.14	15.80	-	-	-
miR164	14	3	18	2	0.18	1.69	7.90	-	-	-
miR2911	47	35	27	645	0.64	0.76	0.87	-	-	-
miR2916	0	1	3	345	-	-	6.77	-	-	-
miR2950	838	887	421	132	0.91	0.66	0.97	-	-	-
miR397	6	6	9	10	0.86	1.97	3.39	-	-	-
miR399	79	123	64	36	1.34	1.07	1.05	-	-	-
miR529	62	26	42	1	0.36	0.89	0.13	-	-	-
miR5368	181	326	126	58	1.55	0.92	1.48	-	-	-

^a Calculated from (reads of a specific family) ÷ (total clean reads) × 1,000,000

^b FC: fold change. Reads of a specific family was first normalized with total miRNA counts within the library, and then compared between libraries to obtain the fold change index.

^c Fold change calculated from qRT-PCR results by $\Delta\Delta Ct$ -method using miR399 as reference and the value of Mi was arbitrarily set as 1.

^d Numbers in red indicates statistical significant ($P \leq 0.05$).

^e -: not determined.

Table 5. Putative target genes of ORSV infection responsive miRNAs.

miRNA Family	Putative target gene ^a	Arabidopsis homolog	Annotation	Biological process
miR156	PATC135707	AT5G50670	SQUAMOSA PROMOTER-BINDING PROTEIN LIKE (SPL) 13	phase transition, regulation of transcription
	PATC143407	AT5G43270	SQUAMOSA PROMOTER BINDING PROTEIN-LIKE (SPL) 2	
	PATC148826			
	PATC153064			
	PATC135103	-	SQUAMOSA PROMOTER-BINDING PROTEIN LIKE (SPL) 12	
	PATC141751	AT3G15270	SQUAMOSA PROMOTER BINDING PROTEIN-LIKE (SPL) 5	
	PATC024123	AT4G20140	GASSHO1 (GSO1)	embryo and epidermis development; protein phosphorylation
	PATC130083	-	PHD-finger homeodomain protein	chromosome organization, regulation of transcription
	PATC136866	AT1G60220	UB-LIKE PROTEASE 1D (ULP1D)	protein desumoylation, cell wall organization, root hair and trichome morphogenesis, response to salt stress
	PATC136943	AT3G26782	mitochondrion located Tetratricopeptide repeat (TPR)-like superfamily protein	unknown
	PATC141616			
	PATC144388	AT5G08170	EMBRYO DEFECTIVE 1873 (EMB1873)	polyamine and putrescine biosynthesis process
	PATC147320	AT4G17830	Peptidase M20/M25/M40 family protein	proteolysis, metabolic process
	PATC149565	AT1G12430	kinesin-like protein (PAK)	flower morphogenesis, microtubule-based movement
	PATC161070	AT5G40840	Sister chromatid cohesion 1	cell cycle process
	PATC012624	-	hypothetical protein	unknown
	PATC042847	-	hypothetical protein	unknown
PATC049704	-	hypothetical protein	unknown	
PATC133938	-	predicted protein	unknown	
PATC134878	-	hypothetical protein	unknown	
miR168	PATC143303	AT1G48410	ARGONAUTE 1 (AGO1)	RNA silencing
miR171	PATC143284	AT4G00150	HAIRY MERISTEM 3 (HAM3) / LOST MERISTEMS 3 (LOM3)	cell differentiation
	PATC149190			
	PATC149532			
	PATC154363	AT3G13670	Protein kinase family protein	protein phosphorylation
	PATC049290	AT4G08250	GRAS family transcription factor	regulation of transcription
PATC023657	-	GRAS family transcription factor (GRAS40)	regulation of transcription	
PATC124992	-	hypothetical protein	unknown	

(continued)

Table 5. Putative target genes of ORSV infection responsive miRNAs. (continued)

miRNA Family	Putative target gene ^a	Arabidopsis homolog	Annotation	Biological process
miR5139	PATC139307	AT1G48710	copla-like retrotransposon	unknown
	PATC156350	AT2G24940	membrane-associated progesterone binding protein 2 (MAPR2)	heme binding
	PATC022793	-	predicted protein	unknown
	PATC143291	-	hypothetical protein	unknown
miR528	PATC127027	AT1G71440	chloroplast localized tubulin-folding cofactor E	cytokinesis, tubulin complex assembly
	PATC156396			
miR535	PATC126341	AT5G28150	nucleus localized unknown protein	unknown
	PATC127350	AT1G80550	mitochondrion localized Pentatricopeptide repeat (PPR) superfamily protein	unknown
	PATC127615	AT1G27600	IRREGULAR XYLEM 9 HOMOLOG (I9H)	glucuronoxylan biosynthesis, protein glycosylation, secondary cell wall biogenesis
	PATC128040	AT2G12400	plasmodesmo local localized unknown protein	unknown
	PATC128688	AT1G10960	Ferredoxin 1 (FD1)	ABA biosynthetic process, electron transport chain
	PATC129893	AT1G74530	chloroplast localized unknown protein	unknown
	PATC130349	AT4G19880	Glutathione S-transferase family protein	response to cadmium ion
	PATC130662	AT1G72340	NagB/RpiA/CoA transferase-like superfamily protein	cellular metabolic process, translational initiation
	PATC133246	AT4G14480	Protein kinase superfamily protein	protein phosphorylation
	PATC134561	AT5G13770	Pentatricopeptide repeat (PPR-like) superfamily protein	chloroplast organization
	PATC135523	AT2G03530	UREIDE PERMEASE 2 (UPS2)	uracil:cation symporter activity
	PATC138376	AT5G19940	Plastid-lipid associated PAP/fibrillin family protein	light reaction, regulation of protein dephosphorylation
	PATC138531	AT2G14850	nucleus localized unknown protein	unknown
	PATC138729	AT2G38920	SPX (SYG1/Pho81/XPR1) domain-containing zinc finger protein	response to phosphate starvation, fatty acid catabolic process, phosphate ion transport
	PATC142441	AT1G34120	MYO-INOSITOL POLYPHOSPHATE 5-PHOSPHATASE 1 (IP5P1)	inositol trisphosphate metabolic process
	PATC145620	AT5G07120	SORTING NEXIN 2B (SNX2B)	signal transduction, vesicle-mediated transport
	PATC146667	AT3G04070	NAC domain containing protein 47 (NAC047)	organ senescence, amino acid transport
	PATC147167	AT1G74530	chloroplast localized unknown protein	unknown
	PATC151754	-	reverse transcriptase	unknown
	PATC152377	-	predicted retrotransposon	unknown
PATC154063	AT4G34660	SH3 domain-containing protein	clathrin binding	

^a Orchidstra database (<http://orchidstra.abrc.sinica.edu.tw>) accession numbers. Targets also reported in *A. thaliana* were indicated in bold.

Table 6. Summary of total reads in small RNA libraries constructed from mock-, CymMV-, and CymMV and ORSV mixedly-inoculated tissues.

	Mi-2 ^a	Mc-2	Ci	Cc	Di	Dc	Dsc
raw data input							
Total reads	5,384,213	5,230,602	5,049,276	5,680,202	5,326,905	5,312,076	5,233,409
Poor quality reads filtered ^b	5,093,963	4,964,619	4,853,176	5,471,939	5,183,147	5,126,864	4,960,095
15-27 nt	4,261,332	3,878,205	3,979,112	4,435,124	4,423,049	4,160,257	4,051,878
low frequency reads filtered ^c	3,644,782	3,343,199	3,270,176	3,674,964	3,879,317	3,618,508	3,382,737
sRNAs from microbes							
Contaminants ^d	903	1,089	808	882	554	1,177	855
ORSV ^e	1	3	6	10	514,753 (13.27%)	294 (0.01%)	76 (<0.01%)
CymMV	5	13	190,786 (5.83%)	858 (0.02%)	1,082,211 (27.9%)	283,087 (7.82%)	60 (<0.01%)
CMV ^f	2	1	3	0	2	1	0
TSWV	0	1	0	1	1	1	1
sRNAs from <i>Phalaenopsis</i>							
clean reads ^g	3,643,873	3,342,094	3,078,576	3,673,214	2,281,799	3,333,950	3,381,746
<i>P. aphrodite</i> ESTs	2,169,102	2,025,187	1,729,124	2,152,097	1,068,763	1,883,749	2,018,058
structure RNA (Rfam)	342,694	310,040	241,965	315,070	299,037	370,710	273,268
<i>P. aphrodite</i> chloroplast	150,321	138,323	197,080	203,601	101,502	211,942	199,328
miRNA ^h	1,308,744 (35.92%)	1,198,256 (35.85%)	1,020,228 (33.14%)	1,304,899 (35.53%)	481,727 (21.11%)	1,004,585 (30.13%)	1,137,795 (33.65%)

^a Mi-2, Ci, Di: inoculated (i) tissues of mock (M)-, CymMV (C)-, and doubly (D)-inoculated plants. Mc-2, Cc, Dc, Dsc: non-inoculated (c) tissues of mock (M)-, CymMV (C)-, and doubly (D)-inoculated plants.

^b Adapter trimming and removal of poly-A/T/C/G or N (null)-calling bases containing tas.

^c Reads with only 1 counts is defined as low frequency reads and filtered before further analysis.

^d Reads matched to *Escherichia coli* and other microbes.

^e The numbers in grey stand for the percentage of ORSV and CymMV viral siRNAs in low frequency reads - filtered totalsmall RNAs.

^f Besides *Cymbidium mosaic virus* (CymMV) and *Odontoglossum ringspot virus* (ORSV), matching reads to genomes of some prevalent orchid viruses [*Capsicum chlorotic virus* (CaCV), *Carnation mosaic virus* (CarMV), *Cucumber mosaic virus* (CMV), *Impatiens necrotic spot virus* (INSV), *Orchid fleck virus* (OFV), *Phalaenopsis chlorotic spot virus* (PhCSV), and *Tomato spotted wilt virus* (TSWV)] was performed and only perfect matched reads are shown.

^g Contaminants and viral siRNA excluded reads. ^h The numbers in grey stand for the percentage of miRNAs in total clean reads.

Table 7. Summary of total unique reads in small RNA libraries constructed from mock-, CymMV-, and CymMV and ORSV mixedly-inoculated tissues.

	Mi-2 ^a	Mc-2	Ci	Cc	Di	Dc	Dsc
raw data input							
Total unique reads (tags)	1,419,817	1,320,711	1,521,218	1,635,298	1,310,002	1,321,948	1,475,658
Poor quality filtered tags ^b	1,243,341	1,122,813	1,369,862	1,449,080	1,090,673	1,139,151	1,315,318
15-27 nt	1,188,722	1,046,333	1,301,852	1,375,690	982,234	1,067,940	1,238,779
low frequency tags filtered ^c	572,172	511,327	592,916	615,530	438,502	526,191	569,638
sRNAs from microbes							
Contaminants ^d	397	534	419	400	263	455	447
ORSV	1	3	6	9	383,337	268	72
CymMV	5	13	14,801	618	31,964	18,920	57
CMV ^e	1	1	2	0	1	1	0
TSWV	0	1	0	1	1	1	1
sRNAs from <i>Phalaenopsis</i>							
clean tags ^f	571,769	510,777	577,690	614,503	367,938	506,548	569,062
<i>P. aphrodite</i> ESTs	99,030	89,803	99,431	106,978	73,390	95,591	100,539
structure RNA (Rfam)	22,690	22,591	22,186	24,647	22,617	25,641	23,438
<i>P. aphrodite</i> chloroplast	12,640	12,073	11,938	13,073	8,829	14,012	11,234
miRNA (tag counts)	1,830	1,913	2,291	2,316	1,652	1,993	2,003
miRNA (family categories)	69	67	79	70	66	59	62

^a Mi-2, Ci, Di: inoculated (i) tissues of mock (M)-, CymMV (C)-, and doubly (D)-inoculated plants. Mc-2, Cc, Dc, Dsc: non-inoculated (c) tissues of mock (M)-, CymMV (C)-, and doubly (D)-inoculated plants.

^b Adapter trimming and removal of poly-A/T/C/G or N (null)-calling bases containing tags.

^c Reads with only 1 counts is defined as low frequency reads and filtered before further analysis.

^d Reads matched to *Escherichia coli* and other microbes.

^e Besides *Cymbidium mosaic virus* (CymMV) and *Odontoglossum ringspot virus* (ORSV), matching reads to genomes of some prevalent orchid viruses [*Capsicum chlorotic virus* (CaCV), *Carnation mosaic virus* (CarMV), *Cucumber mosaic virus* (CMV), *Impatiens necrotic spot virus* (INSV), *Orchid fleck virus* (OFV), *Phalaenopsis chlorotic spot virus* (PhCSV), and *Tomato spotted wilt virus* (TSWV)] was performed and only perfect matched reads are shown.

^f Contaminants and viral siRNA excluded tags.

Table 8. Potential ORSV vsRNA targeting *Phalaenopsis* genes.

ID	library ^a	Site ^b	Score ^c	MFE ratio ^d	vsRNA 3'-5'	Target ^e	Target site	Target annotation
9472785	Di	1498-1478	3	0.984	AGUUUUUAA-ACUGCUA-UGUCA	PATC146758	832-854	AtBRCA1, an ortholog of the human breast cancer susceptibility gene 1
10176148	Di	5999-6019	3	0.804	AG-AUGGAGCUAAUAAGAUAAU	PATC149930	219-240	Ureide permease 2, Mediate high-affinity uracil and 5-FU (a toxic uracil analogue) transport
3373159	Di	3320-3340	3	0.783	CCCAGUAGUCGGACAAUAG	PATC126788	1-19	OSBP(oxysterol binding protein)-related protein 4B (ORP4B), involved in steroid metabolic process
8699519	Di	1085-1105	3	0.742	UCGUAACGGUUUCA- AAGAAU	PATC137286	308-329	Ribosomal L38e protein family, involved in translation and ribosome biogenesis
10176148	Di	5999-6019	3.5	0.897	AGA-UGGAGCUAAUAA-GAUA-AU	PATC068319	650-673	di- and tri-peptide transporter involved in responses to wounding, virulent bacterial pathogens, and high NaCl concentrations
8125631	Di	634-614	3.5	0.874	UCUGACAAGAAUGAGGCAAC-U	PATC127112	818-839	EUKARYOTIC TRANSLATION INITIATION FACTOR 2 BETA SUBUNIT (EIF2 BETA)
8125631	Di	634-614	3.5	0.874	UCUGACAAGAAUGAGGCAAC-U	PATC127113	795-816	EUKARYOTIC TRANSLATION INITIATION FACTOR 2 BETA SUBUNIT (EIF2 BETA)
8125631	Di	634-614	3.5	0.874	UCUGACAAGAAUGAGGCAAC-U	PATC140938	351-372	EUKARYOTIC TRANSLATION INITIATION FACTOR 2 BETA SUBUNIT (EIF2 BETA)
840672	Di	1019-999	3.5	0.863	CUA-UGAAUA-AAGGAA-AAGGCU	PATC137746	695-718	NAD(P)-binding Rossmann-fold superfamily protein, involved in oxidation reduction
1072910	Di	2226-2246	3.5	0.824	CCG-UGGUAUCUGUAGGAAAUC	PATC104536	55-76	disulfide isomerase 2 precursor

^a Indicating the from which the library vsRNA tag was in the top 50 abundant list.

^b The viral genome position of the vsRNA. Sites are based on genomic sequence of a Taiwan strain (DQ139262).

^c Position-dependent scoring matrix for miRNA:mRNA pairing assessment described by Fahlgren and Carrington (2010).

^d MFE ratio = $\Delta G_{\text{target}}/\Delta MFE$, the ratio between minimum folding energy for the vsRNA:mRNA duplex and a hypothetical perfect paired duplex of the vsRNA.

^e Orchidstra database (<http://orchidstra.abrc.sinica.edu.tw>) accession numbers of potential targets.

(continued)

Table 8. Potential ORSV vsRNA targeting *Phalaenopsis* genes. (continued)

ID	library ^a	Site ^b	Score ^c	MFE ratio ^d	vsRNA 3'-5'	Target ^e	Target site	Target annotation
8850722	Di	2662-2642	3.5	0.821	C-UCUCGAUUAUU-CAGACCUGU	PATC127561	364-386	structural core component of a COMPASS-like H3K4 histone methylation complex that is also involved in the timing of the floral transition and in leaf morphogenesis
7907315	Di	2575-2595	3.5	0.814	GGAGUAGUUUUAAGUGUCAAA	PATC071828	280-300	F-box/RNI-like superfamily protein
10176148	Di	5999-6019	3.5	0.772	AGAUGGAGCUA-AUAAGAUAAU	PATC145084	1821-1842	cellular apoptosis susceptibility protein, putative
10176148	Di	5999-6019	3.5	0.772	AGAUGGAGCUA-AUAAGAUAAU	PATC150396	3146-3167	cellular apoptosis susceptibility protein, putative
9472785	Di	1498-1478	3.5	0.769	AGUUUUUAAACUGCUAUGUCA	PATC155862	101-121	SNF1-related protein kinase
6720991	Di	3310-3330	3.5	0.757	GAAACUGCUCUCCUAG--CUCUU	PATC142665	618-640	N-ethylmaleimide sensitive factor
8540758	Di	1727-1747	3.5	0.739	UC-AAGGCUAUUUC-GUAAUAUU	PATC127377	1275-1297	class I tRNA synthetase, involved in response to cadmium ion and tRNA aminoacylation for protein translation
8540758	Di	1727-1747	3.5	0.739	UC-AAGGCUAUUUC-GUAAUAUU	PATC156769	1275-1297	class I tRNA synthetase, involved in response to cadmium ion and tRNA aminoacylation for protein translation
8540758	Di	1727-1747	3.5	0.739	UC-AAGGCUAUUUC-GUAAUAUU	PATC157924	1275-1297	class I tRNA synthetase, involved in response to cadmium ion and tRNA aminoacylation for protein translation
840672	Di	1019-999	3.5	0.737	CUAUGAAU-AAA-GGAAAAGGCU	PATC155842	550-572	CCHC-type zinc finger protein
7907315	Di	2575-2595	3.5	0.73	GGAGUAGUUUUAAGUGUCAAA	PATC031461	185-205	eukaryotic translation initiation factor 1

^a Indicating the from which the library vsRNA tag was in the top 50 abundant list

^b The viral genome position of the vsRNA. Sites are based on genomic sequence of a Taiwan strain (DQ139262).

^c Position-dependent scoring matrix for miRNA:mRNA pairing assessment described by Fahlgren and Carrington(2010).

^d MFE ratio = $\Delta G_{\text{target}}/\Delta MFE$, the ratio between minimum folding energy for the vsRNA:mRNA duplex and a hypothetical perfect paired duplex of the vsRNA.

^e Orchidstra database (<http://orchidstra.abrc.sinica.edu.tw>) accession numbers of potential targets.

(continued)

Table 8. Potential ORSV vsRNA targeting *Phalaenopsis* genes. (continued)

ID	library ^a	Site ^b	Score ^c	MFE ratio ^d	vsRNA 3'-5'	Target ^e	Target site	Target annotation
4561576	Oi,Di	5833-5854	3	0.81	UGUCAAA-CAAGCUCGAACAACAC	PATC038602	121-143	UDP-Glycosyltransferase superfamily protein
9392694	Oi	5832-5852	1.5	0.927	UCAA-CAAGCUCGAACAACACA	PATC038602	123-144	UDP-Glycosyltransferase superfamily protein
280101	Oi	5842-5862	2.5	0.744	CGACAACUUGUCAACAAGCUC	PATC148505	714-734	Pentatricopeptide repeat (PPR) superfamily protein
280101	Oi	5842-5862	2.5	0.744	CGACAACUUGUCAACAAGCUC	PATC148513	1256-1276	Pentatricopeptide repeat (PPR) superfamily protein
1706093	Oi	6158-6178	3	0.969	UCAG-GUCUGUAGCAGAG-UUUA	PATC155374	33-55	Zinc-binding ribosomal protein family protein, involved in translation and ribosome biogenesis
7719063	Oi	6162-6142	3	0.924	ACAUGUUAGUUCAGAGUA-A-AC	PATC139687	1793-1815	glucose6-Phosphate/phosphate transporter 2
7719063	Oi	6162-6142	3	0.924	ACAUGUUAGUUCAGAGUA-A-AC	PATC155499	1142-1164	glucose6-Phosphate/phosphate transporter 2
7719063	Oi	6162-6142	3	0.924	ACAUGUUAGUUCAGAGUA-A-AC	PATC156934	1138-1160	glucose6-Phosphate/phosphate transporter 2
7719063	Oi	6162-6142	3	0.924	ACAUGUUAGUUCAGAGUA-A-AC	PATC157953	822-844	glucose6-Phosphate/phosphate transporter 2
845480	Oi	6156-6176	3	0.876	AG-GUCUGUAGCAGAG-UUUACU	PATC155374	35-57	Zinc-binding ribosomal protein family protein, involved in translation and ribosome biogenesis
6947413	Oi	4900-4920	3	0.846	UUUAAGUC-UCUAAAACUACGA	PATC130390	300-321	YUCCA6 (YUC6), oxidoreductase activity. Involved in auxin biosynthetic process
1706093	Oi	6158-6178	3	0.82	UCAG-GUCUGUAGCAGAGUUUA	PATC155374	33-54	Zinc-binding ribosomal protein family protein, involved in translation and ribosome biogenesis
280101	Oi	5842-5862	3	0.768	CGA-CAACUUGUCAACAAGCUC	PATC138320	116-137	Urb2/Npa2, involved in nucleolar 27S pre-rRNA processing

^a Indicating the from which the library vsRNA tag was in the top 50 abundant list.

^b The viral genome position of the vsRNA. Sites are based on genomic sequence of a Taiwan strain (DQ139262).

^c Position-dependent scoring matrix for miRNA:mRNA pairing assessment described by Fahlgren and Carrington(2010).

^d MFE ratio = $\Delta G_{\text{target}}/\Delta MFE$, the ratio between minimum folding energy for the vsRNA:mRNA duplex and a hypothetical perfect paired duplex of the vsRNA.

^e Orchidstra database (<http://orchidstra.abrc.sinica.edu.tw>) accession numbers of potential targets.

(continued)

Table 8. Potential ORSV vsRNA targeting *Phalaenopsis* genes. (continued)

ID	library ^a	Site ^b	Score ^c	MFE ratio ^d	vsRNA 3'-5'	Target ^e	Target site	Target annotation
81070	Oi	6043-6063	3	0.746	CUCAACGUAGAUUACAAAG-GC	PATC153187	3145-3166	WD-40 repeat family protein, involved in vesicle-mediated transport and methylation
2180236	Oi	992-1012	3.5	1.009	UC--CUUUAUUCAUAGAUGGA-AC	PATC143800	5772-5795	armadillo (ARM) repeat superfamily protein
1960633	Oi	2443-2423	3.5	0.932	CCGGC-AGAGAA-GUCU-AAGGGA	PATC126327	357-380	PECTIN METHYLESTERASE 1 (PME1)
5032603	Oi	89-110	3.5	0.886	UGG-UCGGAGU-UAUUGAAACAAC	PATC146635	3446-3469	aminoacyl-tRNA ligases, involved in tRNA aminoacylation for protein translation
6947413	Oi	4900-4920	3.5	0.834	UUUAAGUCUCUAAAACUA-CGA	PATC128836	522-543	STARCH-EXCESS 4 (SEX4), a plant-specific glucan phosphatase
6947413	Oi	4900-4920	3.5	0.804	UUUA-AGUCUCUAAAACUACGA	PATC132649	1230-1251	armadillo (ARM) repeat superfamily protein
6947413	Oi	4900-4920	3.5	0.767	UUUAAGUCUCUA-AAACUACGA	PATC145869	368-389	zinc finger-homeodomain transcription factor ZHD5
5145985	Oi	6272-6292	3.5	0.75	UUUUGGGAAGCUAAAUUCACC	PATC138657	103-123	DWD(DDB1 binding WD40) protein, involved in the negative regulation of ABA responses

^a Indicating the from which the library vsRNA tag was in the top 50 abundant list.

^b The viral genome position of the vsRNA. Sites are based on genomic sequence of a Taiwan strain (DQ139262).

^c Position-dependent scoring matrix for miRNA:mRNA pairing assessment described by Fahlgren and Carrington(2010).

^d MFE ratio = $\Delta G_{\text{target}}/\Delta MFE$, the ratio between minimum folding energy for the vsRNA:mRNA duplex and a hypothetical perfect paired duplex of the vsRNA.

^e Orchidstra database (<http://orchidstra.abrc.sinica.edu.tw>) accession numbers of potential targets.

Table 9. Potential Di library-specific ORSV vsRNA targeting *Phalaenopsis* genes.

ID	Site ^a	Score ^b	MFE ratio ^c	vsRNA 3'-5'	Target ^d	Target site	Target annotation
2979262	1902-1921	2	0.974	CCACUUUCUCGUAGGCUAAU	PATC125276	130-149	Zinc finger C-x8-C-x5-C-x3-H type family protein, functions in zinc ion binding and nucleic acid binding
5497155	5479-5498	2.5	0.792	UCGGAUCGUCGGUAUCCUUG	PATC129343	101-120	flavin-dependent monooxygenases (FMO), is required for full expression of TIR-NB-LRR conditioned resistance to avirulent pathogens
5497155	5479-5498	2.5	0.778	UCGGAUCGUCGGUAUCCUUG	PATC126936	477-496	oxidoreductase, 2OG-Fe(II) oxygenase family protein
2452139	5480-5498	2.5	0.776	UCGGAUCGUCGGUAUCCUU	PATC129343	101-119	flavin-dependent monooxygenases (FMO), is required for full expression of TIR-NB-LRR conditioned resistance to avirulent pathogens
2452139	5480-5498	2.5	0.762	UCGGAUCGUCGGUAUCCUU	PATC126936	477-495	oxidoreductase, 2OG-Fe(II) oxygenase family protein
2452139	5480-5498	3	0.796	UCGGAUCGUCGGUAUCCUU	PATC143200	1233-1251	armadillo (ARM) repeat superfamily protein
3512506	2866-2847	3.5	1.004	AAAUAUUUGU--CUCACCGUUU	PATC138651	544-565	LOB domain-containing protein 15, involved in leaf morphogenesis
2880184	4577-4558	3.5	0.98	UCCGUUUUAAUAUAGCA--UUC	PATC139502	755-776	CONSTITUTIVE PHOTOMORPHOGENIC 1 (COP1), represses photomorphogenesis and induces skotomorphogenesis in the dark
4606561	1902-1922	3.5	0.924	GCCACUUUCUCGUAGGCUAAU	PATC137889	395-415	arogenate dehydrogenase, involved in tyrosine biosynthetic process
2979262	1902-1921	3.5	0.918	CCACUUUCUCGUAGGCUAAU	PATC137889	396-415	arogenate dehydrogenase, involved in tyrosine biosynthetic process

^a The viral genome position of the vsRNA. Sites are based on genomic sequence of a Taiwan strain (DQ139262).

^b Position-dependent scoring matrix for miRNA:mRNA pairing assessment described by Fahlgren and Carrington(2010).

^c MFE ratio = $\Delta G_{\text{target}}/\Delta MFE$, the ratio between minimum folding energy for the vsRNA:mRNA duplex and a hypothetical perfect paired duplex of the vsRNA.

^d Orchidstra database (<http://orchidstra.abrc.sinica.edu.tw>) accession numbers of potential targets.

(continued)

Table 9. Potential Di library-specific ORSV vsRNA targeting *Phalaenopsis* genes. (continued)

ID	Site ^a	Score ^b	MFE ratio ^c	vsRNA 3'-5'	Target ^d	Target site	Target annotation
8455787	5479-5500	3.5	0.795	ACUCGGAUCGUCGGUAUCCUUG	PATC129343	99-120	flavin-dependent monooxygenases (FMO), is required for full expression of TIR-NB-LRR conditioned resistance to avirulent pathogens
10193462	5480-5502	3.5	0.79	GAACUCGGAUCGUCGGUA--UCCUU	PATC137498	1036-1060	galacturonosyltransferase
2979262	1902-1921	3.5	0.755	CCACUUUCUCGUAGGCUA-UU	PATC146573	405-425	DEG15 protease, responsible for peroxisomal processing
2452139	5480-5498	3.5	0.738	UCGGAUCGUCGGUA--UCCUU	PATC137498	1040-1060	galacturonosyltransferase

^a The viral genome position of the vsRNA. Sites are based on genomic sequence of a Taiwan strain (DQ139262).

^b Position-dependent scoring matrix for miRNA:mRNA pairing assessment described by Fahlgren and Carrington(2010).

^c MFE ratio = $\Delta G_{\text{target}}/\Delta MFE$, the ratio between minimum folding energy for the vsRNA:mRNA duplex and a hypothetical perfect paired duplex of the vsRNA.

^d Orchidstra database (<http://orchidstra.abrc.sinica.edu.tw>) accession numbers of potential targets.

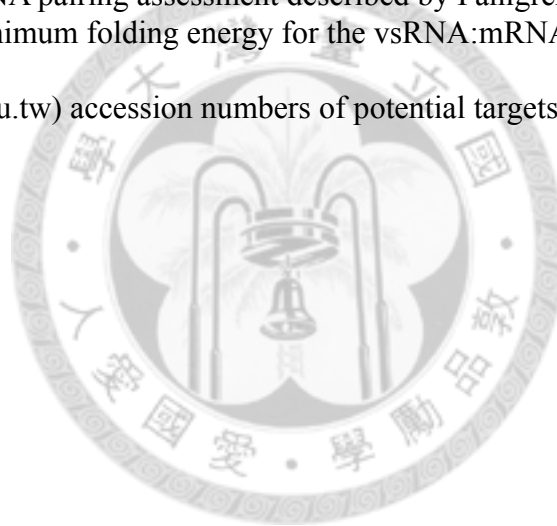


Table 10. Potential CymMV vsRNA targeting *Phalaenopsis* genes.

ID	library ^a	Site ^b	Score ^c	MFE ratio ^d	vsRNA 3'-5'	Target ^e	Target site	Target annotation
8552386	Di	1533-1553	0.5	0.917	ACAGAUCUCCUAGUUUCAAC	PATC096516	3-23	beta-galactosidase 2 (BGAL2), involved in lactose catabolic and carbohydrate metabolic process process
7846663	Di	1377-1357	3	1.006	UCUGGAUGG--UACGCUACUUAU	PATC157852	499-521	ADP-ribosylation factor
3391029	Di	2451-2468	3.5	0.913	GUCGAUGUAAUGCCACC-C	PATC108415	7-25	glycoside hydrolase family 13 andglycosyltransferase
4702849	Di	2166-2188	3.5	0.837	CGAAGGCUA-GAAUAACUCGGUCA	PATC125780	924-947	FAD-binding Berberine family protein, involved in oxidation reduction
7935383	Di	216-236	3.5	0.828	G-CUCUAAAAGCUCUGUCAGCC	PATC137910	2199-2220	Transducin/WD40 repeat-like superfamily protein
34729	Di	168-188	3.5	0.785	UCAA AUGCUCA-CGGCUC CGUU	PATC140675	1834-1855	Ortholog of breast cancer susceptibility protein 2, essential at meiosis.
3618470	Di	1947-1967	3.5	0.76	AGGGUC-AGGAUGAU AAGAAUU	PATC128821	920-941	RNase III-like enzyme that catalyzes processing of trans-acting small interfering RNA precursors
6827705	Di	2568-2588	3.5	0.755	GAACGAAGUAAGAUCUCCAU	PATC134966	2119-2139	Homeodomain protein required for ovule identity
3391029	Di	2451-2468	3.5	0.748	GUCGAUGUAAUGCCACC-C	PATC136376	308-326	single cystathionine beta-synthase domain-containing protein. Modulates development by regulating the thioredoxin system.
9389731	Dc	3044-3065	0	1	CCCAAAGCAGGAAACGACAAC	PATC108373	47-68	metal homeostasis related oligopeptide transporter
8181372	Di,Dc	572-593	3	0.752	CCCAACGGUCGUCUAAAAGUC	PATC143230	265-286	Galactose mutarotase-like superfamily protein, involved in galactose, hexose, carbohydrate metabolic process

^a Indicating the from which the library vsRNA tag was in the top 50 abundant list.

^b The viral genome position of the vsRNA. Sites are based on genomic sequence of the Taichung strain.

^c Position-dependent scoring matrix for miRNA:mRNA pairing assessment described by Fahlgren and Carrington(2010).

^d MFE ratio = $\Delta G_{\text{target}}/\Delta MFE$, the ratio between minimum folding energy for the vsRNA:mRNA duplex and a hypothetical perfect paired duplex of the vsRNA.

^e Orchidstra database (<http://orchidstra.abrc.sinica.edu.tw>) accession numbers of potential targets.

(continued)

Table 10. Potential CymMV vsRNA targeting *Phalaenopsis* genes. (continued)

ID	library ^a	Site ^b	Score ^c	MFE ratio ^d	vsRNA 3'-5'	Target ^e	Target site	Target annotation
8984112	Di,De	3204-3224	3.5	0.805	UCUCUGCUGCAAGUUUUCCUU	PATC132840	1195-1215	chloroplastic glutaminyl-tRNA synthase, involved in translation
1645244	Ci,De	4510-4490	0	1	AAGAGUGUGUCAGGGUGUAAC	PATC090502	580-600	hexosaminidase
1645244	Ci,De	4510-4490	0	1	AAGAGUGUGUCAGGGUGUAAC	PATC115656	769-789	geranyl diphosphate synthase
1645244	Ci,De	4510-4490	0	1	AAGAGUGUGUCAGGGUGUAAC	PATC117468	249-269	lysine-sensitive aspartate kinase
5324354	Ci,De	3221-3241	3	0.875	UCG-AA-ACGUCUACAAGGUCUC	PATC130795	1381-1403	xyloglucan galactosyltransferase responsible for actin organization and the synthesis of cell wall materials
1608330	Ci,De	3187-3207	3.5	0.913	CCUUG-UCCGAGUACUCCAUCU	PATC129995	1031-1052	SKP1 interacting partner (SKIP4), response to cold
1341912	Ci,Di	3762-3782	3.5	0.801	U-CGUAAGUCAUAAC-CGCAGCU	PATC140948	610-632	Acyl-CoA independent ceramide synthase
1341912	Ci,Di	3762-3782	3.5	0.801	U-CGUAAGUCAUAAC-CGCAGCU	PATC239643	263-285	Acyl-CoA independent ceramide synthase
525483	Ci	2930-2951	0	1	CCAGUUCACGUCUUUAUGCAUU	PATC189557	5-26	26S ribosomal RNA gene
10058797	Ci	1059-1038	3	0.918	CCGUUAACUAGGG-CUGAA-GACU	PATC147592	307-330	ATP-dependent MRP-like ABC transporter able to transport glutathione-conjugates as well as chlorophyll catabolites
3738595	Ci	3508-3528	3	0.854	AGGAGGCCUCAGAAAA--GUGUU	PATC140493	981-1003	RNA-binding KH domain-containing protein
3738595	Ci	3508-3528	3	0.778	AGGAG-GCCUCAGAAAAGUGUU	PATC135541	162-183	putative cytochrome P450

^a Indicating the from which the library vsRNA tag was in the top 50 abundant list.

^b The viral genome position of the vsRNA. Sites are based on genomic sequence of the Taichung strain.

^c Position-dependent scoring matrix for miRNA:mRNA pairing assessment described by Fahlgren and Carrington(2010).

^d MFE ratio = $\Delta G_{\text{target}}/\Delta \text{MFE}$, the ratio between minimum folding energy for the vsRNA:mRNA duplex and a hypothetical perfect paired duplex of the vsRNA.

^e Orchidstra database (<http://orchidstra.abrc.sinica.edu.tw>) accession numbers of potential targets.

(continued)

Table 10. Potential CymMV vsRNA targeting *Phalaenopsis* genes. (continued)

ID	library ^a	Site ^b	Score ^c	MFE ratio ^d	vsRNA 3'-5'	Target ^e	Target site	Target annotation
4798235	Di,Dc,Ci	1526-1546	0	1	UCCUAGUUUCAACCCCGUU	PATC096516	10-30	beta-galactosidase 2 (BGAL2), involved in lactose catabolic and carbohydrate metabolic process process
1254676	Di,Dc,Ci	2933-2953	0	1	GUCCAGUUCACGUCUUUAUGC	PATC189557	3-23	26S ribosomal RNA gene
8297013	Di,Dc,Ci	2830-2850	0.5	1	UCGGCAAGUCAACAAGGAGU	PATC182738	4-24	abscisic acid response protein
2838623	Di,Dc,Ci	4670-4690	0.5	0.95	ACCCACGCUGAUCUCAUCAUC	PATC115131	23-43	basic helix-loop-helix (bHLH) DNA-binding superfamily protein
938095	Di,Dc,Ci	867-887	1	0.946	GCUUACAGGCGUCAAACCCAC	PATC103314	21-41	Phosphoglucomutase
2838623	Di,Dc,Ci	4670-4690	1	0.85	ACCCACGCUGAUCUCAUCAUC	PATC094296	3-23	iron/ascorbate-dependent oxidoreductase
2838623	Di,Dc,Ci	4670-4690	1	0.85	ACCCACGCUGAUCUCAUCAUC	PATC105182	3-23	SAP domain-containing protein, functions in nucleic acid binding
2838623	Di,Dc,Ci	4670-4690	1	0.85	ACCCACGCUGAUCUCAUCAUC	PATC107513	23-43	chromatin remodeling 24 (CHR24), helicase activity
8206317	Di,Dc,Ci	3078-3098	2	1.022	AUCUCUCAGAUCGCAGAU-A-C-C	PATC091436	16-38	TOPLESS-related 2 (TPR2), involved in primary shoot apical meristem specification
8206317	Di,Dc,Ci	3078-3098	2	1.022	AUCUCUCAGAUCGCAGAU-A-C-C	PATC108373	14-36	metal homeostasis related oligopeptide transporter
8206317	Di,Dc,Ci	3078-3098	2	0.865	AUCUCUCAGAUCGCAGAUACC	PATC091436	16-36	TOPLESS-related 2 (TPR2), involved in primary shoot apical meristem specification
8206317	Di,Dc,Ci	3078-3098	2	0.865	AUCUCUCAGAUCGCAGAUACC	PATC108373	14-34	metal homeostasis related oligopeptide transporter

^a Indicating the from which the library vsRNA tag was in the top 50 abundant list.

^b The viral genome position of the vsRNA. Sites are based on genomic sequence of the Taichung strain.

^c Position-dependent scoring matrix for miRNA:mRNA pairing assessment described by Fahlgren and Carrington(2010).

^d MFE ratio = $\Delta G_{\text{target}}/\Delta MFE$, the ratio between minimum folding energy for the vsRNA:mRNA duplex and a hypothetical perfect paired duplex of the vsRNA.

^e Orchidstra database (<http://orchidstra.abrc.sinica.edu.tw>) accession numbers of potential targets.

(continued)

Table 10. Potential CymMV vsRNA targeting *Phalaenopsis* genes. (continued)

ID	library ^a	Site ^b	Score ^c	MFE ratio ^d	vsRNA 3'-5'	Target ^e	Target site	Target annotation
8206317	Di,Dc,Ci	3078-3098	3	0.845	AUCUCUCAGAUCGCAGAUACC	PATC091436	16-36	TOPLESS-related 2 (TPR2), involved in primary shoot apical meristem specification
8206317	Di,Dc,Ci	3078-3098	3	0.845	AUCUCUCAGAUCGCAGAUACC	PATC108373	14-34	metal homeostasis related oligopeptide transporter
2715066	Di,Dc,Ci	2954-2974	3	0.818	GAGCGCUCUCACGAAAAGGCC	PATC154905	611-631	ribosomal protein S5
1216119	Di,Dc,Ci	950-970	3.5	0.978	UCGAGAUGCA-AAC-CUGUUACC	PATC127960	847-869	GDSL-like Lipase/Acylhydrolase superfamily protein, involved in lipid metabolic process
2384603	Di,Dc,Ci	1040-1060	3.5	0.963	GAGUCUUCAGCCCUAG-UUAAC	PATC155458	3798-3819	LMBR1-like membrane protein
1254676	Di,Dc,Ci	2933-2953	3.5	0.927	GUCCAGUUCACGUCU--UUAUGC	PATC139961	691-713	Encodes NUFIP that directs assembly of C/D snoRNP (small nucleolar ribonucleoprotein)
8467258	Di,Dc,Ci	1983-2003	3.5	0.896	UCCGAAAGGUCCCGUACA-AGU	PATC132568	708-729	chloroplastic Ribonuclease III family protein
1254676	Di,Dc,Ci	2933-2953	3.5	0.83	G-UCCAGUUCACGUCUU-UAUGC	PATC127096	951-973	serine carboxypeptidase-like 5 (scpl5), involved in proteolysis
1254676	Di,Dc,Ci	2933-2953	3.5	0.77	GUCCAGUUCACGUCUUU-AUGC	PATC131935	217-238	P-type ATPase HMA5, involved in Cu detoxification
7685056	Di,Dc,Ci	1575-1555	3.5	0.761	CCC-GUUCAGGUAAUAGCA-ACU	PATC140195	184-206	Encodes a protein with similarity to mammalian RACK, functions to shuttle activated protein kinase C to different subcellular sites and may also function as a scaffold through physical interactions with other proteins.

^a Indicating the from which the library vsRNA tag was in the top 50 abundant list.

^b The viral genome position of the vsRNA. Sites are based on genomic sequence of the Taichung strain.

^c Position-dependent scoring matrix for miRNA:mRNA pairing assessment described by Fahlgren and Carrington(2010).

^d MFE ratio = $\Delta G_{\text{target}}/\Delta MFE$, the ratio between minimum folding energy for the vsRNA:mRNA duplex and a hypothetical perfect paired duplex of the vsRNA.

^e Orchidstra database (<http://orchidstra.abrc.sinica.edu.tw>) accession numbers of potential targets.

(continued)

Table 10. Potential CymMV vsRNA targeting *Phalaenopsis* genes. (continued)

ID	library ^a	Site ^b	Score ^c	MFE ratio ^d	vsRNA 3'-5'	Target ^e	Target site	Target annotation
4798235	Di,Dc,Ci	1526-1546	3.5	0.759	UCCUAGUUUCAACCCCGGUU	PATC138432	10-30	single cystathionine beta-synthase domain-containing protein. Modulates development by regulating the thioredoxin system.
938095	Di,Dc,Ci	867-887	3.5	0.753	GCUUACAGGCGUCAAACCCAC	PATC148106	2202-2222	cytosolic glutamine synthetase

^a Indicating the from which the library vsRNA tag was in the top 50 abundant list.

^b The viral genome position of the vsRNA. Sites are based on genomic sequence of the Taichung strain.

^c Position-dependent scoring matrix for miRNA:mRNA pairing assessment described by Fahlgren and Carrington(2010).

^d MFE ratio = $\Delta G_{\text{target}}/\Delta MFE$, the ratio between minimum folding energy for the vsRNA:mRNA duplex and a hypothetical perfect paired duplex of the vsRNA.

^e Orchidstra database (<http://orchidstra.abrc.sinica.edu.tw>) accession numbers of potential targets.



Table 11. Potential Di library-specific CymMV vsRNA targeting *Phalaenopsis* genes.

ID	Site ^a	Score ^b	MFE ratio ^c	vsRNA 3'-5'	Target ^d	Target site	Target annotation
3312278	1255-1238	0	1	GUUAAAUUAGUUGACGAG	PATC157382	39-56	similar to tobacco hairpin-induced gene (HIN1) and Arabidopsis non-race specific disease resistance gene (NDR1)
697298	2170-2187	1.5	0.904	GAAGGCUA-GAAUACUCG	PATC125780	925-943	chromatin remodeling 24 (CHR24), helicase activity
1791194	3093-3074	1.5	0.802	CGAUGGUAUCUGCGAUCUGA	PATC198052	146-165	ubiquitin, attached to proteins destined for degradation
4162772	346-329	2	1.08	GAAGGA-UUUCUUGGGAG-G	PATC125751	107-126	appr-1-p processing enzyme family protein, contains cellular retinaldehyde-binding
11982790	3364-3381	2	0.984	CGAGGUUAAAA-GAGUAAA	PATC135457	31-49	HD-GLABRA2 group homeodomain protein, involved in the accumulation of anthocyanin and in root development
12695775	5841-5860	2	0.849	GUCGUAGUCUAAGGUGUGGU	PATC152194	3896-3915	aminophospholipid translocase (p-type ATPase) involved in chilling response
2895625	1122-1104	2	0.754	UGAAUGAUAGUAGUCAGU	PATC148220	943-961	homolog of the yeast SRS2 (Suppressor of RAD Six-screen mutant 2) helicase, disrupts recombinogenic DNA intermediates and facilitates single strand annealing
3239158	275-259	2	0.733	GUAGGUUUGCGUAUGUG	PATC135205	757-773	chloroplastic pentatricopeptide repeat (PPR) superfamily protein
5006172	3362-3381	2.5	1.02	CGAGGUUAAAA-GAGUAAA-AA	PATC135457	31-52	HD-GLABRA2 group homeodomain protein, involved in the accumulation of anthocyanin and in root development
5006172	3362-3381	2.5	0.893	CGAGGUU--AAAAGAGUAAAA	PATC127059	548-569	armadillo (ARM) repeat superfamily protein
11391303	3546-3528	2.5	0.838	UGAAGUUUUUAAGUAUGA	PATC139030	4655-4673	S-adenosyl-L-methionine-dependent methyltransferases
11982790	3364-3381	2.5	0.883	CGAGGUU--AAAAGAGUAAA	PATC127059	548-567	armadillo (ARM) repeat superfamily protein

^a The viral genome position of the vsRNA. Sites are based on genomic sequence of the Taichung strain.

^b Position-dependent scoring matrix for miRNA:mRNA pairing assessment described by Fahlgren and Carrington(2010).

^c MFE ratio = $\Delta G_{\text{target}}/\Delta MFE$, the ratio between minimum folding energy for the vsRNA:mRNA duplex and a hypothetical perfect paired duplex of the vsRNA.

^d Orchidstra database (<http://orchidstra.abrc.sinica.edu.tw>) accession numbers of potential targets.

(continued)

Table 11. Potential Di library-specific CymMV vsRNA targeting *Phalaenopsis* genes. (continued)

ID	Site ^b	Score ^c	MFE ratio ^d	vsRNA 3'-5'	Target ^e	Target site	Target annotation
12585279	2674-2656	2.5	0.828	UUAGGUU-UAAAACUAUCUG	PATC135769	923-942	protein serine/threonine kinase
11543353	1118-1099	2.5	0.809	GUUAAUGAAUGAUAGUAGU	PATC015993	32-51	tRNA/tRNA methyltransferase (SpoU)
697298	2170-2187	2.5	0.798	GAAGGCUAGAAUACUCG	PATC136935	2791-2808	PHD-finger protein, required for embryonic root meristem initiation
697298	2170-2187	2.5	0.783	GAAGGCUAGAAU-ACUCG	PATC232148	20-38	EMBRYO DEFECTIVE 2765 (EMB2765)
6213507	2211-2192	2.5	0.759	CUUGUUUGCUUAGUUUUUG	PATC136701	94-113	Zinc finger C-x8-C-x5-C-x3-H type family protein, functions in zinc ion and nucleic acid binding
6213507	2211-2192	2.5	0.759	CUUGUUUGCUUAGUUUUUG	PATC153742	1285-1304	Zinc finger C-x8-C-x5-C-x3-H type family protein, functions in zinc ion and nucleic acid binding
11982790	3364-3381	3	1.032	CGAG-GUAAAAGA-GUAAA	PATC125175	2298-2317	WD-40 protein, integrating auxin signaling in the organization and maintenance of the apical meristems
5006172	3362-3381	3	1	CGAG-GUAAAAGA-GUAAAA	PATC125175	2298-2319	WD-40 protein, integrating auxin signaling in the organization and maintenance of the apical meristems
3239158	275-259	3	0.986	GUA-GGUUUGCGUAUGUG	PATC104641	50-67	CYP86A subfamily of cytochrome p450 genes
697298	2170-2187	3	0.953	GAAGGCUAGAAUACUC-G	PATC136935	2791-2809	PHD-finger protein, required for embryonic root meristem initiation
2895625	1122-1104	3	0.937	UGAAUGAUAGUAGUCA-GU	PATC148220	943-962	homolog of the yeast SRS2 (Suppressor of RAD Six-screen mutant 2) helicase, disrupts recombinogenic DNA intermediates and facilitates single strand annealing
3239158	275-259	3	0.906	GUAGGUUUGCG-UAUGUG	PATC143848	1634-1651	auxin response factor
11543353	1118-1099	3	0.888	GUUAAUGAAUG-AUAAGUAGU	PATC139706	5403-5423	callose synthase 1 catalytic subunit

^a The viral genome position of the vsRNA. Sites are based on genomic sequence of the Taichung strain.

^b Position-dependent scoring matrix for miRNA:mRNA pairing assessment described by Fahlgren and Carrington(2010).

^c MFE ratio = $\Delta G_{\text{target}}/\Delta MFE$, the ratio between minimum folding energy for the vsRNA:mRNA duplex and a hypothetical perfect paired duplex of the vsRNA.

^d Orchidstra database (<http://orchidstra.abrc.sinica.edu.tw>) accession numbers of potential targets.

(continued)

Table 11. Potential Di library-specific CymMV vsRNA targeting *Phalaenopsis* genes. (continued)

ID	Site ^b	Score ^c	MFE ratio ^d	vsRNA 3'-5'	Target ^e	Target site	Target annotation
11982790	3364-3381	3	0.886	CGAGGUUAAAAGAGUU-AA	PATC158243	669-687	hydroxyproline-rich glycoprotein family protein
3239158	275-259	3	0.869	GUAG-GUUUGCGUAUGUG	PATC080935	271-288	class III type alcohol dehydrogenas
9689144	300-281	3	0.818	CGU--CGAUUUUGACAACUUUU	PATC135356	1354-1375	CC1-like splicing factor, involved in mRNA processing
3075964	787-768	3	0.781	U-AGGAAACUUUCAUUUCUUU	PATC153454	568-588	dihydrosphingosine phosphate lyase (DPL1), involved in sphingolipid catabolic process
9633694	5733-5715	3	0.77	GCAGGUUCUCACGAUGGG-A	PATC146005	754-773	armadillo (ARM) repeat superfamily protein
3239158	275-259	3	0.77	GUAGGUUUGCGUAUGUG	PATC152330	162-178	GPI transamidase component Gpi16 subunit family protein
3239158	275-259	3	0.77	GUAGGUUUGCGUAUGUG	PATC152331	1627-1643	GPI transamidase component Gpi16 subunit family protein
3239158	275-259	3	0.77	GUAGGUUUGCGUAUGUG	PATC152332	1360-1376	GPI transamidase component Gpi16 subunit family protein
3239158	275-259	3	0.75	GUAGGUUUGCGUAUGUG	PATC139037	1599-1615	light-dependent NADPH:protochlorophyllide oxidoreductase A
3239158	275-259	3	0.75	GUAGGUUUGCGUAUGUG	PATC155114	1599-1615	light-dependent NADPH:protochlorophyllide oxidoreductase A
3239158	275-259	3	0.75	GUAGGUUUGCGUAUGUG	PATC158427	1599-1615	light-dependent NADPH:protochlorophyllide oxidoreductase A
3239158	275-259	3	0.75	GUAGGUUUGCGUAUGUG	PATC150226	1599-1615	light-dependent NADPH:protochlorophyllide oxidoreductase A
5006172	3362-3381	3	0.735	CGAGGUUAAAA-GAGUUA-AAA	PATC146288	1282-1303	AT hook motif DNA-binding family protein
11982790	3364-3381	3	0.735	CGAGGUUAAAA-GAGUUA-A	PATC146288	1282-1301	AT hook motif DNA-binding family protein

^a The viral genome position of the vsRNA. Sites are based on genomic sequence of the Taichung strain.

^b Position-dependent scoring matrix for miRNA:mRNA pairing assessment described by Fahlgren and Carrington(2010).

^c MFE ratio = $\Delta G_{\text{target}}/\Delta MFE$, the ratio between minimum folding energy for the vsRNA:mRNA duplex and a hypothetical perfect paired duplex of the vsRNA.

^d Orchidstra database (<http://orchidstra.abrc.sinica.edu.tw>) accession numbers of potential targets.

(continued)

Table 11. Potential Di library-specific CymMV vsRNA targeting *Phalaenopsis* genes. (continued)

ID	Site ^b	Score ^c	MFE ratio ^d	vsRNA 3'-5'	Target ^e	Target site	Target annotation
3239158	275-259	3.5	1.164	GUAGGUUUGCGU--AU-GUG	PATC139037	1599-1618	light-dependent NADPH:protochlorophyllide oxidoreductase A
3239158	275-259	3.5	1.164	GUAGGUUUGCGU--AU-GUG	PATC150226	1599-1618	light-dependent NADPH:protochlorophyllide oxidoreductase A
3239158	275-259	3.5	1.164	GUAGGUUUGCGU--AU-GUG	PATC155114	1599-1618	light-dependent NADPH:protochlorophyllide oxidoreductase A
3239158	275-259	3.5	1.164	GUAGGUUUGCGU--AU-GUG	PATC158427	1599-1618	light-dependent NADPH:protochlorophyllide oxidoreductase A
11982790	3364-3381	3.5	1.022	CGAGGUUA-AA-AGAG-UUAA	PATC211670	89-109	Translation elongation factor EF1A/initiation factor IF2gamma family protein
11982790	3364-3381	3.5	1.02	CGAGGU-U-AAAAGAG-UUAA	PATC127232	261-281	Glycosyl hydrolase family, involved in mannose and carbohydrate metabolic process
9689144	300-281	3.5	1.004	CGUCGAUUUUGACAA-CUUUU	PATC140537	1317-1337	protein disulfide isomerase-like (PDIL) protein
9689144	300-281	3.5	1	C-GUCGAUUUUGA-CAACUUUU	PATC136877	1856-1877	chloroplastic P-loop containing nucleoside triphosphate hydrolases
12585279	2674-2656	3.5	0.946	UUAGGUUUAAAACUA-UC-UG	PATC130040	1709-1729	oligomeric Golgi complex component-related protein
4162772	346-329	3.5	0.935	GAAGGA-UUUC-UUGGGAGG	PATC129877	103-122	EMB2780 (EMBRYO DEFECTIVE 2780), functions in nucleic acid binding
3312278	1255-1238	3.5	0.901	G-UUAAAUUAGUUGA-CGAG	PATC131945	604-623	XB3 ortholog 3 in <i>Arabidopsis thaliana</i> (XBAT33), ubiquitin-protein ligase activity
12695775	5841-5860	3.5	0.855	GUCGUAGUC-UAAG-GUGUGGU	PATC153656	535-556	methylthioalkylmalate isomerase, involved in glucosinolate biosynthesis
3239158	275-259	3.5	0.851	GUAGG-UUUGCGUAUGUG	PATC148376	947-964	P-glycoprotein 20 (PGP20), involved in transmembrane transport

^a The viral genome position of the vsRNA. Sites are based on genomic sequence of the Taichung strain.

^b Position-dependent scoring matrix for miRNA:mRNA pairing assessment described by Fahlgren and Carrington(2010).

^c MFE ratio = $\Delta G_{\text{target}}/\Delta MFE$, the ratio between minimum folding energy for the vsRNA:mRNA duplex and a hypothetical perfect paired duplex of the vsRNA.

^d Orchidstra database (<http://orchidstra.abrc.sinica.edu.tw>) accession numbers of potential targets.

(continued)

Table 11. Potential Di library-specific CymMV vsRNA targeting *Phalaenopsis* genes. (continued)

ID	Site ^b	Score ^c	MFE ratio ^d	vsRNA 3'-5'	Target ^e	Target site	Target annotation
9527620	397-378	3.5	0.849	CGAUGGAUGCU-GCGCGGCGG	PATC125622	538-558	protein similar to animal presenilin
11982790	3364-3381	3.5	0.849	CGAGGUUA-AAAGA-GUUA	PATC152658	471-490	WPP family members contains an NE targeting domain
12695775	5841-5860	3.5	0.844	GUCGUAGUCU-AAGGU-GUGGU	PATC131475	90-111	mitochondrial half-molecule ABC transporter, involved in heavy metal resistance
11982790	3364-3381	3.5	0.832	CGAGGUUAAAAGAG-UUA	PATC129650	900-918	embryo defective 1865 (EMB1865), involved in embryo development ending in seed dormancy
4162772	346-329	3.5	0.828	GAAGGAUUUC-UUGGGAGG	PATC142815	334-352	ATP-dependent protease La (LON) domain protein, involved in proteolysis
4162772	346-329	3.5	0.825	GAAGGAUUUC-UUGGGAGG	PATC215040	6-24	pentatricopeptide repeat (PPR) gene family
3312278	1255-1238	3.5	0.822	GUUAAAUA-G-UUGACGAG	PATC128857	20-39	Prolyl oligopeptidase family protein, serine-type peptidase activity. Involved in proteolysis
3312278	1255-1238	3.5	0.822	GUUAAAUA-G-UUGACGAG	PATC128859	20-39	Prolyl oligopeptidase family protein, serine-type peptidase activity. Involved in proteolysis
3312278	1255-1238	3.5	0.822	GUUAAAUA-G-UUGACGAG	PATC133017	20-39	Prolyl oligopeptidase family protein, serine-type peptidase activity. Involved in proteolysis
3312278	1255-1238	3.5	0.822	GUUAAAUA-G-UUGACGAG	PATC150326	20-39	Prolyl oligopeptidase family protein, serine-type peptidase activity. Involved in proteolysis
4162772	346-329	3.5	0.805	GAA-GGAUUUCUUGGGAGG	PATC129594	2564-2582	armadillo (ARM) repeat superfamily protein
12585279	2674-2656	3.5	0.803	UUAGGUUAAAA-C-UAUCUG	PATC151426	152-172	GCN subfamily protein, predicted to be involved in stress-associated protein translation control
3312278	1255-1238	3.5	0.802	GUU-AAAUAGUUGACGAG	PATC130821	648-666	poly(ADPribose) glycohydrolase (PARG1), plays a role in abiotic stress responses
4162772	346-329	3.5	0.798	GAAGGAUUUCUUG-G-GAGG	PATC146474	978-997	Glycosyl hydrolase, involved in carbohydrate metabolic process

^a The viral genome position of the vsRNA. Sites are based on genomic sequence of the Taichung strain.

^b Position-dependent scoring matrix for miRNA:mRNA pairing assessment described by Fahlgren and Carrington(2010).

^c MFE ratio = $\Delta G_{\text{target}}/\Delta MFE$, the ratio between minimum folding energy for the vsRNA:mRNA duplex and a hypothetical perfect paired duplex of the vsRNA.

^d Orchidstra database (<http://orchidstra.abrc.sinica.edu.tw>) accession numbers of potential targets.

(continued)

Table 11. Potential Di library-specific CymMV vsRNA targeting *Phalaenopsis* genes. (continued)

ID	Site ^b	Score ^c	MFE ratio ^d	vsRNA 3'-5'	Target ^e	Target site	Target annotation
697298	2170-2187	3.5	0.791	GAAG-GCUAGAAUA-ACUCG	PATC129147	3176-3195	RNA recognition motif (RRM)-containing protein
11982790	3364-3381	3.5	0.785	CGAGGU-UAAAAGAGUAAA	PATC149074	730-748	embryo defective 1967 (emb1967)
5006172	3362-3381	3.5	0.784	CGAGGUUA-AAAGAGUAAAA	PATC133803	1073-1093	esterase/lipase/thioesterase family protein
6213507	2211-2192	3.5	0.781	C-UUGUUUGCUUAUAGUUUUG	PATC022997	557-577	UDP-glucose dehydrogenase
12585279	2674-2656	3.5	0.78	UUAGGUUAAAACUAUC-UG	PATC126630	782-801	Ankyrin repeat family protein
9208604	3058-3038	3.5	0.779	GUCGUAGUUGUCCGUUUC-CUG	PATC130629	1928-1949	cytosolic chaperone DnaJ-domain superfamily protein, functions in heat shock protein binding
3239158	275-259	3.5	0.779	GUAGGU-UUGCGUAU-GUG	PATC142565	1456-1474	glycosyl hydrolase 9B13 (GH9B13), involved in carbohydrate metabolic process
12585279	2674-2656	3.5	0.774	UUAGGUUAAAACUAU-CUG	PATC154231	2096-2115	2-oxoglutarate (2OG) and Fe(II)-dependent oxygenase, oxidoreductase activity. Involved in aging and cellular response to starvation
2895625	1122-1104	3.5	0.771	UGAAUGAUAAGUA-GUCAGU	PATC147630	48-67	RELA/SPOT homolog 1 (RSH1), response to wounding
2895625	1122-1104	3.5	0.771	UGAAUGAUAAGUA-GUCAGU	PATC153713	2380-2399	RELA/SPOT homolog 1 (RSH1), response to wounding
1791194	3093-3074	3.5	0.768	CGAUGGUAUCUGCGAUCUGA	PATC154177	525-544	RAB GTPase homolog G3A (RABG3A), involved in protein transport and small GTPase mediated signal transduction
11391303	3546-3528	3.5	0.765	U-GAAGUUUUUAAGUAUGA	PATC147311	3474-3493	homolog of yeast autophagy 18 (ATG18) F (G18F)
11982790	3364-3381	3.5	0.764	CGAGGUUA-AAAGAGUAAA	PATC133803	1073-1091	esterase/lipase/thioesterase family protein
5006172	3362-3381	3.5	0.761	CGAGGUUAAAAGAGUAAAA	PATC158243	669-688	hydroxyproline-rich glycoprotein family protein

^a The viral genome position of the vsRNA. Sites are based on genomic sequence of the Taichung strain.

^b Position-dependent scoring matrix for miRNA:mRNA pairing assessment described by Fahlgren and Carrington (2010).

^c MFE ratio = $\Delta G_{\text{target}}/\Delta MFE$, the ratio between minimum folding energy for the vsRNA:mRNA duplex and a hypothetical perfect paired duplex of the vsRNA.

^d Orchidstra database (<http://orchidstra.abrc.sinica.edu.tw>) accession numbers of potential targets.

(continued)

Table 11. Potential Di library-specific CymMV vsRNA targeting *Phalaenopsis* genes. (continued)

ID	Site ^b	Score ^c	MFE ratio ^d	vsRNA 3'-5'	Target ^e	Target site	Target annotation
3239158	275-259	3.5	0.76	GUAGGUUUGCGUAUGUG	PATC131276	2285-2301	ERD (early-responsive to dehydration stress)
9689144	300-281	3.5	0.758	CGUC--GAUUUUGACAACUUUU	PATC154065	1616-1637	ALWAYS EARLY 3 (ALY3), functions in DNA binding
11543353	1118-1099	3.5	0.752	GUUAAUGAAUGA-UAAGUAGU	PATC143101	54-74	Ribosomal L18p/L5e family protein involved in translation and ribosome biogenesis
697298	2170-2187	3.5	0.752	GAAGGCUAGAAUACUC-G	PATC146419	315-333	Regulator of Vps4 activity in the MVB pathway protein
11982790	3364-3381	3.5	0.743	CGAGGUUAA-AAGAGUAAA	PATC129611	198-216	plastidial thioredoxin (TRX) isoform, disulfide reductase activity
7178992	416-397	3.5	0.741	GUU-GUUGUUUCUGUAUAAAG	PATC140288	742-762	ATMAP4K ALPHA1, protein serine/threonine kinase activity
11982790	3364-3381	3.5	0.74	CGAGGUUA-AAAGAGUUA-A	PATC143615	749-768	NBR1, a selective autophagy substrate
3239158	275-259	3.5	0.734	GUAG-GUUUGCG-UAUGUG	PATC151547	839-857	zinc induced facilitator-like 2 (ZIFL2), involved in carbohydrate transmembrane transport

^a The viral genome position of the vsRNA. Sites are based on genomic sequence of the Taichung strain.

^b Position-dependent scoring matrix for miRNA:mRNA pairing assessment described by Fahlgren and Carrington(2010).

^c MFE ratio = $\Delta G_{\text{target}}/\Delta MFE$, the ratio between minimum folding energy for the vsRNA:mRNA duplex and a hypothetical perfect paired duplex of the vsRNA.

^d Orchidstra database (<http://orchidstra.abrc.sinica.edu.tw>) accession numbers of potential targets.

Table 12. The major sequences and total reads of abundant miRNAs in small RNA libraries constructed from mock-, CymMV-, and CymMV and ORSV mixedly-inoculated tissues.

ID	Family	Size	Sequence	Reads ^a						
				Mi-2	Mc-2	Ci	Cc	Di	Dc	Dsc
4565061	miR156	21	CUGACAGAAGAUAGAGAGCAC	170	198	187	193	100	399	111
4228356	miR156	20	UGACAGAAGAGAGUGAGCAC	340	265	467	383	162	506	341
	miR156		total^b	602	539	776	681	317	1,061	501
1751961	miR159	21	UCUGGAUUGAAGGGAGCUCUG	0	1	121	67	1	1	2
4420694	miR159	21	UGUGGAUUGAAGGGAGCUCUG	0	0	130	63	2	7	16
1027789	miR159	23	UUUGGAUUGAAGGGAGCUCUAUU	94	108	42	55	27	33	49
2658446	miR159	21	UAUGGAUUGAAGGGAGCUCUA	0	2	245	172	0	9	10
6600183	miR159	22	UUUGGAUUGAAGGGAGCUCUAC	60	47	94	109	30	65	128
1787503	miR159	22	UUUGGAUUGAAGGGAGCUCUAU	80	58	109	142	36	89	127
6523503	miR159	21	UCUGGAUUGAAGGGAGCUCUA	0	1	397	242	2	2	7
612588	miR159	21	UGUGGAUUGAAGGGAGCUCUA	1	2	397	253	9	22	35
6789462	miR159	21	UUUGGAUUGAAGGGAGCUCUU	106	111	93	147	53	125	158
5173640	miR159	19	UUUGGAUUGAAGGGAGCUC	812	822	857	1,014	407	989	1,088
4920752	miR159	21	UUGGAUUGAAGGGAGCUCUGC	1,133	983	1,397	1,649	869	1,842	1,409
5852294	miR159	20	UUUGGAUUGAAGGGAGCUCU	4,372	4,144	3,920	4,360	1,278	3,557	6,073
2344141	miR159	21	UUUGGAUUGAAGGGAGCUCUG	7,087	8,260	8,272	9,595	4,175	8,495	9,663
867925	miR159	21	UUUGGAUUGAAGGGAGCUCUA	15,957	18,061	26,567	34,658	9,818	27,678	46,863
	miR159		total	30,779	33,778	44,236	54,335	17,353	44,295	67,496

^a Sequences with the more than 100 reads or being the tag with the highest read within the family was designated as abundant miRNAs.

^b Sub-totaled reads within a single miRNA family

(continued)

Table 12. The major sequences and total reads of abundant miRNAs in small RNA libraries constructed from mock-, CymMV-, and CymMV and ORSV mixedly-inoculated tissues. (continued)

ID	Family	Size	Sequence	Reads ^a						
				Mi-2	Mc-2	Ci	Cc	Di	Dc	Dsc
1307734	miR162	18	UCGAUAAACCUCUGCAUC	80	101	174	184	71	193	186
2768096	miR162	22	UCGAUAAACCUCUGCAUCCGGU	929	1,010	1,197	1,378	614	1,564	1,220
9227853	miR162	21	UCGAUAAACCUCUGCAUCCGG	8,955	11,875	9,147	11,375	5,512	11,779	10,029
	miR162		total^b	10,231	13,287	11,085	13,565	6,456	14,025	11,856
3025792	miR165	21	UCGGACCAGGCUUCAUCCCC	132	134	127	145	52	97	96
	miR165		total	198	197	184	246	82	147	162
1340164	miR166	21	UACGGACCAGGCUUCAUCCCC	1	0	143	100	2	9	10
4030770	miR166	21	UCCGGACCAGGCUUCAUCCCC	0	3	230	135	1	2	6
10050345	miR166	21	UCGGACCACGCUUCAUCCCC	104	43	40	48	10	125	21
1027979	miR166	21	UGCGGACCAGGCUUCAUCCCC	1	1	206	144	2	22	21
7649985	miR166	21	UCCGACCAGGCUUCAUCCCC	35	22	5	6	62	132	143
7877325	miR166	21	UCGGACCAGGCUUCAUUCGCC	46	182	26	62	23	35	34
6512923	miR166	21	UCGGACCAUGCUUCAUCCCC	102	76	53	73	13	104	30
3501726	miR166	21	UCGGAGCAGGCUUCAUCCCC	45	39	66	72	40	89	108
3411178	miR166	21	UCGGACCAGGCUUCAUCCUC	39	92	87	122	23	57	51
5105791	miR166	19	GGACCAGGCUUCAUCCCC	104	73	65	73	35	61	80
849600	miR166	21	UCGGACCAAGCUUCAUCCCC	131	76	73	80	20	112	41
2811658	miR166	21	UCGGAUCAGGCUUCAUCCCC	102	67	80	102	29	84	99

^a Sequences with the more than 100 reads or being the tag with the highest read within the family was designated as abundant miRNAs.

^b Sub-totaled reads within a single miRNA family

(continued)

Table 12. The major sequences and total reads of abundant miRNAs in small RNA libraries constructed from mock-, CymMV-, and CymMV and ORSV mixedly-inoculated tissues. (continued)

ID	Family	Size	Sequence	Reads ^a						
				Mi-2	Mc-2	Ci	Cc	Di	Dc	Dsc
7226803	miR166	21	UCGGACCAGUCUUCAUUCCCC	149	122	57	88	26	71	60
6441303	miR166	21	UCGGACCAGGCUUCUUUCCCC	126	95	73	107	29	71	102
8256050	miR166	22	UCGGACCAGGCUUCAUUCCCCC	95	97	83	90	109	60	75
9570908	miR166	21	UCGGACCAGCCUUCAUUCCCC	149	90	111	88	24	82	67
515279	miR166	21	UCGGACCAGGCUGCAUUCCCC	29	129	26	99	48	134	165
6982131	miR166	21	UCGGACCAGGCUACAUUCCCC	62	117	96	123	35	107	113
274081	miR166	21	UCGGACCAGGCUCCAUUCCCC	112	126	96	121	37	82	111
4804583	miR166	21	UCGGACCAGGCUUCGUUCCCC	134	145	88	113	47	75	100
720348	miR166	21	UCGGACAAGGCUUCAUUCCCC	162	119	94	124	35	108	61
7570448	miR166	21	UCGGACCAGGCUUGAUUCCCC	117	129	37	58	61	124	186
1131391	miR166	21	UCGGACCAGGCUUCAUUCCCA	90	56	162	171	61	107	85
6518757	miR166	21	UCGGACCAGGCUUCAUUCCGC	27	355	194	171	17	20	22
220884	miR166	21	UCGGACCAGGCUUCCUUCCCC	212	327	36	89	41	61	130
4517667	miR166	21	UCGGACCAGGCUUCAUUCACC	130	225	97	273	64	119	81
9033509	miR166	21	UCGGGCCAGGCUUCAUUCCCC	311	148	73	129	47	121	210
3758512	miR166	21	UCGGACCAGGCUUCAUUGCCC	99	172	56	146	130	237	239
2770477	miR166	21	UCGGACCAGACUUCAUUCCCC	284	233	185	159	51	110	102

^a Sequences with the more than 100 reads or being the tag with the highest read within the family was designated as abundant miRNAs.

^b Sub-totaled reads within a single miRNA family

(continued)

Table 12. The major sequences and total reads of abundant miRNAs in small RNA libraries constructed from mock-, CymMV-, and CymMV and ORSV mixedly-inoculated tissues. (continued)

ID	Family	Size	Sequence	Reads ^a						
				Mi-2	Mc-2	Ci	Cc	Di	Dc	Dsc
3030416	miR166	21	CCGGACCAGGCUUCAUUC CCC	169	98	253	209	65	156	181
9769609	miR166	21	UCGGACCAGGCUUCACU CCC	115	140	138	148	101	252	273
5033830	miR166	21	UCGGCCCAGGCUUCAUUC CCC	309	479	44	50	52	38	205
3046882	miR166	21	UAGGACCAGGCUUCAUUC CCC	54	61	52	129	142	344	396
3595554	miR166	21	UCGGACCAGGCUUCAUUC CAC	69	200	301	354	108	167	67
1537655	miR166	20	CGGACCAGGCUUCAUUC CCC	83	54	249	356	158	261	180
7416352	miR166	21	UCGGACCAGGCCUCAUUC CCC	163	171	346	354	51	123	142
6763642	miR166	21	UCGGACCAGGCUUCAUUA CCC	134	230	208	408	93	148	159
9044926	miR166	21	UCGGACCGGGCUUCAUUC CCC	84	120	262	118	182	304	312
7491037	miR166	21	UCGGACCAGGUUCAUUC CCC	189	179	336	307	61	173	155
1639010	miR166	19	UCGGACCAGGCUUCAUUC C	169	157	160	224	342	165	206
1626117	miR166	21	ACGGACCAGGCUUCAUUC CCC	154	314	296	283	94	150	151
6175229	miR166	21	UUUCGGACCAGGCUUCAUUC C	217	289	188	205	69	215	278
4253006	miR166	22	UCUCGGACCAGGCUUCAUUC CC	181	226	253	221	164	250	220
6380141	miR166	21	UCUCGGACCAGGCUUCAUUC C	142	202	170	270	97	297	358
9201857	miR166	21	UCGGACCAGGCAUCAUUC CCC	50	34	785	588	23	34	26
4033576	miR166	21	UCGGACCAGGCUUCAUUC CUCC	233	274	211	330	92	283	211
847283	miR166	21	UCGGACCAGGAUCAUUC CCC	153	200	649	456	37	76	74
3554030	miR166	21	UCGGACCAGGCUUAAUUC CCC	447	380	198	171	71	101	303

^a Sequences with the more than 100 reads or being the tag with the highest read within the family was designated as abundant miRNAs.

^b Sub-totaled reads within a single miRNA family

(continued)

Table 12. The major sequences and total reads of abundant miRNAs in small RNA libraries constructed from mock-, CymMV-, and CymMV and ORSV mixedly-inoculated tissues. (continued)

ID	Family	Size	Sequence	Reads ^a						
				Mi-2	Mc-2	Ci	Cc	Di	Dc	Dsc
9371738	miR166	21	UCAGACCAGGCUUCAUUCCCC	229	115	147	144	182	432	566
1051268	miR166	21	UGGGACCAGGCUUCAUUCCCC	30	40	34	41	266	642	782
7087901	miR166	22	UCGGACCAGGCUUCAUUCCCCU	286	279	223	262	602	191	249
4014606	miR166	21	UCGGACCAGGCUUUUAUUCCCC	469	469	239	327	112	298	352
8003442	miR166	21	UCGGACCAGGCUUCAGUCCCC	18	84	355	225	316	630	785
9267547	miR166	21	UCGGACCAGGCGUCAUUCCCC	77	43	1,462	1,157	32	48	32
8517396	miR166	22	CUCGGACCAGGCUUCAUUCCCC	585	517	456	596	194	440	486
7688138	miR166	21	UCGGACCAGGCUUCAUUUCCC	549	676	465	873	257	739	444
8880687	miR166	20	UCGGACCAGGCUUCAUUCCC	672	621	579	679	749	445	549
9527939	miR166	21	GCGGACCAGGCUUCAUUCCCC	1,147	300	420	2,460	91	162	209
7003658	miR166	21	UUGGACCAGGCUUCAUUCCCC	169	141	10,056	6,641	86	171	196
6100862	miR166	21	CUCGGACCAGGCUUCAUUCCC	1,282	2,100	3,612	2,634	2,509	2,461	3,085
5650228	miR166	21	UUCGGACCAGGCUUCAUUCCC	22,447	26,601	17,496	21,322	7,616	21,232	22,451
3004100	miR166	21	UCGGACCAGGCUUCAUUCCCC	1,141,714	1,028,192	817,305	1,072,147	386,882	805,360	925,831
	miR166		total^b	1,177,426	1,069,229	862,553	1,119,886	404,168	840,777	964,080
4686497	miR167	21	UGAAGCUGCCAGCUUGAUCUG	61	64	89	132	24	41	127
8797107	miR167	22	UUAAGCUGCCAGCAUGAUCUGU	12	27	319	160	4	20	4
3539608	miR167	23	UGAAGCUGCCAGCAUGAUCUGUU	95	71	154	157	54	96	102

^a Sequences with the more than 100 reads or being the tag with the highest read within the family was designated as abundant miRNAs.

^b Sub-totaled reads within a single miRNA family

(continued)

Table 12. The major sequences and total reads of abundant miRNAs in small RNA libraries constructed from mock-, CymMV-, and CymMV and ORSV mixedly-inoculated tissues. (continued)

ID	Family	Size	Sequence	Reads ^a						
				Mi-2	Mc-2	Ci	Cc	Di	Dc	Dsc
1093010	miR167	19	UGAAGCUGCCAGCAUGAUC	166	107	177	173	55	123	122
6578147	miR167	22	UGAAGCUGCCAGCAUGAUCUGG	174	148	446	474	83	224	218
4422450	miR167	21	UGAAGCUGCCAGCAUGAUCUG	878	907	949	1,043	611	1,121	905
8116347	miR167	22	UGAAGCUGCCAGCAUGAUCUGA	9,746	7,893	16,221	15,339	6,245	16,195	13,164
9798196	miR167	22	UGAAGCUGCCAGCAUGAUCUGU	34,484	27,324	31,009	36,974	10,100	28,404	29,373
	miR167		total^b	46,225	37,111	50,400	55,460	17,547	47,093	44,718
6967635	miR168	22	UCGCUUGGUGCAGGUCGGGAUU	32	14	25	10	250	20	20
10684205	miR168	21	UUCGCUUGGUGCAGGUCGGGA	127	117	92	108	60	93	110
5143698	miR168	21	CGCUUGGUGCAGGUCGGGAAU	10	52	463	219	210	257	359
9455314	miR168	20	UCGCUUGGUGCAGGUCGGGA	94	271	964	703	473	784	1,147
9237120	miR168	21	UCGCUUGGUGCAGGUCGGGAC	1,918	1,923	1,244	1,467	4,408	1,154	1,628
4108757	miR168	21	UCGCUUGGUGCAGGUCGGGAA	1,045	1,102	3,367	3,119	926	2,435	2,902
5435433	miR168	21	UCGCUUGGUGCAGGUCGGGAU	3,213	1,941	2,030	1,734	4,897	1,343	2,216
	miR168		total	6,927	5,923	8,883	7,992	11,910	6,560	9,014
92645	miR169	20	UAGCCAAGGAUGACUUGCCU	163	107	83	108	48	111	94
	miR169		total	169	111	93	111	52	112	96
6992510	miR171	21	UUGAGCCGUGCCAAUAUCGCG	99	96	155	193	45	111	287
901181	miR171	21	UUGAGCCGCGUCAAAUAUCUCC	312	326	391	412	255	351	385

^a Sequences with the more than 100 reads or being the tag with the highest read within the family was designated as abundant miRNAs.

^b Sub-totaled reads within a single miRNA family

(continued)

Table 12. The major sequences and total reads of abundant miRNAs in small RNA libraries constructed from mock-, CymMV-, and CymMV and ORSV mixedly-inoculated tissues. (continued)

ID	Family	Size	Sequence	Reads ^a						
				Mi-2	Mc-2	Ci	Cc	Di	Dc	Dsc
	miR171	total		522	527	753	841	375	604	920
8576633	miR172	21	CGAAUCUUGAUGAUGCUGCAU	71	36	98	81	38	58	74
	miR172	total^b		77	46	114	92	45	67	83
5145149	miR2950	21	UUCCAUCUCUUGCACACUGGA	192	177	290	383	106	283	367
	miR2950	total		216	218	319	423	131	315	413
2288091	miR319	22	UUGGACUGAAGGGAGCUCCCUU	169	149	203	248	130	251	123
9593653	miR319	20	UUGGACUGAAGGGAGCUCCC	312	242	273	327	232	496	243
2485503	miR319	22	CUUGGACUGAAGGGAGCUCCCU	689	737	575	682	477	796	541
6920538	miR319	21	UUGGACUGAAGGGAGCUCCCU	1,291	1,270	1,579	1,943	1,774	2,662	1,312
	miR319	total		2,592	2,513	2,876	3,447	2,724	4,394	2,356
1365095	miR393	22	UCCAAAGGGAUCGCAUUGAUCU	659	422	955	1,264	643	843	758
	miR393	total		701	460	1,041	1,363	671	918	821
9450147	miR396	21	UCCACAGCUUUCUUGAACUG	5	2	135	96	1	10	8
5403016	miR396	21	UGCCACAGCUUUCUUGAACUG	0	1	128	101	3	16	16
9430746	miR396	22	UUCCACAGCUUUCUUGAACUUU	74	88	86	115	37	115	92
3930814	miR396	21	UUCCACACCUUUCUUGAACUG	44	144	49	96	19	225	39
3519222	miR396	21	UUCCAUAGCUUUCUUGAACUG	73	105	74	121	41	122	87
1688761	miR396	19	CCACAGCUUUCUUGAACUG	77	61	75	141	67	204	110

^a Sequences with the more than 100 reads or being the tag with the highest read within the family was designated as abundant miRNAs.

^b Sub-totaled reads within a single miRNA family

(continued)

Table 12. The major sequences and total reads of abundant miRNAs in small RNA libraries constructed from mock-, CymMV-, and CymMV and ORSV mixedly-inoculated tissues. (continued)

ID	Family	Size	Sequence	Reads ^a						
				Mi-2	Mc-2	Ci	Cc	Di	Dc	Dsc
4752899	miR396	21	UUCCACAGCUUUCUUGAACUA	65	61	123	163	65	152	121
2351483	miR396	21	UUCCACAUCUUCUUGAACUG	124	355	113	216	33	320	80
4381227	miR396	22	UUCCACAGCUUUCUUGAACUGC	183	182	181	303	106	268	215
5278057	miR396	21	CUUCCACAGCUUUCUUGAACU	404	466	266	338	87	283	262
5534103	miR396	21	UUCCACAGCUUUCUUGAACUC	559	901	597	979	290	623	747
4197730	miR396	19	UUCCACAGCUUUCUUGAAC	441	635	653	1,099	409	921	728
6824584	miR396	20	UUCCACAGCUUUCUUGAACU	863	999	798	1,157	609	1,163	1,144
5944696	miR396	18	CACAGCUUUCUUGAACUG	1,370	1,566	1,314	1,951	557	1,796	1,729
10189858	miR396	21	UUCCACAGCUUUCUUGAACUU	1,453	1,896	1,606	2,591	740	2,158	2,077
10285039	miR396	21	UUCCACAGCUUUCUUGAACUG	11,225	14,439	12,547	18,545	6,249	20,006	14,405
	miR396		total^b	17,645	22,811	19,787	29,433	9,747	29,531	22,701
11035586	miR397	21	UCGAGGGCAGCGUUGAUGAAA	0	0	135	39	0	0	0
9395939	miR397	22	UUGAGGGCAGCGUUGAUGAAAA	58	22	52	28	5	13	14
	miR397		total	195	143	567	296	33	78	76
13034247	miR398	21	UUUGUUCUCAGGUCGCCCCUG	2	1	201	82	0	1	4
2192559	miR398	21	UGUGUUCUCAGGUCGCCCCGG	125	88	207	131	43	51	48
	miR398		total	580	395	741	450	138	184	203
1359557	miR399	21	UGCCAAAGGAGAGUUGCCCUG	77	66	100	111	42	93	103
	miR399		total	100	108	133	134	55	109	120

^a Sequences with the more than 100 reads or being the tag with the highest read within the family was designated as abundant miRNAs.

^b Sub-totaled reads within a single miRNA family

(continued)

Table 12. The major sequences and total reads of abundant miRNAs in mock-, CymMV-, or double infected tissues. (continued)

ID	Family	Size	Sequence	Reads ^a						
				Mi-2	Mc-2	Ci	Cc	Di	Dc	Dsc
9746162	miR408	21	UGCACUGCCUCUUCCCUGGCU	184	176	207	163	113	152	111
7920685	miR408	22	UGCACUGCCUCUUCCCUGGCUU	4,155	3,631	4,290	3,751	1,542	2,601	2,153
	miR408		total	4,517	3,996	4,765	4,110	1,724	2,882	2,362
9098106	miR5139	22	UCGAAACCUGGCUCUGAUACCA	131	82	82	106	57	106	84
8279168	miR5139	18	AACCUGGCUCUGAUACCA	379	376	327	393	309	427	406
	miR5139		total^b	1,145	935	819	967	617	922	943
5236541	miR528	20	UGAAGGGGCAUGCAGAGGAG	62	135	77	99	11	38	47
8668768	miR528	21	UGUAAGGGGCAUGCAGAGGAG	89	130	126	155	12	72	51
	miR528		total	358	536	445	546	70	267	260
3728764	miR535	21	UUGACAAAGAGAGAGACACG	322	415	824	842	201	1,017	753
1824587	miR535	21	UGACAACGAGAGAGACACGC	634	398	2,997	2,747	759	2,957	1,924
	miR535		total	1,078	902	4,106	3,831	1,037	4,153	2,833
5227291	miR894	24	GUUCGUUUCACGUCGGGUUCACCA	194	99	137	164	74	122	103
8533642	miR894	22	UCGUUUCACGUCGGGUUCACCA	233	130	155	199	87	143	135
7118193	miR894	23	UUCGUUUCACGUCGGGUUCACCA	522	376	324	388	178	322	291
6938561	miR894	21	CGUUUCACGUCGGGUUCACCA	538	364	396	564	182	395	388
2584993	miR894	20	GUUUCACGUCGGGUUCACCA	1,074	761	528	764	316	648	632
5444280	miR894	19	UUUCACGUCGGGUUCACCA	2,618	1,548	887	1,486	678	1,308	1,124
	miR894		total	5,514	3,559	2,696	3,889	1,646	3,205	2,885

^a Sequences with the more than 100 reads or being the tag with the highest read within the family was designated as abundant miRNAs.

^b Sub-totaled reads within a single miRNA family

Table 13. Expression fold-changes of some abundant miRNAs in mock-, CymMV-, or mixedly-infected tissues.

miRNA Family	TPM (Tags per million) ^a							FC (miR%) ^c							FC (wRT-PCR) ^d						
	Mi-2	Mc-2	Ci	Cc	Di	Dc	Dsc	mc/mi ^b	Ci/mi	Cc/mc	Di/mi	Dc/mc	Dsc/mc	mc	Ci	Cc	Di	Dc	Dsi	Dsc	
miR156	602	539	776	681	317	1061	501	0.88	1.06	0.92	0.93	1.68	0.75	1.3	2.4 ^e	2.4	2.9	3.3	3.1	4.8	
miR159	30,779	33,778	44,236	54,335	17,353	44,295	67,496	1.08	1.18	1.18	0.99	1.12	1.60	1.2	1.3	1.1	0.9	1.3	0.9	1	
miR162	10,231	13,287	11,085	13,565	6,456	14,025	11,856	1.28	0.89	0.75	1.11	0.90	0.72	1.1	1.1	1.2	1.2	1.5	1.4	1.5	
miR165	198	197	184	246	82	147	162	0.98	0.76	0.91	0.73	0.64	0.66	0.9	1.2	0.9	1.3	0.9	1.1	1.3	
miR166	1,177,426	1,069,229	862,553	1,119,886	404,168	840,777	964,080	0.89	0.60	0.77	0.60	0.67	0.72	0.9	1.2	1	1.2	0.9	1.1	1.3	
miR167	46,225	37,111	50,400	55,460	17,547	47,093	44,718	0.79	0.90	1.09	0.67	1.08	0.97	0.8	1	1.1	1	1.1	0.8	1.1	
miR168	6,927	5,923	8,883	7,992	11,910	6,560	9,014	0.84	1.06	0.99	3.03	0.95	1.22	1.1	1.6	1.3	1.8	1.3	1.8	1.1	
miR169	169	111	93	111	52	112	96	0.65	0.45	0.73	0.54	0.86	0.69	1	1	0.8	1.1	0.6	12.4	13.3	
miR171	522	527	753	841	375	604	920	0.99	1.19	1.17	1.27	0.98	1.40	1	1.3	1.4	1.1	1.2	1	1.3	
miR172	77	46	114	92	45	67	83	0.59	1.22	1.46	1.03	1.24	1.45	0.9	1.2	0.9	1.2	0.9	1.2	1.2	
miR319	2,592	2,513	2,876	3,447	2,724	4,394	2,356	0.95	0.91	1.00	1.85	1.49	0.75	1.1	1.5	0.9	1.4	0.7	1.4	2.5	
miR393	701	460	1041	1363	671	918	821	0.64	1.22	2.16	1.69	1.70	1.43	0.9	1.3	0.8	1.2	0.9	0.9	1.5	
miR394	7	4	4	5	4	4	7	0.56	0.47	0.91	1.01	0.85	1.40	0.8	1.3	1.2	0.9	1.3	3.3	4.7	
miR396	17,645	22,811	19,787	29,433	9,747	29,531	22,701	1.27	0.92	0.94	0.97	1.11	0.80	1.3	1.1	1.5	1.2	1.6	1.4	1.2	
miR398	580	395	741	450	138	184	203	0.67	1.05	0.83	0.42	0.40	0.41	0.9	0.8	0.5	0.7	0.5	0.4	0.3	
miR408	4,517	3,996	4,765	4,110	1,724	2,882	2,362	0.87	0.87	0.75	0.67	0.62	0.47	0.9	1.2	0.6	0.7	0.5	0.2	0.2	
miR5139	1145	935	819	967	617	922	943	0.80	0.59	0.76	0.95	0.84	0.81	0.9	1	1.1	1.5	1.4	1.1	0.7	
miR528	358	536	445	546	72	267	260	1.47	1.02	0.74	0.35	0.43	0.39	0.9	1.1	0.4	1.4	0.4	0.2	0.3	
miR535	1,078	902	4,106	3,831	1,037	4,153	2,833	0.82	3.14	3.10	1.69	3.93	2.52	1.1	1.3	0.9	1	0.5	0.9	0.8	
miR894	5,514	3,559	2,696	3,889	1,646	3,205	2,885	0.63	0.40	0.80	0.53	0.77	0.65	0.9	2.1	1.4	2.2	0.9	8.9	32.6	
miR1318	18	20	28	29	43	29	30	1.09	1.28	1.06	4.21	1.24	1.20	- ^f	-	-	-	-	-	-	
miR164	18	6	34	19	8	20	19	0.33	1.55	2.31	0.78	2.85	2.54	-	-	-	-	-	-	-	
miR2911	109	145	30	27	38	28	18	1.31	0.23	0.14	0.61	0.16	0.10	-	-	-	-	-	-	-	
miR2950	216	218	319	423	131	315	413	0.99	1.22	1.42	1.07	1.23	1.52	-	-	-	-	-	-	-	
miR397	195	143	567	296	33	78	76	0.72	2.39	1.51	0.30	0.47	0.43	-	-	-	-	-	-	-	
miR399	100	108	133	134	55	109	120	1.06	1.09	0.91	0.97	0.86	0.89	-	-	-	-	-	-	-	
miR529	37	16	29	39	3	16	57	0.42	0.65	1.78	0.14	0.85	2.86	-	-	-	-	-	-	-	
miR5368	33	16	32	28	19	42	23	0.48	0.80	1.28	1.01	2.24	1.15	-	-	-	-	-	-	-	

^a Calculated from (reads of a specific family) ÷ (total clean reads) × 1,000,000. ^b mi: Mi, mc: Mc.

^c FC: fold change. Reads of a specific family was first normalized with total miRNA counts, and then compared between libraries to obtain the fold change index.

^d Fold change calculated from qRT-PCR results by $\Delta\Delta C_t$ -method using miR399 as reference and the value of Mi was arbitrarily set as 1.

^e Numbers in red indicates statistical significant ($P \leq 0.05$).

^f - : not determined.

Table 14. Putative target genes of virus infection-responsive miRNAs.

miR Family	Putative target gene ^a	Arabidopsis homolog	Annotation	Biological process	
miR162	PATC140870	AT1G01040	DICER-LIKE 1 (DCL1)	RNA silencing	
	PATC135020	AT2G04940	mitochondrion and plastid located scramblase-related protein	unknown	
	PATC147200	AT3G20260	unknown protein	acetyl-CoA metabolic process, cell proliferation, microtubule cytoskeleton organization	
miR169	PATC129283	AT1G54160 AT5G06510	NUCLEAR FACTOR Y A5 (NFYA5)	ABA signaling	
	PATC150676				
	PATC126444				
miR319	PATC134871	AT1G30210	TEOSINTE BRANCHED 1/ CYCLOIDEA AND PCF TRANSCRIPTION FACTOR 24 (TCP24)	leaf differentiation, MAPK cascade, SA mediated signaling, defense response, phase transition	
	PATC135086				
	PATC138402	AT1G53230	TEOSINTE BRANCHED 1/ CYCLOIDEA AND PCF TRANSCRIPTION FACTOR 3 (TCP3)		
	PATC089381	AT1G03920	Protein kinase family protein		protein phosphorylation
	PATC125994	AT3G48200	unknown protein		chloroplast relocation, mRNA modification, metabolic process
	PATC128474	AT1G53380	unknown protein		oligopeptide transport
	PATC129076	AT3G55160	chloroplast and cytosol localized unknown protein		nucleotide biosynthetic process
	PATC131148	AT3G23310	AGC (cAMP-dependent, cGMP-dependent and protein kinase C) kinase family protein		nucleotide biosynthetic process
	PATC139252	AT1G69370	CHORISMATE MUTASE 3 (CM3)		aromatic amino acid family biosynthetic process
	PATC148783	AT5G06100	MYB DOMAIN PROTEIN 33, MYB33		regulation of transcription, GA and ABA mediated signaling pathway, pollen cell differentiation programmed cell death
	PATC023828	-	transcription factor MYB101		regulation of transcription
miR393	PATC157696	AT3G62980	TRANSPORT INHIBITOR RESPONSE 1 (TIR1)	auxin mediated signaling pathway	
	PATC149677				
miR394	PATC129841	AT1G27340	LEAF CURLING RESPONSIVENESS (LCR)	leaf vascular tissue pattern formation; regulation of auxin mediated signaling pathway	

(continued)

Table 14. Putative target genes of virus infection-responsive miRNAs (continued)

miR Family	Putative target gene ^a	Arabidopsis homolog	Annotation	Biological process
miR396	PATC130257	AT4G37740	GROWTH-REGULATING FACTOR 2 (GRF2)	embryo and leaf development; response to ABA
	PATC144187	AT2G22840	GROWTH-REGULATING FACTOR 1 (GRF1)	
	PATC133318			
	PATC125749	AT3G51895	SULFATE TRANSPORTER 3;1 (SULTR3;1)	sulfate transport
	PATC125758	AT5G13650	SUPPRESSOR OF VARIATION 3 (SVR3)	chloroplast RNA processing, response to reactive oxygen species
	PATC127048	AT5G53060	REGULATOR OF CBF GENE EXPRESSION 3 (RCF3)	RNA binding
	PATC129416	AT3G13870	GOLGI MUTANT 8 (GOM8)/ROOT HAIR DEFECTIVE 3 (RHD3)	Golgi vesicle transport, cell wall biogenesis, cell growth and differentiation
	PATC129482	AT4G33110	S-adenosyl-L-methionine-dependent methyltransferase	lipid biosynthetic process
	PATC130150	AT1G65010	unnamed protein	flower development, microtubule nucleation
	PATC131246	AT5G20490	type XI myosin protein	root hair and trichome development, organelle trafficking
	PATC137791	AT1G76390	PLANT U-BOX 43 (PUB43)	protein ubiquitination
	PATC144370	AT2G15790	cyclophilin 40 (CyP40) homolog	protein folding, phase transition
	PATC149114	AT1G15240	Phox-associated domain protein	signal transduction
	PATC149117			
	PATC150890	AT1G78570	RHAMNOSE BIOSYNTHESIS 1 (RHM1)	UDP-rhamnose and flavonoid biosynthesis
	PATC151850	AT1G72560	PAUSED (PSD) karyopherin	protein myristoylation, transport between nucleus and cytosol, phase transition
PATC152055	AT5G45340	ABA 8'-hydroxylase	ABA catabolism, redox process	
PATC076655	-	hypothetical protein	unknown	
miR398	PATC143343	AT2G28190	COPPER/ZINC SUPEROXIDE DISMUTASE 2 (CSD2)	response to light stimulus and oxidative stress
	PATC152430			
	PATC143977	AT3G15640	Rubredoxin-like superfamily protein	glucose catabolic process
miR408	PATC113957	AT2G30210	LACCASE 3 (LAC3)	lignin catabolic and redox process
	PATC003794			
	PATC146846	AT2G02850	plantacyanin	phase transition; respond to ABA and freezing
	PATC128673	AT1G07090	LIGHT SENSITIVE HYPOCOTYLS 6 (LSH6)	unknown
	PATC149690	AT1G76630	Tetratricopeptide repeat (TPR)-like superfamily protein	RNA interference, methylation-dependent chromatin silencing

^a Orchidstra database (<http://orchidstra.abrc.sinica.edu.tw>) accession numbers. Targets also reported in *A. thaliana* are indicated in bold.

Table S1. Primers used in RT-PCR and stem-loop qRT-PCR.

Identifier	Sequence	Amplification target	Position
CymMV CP-F1 ^a	ATGGGAGAGYCCACTCCARCYCCAGC	CymMV CP	CP gene 1-26 nt
CymMV CP-R1	TTCAGTAGGGGGTGCAGGCA	CymMV CP	CP gene 669-650 nt
ORSV CP-F1	ATGTCTTACACTATTACAGACCCG	ORSV CP	CP gene 1-24 nt
ORSV CP-R1	GGAAGAGGTCCAAGTAAGTCC	ORSV CP	CP gene 474-454 nt
ORSV-3	ATGTCTTACACTATTACAGACCCGTCTAAG	ORSV CP	genome 5721-5750 (U34586)
ORSV-6	TTAGGAAGAGGTCCAAGTAAGCCGCTCGAGCGG	ORSV CP	genome 6197-6177 (U34586)
CymRdRp-R	GCTCTAGAGCGCCCCTATGTTCCAGCATCAA	CymMV RdRp	genome 3025-3045 (U62963)
CymRdRp-F	CCGCTCGAGCGGTCTGGTGGCATTGTAGGCAATAGA	CymMV RdRp	genome 3781-3804 (U62963)
OR-RdRp-F	ATTGGCGACGAGTGGCCGTC	ORSV RdRp	genome 2411-2430 (AY571290)
OR-RdRp-R	TGCAACAAGAACGTGCGGTGA	ORSV RdRp	genome 3270-3250 (AY571290)
CyRdRp1319-F	GCCTCTGCCATCTTTAGTGAGT	CymMV RdRp	genome 2404-2425 (EF125180)
CyRdRp1319-R	GTCCCGAGGAAGATTCAGC	CymMV RdRp	genome 3722-3703 (EF125180)
OR-CP3UTR-F	AAgCTCggCTTgggCTgACC	ORSV CP+3'UTR	genome5763-5782 (AY571290)
OR-CP3UTR-R	gCCTTACCCgAggTAAgggggA	ORSV CP+3'UTR	genome6609-6587 (AY571290)
URP ^b	gTgCAgggTCCgAggT	universal reverse primer for miRNA detection	
miR156-F ^c	gCggCgg CTGACAGAAGATAGA		
miR156-R	gTTggCTCTggTgCAgggTCCgAggTATTCgCACCAgAgCCAAC GTGCTC		
miR159-F	gCggCgg TTTggATTgAAgggA		
miR159-R	gTTggCTCTggTgCAgggTCCgAggTATTCgCACCAgAgCCA ACTAgAgC		

^a CymMV CP-F1/R1, ORSV CP-F1/R1 primer pairs are adopted from Lee and Chang (2006). R nucleotide represents A or G.

^b Stem-loop qRT-PCR primers were designed based on the methods described by Varkonyi-Gasic and Hellens (2010). Characters in bold indicates mature sequence of miRNA.

(continued)

Table S1. Primers used in RT-PCR and stem-loop qRT-PCR. (continued)

Identifier	Sequence	Amplification target	Position
miR162-F ^a	gCggCgg TCGATAAACCTCTGC		
miR162-R	gTTggCTCTggTgCAgggTCCgAggTATTCgCACCAgAgCCAACCCGGAT		
miR165-F ^a	gCggCgg TCggACCAggCTTCA		
miR165-R	gTTggCTCTggTgCAgggTCCgAggTATTCgCACCAgAgCCAACgggggA		
miR166-F	gCggCgg TCggACCAggCTTCA		
miR166-R	gTTggCTCTggTgCAgggTCCgAggTATTCgCACCAgAgCCAACggggAA		
miR167-F	gCggCgg TGAAGCTGCCAGCATG		
miR167-R	gTTggCTCTggTgCAgggTCCgAggTATTCgCACCAgAgCCAACACAGAT		
miR168-F	gCggCgg TCgCTTggTgCaggT		
miR168-R	gTTggCTCTggTgCAgggTCCgAggTATTCgCACCAgAgCCAACgTCCCg		
miR169-F	gCggCgg TAGCCAAGGATGAC		
miR169-R	gTTggCTCTggTgCAgggTCCgAggTATTCgCACCAgAgCCAACAGGCAA		
miR171-F	gCggCgg TTGAGCCGCGTCAAT		
miR171-R	gTTggCTCTggTgCAgggTCCgAggTATTCgCACCAgAgCCAACGGAGAT		
miR319-F	gCggCgg TTGACTGAAGGGAG		
miR319-R	gTTggCTCTggTgCAgggTCCgAggTATTCgCACCAgAgCCAACAGGGAG		
miR393-F	gCggCgg TCCAAAgggATCgCAT		
miR393-R	gTTggCTCTggTgCAgggTCCgAggTATTCgCACCAgAgCCAACAgATCA		

^a Stem-loop qRT-PCR primers were designed based on the methods described by Varkonyi-Gasic and Hellens (2010). Characters in bold indicates mature sequence of miRNA. (continued)

Table S1. Primers used in RT-PCR and stem-loop qRT-PCR. (continued)

Identifier	Sequence	Amplification target	Position
miR394-F	gCggCgg TTGGCATTCTGTCC		
miR394-R	gTTggCTCTggTgCAgggTCCgAggTATTCgCACCAgAgCCAAC GGAGGT		
miR396-F	gCggCgg TTCCACA gCTTTCTT		
miR396-R	gTTggCTCTggTgCAgggTCCgAggTATTCgCACCAgAgCCAAC CAgTTC		
miR398-F	gCggCgg TgTgTTCTCA g gTCg		
miR398-R	gTTggCTCTggTgCAgggTCCgAggTATTCgCACCAgAgCCAAC CAgggg		
miR399-F	gCggCgg TGCCAAAGGAGAGTT		
miR399-R	gTTggCTCTggTgCAgggTCCgAggTATTCgCACCAgAgCCAAC CAAGGCGC		
miR408-F	gCggCgg TGCACTGCCTCTTCCC		
miR408-R	gTTggCTCTggTgCAgggTCCgAggTATTCgCACCAgAgCCAAC CAAGCCA		
miR5139-F	gCggCgg AACCTGGCTCTG		
miR5139-R	gTTggCTCTggTgCAgggTCCgAggTATTCgCACCAgAgCCAAC CTGGTAT		
miR528-F	gcggcgg TGTAAGGGGCATGCA		
miR528-R	gttgctctggtgcagggctccaggtattgcaccagagccaac CTCCTC		
miR535-F	gcggcgg TTGACAAAGAGAGAG		
miR535-R	gttgctctggtgcagggctccaggtattgcaccagagccaac CGTGCT		
miR894-F	gCggCgg TTTCACGTCGGGT		
miR894-R	gTTggCTCTggTgCAgggTCCgAggTATTCgCACCAgAgCCAAC CTGGTGA		

^a Stem-loop qRT-PCR primers were designed based on the methods described by Varkonyi-Gasic and Hellens (2010). Characters in bold indicates mature sequence of miRNA.

Table S2. Information about the super-abundant miR166 (ID:3004100) tag small RNA libraries constructed from mock- and ORSV-infected tissues.

	Mi	Mc	Oi	Oc
15-27 reduced reads ^a	5,995,466	6,435,986	8,298,644	3,495,508
Total clean reads ^b	5,990,907	6,428,789	5,839,287	3,489,671
Reads				
Total miRNA	1,134,103	901,940	608,497	325,957
Total miRNA-166 ^c	229,855	266,639	174,753	101,600
% in total clean reads				
Total miRNA	18.9%	14.0%	10.4%	9.3%
Total miRNA – 166 ^d	3.8%	4.1%	3.0%	2.9%
Information of miR166 (ID:3004100)				
Reads	904,248	635,301	433,744	224,357
% in total miRNA	79.7%	70.4%	71.3%	68.8%
% in total clean reads	15.1%	9.9%	7.4%	6.4%

^a Adapter and low quality sequences trimmed reads with further filtering of low frequency (tags with only 1 read in only 1 library was removed).

^b Total reads of 15-27 reduced tags after vsRNA and microbe contaminant tags were removed.

^{c,d} Reads and percentage of total miRNA re-calculated after the ID: 3004100 miR166 tag was removed.

Table S3. The non-redundant list of the top 50 abundant CymMV vsRNAs in Ci, Di and Dc libraries.

ID	Sequence	Length	Polarity	Start ^a	End	Library ^b
34729	UUGCCUCGGCACUCGUAAACU	21	+	168	188	Di
316385	CCUUCGACGCCAAUACUGAAU	21	+	3759	3779	Ci,Dc
525483	UUACGUUUUCUGCACUUGACC	22	+	2930	2951	Ci
606459	CCAGUCAACAACGUAGUUAUC	21	+	2234	2254	Ci,Di,Dc
778771	CUCAAGCUCUGAAACCGAGGA	21	+	1453	1473	Dc
782058	CUAAGAAACUUGAUGCAUGCC	21	+	4008	4028	Ci,Di,Dc
914102	UCUGAAACCGAGGACUCUGAG	21	+	1460	1480	Ci,Di,Dc
938095	CACCCAAACUGCGGACAUUCG	21	+	867	887	Ci,Di,Dc
1014359	UCAGUUCUCGAGCUUCCGCCU	21	+	1914	1934	Ci,Dc
1103073	UGUAGCUGAACUCGCUUGCCU	21	+	2461	2481	Ci,Di,Dc
1216119	CCAUUGUCCAAACGUAGAGCU	21	+	950	970	Ci,Di,Dc
1254676	CGUAUUUCUGCACUUGACCUG	21	+	2933	2953	Ci,Di,Dc
1341912	UCGACGCCAAUACUGAAUGCU	21	+	3762	3782	Ci,Di
1575880	CUGACCGUGAACGUGCUGCGCA	22	+	5994	6015	Ci,Dc
1608330	UCUACCUCAUGAGCCUGUUC	21	+	3187	3207	Ci,Dc
1645244	CAAUGUGGGACUGUGUGAGAA	21	-	4510	4490	Ci,Dc
1815323	UAAGAAACUUGAUGCAUGCCU	21	+	4009	4029	Ci,Di,Dc
2384603	CAAUUGAUCCCGACUUCUGAG	21	+	1040	1060	Ci,Di,Dc
2389913	UACUUGAACACUGGUACACACA	21	+	3543	3563	Ci,Di,Dc
2715066	CCGAAAAGCACUCUCGCGAG	21	+	2954	2974	Ci,Di,Dc
2838623	CUACUACUCUAGUCGCACCCA	21	+	4670	4690	Ci,Di,Dc
3171235	UGGCUGUGGCAAUCUUAUGC	21	+	2068	2088	Ci
3391029	CCCACCGUAAUGUAGCUG	18	+	2451	2468	Di
3618470	UUAAGAAUAGUAGGACUGGGA	21	+	1947	1967	Di
3646483	AUACUGAAUGCUCUAUUGCCU	21	+	3771	3791	Ci,Di,Dc
3738595	UUGUGAAAAGACUCCGGAGGA	21	+	3508	3528	Ci
3841209	CCGAGAUUUUCGAGACAGUCG	21	-	237	217	Ci,Di,Dc
3870341	UGCCCAACUCUAGAACUACGU	21	+	2141	2161	Ci,Dc
3921833	UUUCCUCCGUUUCUUCGUAUG	21	+	1125	1145	Di,Dc
4145901	UCACGCCGAGAUUUUCGAGAC	21	-	242	222	Ci,Di,Dc
4203274	UCCCAACUCGCAGGCUUUCUG	21	+	2758	2778	Ci,Di,Dc
4702849	ACUGGCUCAAUAGAUCGGAAGC	23	+	2166	2188	Di
4744517	UCACCCGUGGGCUUGUACAGCU	22	-	1791	1770	Ci
4798235	UUGCCCCCAAACUUUGAUCCU	21	+	1526	1546	Ci,Di,Dc
5040346	UCUCUUUAAUACCUGAUGCCU	21	+	2388	2408	Ci,Di,Dc
5104944	UUUCCAUCAUGCGCCUAUCUG	21	+	3726	3746	Di
5242767	CAAUUGAUCCCGACUUCUGAGU	22	+	1040	1061	Ci,Di,Dc
5324354	CUCUGGAACAUCUGCAAAGCU	21	+	3221	3241	Ci,Dc
5338737	CUAAGAAACUUGAUGCAUGCCU	22	+	4008	4029	Ci,Di,Dc
5626849	UGACCGUGAACGUGCUGCGCA	21	+	5995	6015	Ci
6422152	CCGAAAAGCACUCUCGCGAGA	22	+	2954	2975	Dc
6743361	AAAAGAAACUGAAAUUGACCU	21	+	3900	3920	Ci,Di,Dc
6827705	UACCCUCUAGAAUGAAGCAAG	21	+	2568	2588	Di
6984015	UUGGGCAUACCACAGUAGCUG	21	-	2147	2127	Di
7501856	UAGAGGAUCAAGUUUGGGGGC	22	-	1549	1528	Ci
7685056	UCAACGAUAAUGGACUUGCCC	21	-	1575	1555	Ci,Di,Dc
7803887	UUCUGCUGGCAACCCUGGUCC	21	+	579	599	Di

(continued)

Table S3. The non-redundant list of the top 50 abundant CymMV vsRNAs in Ci, Di and Dc libraries. (continued)

ID	Sequence	Length	Polarity	Start	End	Library
7846663	UAUUCAUCGCAUGGUAGGUCU	21	-	1377	1357	Di
7935383	CCGACUGUCUCGAAAAUCUCG	21	+	216	236	Di
7979091	CUGAAAAUUCUGCUGGCAACC	21	+	572	592	Ci,Di,Dc
8085598	UAAAGAUCGCGUUCGCUCACC	21	-	1026	1006	Ci,Di,Dc
8181372	CUGAAAAUUCUGCUGGCAACCC	22	+	572	593	Di,Dc
8206317	CCAUAGACGCUAGACUCUCUA	21	+	3078	3098	Ci,Di,Dc
8297013	UGAGGAACAAACUGAACGGCU	21	+	2830	2850	Ci,Di,Dc
8399676	CAACUCUAGAACUACGUAAUG	21	+	2145	2165	Di,Dc
8467258	UGAACAUGCCUGGAAAGCCU	21	+	1983	2003	Ci,Di,Dc
8552386	CAAACUUUGAUCCUCUAGACA	21	+	1533	1553	Di
8560024	CGAGACUACCGUAGCCACAGCG	22	+	4213	4234	Ci,Di,Dc
8658681	UUGAGUGACAUAGGCGAGAGA	21	-	2023	2003	Ci
8715788	UUGACUGUCACGCCGAGAUUU	21	-	249	229	Ci,Di,Dc
8794800	CGCAUUCAUACCCUUAGGAUG	21	-	943	923	Ci,Di,Dc
8822573	CUCCGGAGGACUCAAUAAAUU	22	+	3519	3540	Ci,Dc
8984112	UUCUUUUUGAACUCGUCUCU	21	+	3204	3224	Di,Dc
9005510	CUGACGAGGAAGUGUACAACU	21	+	4818	4838	Di,Dc
9185375	CACAAGACUCGUCAUCGUAACG	22	-	470	449	Di,Dc
9389731	CAACAGGCAAAGGACGAAACCC	22	+	3044	3065	Dc
9515535	CCCGAGACUACCGUAGCCACA	21	+	4211	4231	Di,Dc
9745462	UUAUACCUGAUGCCUCUGCC	21	+	2393	2413	Ci,Di,Dc
10058797	UCAGAAGUCGGGAUCAAUUGCC	22	-	1059	1038	Ci
10091781	CCAUCUAUACUUUGAACUACC	21	+	642	662	Di,Dc
10530383	CUCUAGAACUACGUAAUGACU	21	+	2148	2168	Ci,Di,Dc
10538747	UUAUUGAAGACGUCACCCAAG	21	+	3813	3833	Di

^a The viral genome position of the vsRNA. Sites are based on genomic sequence of the Taichung strain.

^b Indicating the for which library vsRNA tag was in the top 50 abundant list.

Table S4. The non-redundant list of the top 50 abundant ORSV vsRNAs in Oi and Di libraries.

ID	Sequence	Length	Polarity	Start ^a	End	Library ^b
76683	UAAAUCUGUUAGUGUCCCGAG	21	+	3599	3619	Di
81070	CGGAAACAUUAGAUGCAACUC	21	+	6043	6063	Oi
173402	UCUGUCAACAAAAAGAAACCU	21	+	5512	5532	Oi
280101	CUCGAACAACUGUUCAACAGC	21	+	5842	5862	Oi
329364	UCAAGUAGGAACCGGCUGCC	21	-	5898	5878	Oi
369199	UUAUACGUCAAGGCUUUGUCU	21	-	1309	1289	Di
840672	UCGAAAAGGAAUAAGUAUC	21	-	1019	999	Di
845480	UCAUUUGAGACGAUGUCUGGA	21	+	6156	6176	Oi
913828	CGAGAUUACGUCCAUUGCUGU	21	+	420	440	Oi,Di
1030613	AUACUUUGUCUGAUUAUGAUU	21	+	5021	5041	Oi
1072910	CUAAAGGAUGUCUAUGGUGCC	21	+	2226	2246	Di
1137936	UAACGUUGAUAGUGUUGAACU	21	+	6213	6233	Oi
1243319	UAACUCUAGAACUCCAUGGCC	22	-	4199	4178	Di
1424549	UCCACUAAAUCGAAGGGUUG	21	+	6487	6507	Oi,Di
1602970	UUAGAGAGGAUAGACAGUAGC	21	+	4086	4106	Di
1706093	AUUUGAGACGAUGUCUGGACU	21	+	6158	6178	Oi
1864616	UUACAGGCGUUAUCAUGACU	21	+	1401	1421	Di
1893580	CGUAGUCUCAAGAAGCAGAUU	21	-	779	759	Oi
1938541	UGAAGAACUAUAUGGAUUACC	21	+	2161	2181	Oi,Di
1960633	AGGGAUCUGAAGAGACGGCC	21	-	2443	2423	Oi
2097716	UUUAUCCCGUUGUGUACACG	21	+	6333	6353	Oi,Di
2180236	CAAGGUAGAUACUUAUUUCCU	21	+	992	1012	Oi
2224524	UUCCGGGAAAACAACGCUG	21	+	637	657	Di
2298819	UUACGUCCAUUGCUGUAUGCC	21	+	425	445	Oi
2366968	CUGCAGAUAGUAGGUUCCU	21	+	6296	6316	Oi
2487467	CUAGAACUCCAUUGGCACCG	21	-	4194	4174	Oi,Di
2708917	AGGCAUCUGAAGUCAUCGGUG	21	-	3852	3832	Oi
2724343	CCUUUACAACACUCAACUCG	21	+	277	297	Di
2892466	GAGAUACGUCCAUUGCUGUA	21	+	421	441	Oi
3137167	UACGGAAACAUUAGAUGCAACU	22	+	6041	6062	Oi,Di
3291517	UUUGCCACUCUGUUUAUAAAG	21	-	2866	2846	Di
3293887	UUCAGACGUUGUUAAGCUGCU	21	+	2467	2487	Oi
3327177	AAAGACUUGAGCCUAGCAGCC	21	-	5507	5487	Oi
3373159	GAUAACAGGCUGAUGACCC	19	+	3320	3340	Di
3522752	UAUCGGUUGUUCGUUUGACAC	21	+	3199	3219	Di
3900368	AGCGCACUUAUAUAAAGGACG	21	+	401	421	Oi
4226530	UAACAUCUGCCGGGCAUCUAAG	22	-	2952	2931	Di
4369547	UAACUCUAGAACUCCAUUGG	21	-	4199	4179	Di
4440777	CACACGAGACCUAUUUGACUC	21	-	1349	1329	Oi
4468189	UACAGACCCGUCUAAGCUGGCU	22	+	5735	5756	Oi
4561576	CACAACAAGCUCGAACAACUGU	22	+	5833	5854	Oi,Di
4688003	UUCCGGGUGUAAAACAAAAUU	22	-	4129	4108	Di

(continued)

Table S4. The non-redundant list of the top 50 abundant ORSV vsRNAs in Oi and Di libraries. (continued)

ID	Sequence	Length	Polarity	Start ^a	End	Library ^b
4839798	CUGAACGUCCACGUAGUGCUG	21	+	3661	3681	Oi,Di
4842582	UUGAUCCAGACGUCGUGGCGA	21	+	1816	1836	Di
5032603	CAACAAAGUUAUUGAGGCUGGU	22	+	89	110	Oi
5092991	UACAGACCCGUCUAAGCUGGC	21	+	5735	5755	Oi
5145985	CCACUUAUUUCGAAGGGUUUU	21	+	6272	6292	Oi
5150094	UGAGUAUCUGUCUUGUAGACA	21	+	5141	5161	Oi
5309030	UUUCUGCAGACUCUGGGUCGG	21	-	2265	2245	Di
5487552	UUACAGACCCGUCUAAGCUGGC	22	+	5734	5755	Oi
5965634	CUCUAGAACUCCAUUGGCACC	22	-	4196	4175	Di
6219210	CCAGAUAAAGUAGAAACAGUAUC	22	-	510	489	Di
6683200	UUACGUCCAUUGCUGUAUGCCU	22	+	425	446	Di
6720991	UUCUCGAUCCUCUCGUCAAAG	21	+	3310	3330	Di
6723019	UUCGGAUAAAGGGAAAUUUGCC	21	-	2881	2861	Di
6754836	CGCACAAUCUGAUUCGUUAUUG	21	+	5697	5717	Oi
6877727	AUGUCUGGACUUACUUGGACC	21	+	6168	6188	Oi
6947413	AGCAUCAAAAUCUCUGAAUUU	21	+	4900	4920	Oi
6978017	CAACCGAUACGUCUUCAAAGG	21	-	3207	3187	Di
7100261	UCGUAGACUCCAGACUUUUUCU	21	-	2281	2261	Di
7179774	CUUUUAAAAAUCCAACGCCUG	21	+	1876	1896	Di
7447200	CCACUGCCGACGCUCUUAAG	21	+	5261	5281	Di
7719063	CAAUUGAGACUUGAUUGUACA	21	-	6162	6142	Oi
7907315	AAACUGUGAAUUUUGAUGAGG	21	+	2575	2595	Di
8125631	UCAACGGAGUAAGAACAGUCU	21	-	634	614	Di
8168936	ACGGAAACAUAUGAUGCAACU	21	+	6042	6062	Oi
8207743	UUACCUCGGGUAGAGGCC	19	+	6592	6610	Oi
8210134	CAGCCGGUCCUACUUUGACC	21	+	5880	5900	Oi
8227972	AGCAAAAGAUCAAGUCGUACU	21	+	1448	1468	Oi
8300098	CAUGUCCAGACUUAUUAGCUC	21	-	2664	2644	Di
8540758	UUAUAAUGCUUUAUCGGAACU	21	+	1727	1747	Di
8598473	UUCCAAAGGGACUUGAUCUCC	22	+	4498	4519	Di
8699519	UAAGAAAACUUUGGCAAUGCU	21	+	1085	1105	Di
8728174	UCGAGCGGAGCAGACGUAGUC	21	-	793	773	Di
8814023	CGAGAUUACGUCCAUUGCUGUA	22	+	420	441	Oi,Di
8850722	UGUCCAGACUUAUUAGCUCUC	21	-	2662	2642	Di
8958524	ACGAGAUUACGUCCAUUGCUG	21	+	419	439	Oi
9289445	ACUGUAGCAAUAAGAUCUGCA	21	+	6081	6101	Oi
9310450	AGGAACCGGCUGCCAAACAUC	21	-	5891	5871	Oi
9353671	UCUAGAACUCCAUUGGCACC	21	-	4195	4175	Di
9392694	ACACAACAAGCUCGAACAACU	21	+	5832	5852	Oi
9409393	UCGCGAAAGAUCGUCCUUUCG	21	-	1132	1112	Di
9472785	ACUGUAUCGUCAAUUUUUGA	21	-	1498	1478	Di

(continued)

Table S4. The non-redundant list of the top 50 abundant ORSV vsRNAs in Oi and Di libraries. (continued)

ID	Sequence	Length	Polarity	Start ^a	End	Library ^b
9529651	CCUCCACUAAAUCGAAGGGU	21	+	6269	6289	Oi
9809899	CAGCGCGAUCGCGAAAGAUCG	21	-	1140	1120	Di
9979778	CGGAUGAGUUCGGAGCUGCCU	21	+	688	708	Di
10122434	UCUGAAGUAACCAGCGCCUGC	21	-	5933	5913	Oi,Di
10176148	UAAUAGAAUAAUCGAGGUAGA	21	+	5999	6019	Di
10395509	CAGACCCGUCUAAGCUGGCUU	21	+	5737	5757	Oi
10407909	CGAUGUCUGGACUACUUGGAC	22	+	6166	6187	Oi

^a The viral genome position of the vsRNA. Sites are based on genomic sequence of the Taichung strain.

^b Indicating the for which library vsRNA tag was in the top 50 abundant list.



Table S5. List of ORSV vsRNAs specifically sequenced in Di library.

ID	Sequence	Length	Polarity	Start ^a	End	Reads ^b
264355	AAAGUUCCUAUGGCUGCUAGGCU	23	+	5476	5498	58
454015	AAAGUUCCUAUGGCUGCUAGGCUCA	25	+	5476	5500	32
1443203	UGCUGAAUUGACAUUCUCAUGACU	23	+	4948	4969	38
1477357	CUACUACCGUCAGCUCU AACGGCUGU	26	+	4945	4970	55
1602498	AAAGAAGAAAGAAGAUUUGAACGCU	25	+	5480	5504	32
1711603	AAGUUCCUAUGGCUGCUAGGCUCAAG U	27	+	5477	5503	38
1808182	AAAGUUCCUAUGGCUGCUAGGCUCAA G	27	+	5476	5502	48
2079993	AAGUUCCUAUGGCUGCUAGGCUCAAG	26	+	5477	5502	40
2452139	UUCCUAUGGCUGCUAGGCU	19	+	5480	5498	52
2880184	CUUACGAUAUAUUUUGCCU	20	-	4577	4558	46
2979262	UUAUCGGAUGCUCUUUCACC	20	+	1902	1921	81
3311699	UUCCUAUGGCUGCUAGGCUCAAGU	24	+	5480	5503	32
3512506	UUUGCCACUCUGUUUAUAAA	20	-	2866	2847	44
4120311	AGUUCCUAUGGCUGCUAGGCUCAAGU	26	+	5478	5503	38
4343398	AAGUUCCUAUGGCUGCUAGGCUCA	24	+	5477	5500	37
4357101	ACAUUCGCGAUGUGGCUCGUCACA	24	+	454	477	45
4498907	GUUCCUAUGGCUGCUAGGCUCAAGUC	26	+	5479	5504	31
4606561	UUAUCGGAUGCUCUUUCACCG	21	+	1902	1922	86
4680649	GAGAAAGUUCCUAUGGCUGCUAGGCU	26	+	5473	5498	34
4709390	CCUAUGGCUGCUAGGCUCAAGUCUU	25	+	5482	5506	39
4951352	AAAGUUCCUAUGGCUGCUAGGCUC	24	+	5476	5499	61
5497155	GUUCCUAUGGCUGCUAGGCU	20	+	5479	5498	46
5998569	GAGAAAGUUCCUAUGGCUGCUAGGCU C	27	+	5473	5499	73
6881534	AGAAACUUGGUCUAAAUGGC	20	+	4264	4283	63
7648761	UUCCUAUGGCUGCUAGGCUCAAGUCU U	27	+	5480	5506	112
7925030	AAGUUCCUAUGGCUGCUAGGCUC	23	+	5477	5499	52
8421996	GAAAGUUCCUAUGGCUGCUAGGCUC	25	+	5475	5499	59
8455787	GUUCCUAUGGCUGCUAGGCUCA	22	+	5479	5500	64
10092305	UCCUAUGGCUGCUAGGCUCAAGUCU	25	+	5481	5505	30
10193462	UUCCUAUGGCUGCUAGGCUCAAG	23	+	5480	5502	44
10330019	GAGAAAGUUCCUAUGGCUGC	20	+	5473	5492	48
10348700	UUCCUAUGGCUGCUAGGCUCAAGUCU	26	+	5480	5505	45
12623724	UUGGCAGCCGGUCCUACUUUG	22	+	5876	5897	32
13605836	UUCGCGAUGUGGCUCGUCACAU	22	+	457	478	38

^a The viral genome position of the vsRNA. Sites are based on genomic sequence of a ORSV strain (DQ139262).

^b Indicating the read counts of the tag in Di library.

Table S6. List of CymMV vsRNAs specifically sequenced in Di library.

ID	Sequence	Length	Polarity	Start ^a	End	Reads ^b
697298	GCUCAAUAAGAUCGGAAG	18	+	2170	2187	52
724255	AUGGCGUUCGGAGUUUGUGUUGCU	24	-	921	902	70
768993	AUAUGCUUGCUGAGUGUCGACACCU	24	+	2161	2187	155
1746381	AACACUAGAAUAUUCUAAACC	21	-	4906	4886	208
1791194	AGUCUAGCGUCUAUGGUAGC	20	-	3093	3074	62
2086441	AGUUUCCCGAGAGUCAACCACUGCAGA	27	-	756	730	236
2202084	CAUGGCUUUAAAGGAAAGAGUAAGCU G	27	+	1748	1774	277
2320809	CAUUAUAGCUUUGUAAUUGAC	21	-	3184	3164	131
2352587	GUUUCUUUACUUUCAAGGAU	21	-	788	768	93
2426915	UGGCUUUAAGGAAAGAGUAAGCUG	25	+	1750	1774	103
2735476	UACACUAGAAUAUUCUAAAC	21	-	4907	4887	51
2875561	UUGUAAUUGACAAAAGGAC	20	-	3174	3155	147
2895625	UGACUGAUGAAUAGUAAGU	19	-	1122	1104	82
3075964	UUUCUUUACUUCAAAGGAU	20	-	787	768	90
3239158	GUGUAUGCGUUUGGAUG	17	-	275	259	70
3312278	GAGCAGUUGAUUAAUUG	18	-	1255	1238	54
4162772	GGAGGGUUCUUAGGAAG	18	-	346	329	125
4965267	AGGAACAGGCUCAUGAGGUAG	21	-	3208	3188	75
5006172	AAAUUGAGAAAUUGGAGC	20	+	3362	3381	98
6213507	GUUUUGAUUUCGUUUGUUC	20	-	2211	2192	111
6301898	AGUUUACGAGUGCCGAGGCAAGGACA G	27	-	188	162	57
7178992	GAAUAUUGUCUUUGUUGUUG	20	-	416	397	66
8970474	ACACUGGUCACACAAGCAAGUUG	23	+	3550	3572	102
9138608	AUGGACCAUGUGUGCCUGAGAAGAA G	27	+	3857	3883	114
9208604	GUCCUUUGCCUGUUGAUGCUG	21	-	3058	3038	51
9527620	GGCGGCGGUCGUAGGUAGC	20	-	397	378	50
9601064	UCAAGUAUGAAUUUAUGAAG	21	-	3549	3529	99
9633694	AGGGUAGCACUCUUGGACG	19	-	5733	5715	54
9689144	UUUCAACAGUUUUAGCUGC	20	-	300	281	125
11391303	AGUAUGAAUUUAUGAAGU	19	-	3546	3528	66
11543353	UGAUGAAUAGUAAGUAAUUG	20	-	1118	1099	59
11982790	AAUUGAGAAAUUGGAGC	18	+	3364	3381	68
12585279	GUCUAUCAAAAUUGGAUU	19	-	2674	2656	50
12695775	UGGUGUGGAAUCUGAUGCUG	20	+	5841	5860	61
12953577	CAAGUGUAUAAUGUUUGUCC	21	-	2715	2695	91
14930538	UUAGGCUCA AUGUGUUGAUUU	21	-	438	418	76
16540575	GGUAAAGAAAUUGAGAAAUUGGAGC	27	+	3355	3381	68

^a The viral genome position of the vsRNA. Sites are based on genomic sequence of the Taichung strain.

^b Indicating the read counts of the tag in Di library.

Table S7. The super-abundant miR166 (ID:3004100) tag in small RNA libraries of mock-, CymMV-, and mixedly-inoculated tissues.

	Mi-2	Mc-2	Ci	Cc	Di	Dc	Dsc
15-27 reduced reads	3,644,782	3,343,199	3,270,176	3,674,964	3,879,317	3,618,508	3,382,737
Total clean reads	3,643,873	3,342,094	3,078,515	3,673,121	2,281,799	3,333,950	3,381,746
Reads							
Total miRNA	1,308,744	1,198,256	1,020,228	1,304,899	481,727	1,004,585	1,137,795
Total miRNA-166 ^a	167,030	170,064	202,923	232,752	94,845	199,225	211,964
% in total clean reads							
Total miRNA	35.9%	35.9%	33.1%	35.5%	21.1%	30.1%	33.6%
Total miRNA – 166 ^b	4.6%	5.1%	6.6%	6.3%	4.2%	6.0%	6.3%
% of miR166 (ID:3004100)							
Reads	1,141,714	1,028,192	817,305	1,072,147	386,882	805,360	925,831
% in total miRNA	87.2%	85.8%	80.1%	82.2%	80.3%	80.2%	81.4%
% in total clean reads	31.3%	30.8%	26.5%	29.2%	17.0%	24.2%	27.4%

^a Adapter and low quality sequences trimmed reads with further filtering of low frequency (tags with only 1 read in only 1 library was removed).

^b Total reads of 15-27 reduced tags after vsRNA and microbe contaminant tags were removed.

^{c,d} Reads and percentage of total miRNA re-calculated after the ID: 3004100 miR166 tag was removed.

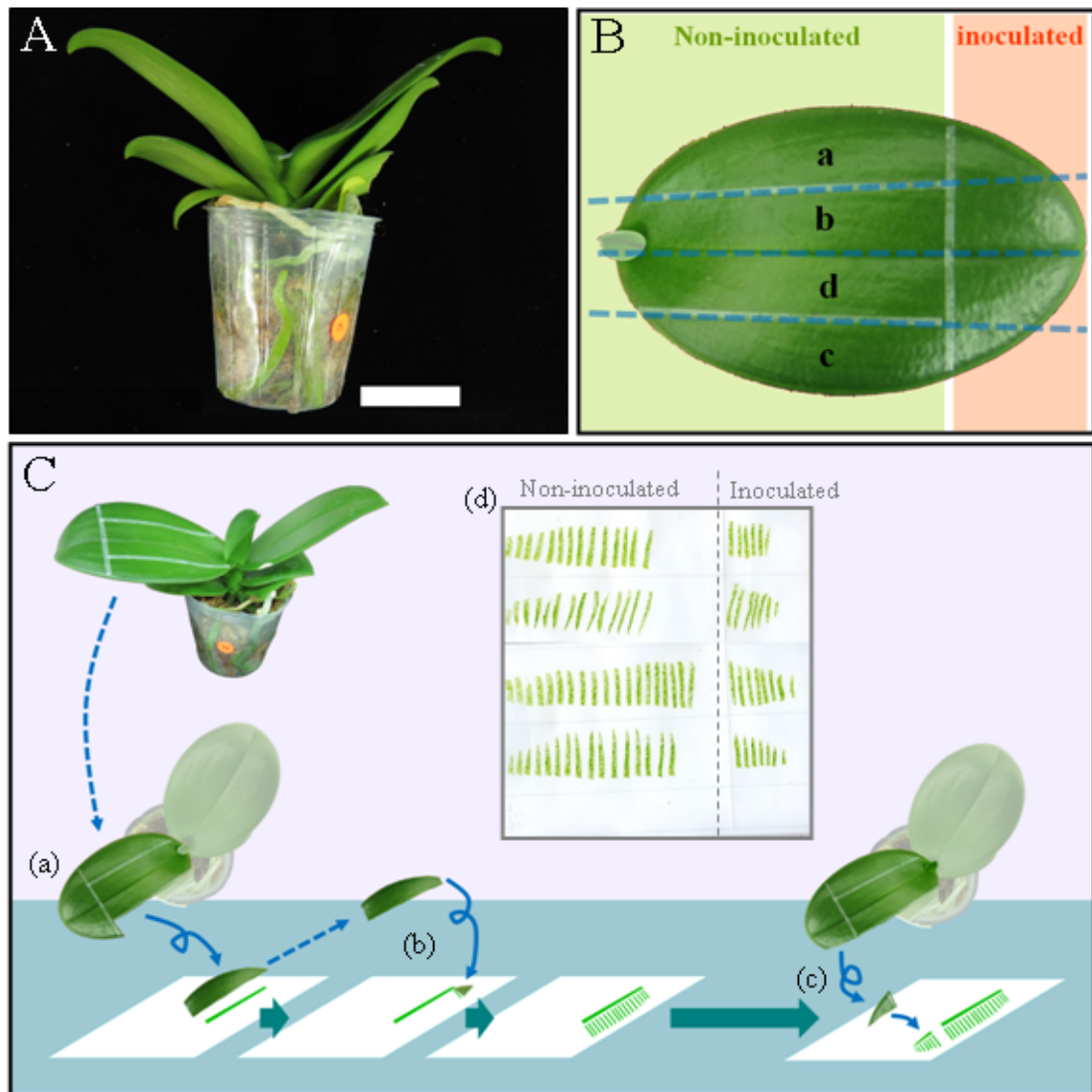


Fig. 1. Diagrams of leaf tip-inoculation and tissue-blotting methods used in the infection time-course assays.

(A) 7.5-cm pot *Phalaenopsis amabilis*. Bar = 5 cm. (B) Virions were inoculated in the tip-side of the inoculated leaf as labeled. Four zones were marked on the inoculated leaf for sampling at different time points (as a-d representing 2, 4, 7, 11, or 5, 10, 20, 30, or 4, 11, 16, 20 days post inoculation according to the schedules) to detect virus infection. (C) The tissue-blotting sampling procedure. a: sliced off the non-inoculated area parallel to the veins. b: sliced perpendicular to the veins from base to tip sides sequentially with about 3 mm spacing. Each single plane cut surface was pressed on Hybond™-N⁺ nylon membranes. c: The inoculated area was also cut and blotted by the same method. d: an example of tissue blot membrane.

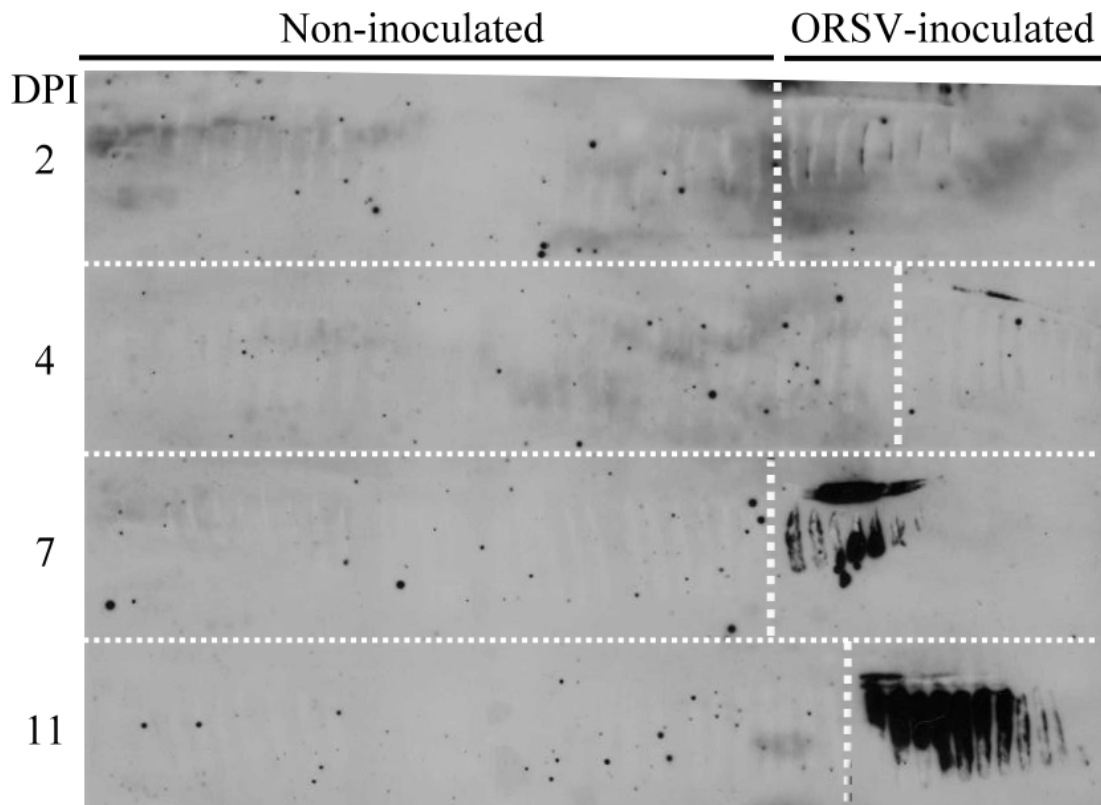


Fig. 2. Time-course detection of ORSV infection in ORSV-inoculated *Phalaenopsis*.

The inoculated leaf was zonally sampled at 2, 4, 7, 11 days post inoculation (DPI) by tissue-blotting and hybridized with DIG-labeled ORSV coat protein (CP) probes. CSPD chemiluminescent signal was recorded on films over 8 h. Vertical dashed lines separate inoculated (right) and non-inoculated (left) areas.

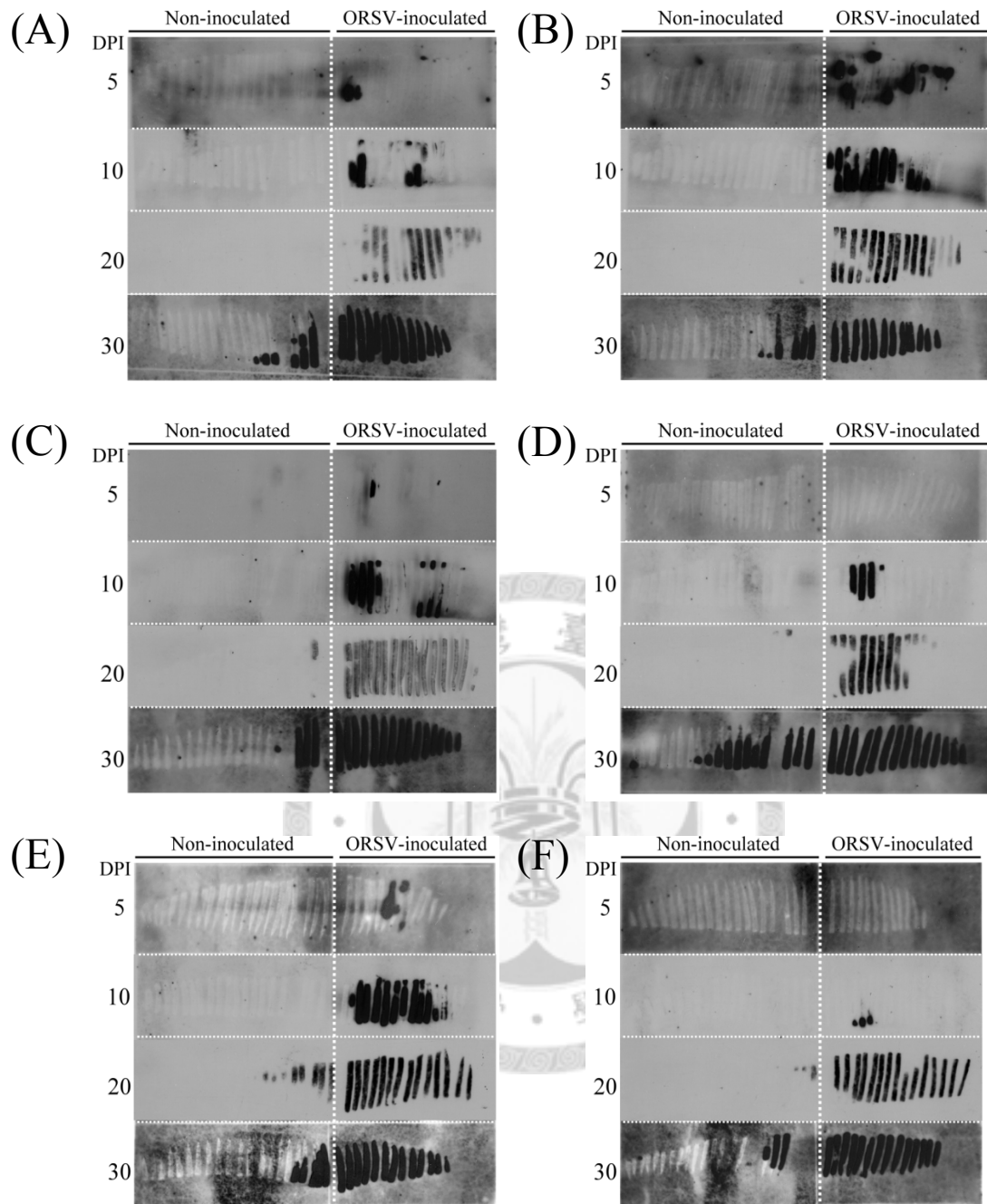


Fig. 3. Time-course detection of ORSV infection in one month period in ORSV-inoculated *Phalaenopsis*.

The inoculated leaf was zonally sampled at 5, 10, 20, 30 days post inoculation (DPI) by tissue-blotting. ORSV infection was detected with DIG-labeled ORSV coat protein (CP) probes. CSPD chemiluminescent signal was recorded on films over 8 h. Vertical dashed lines separate inoculated (right) and non-inoculated (left) areas.(A-F)are 6 independent replicates of ORSV detection.

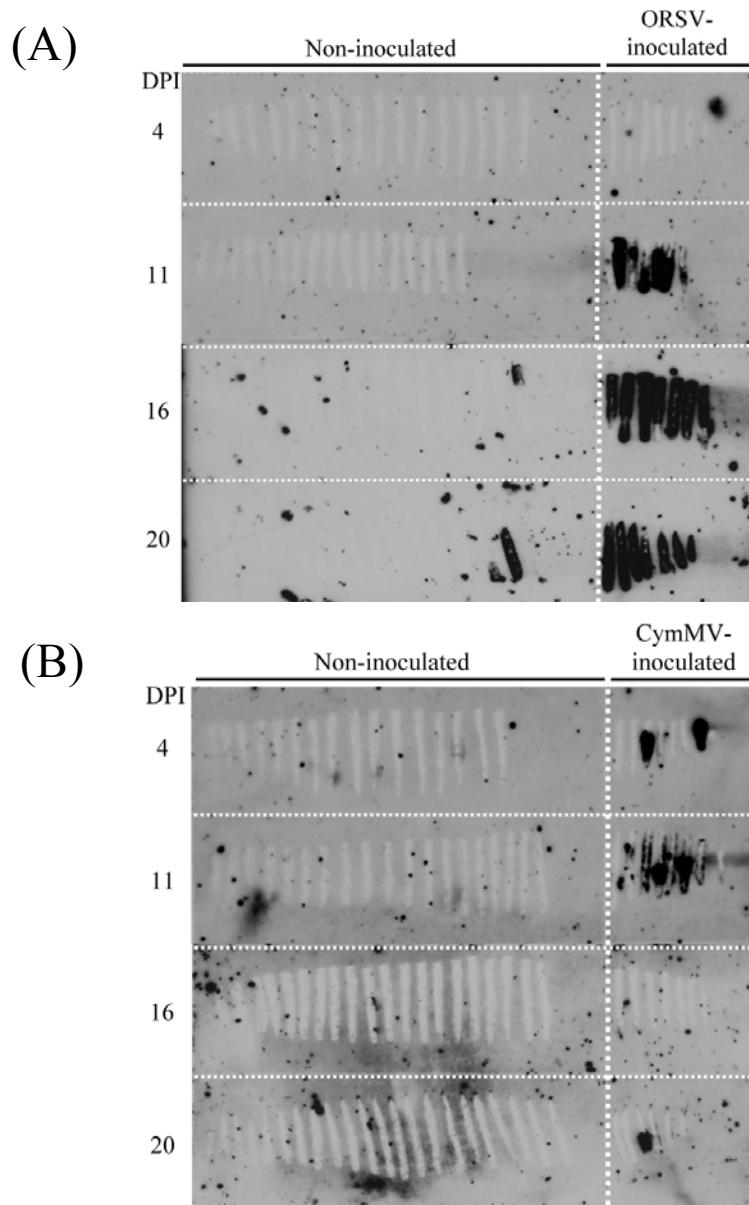
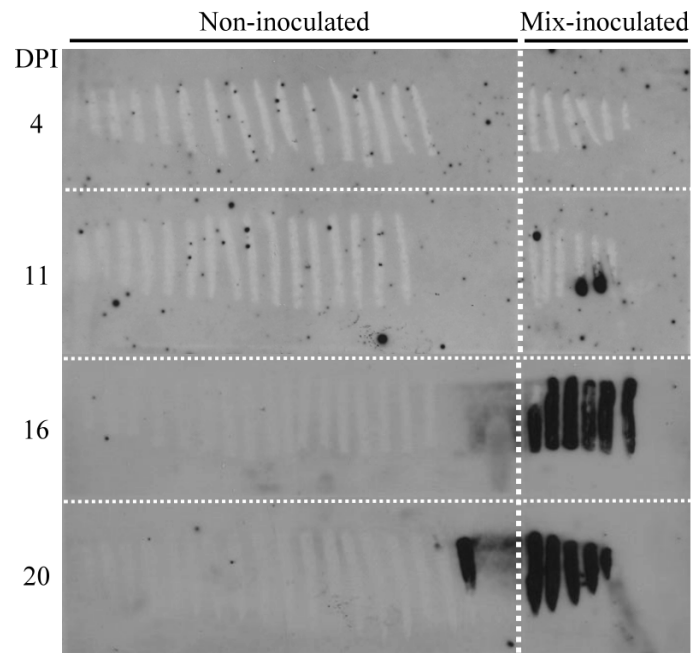


Fig. 4. Time-course detection of virus infection in ORSV or CymMV singly inoculated *Phalaenopsis*.

The inoculated leaf was zonally sampled at 4, 11, 16, 20 days post inoculation (DPI) by tissue-blotting. DIG-labeled CP probes were used to detect (A) ORSV infection in ORSV-inoculated leaf and (B) CymMV infection in CymMV-inoculated leaf. CSPD chemiluminescent signal was recorded on films over 8 h. Vertical dashed lines separate inoculated (right) and non-inoculated (left) areas.

(A)



(B)

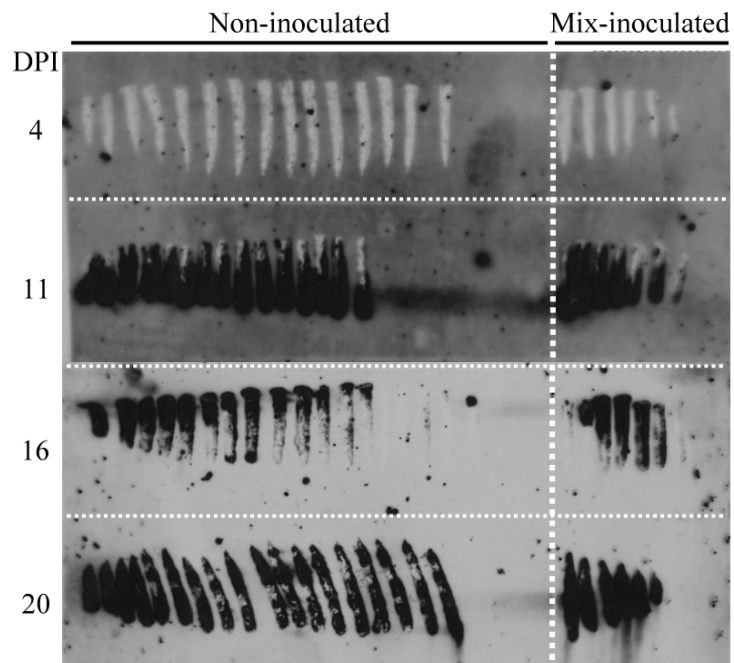


Fig. 5. Time-course detection of virus infection in mixedly-inoculated *Phalaenopsis*. The inoculated leaf was zonally sampled at 4, 11, 16, 20 days post inoculation (DPI) by tissue-blotting. DIG-labeled CP probes were used to detect (A) ORSV infection (B) CymMV infection within the same inoculated leaf. CSPD chemiluminescent signal was recorded on films over 8 h. Vertical dashed lines separate inoculated (right) and non-inoculated (left) areas.

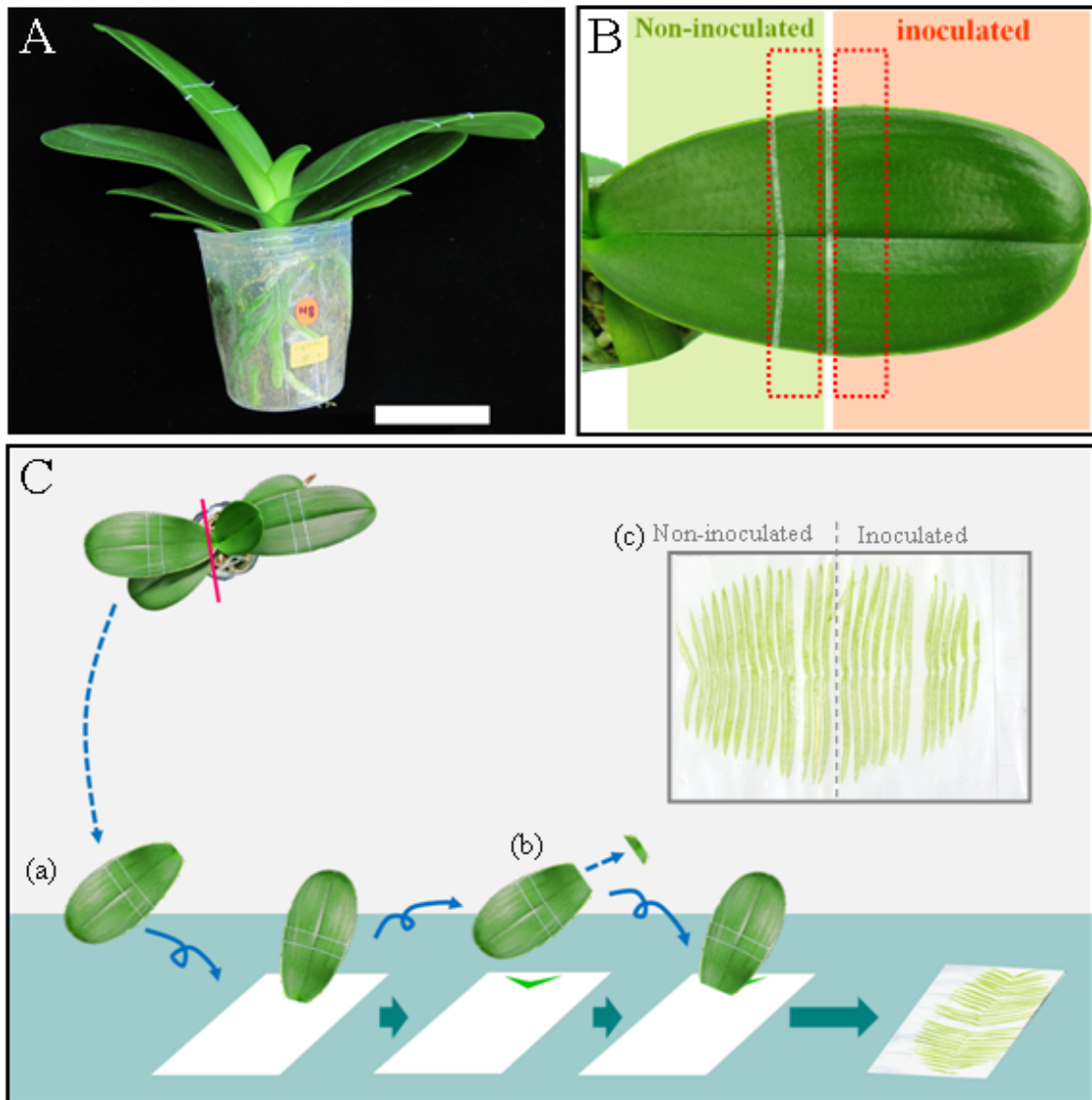


Fig. 6. Diagrams of leaf tip-inoculation and tissue-blotting methods used in the inoculation assays.

(A) 7.5-cm pot *Phalaenopsis amabilis*. Bar = 5 cm. (B) Virions were inoculated in the tip-half of the inoculated leaf as labeled. Red dashed squares indicate areas of inoculated and non-inoculated tissues used for RNA extraction. (C) The tissue-blotting sampling procedure. a: sliced off the whole inoculated leaf from the plant. b: sliced perpendicular to the veins from base (non-inoculated) to tip (inoculated) sides sequentially with about 3 mm spacing. Each single plane cut surface was pressed on Hybond™-N⁺ nylon membranes. c: an example of tissue blot membrane.

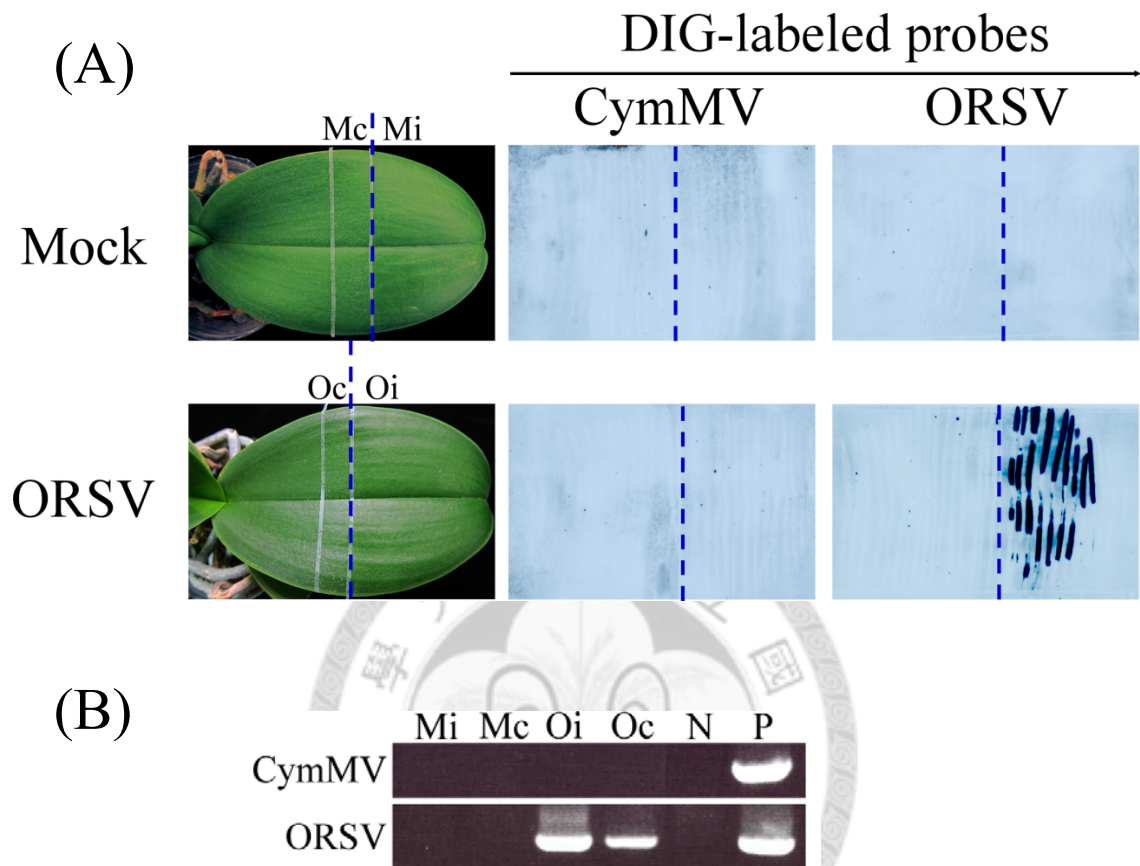


Fig. 7. Virus infection of ORSV-inoculated *Phalaenopsis* at 10 days post inoculation. (A) Phenotype and tissue-blotting detection of mock- and ORSV-inoculated leaves with DIG-labeled CymMV or ORSV CP probes. CSPD chemiluminescent signals were recorded on films for over 8 h. Blue dashed lines separate inoculated (right) and non-inoculated (left) areas. (B) RT-PCR reactions were performed with CymMV or ORSV RdRp-specific primers followed by 40 PCR cycles. Mi, Mc: inoculated (i) or non-inoculated (c) tissues of mock-inoculated plants. Oi, Oc: inoculated (i) or non-inoculated (c) tissues of ORSV-inoculated plants. N: non-template negative control. P: CymMV and ORSV mix-infected *Phalaenopsis* as positive control.

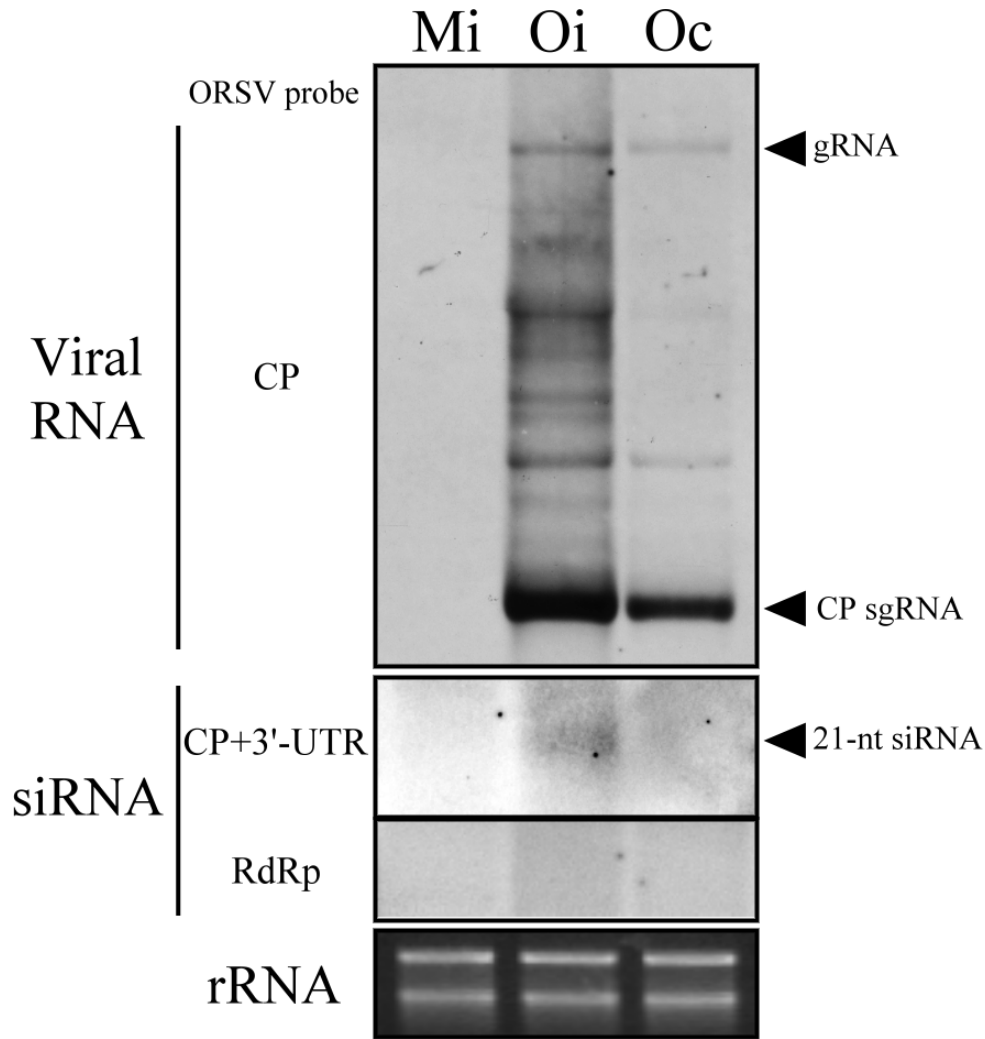
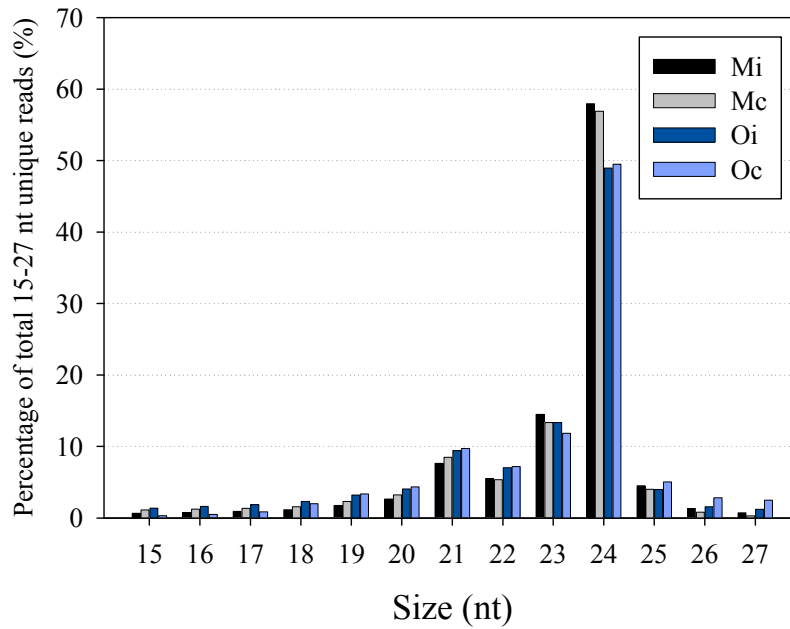


Fig. 8. Accumulation of ORSV viral RNA and virus-specific siRNA in *Phalaenopsis*.

The total RNA of 2 μg or 25 μg , respectively were loaded for viral RNA and siRNA detection by northern blot. Viral genomic RNA (gRNA), subgenomic RNA (sgRNA), and siRNA were detected with ORSV CP, CP to 3'-UTR, and RdRp-specific probes. Ethium bromide stained ribosomal RNA (rRNA) is shown as loading control. Mi: inoculated tissues of mock-inoculated plants. Oi, Oc: inoculated (i) or non-inoculated (c) tissues of ORSV-inoculated plants.

(A) Size distribution of unique reads



(B) Size distribution of total reads

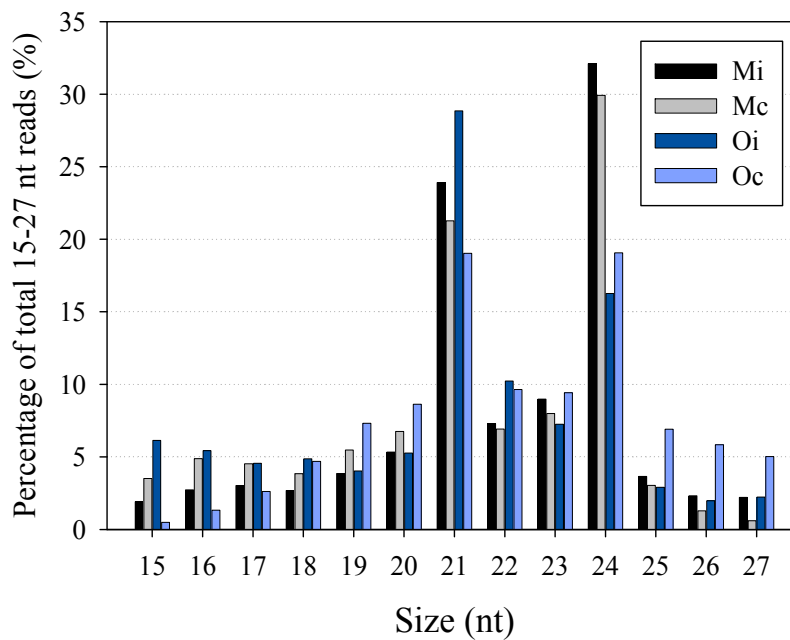


Fig. 9. Size distribution of small RNAs in mock- or ORSV-inoculated *Phalaenopsis*. Percentage and size distribution of 15-27 nt (A) unique reads or (B) redundant reads of small RNA from Solexa sequencing libraries. Mi, Mc: inoculated (i) or non-inoculated (c) tissues of mock-inoculated plants. Oi, Oc: inoculated (i) or non-inoculated (c) tissues of ORSV-inoculated plants.

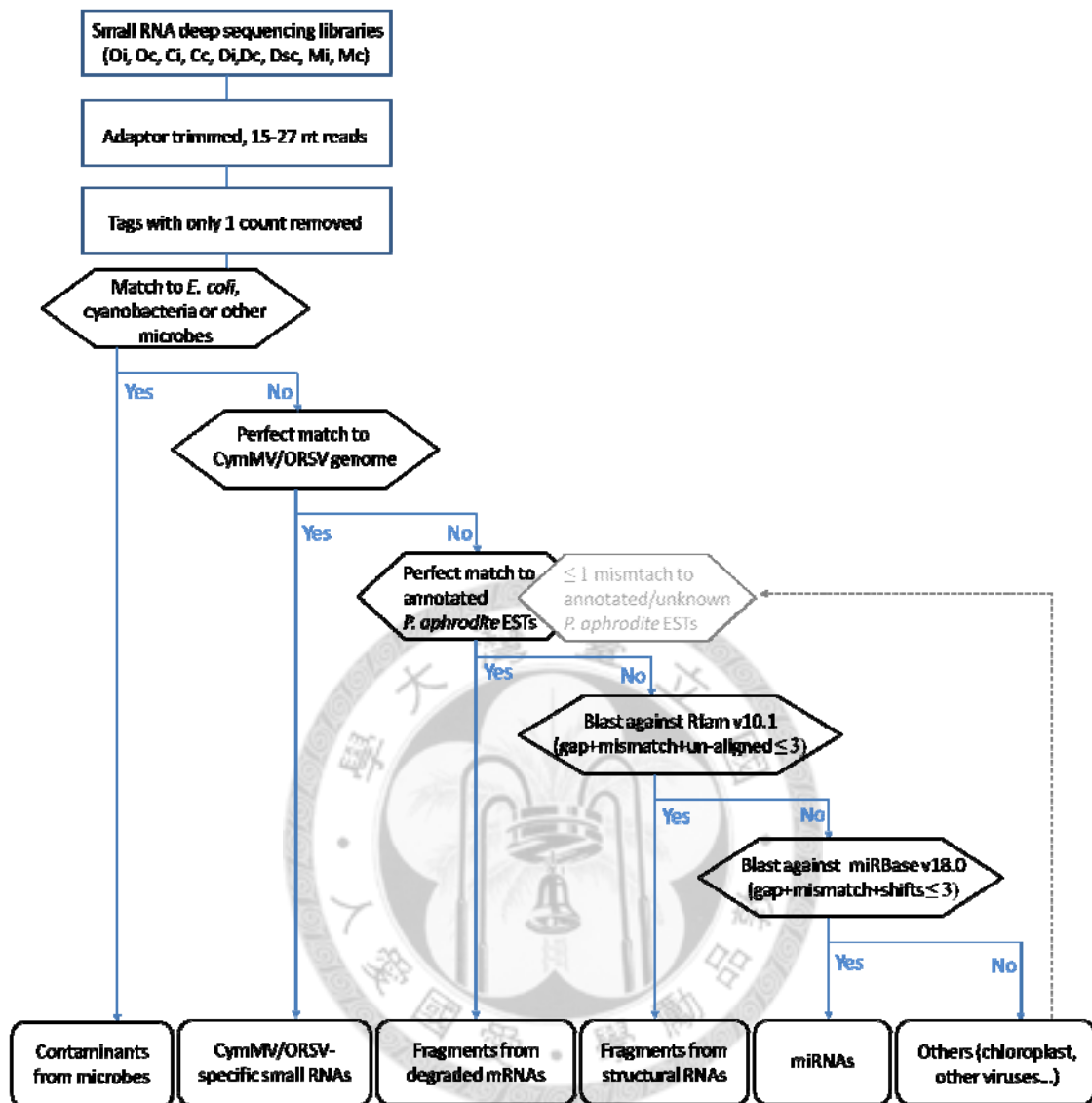


Fig. 10. Annotation procedures of deep sequencing data.

Raw data were trimmed with 3' and 5' adaptors, and filtered with size (15-27 nt). Only tags with at least 2 reads among all 9 libraries were kept for further annotation. Reads were used as queries to search against bacteria genome, virus genome, *Phalaenopsis* transcriptome, Rfam, and miRBase using BLAST algorithm. The criteria and hierarchy are indicated. Reads that not annotated as known categories (classified as "others" at first) were used as queries to search against *P. aphrodite* expression tags (ESTs) again and allowed 1 mismatch in the second round.

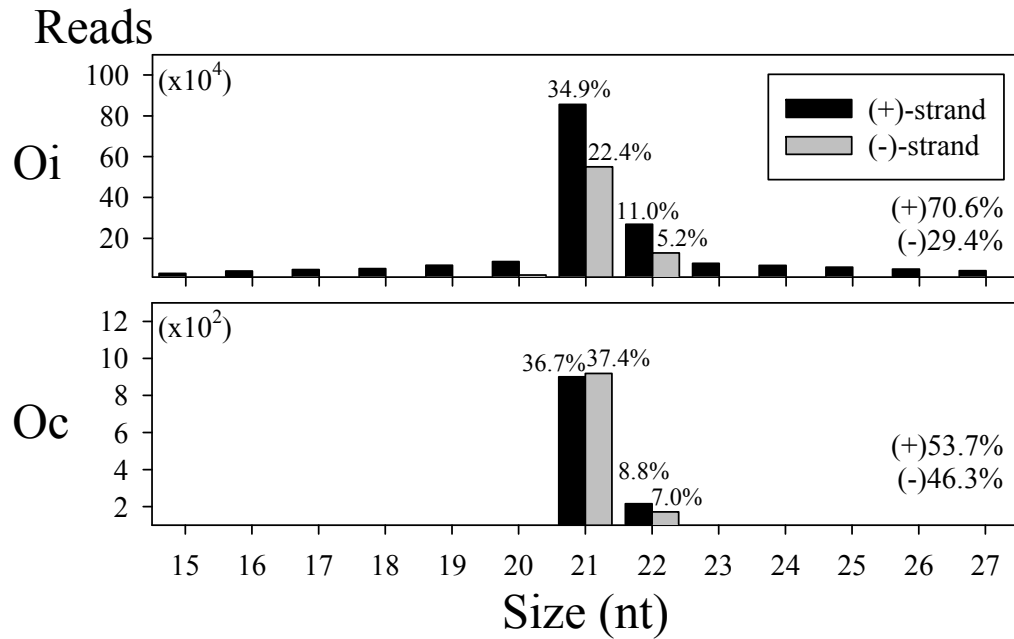


Fig. 11. Abundance and size distribution of ORSV vsRNAs in ORSV-infected *Phalaenopsis*.

Oi, Oc: inoculated (i) or non-inoculated (c) tissues of ORSV-inoculated *Phalaenopsis*. Black bars represents reads matched to ORSV (+)-strand and grey bars represent reads matched to (-)-strand of ORSV genomic RNA. Numbers of percentage above the bar indicate the proportion in total CymMV vsRNAs within the library.

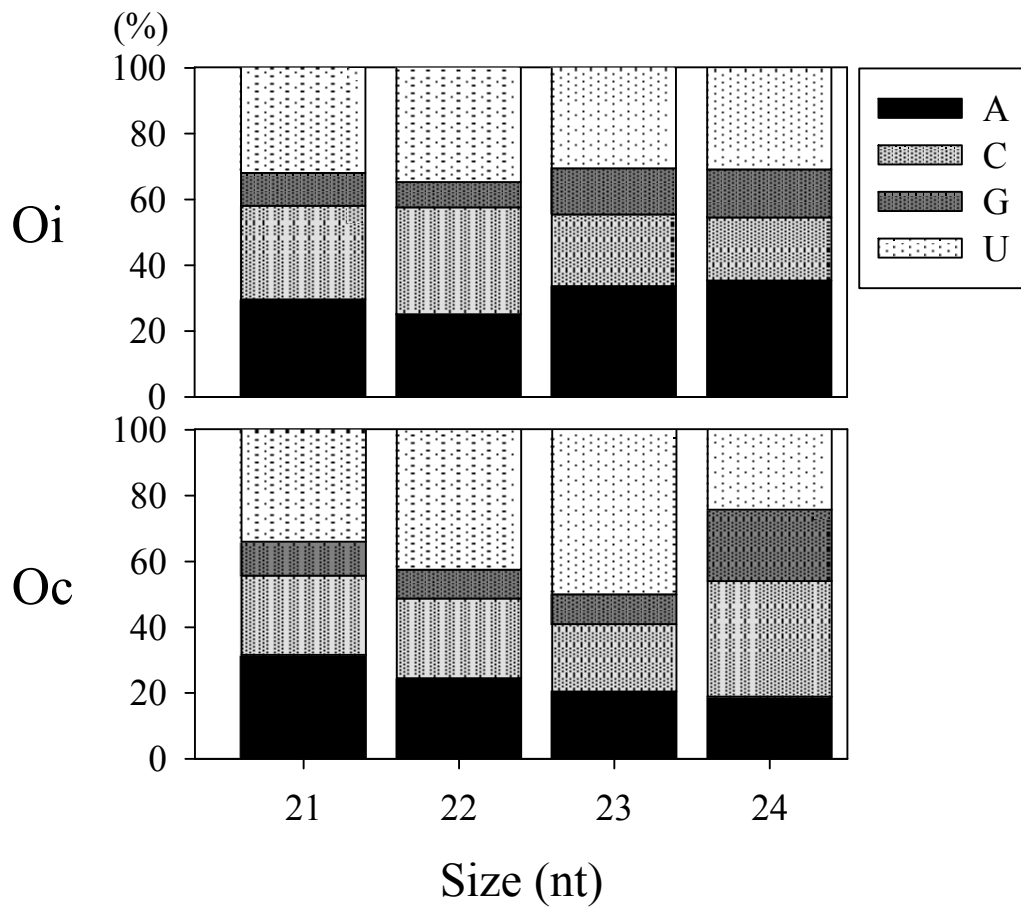


Fig. 12. Nucleotide composition of ORSV vsRNAs in ORSV-infected *Phalaenopsis*.
 The composition of adenine (A), cytosine (C), guanine (G) and uridine (U) were proportioned to 100% within each size classes. Oi, Oc: inoculated (i) or non-inoculated (c) tissues of ORSV-inoculated *Phalaenopsis*.

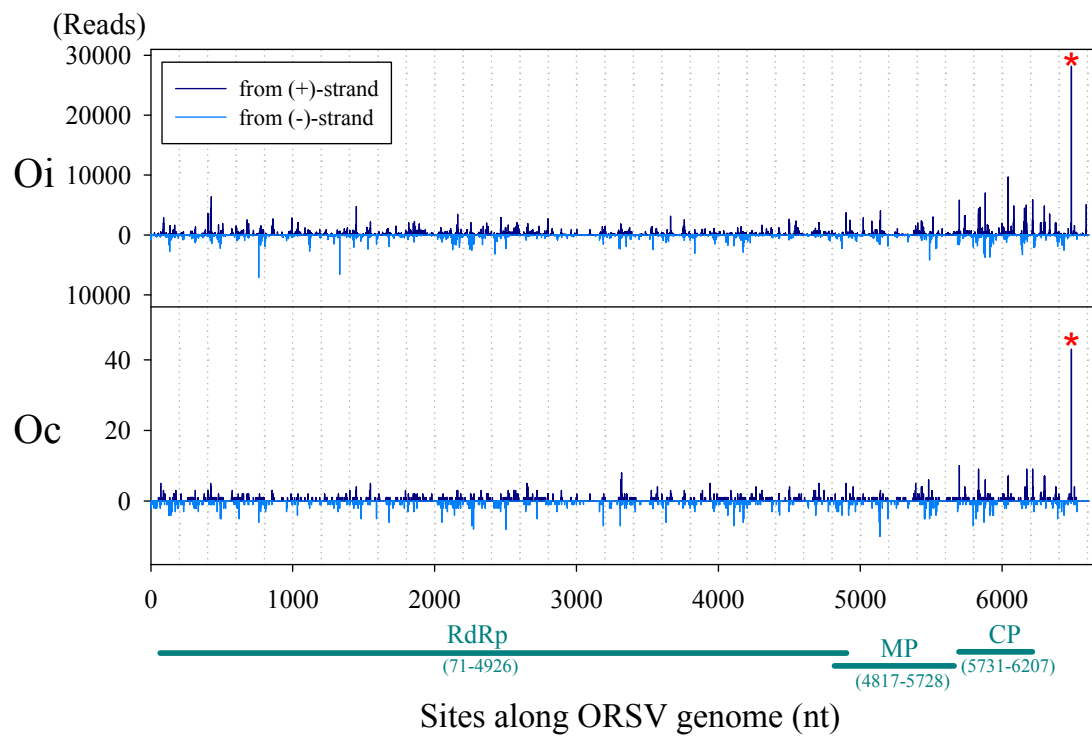


Fig. 13. Distribution of vsRNAs along ORSV genome corresponding to reads from Oi and Oc libraries. Upward dark blue lines representing reads of (+)-polarity and downward light blue lines representing (-)-polarity reads. Genomic sites of RdRp, MP, and CP gene coding regions are indicated below (numbers based on DQ139262). The red asterisks indicate the specific hotspot peak located in the 3'-untranslated region.

```

Bell pepper mottle tobamovirus      -----GGT-ACACACGATAGTGT-ATAGTGTITTTT--CCCTCCACTTAAATCGAA-----GGGTAGTGTCTTGGAACGCGCG-GGTCAAATATAA----
Tomato mosaic virus                  -----T-ACGTACGATAACGT-ACAGTGTITTTT--CCCTCCACTTAAATCGAA-----GGGTAGTGTCTTGGAGCGCGCG-GAGTAAACATATAT--
Rehmannia mosaic virus              -----GGT-GCGTACGATAACGC-ATAGTGTITTTT--CCCTCCACTTAAATCGAA-----GGGTTGTGTCTTGGTTCGCGCG-GGTCAAAGTGTAT----
Tobacco mosaic virus                -----GGT-GCGTACGATAACGC-ATAGTGTITTTT--CCCTCCACTTAAATCGAA-----GGGTTGTGTCTTGGATCGCGCG-GGTCAAATGTAT----
Pepper mild mottle virus            -----GGC-GAGTACGATAACTC-GTAGTGTITTTT--CCCTCCACTTAAATCGAA-----GGGTTGTCTTGGGATGGAACGCAATTAATACA-----
Obuda pepper virus                  -----GGT-GTATGCCATAATAC-ATAGTGTITTTTTCCCTCCACTTAAATCGAA-----GGGTTTGTCTTGGTTTCTTCA-CGGAAAACGT-----
Paprika mild mottle virus           ATGAGGTGGT-ACATACCAAATGT-ACAGTGGTTTT--CCCTCCACTTGAATCGAA-----GGGTTGGTGTGGAGTTTTCA-CGTGA-----
Cactus mild mottle virus            ---CCGCGGTAGCAAGCGATA-TGCTACAGTGTITTC--CAGTCCACTTAAATCGAA---C--TGGT-TGCTGTCTGGATCC--ATACAGTTCA----
Streptocarpus flower break virus    -----TGGT-GCATACTATAATGC-ATAGTGTITTTA--TCCTCCACTTAAATCGAA-----GGATAGTGTCTTCTACTTGA--AGGAAGTTCTG----
Brugmansia mild mottle virus        -----CTTACCATAAAGC-GTAGTGTITTTAC---TCTCCACTTAAATCGAA-----GAGTTGTACATCCGGATCTATAAAGGGAAAAACGTGTGA
Cucumber green mottle mosaic virus  -----GT-GCACACCAAAGTGC-ATAGTGTCTT-TCCCGT-TCACTTAAATCGAA---CGGTTTGTCTCAT-TGGTTTGGGAAACCTCTCACGT----
Cucumber mottle virus               -----GGC-GCTCAGGATAGAGC-GTAGTGTITTT-TCCCGT-CCACTTAAATCGAA---CGGCTTTCTCATCTGGATCGTATTGTCTCTCCC-----
Maracuja mosaic virus               -----GGT-GTACACGATAGTAC-GTAGTGTITTTATCCGTTCCACTGAAATCGAAA---CGGATGATCACCATAATTGGTGTGGTCCGC-----
Passion fruit mosaic virus          -----CATACGAGAATGC-GTAGTGTITTTATCCCGTTCCACTGAAATCGAAA---CGGGTGATCTGCATAATTGCAGTTGCTTGGCTGGA-----
Ribgrass mosaic virus               -----GTGCACACGATAGTGC-ATAGTGTITTTT--CTCTCCACTTAAATCGAA---GAGATATACTTACGGTGTAAATCCGCAAGGGTGGC----
Youcai mosaic virus                 -----GTGGTGCACACGATAGTGC-ACAGTGTITTTT--CTCTCCACTTAAATCGAA---GAGATATACTTACGGTGTAAATCCGTAAGGGT-----
Crucifer tobamovirus                -----GCACACGATAGTGC-ATAGTGTITTTT--CTCTCCACTTAAATCGAA---GAGGTATTCTTACGGTGTAAATCCGTAAGGGTGGCGT--
Turnip vein-clearing virus          -----ATAGCGC-ATAGTGTITTTT--CTCTCCACTTAAATCGAA---GAGATAAACTTACGGTGTAAATCCGTAAGGGTGGCGTAA
Clitoria yellow mottle tobamovirus -----TGCCGAAA-CAGG-TAGTGTITTTA--GCGTCCACTTAAATCGAACGCTAGAAATCAAACGCAGTCACTCTTTGTGCCGTAAGC---
Frangipani mosaic virus             -----TTCGACGATA-TGAACTAGTGTITTTT--CTGTCCACTTAAATCGAAC---AGAA--CAAACGTGGT-GCGTACGAAAACGCATAGTGT
Cucumber fruit mottle mosaic virus  -----TCACGAAA-GATGATAGAGTITTTT--CCCTCCTCTTAAATCGAAG---GGATTGTTTGGCGGGTTTCTACCGAGCCTCTGCTGTGT-
Kyuri green mottle mosaic virus     -----GTAACGATA-TACCCAGAGTITTTT--CCCTCCTCTTAAATCGAAG---GGCTTTCTTACCGGGTTTCTACCAAACCTCTGTCGTG--

```

Fig. 14. Alignment of tobamovirus 3'-untranslated region (3'-UTR) conserved sequence. Identical bases among 22 viruses are highlighted in grey.

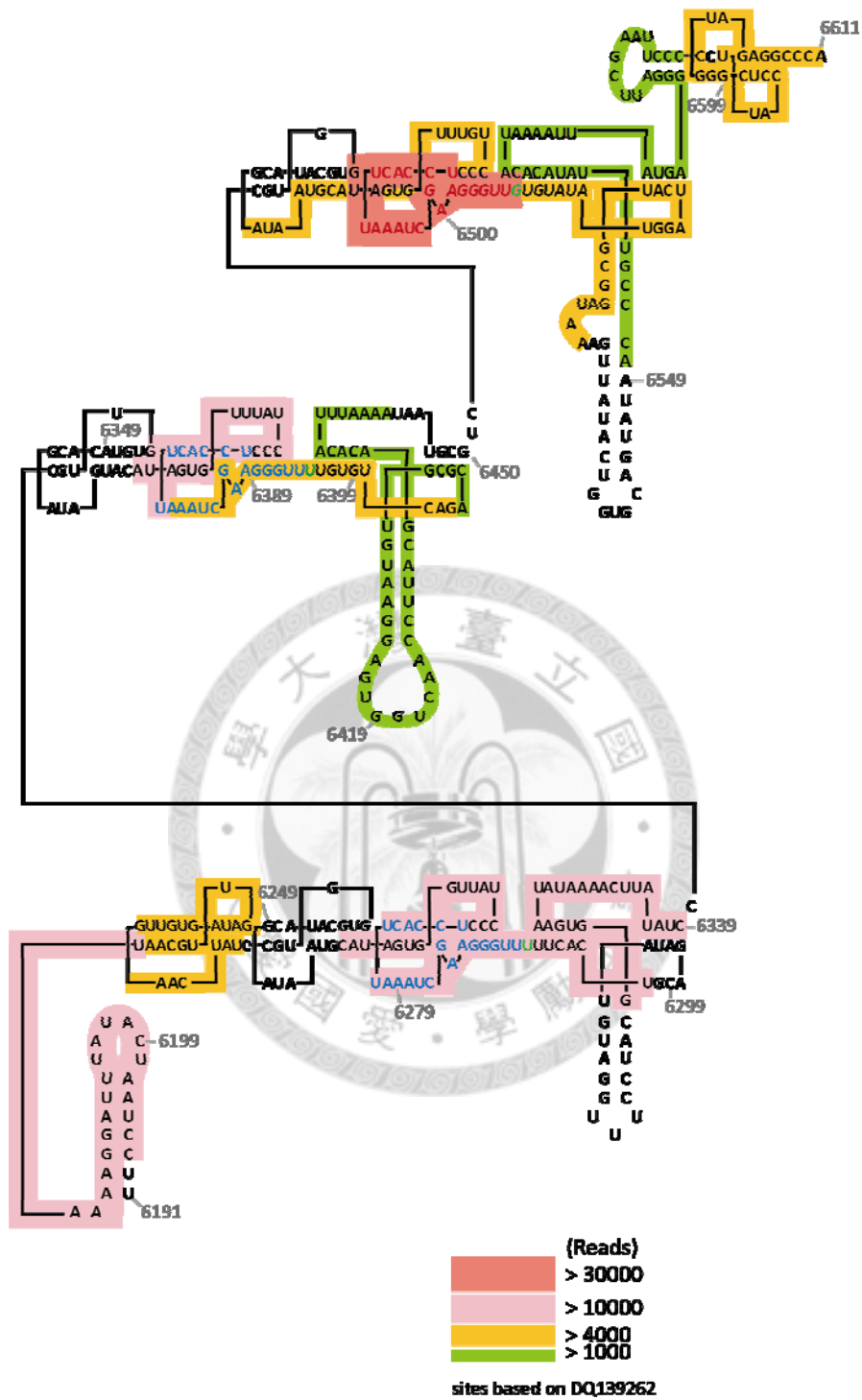


Fig. 15. Location and frequency of abundant 3'-UTR-originating ORSV positive stranded vsRNAs. The hotspot vsRNA and its homologous sequences are indicated in red and blue characters respectively. Gray characters indicating genome sites (based on DQ139262).

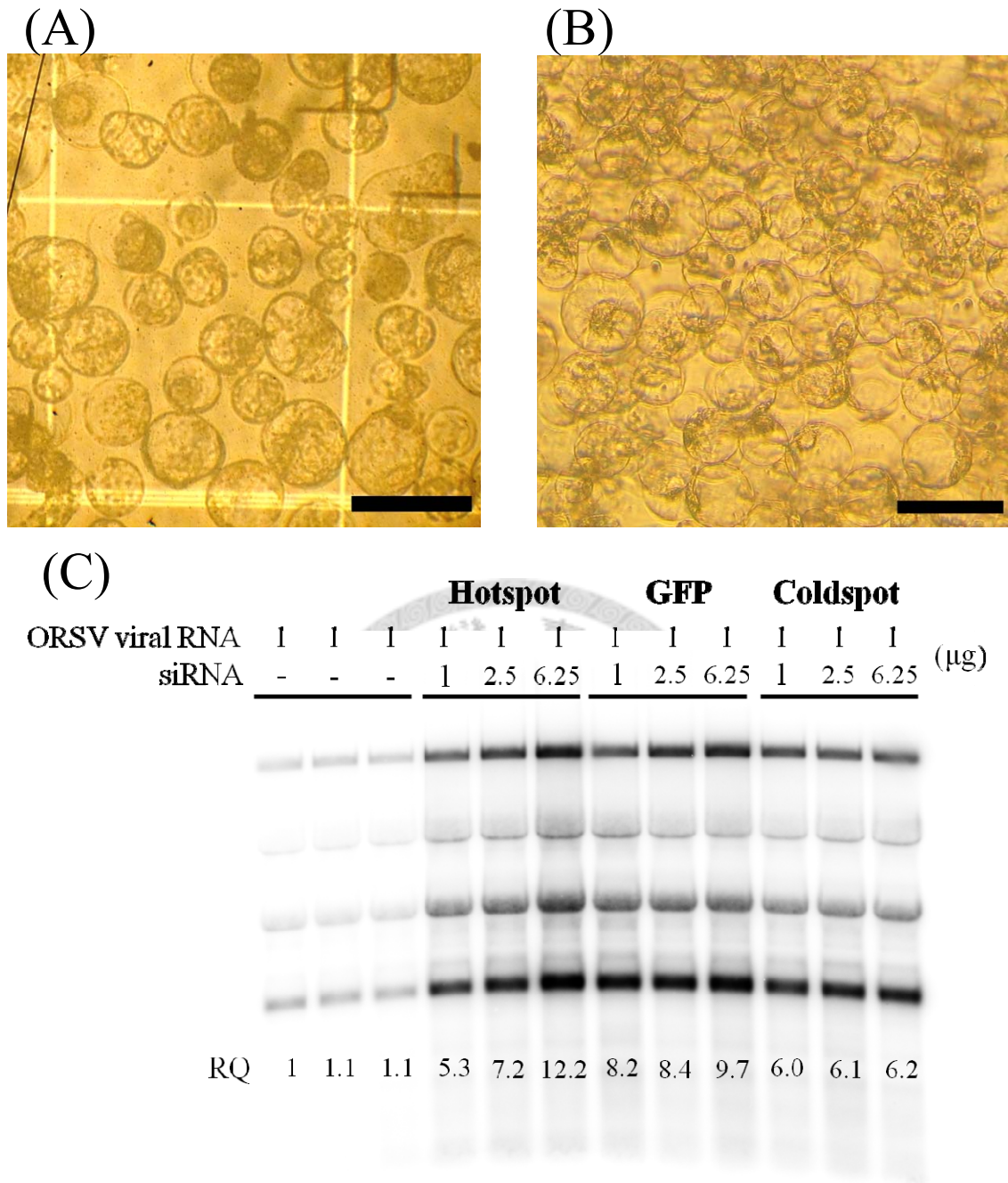


Fig. 16. ORSV viral RNA accumulation in ORSV and synthetic siRNAs co-transfected protoplasts.

(A) *Oncidium* protoplasts isolated from suspension cells (observed on a hemocytometer). (B) Viable protoplasts observed 24 h after transfection. (C) Northern blot analysis of ORSV viral RNA accumulation. Protoplasts were electrotransfected with ORSV viral RNA and synthetic ORSV 3'-UTR hotspot vsRNA, RdRp coldspot vsRNA or GFP siRNA as indicated. Total RNA was collected at 24 h after transfection. RQ: relative quantity of accumulated viral RNA, taken one of replicates of viral RNA-only treatment arbitrarily set as 1. The amount was calculated with the sum of 4 bands per lane by ImageQuant[®] program. Bars represented 100 μm.

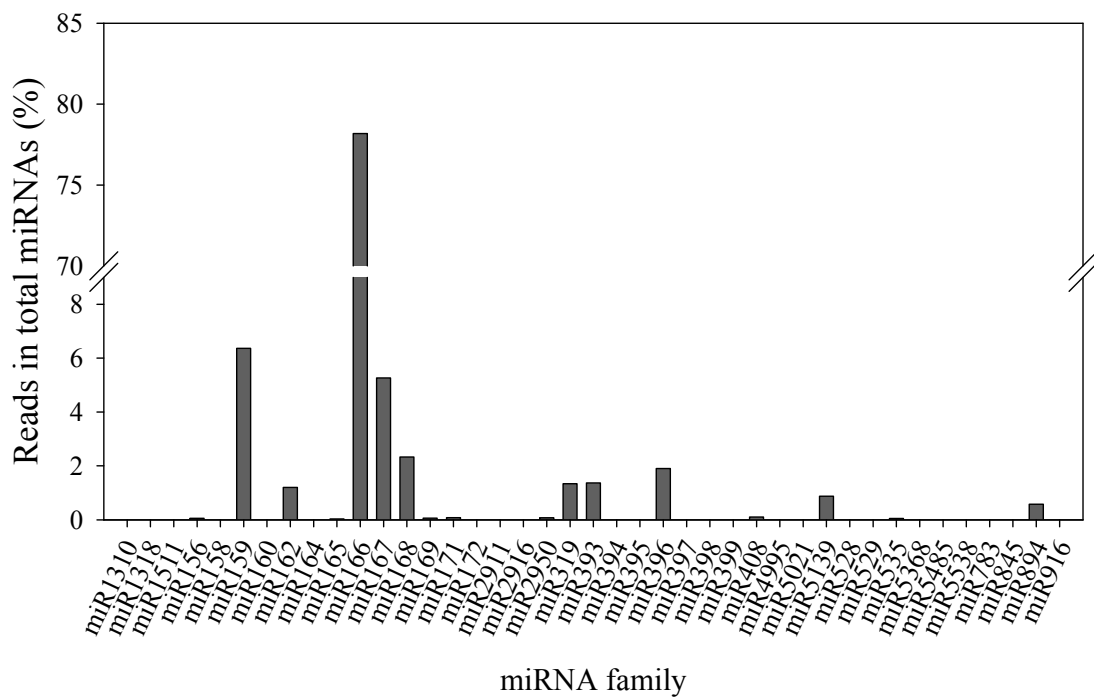


Fig. 17. The abundance of miRNA families in Mi, Mc, Oi, and Oc libraries. The percentage was calculated from sum of Mi, Mc, Oi, and Oc libraries.

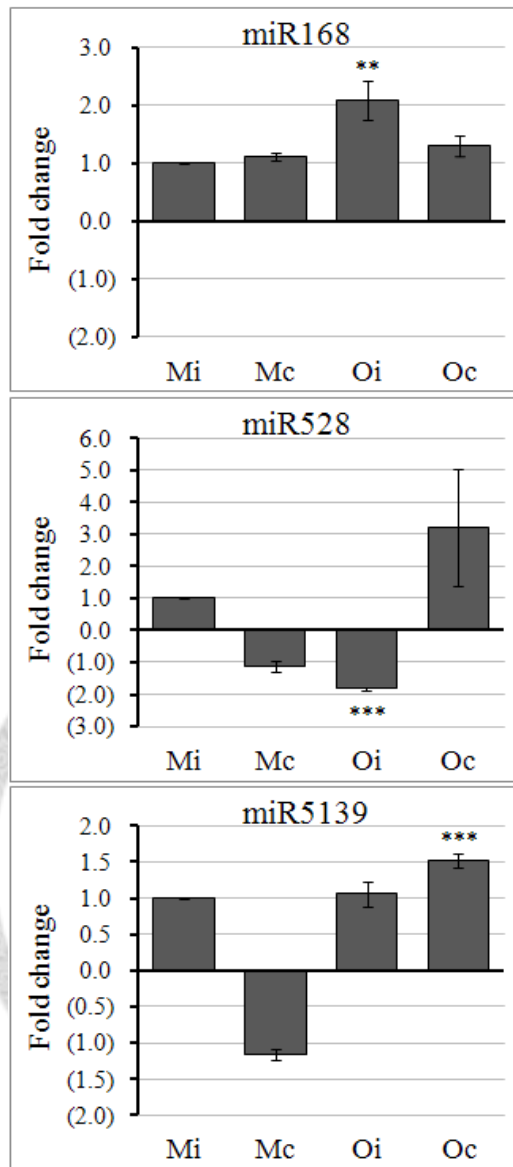


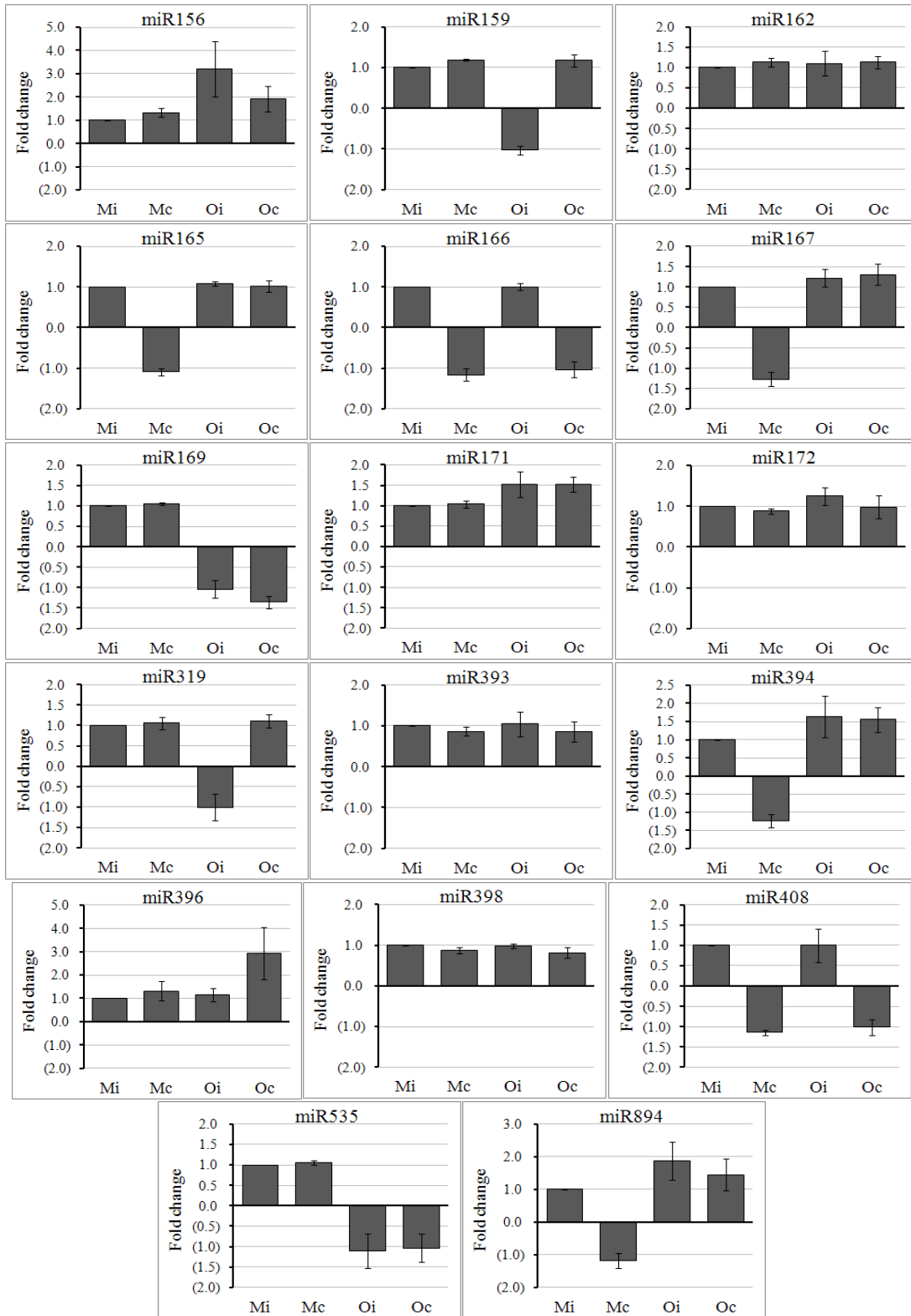
Fig. 18. Expression levels of some ORSV-infection responsive miRNAs validated by stem-loop qRT-PCR.

Fold changes of miR168, miR528, and miR894 are shown. Mi, Mc: inoculated (i) or non-inoculated (c) tissues of mock-inoculated *Phalaenopsis*. Oi, Oc: inoculated (i) or non-inoculated (c) tissues of ORSV-inoculated *Phalaenopsis*. miRNA levels in Mi were arbitrarily set to 1, upward boxes indicate increased and downward boxes indicate repressed expression levels relative to Mi. Bars represents standard deviation from 3 biological replicates. Asterisks indicate statistical significance at $P < 0.05$ (**) and $P < 0.001$ (***) assessed by BootstRatio web tool based on resampling methods.



Fig. 19. Expression of some miRNAs in ORSV- or mock-inoculated tissues validated by stem-loop qRT-PCR.

miRNA levels in Mi were arbitrarily set to 1, upward boxes indicate increased and downward boxes indicate repressed expression levels relative to Mi. Fold changes of miR156, miR159, miR162, miR165, miR166, miR167, miR169, miR171, miR172, miR319, miR393, and miR394, miR396, miR398, miR408, miR535, and miR894 are shown. Mi, Mc: inoculated (i) or non-inoculated (c) tissues of mock-inoculated *Phalaenopsis*. Oi, Oc: inoculated (i) or non-inoculated (c) tissues of ORSV-inoculated *Phalaenopsis*. Bars represents standard deviation from 3 biological replicates.



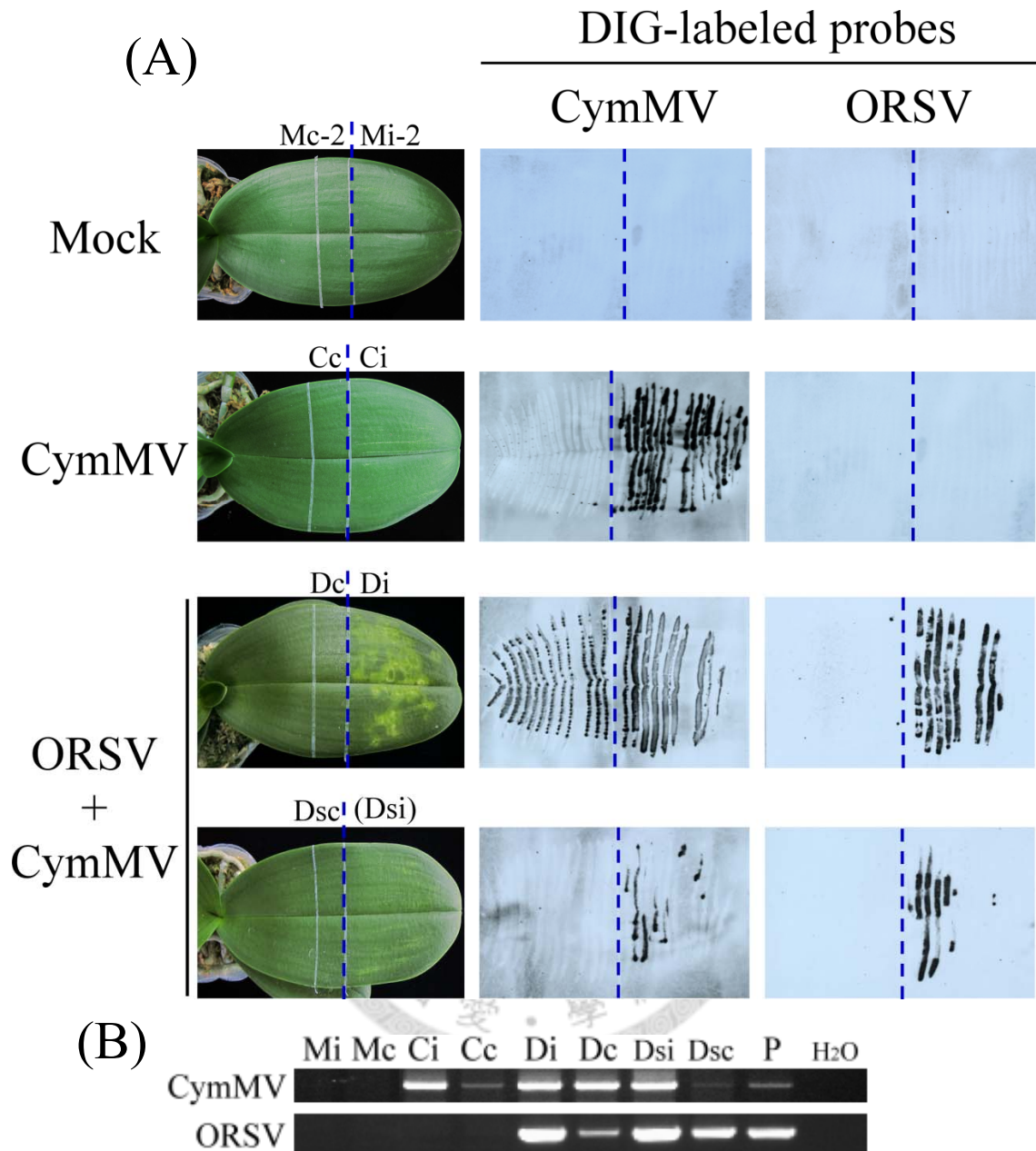


Fig. 20. Virus infection of CymMV- and doubly-inoculated *Phalaenopsis* at 10 days post inoculation (DPI).

(A) Phenotype and tissue-blotting detection of inoculated leaves with DIG-labeled CymMV or ORSV CP probes. CDP-*Star* chemiluminescent signals were recorded on films for 2 h. Blue dashed lines separate inoculated (right) and non-inoculated (left) areas. (B) RT-PCR reactions were performed with CymMV or ORSV CP-specific primers followed by 35 PCR cycles. Mi, Ci, Di, Dsi: inoculated (i) tissues of mock (M)-, CymMV (C)-, and doubly (D)-inoculated plants. Mc, Cc, Dc, Dsc: non-inoculated (c) tissues of mock (M)-, CymMV (C)-, and doubly (D)-inoculated plants. H₂O: non-template negative control. P: CymMV and ORSV mix-infected *Phalaenopsis* as positive control.

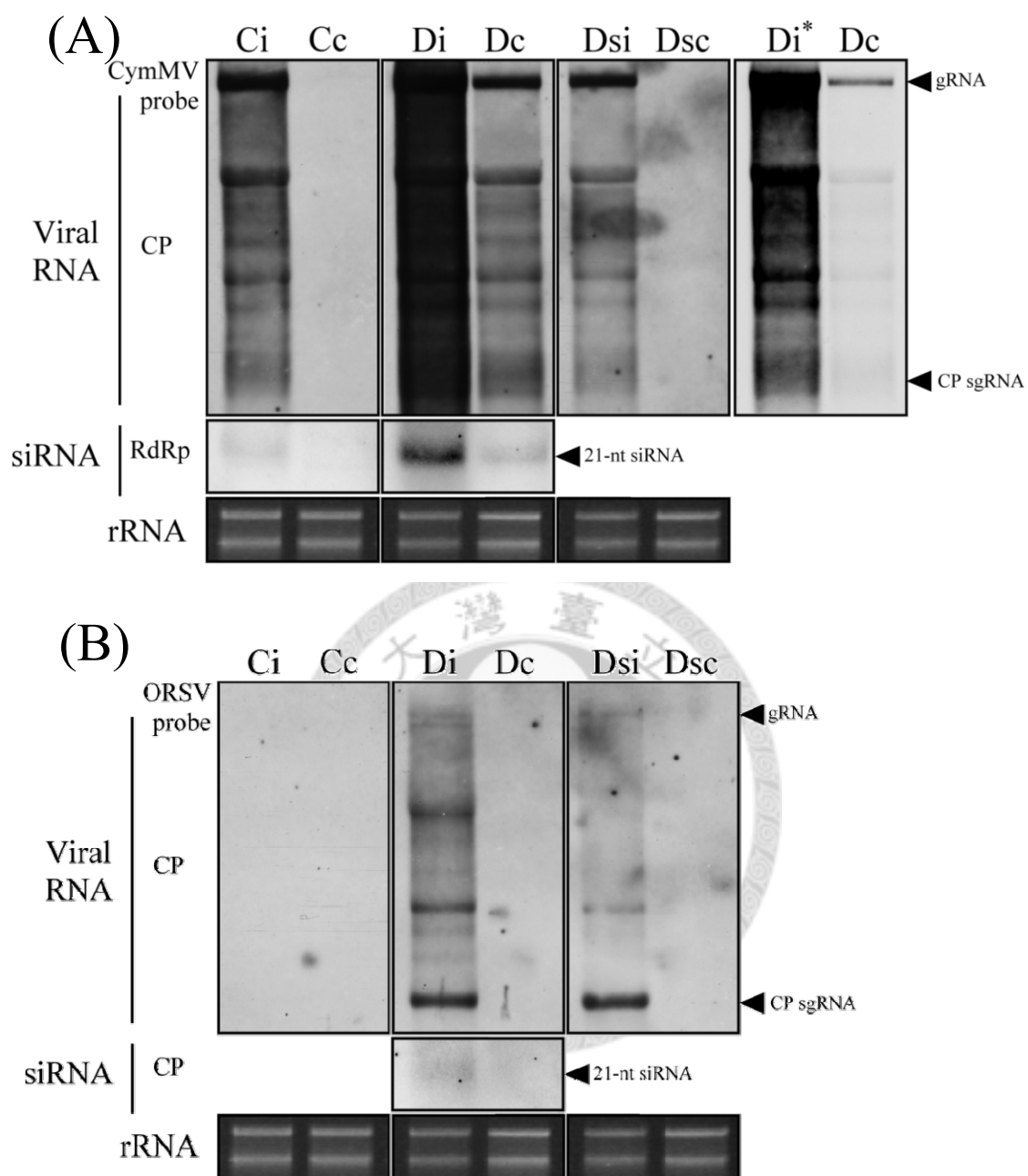
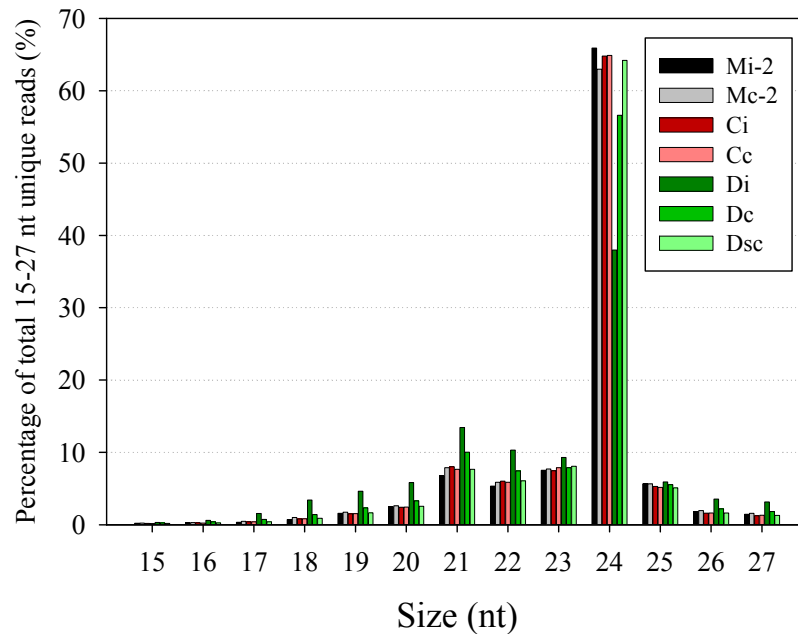


Fig. 21. Accumulation of CymMV and ORSV viral RNA and virus-specific siRNA in *Phalaenopsis*.

The total RNA of 2 μ g or 25 μ g respectively were loaded for viral RNA and siRNA detection by northern blot. Viral genomic RNA (gRNA), subgenomic RNA (sgRNA), and siRNA were detected with CymMV or ORSV CP and RdRp-specific probes. Ethium bromide stained ribosomal RNA (rRNA) is shown as loading control. Ci, Di, Dsi: inoculated (i) tissues of CymMV (C)- and doubly (D)-inoculated plants. Cc, Dc, Dsc: non-inoculated (c) tissues of CymMV (C)-, and doubly (D)-inoculated plants.

(A) Size distribution of unique reads



Size distribution of total reads

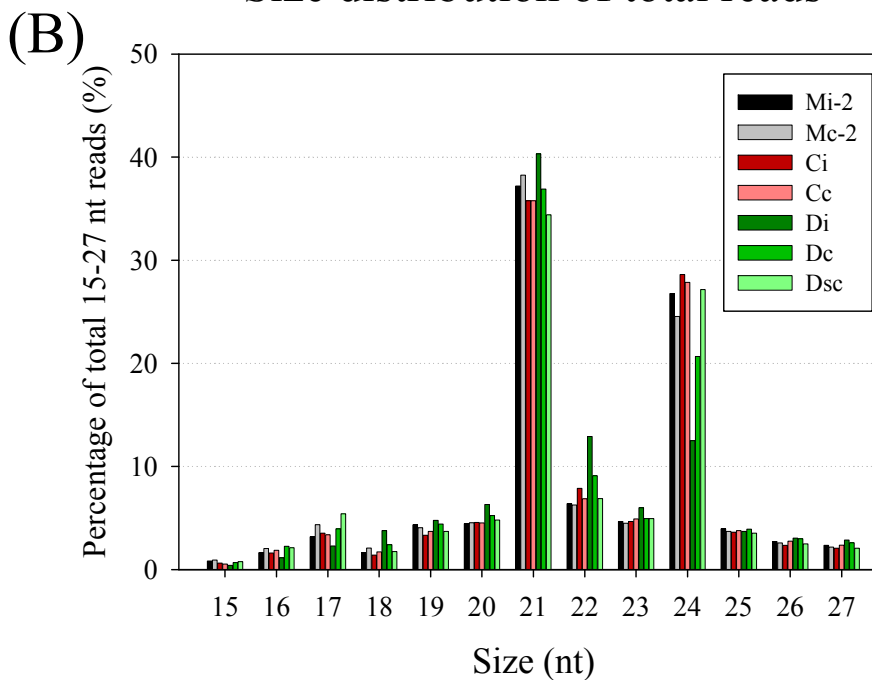


Fig. 22. Size distribution of small RNAs in mock-, CymMV-, or CymMV and ORSV mixedly-inoculated *Phalaenopsis*.

Percentage and size distribution of 15-27 nt (A) unique reads or (B) redundant reads of small RNA from Solexa sequencing libraries. Mi-2, Ci, Di: inoculated (i) tissues of mock (M)-, CymMV (C)-, and doubly (D)-inoculated plants. Mc-2, Cc, Dc, Dsc: non-inoculated (c) tissues of mock (M)-, CymMV (C)-, and doubly (D)-inoculated plants.

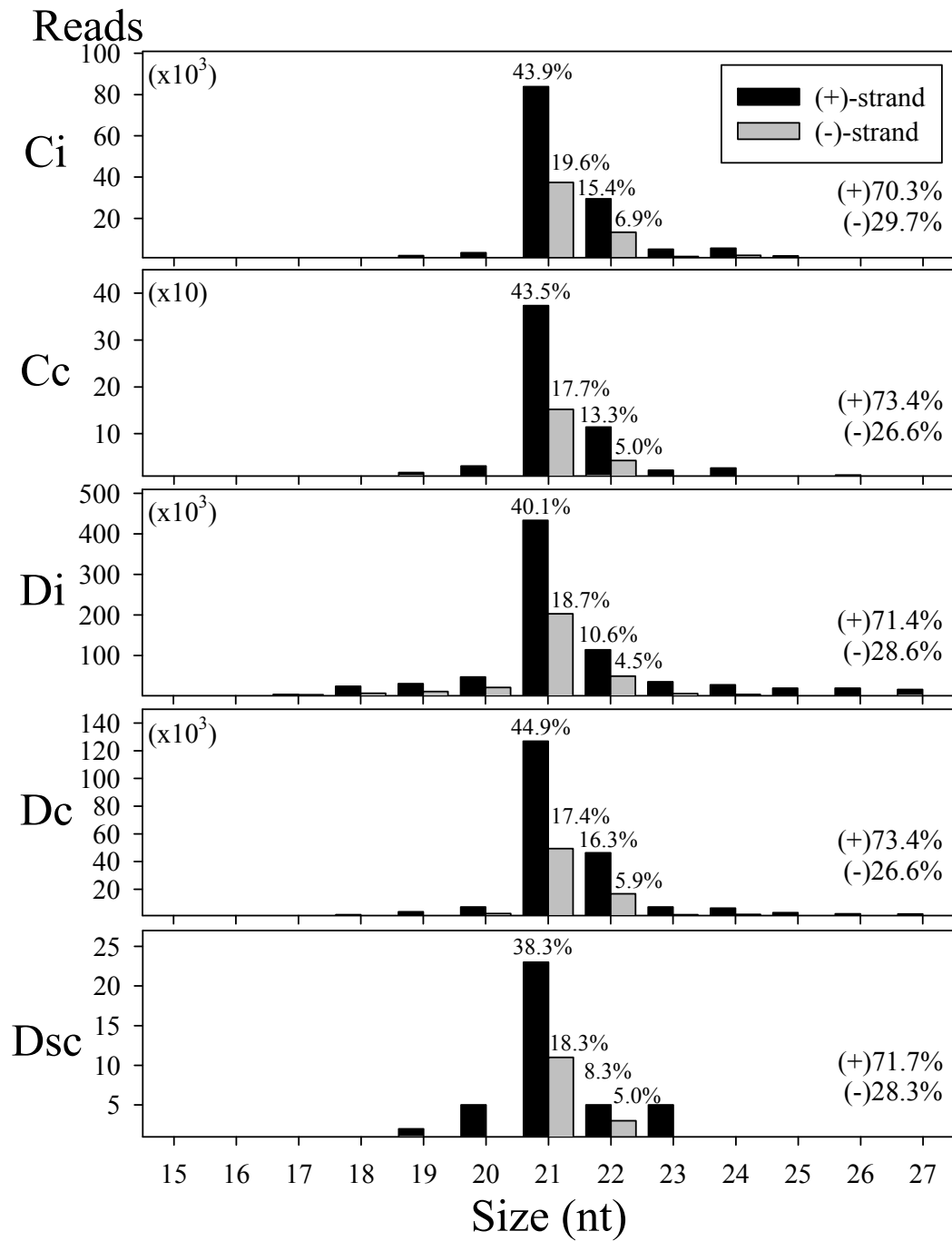


Fig. 23. Abundance and size distribution of CymMV vsRNAs in CymMV, or CymMV and ORSV mixedly-inoculated *Phalaenopsis*. Black bars represent reads matched to (+)-strand and grey bars represent reads matched to (-)-strand of CymMV genomic RNA. Numbers of percentage above the bar indicate the proportion in total CymMV vsRNAs within the library. Ci, Di: inoculated (i) tissues of CymMV (C)- or doubly (D)-inoculated plants. Cc, Dc, Dsc: non-inoculated (c) tissues of CymMV (C)- or doubly (D)-inoculated plants.

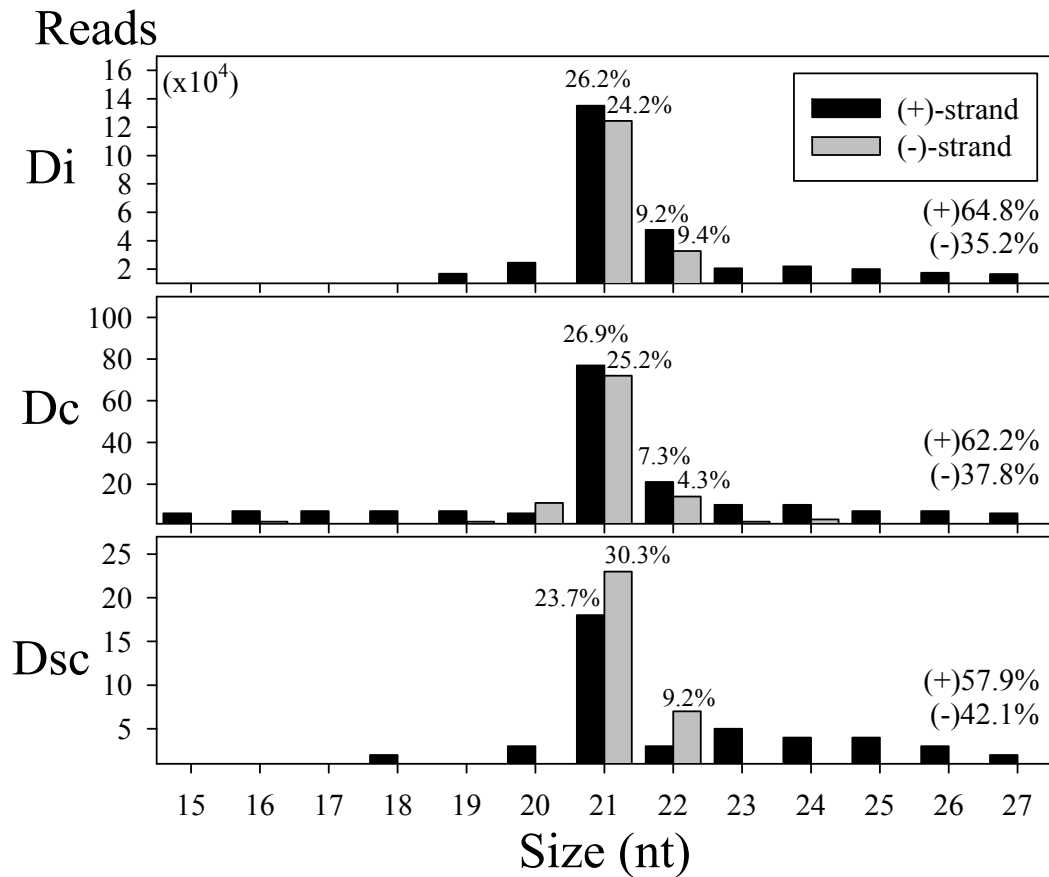


Fig. 24. Abundance and size distribution of ORSV vsRNAs in CymMV and ORSV mixedly-inoculated *Phalaenopsis*. Black bars represent reads matched to (+)-strand and grey bars represent reads matched to (-)-strand of ORSV genomic RNA. Numbers of percentage above the bar indicate the proportion in total ORSV vsRNAs within the library. Di: inoculated tissues of doubly inoculated plants. Dc, Dsc: non-inoculated tissues of doubly inoculated plants.

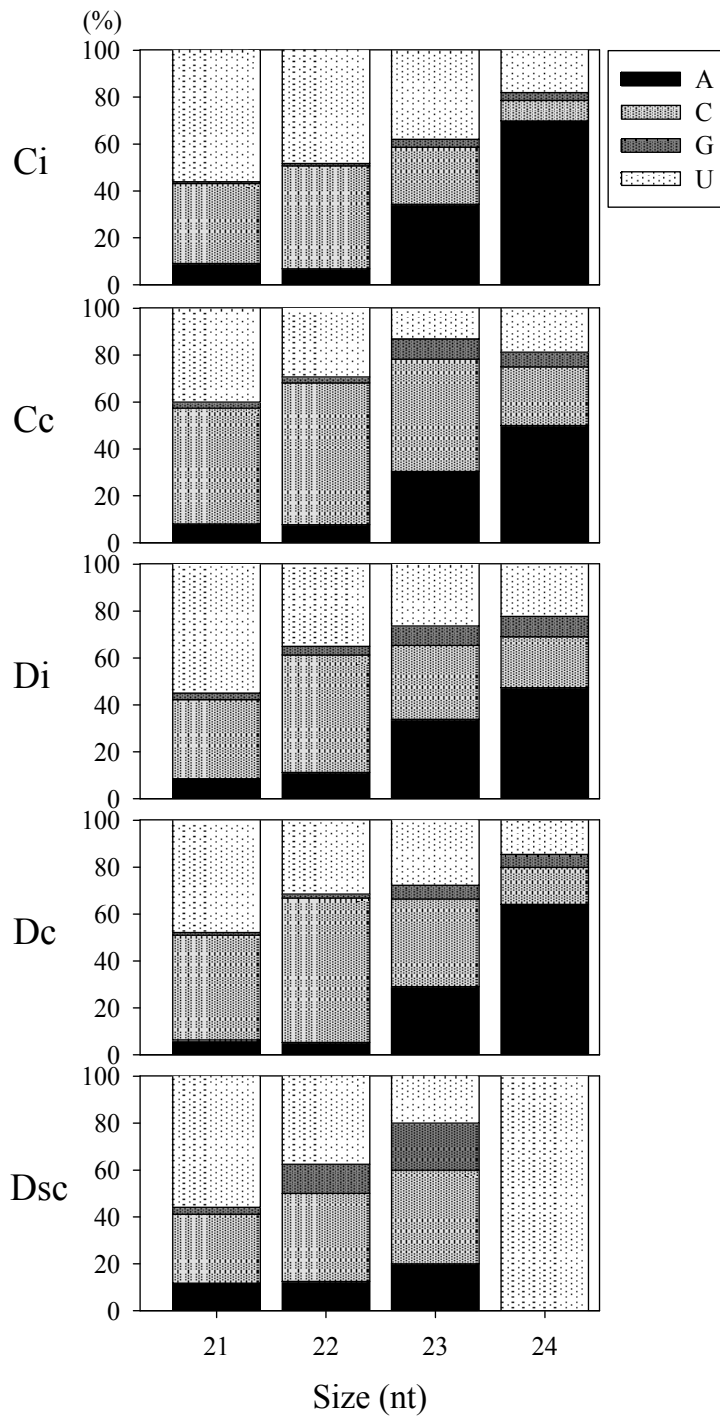


Fig. 25. Nucleotide composition of 5'-end of CymMV vsRNAs in CymMV, or CymMV and ORSV mixedly-inoculated *Phalaenopsis*.

The composition of adenine (A), cytosine (C), guanine (G) and uridine (U) were proportioned to 100% within each size classes. Ci, Di: inoculated (i) tissues of CymMV (C)- or doubly (D)-inoculated plants. Cc, Dc, Dsc: non-inoculated (c) tissues of CymMV (C)- or doubly (D)-inoculated plants.

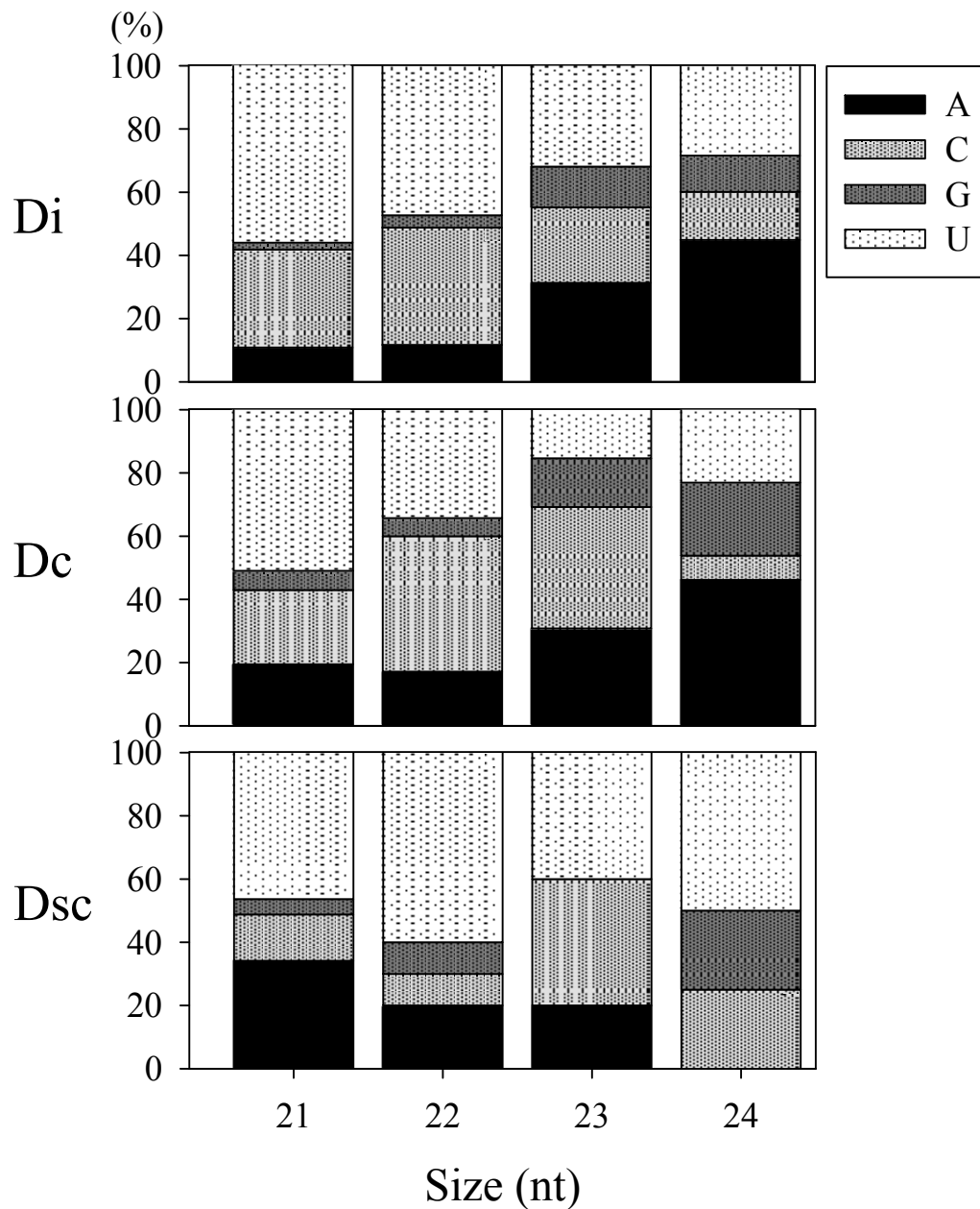
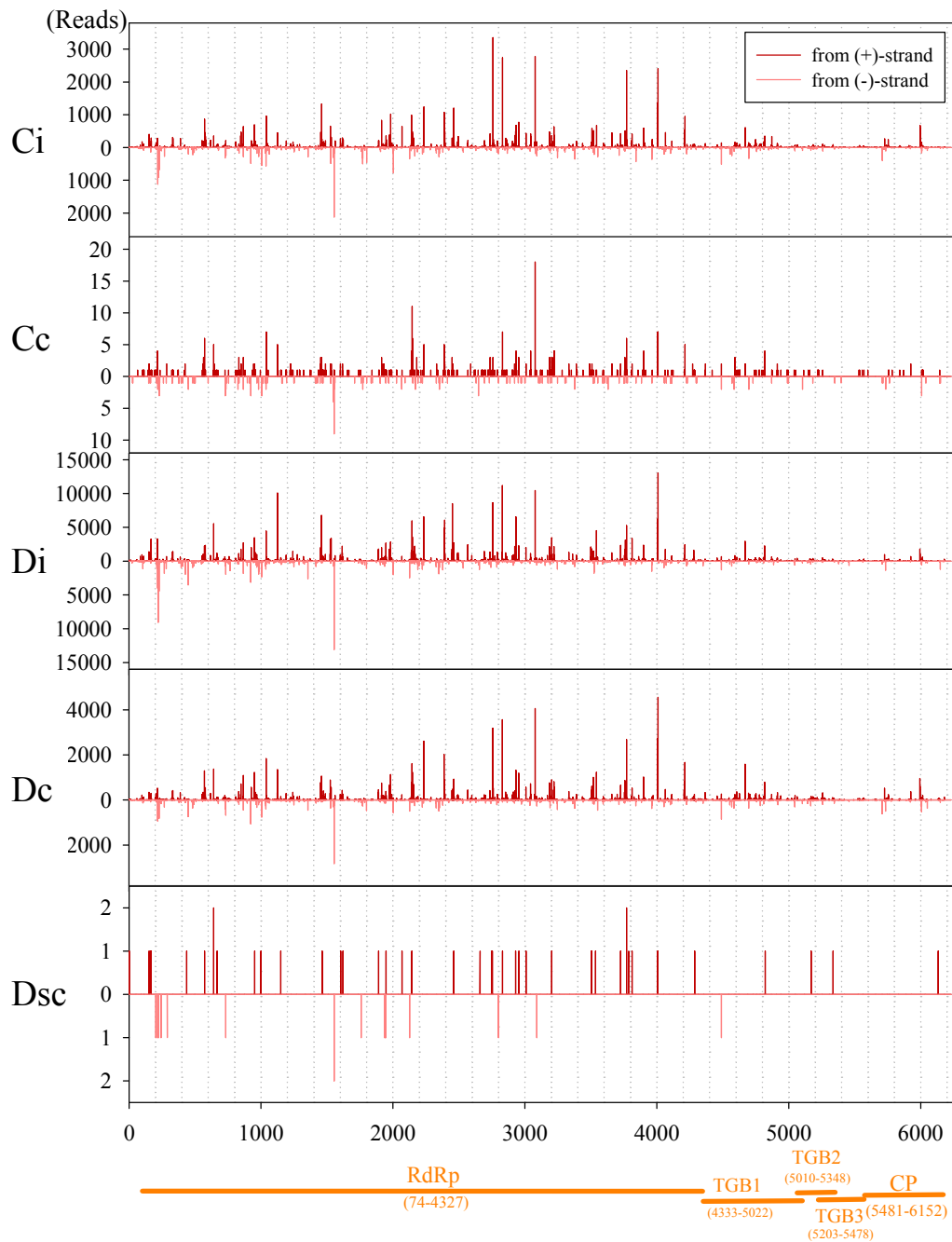


Fig. 26. Nucleotide composition of 5'-end of ORSV vsRNAs in CymMV and ORSV mixedly-inoculated *Phalaenopsis*. The composition of adenine (A), cytosine (C), guanine (G) and uridine (U) were proportioned to 100% within each size classes. Di: inoculated tissues of doubly inoculated plants. Dc, Dsc: non-inoculated tissues of doubly inoculated plants..



Sites along CymMV genome (nt)

Fig. 27. Distribution of vsRNAs along CymMV genome corresponding to reads from Ci, Cc, Di, Dc and Dsc libraries.

Upward red lines representing reads of (+)-polarity and downward pink lines representing (-)-polarity reads. Genomic sites of RdRp, TGBp, and CP gene coding regions are indicated below (numbers based on the Taichung strain of CymMV). Ci, Di: inoculated (i) tissues of CymMV (C)- or doubly (D)-inoculated plants. Cc, Dc, Dsc: non-inoculated (c) tissues of CymMV (C)- or doubly (D)-inoculated

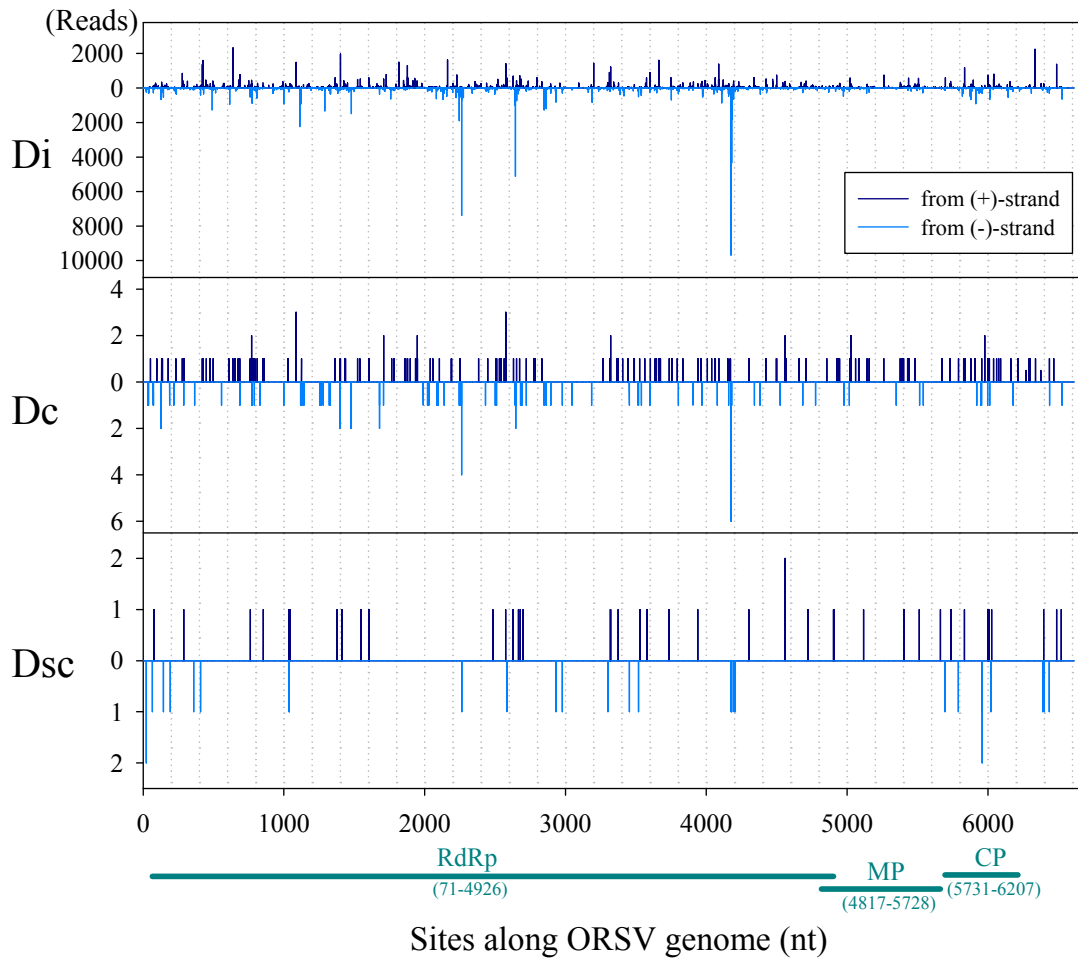


Fig. 28. Distribution of vsRNAs along ORSV genome corresponding to reads from Di, Dc, and Dsc libraries.

Upward dark blue lines representing reads of (+)-polarity and downward light blue lines representing (-)-polarity reads. Genomic sites of RdRp, MP, and CP gene coding regions are indicated below (numbers based on ORSV DQ139262). Di: inoculated tissues of double inoculated plants. Dc, Dsc: non-inoculated tissues of double inoculated plants.

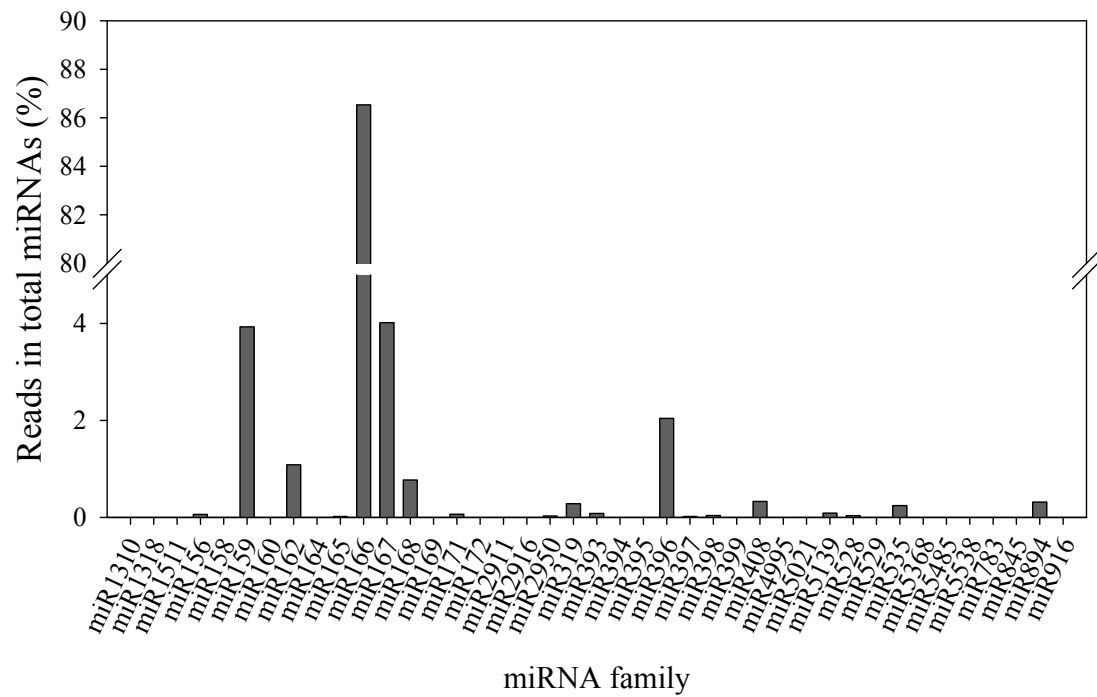
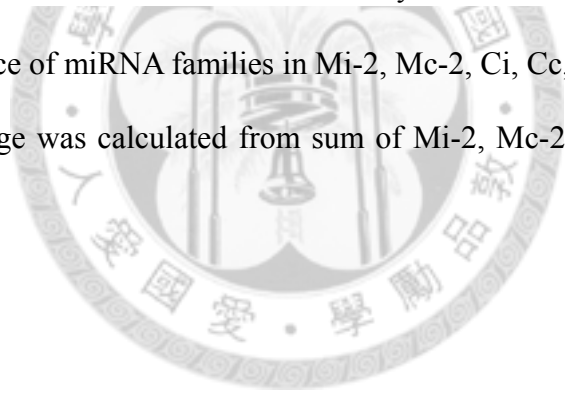


Fig. 29. The abundance of miRNA families in Mi-2, Mc-2, Ci, Cc, Di, Dc, and Dsc libraries. The percentage was calculated from sum of Mi-2, Mc-2, Ci, Cc, Di, Dc and Dsc libraries.



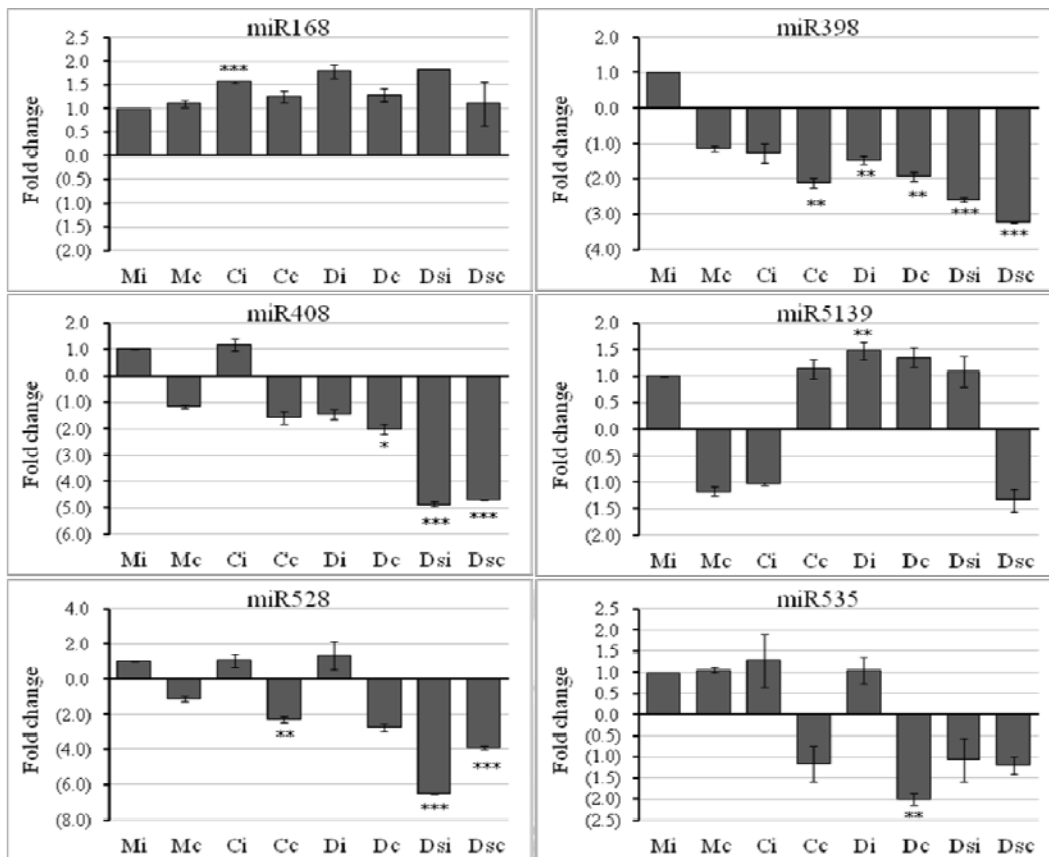


Fig. 30. Fold changes of expression levels of some virus infection-responsive miRNAs in mock-, CymMV-, or CymMV and ORSV mixedly-inoculated *Phalaenopsis* validated by stem-loop qRT-PCR.

miRNA levels in Mi were arbitrarily set to 1, upward boxes indicate increased and downward boxes indicate repressed expression levels relative to Mi. Bars represent standard deviation from 3 biological replicates. Asterisks indicate statistical significance at $P < 0.1$ (*), $P < 0.05$ (**) and $P < 0.001$ (***) assessed by BootstRatio web tool based on resampling methods. Mi (Mi-2), Ci, Di: inoculated (i) tissues of mock (M)-, CymMV (C)-, and doubly (D)-inoculated plants. Mc (Mc-2), Cc, Dc, Dsc: non-inoculated (c) tissues of mock (M)-, CymMV (C)-, and doubly (D)-inoculated plants.

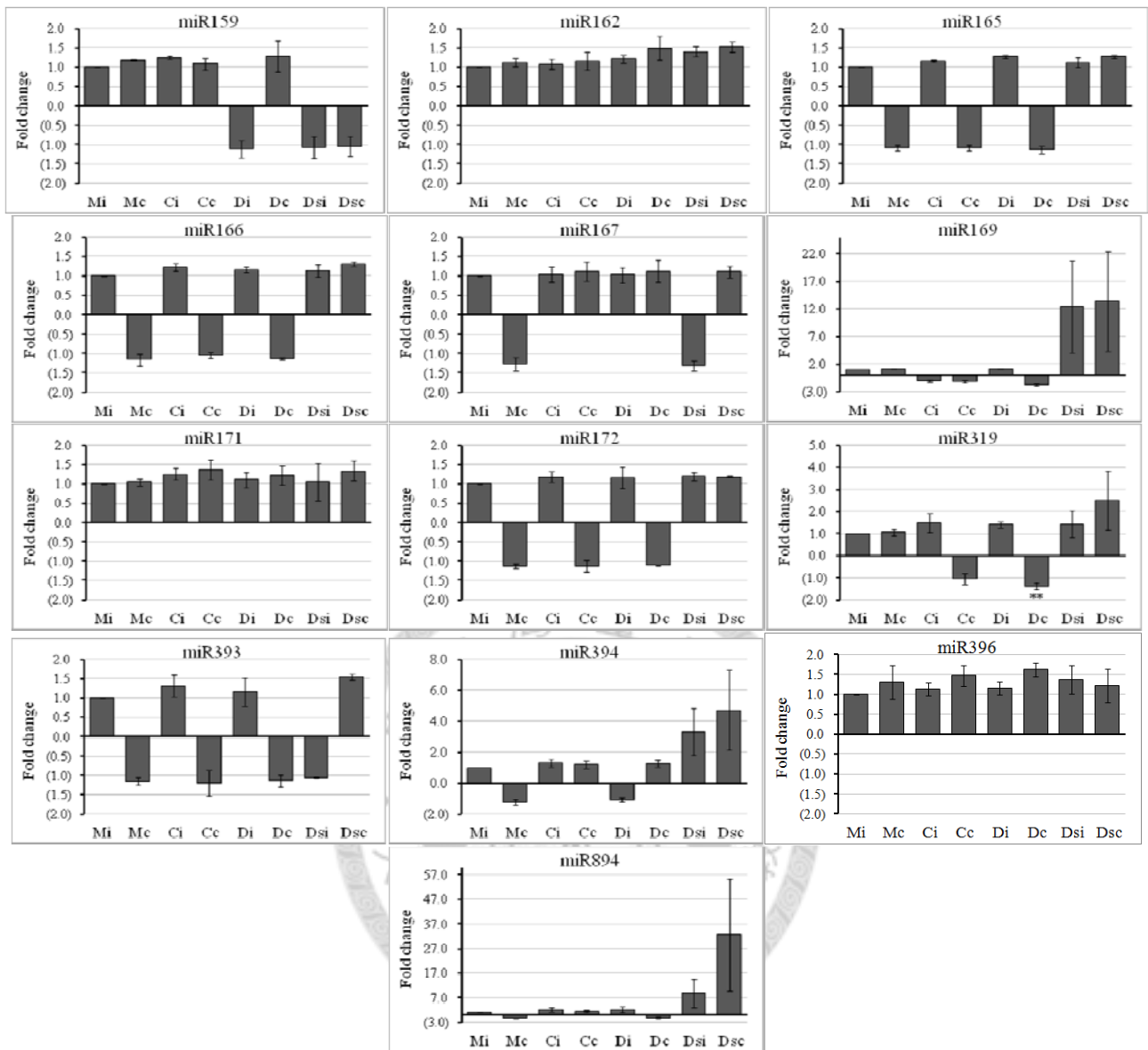
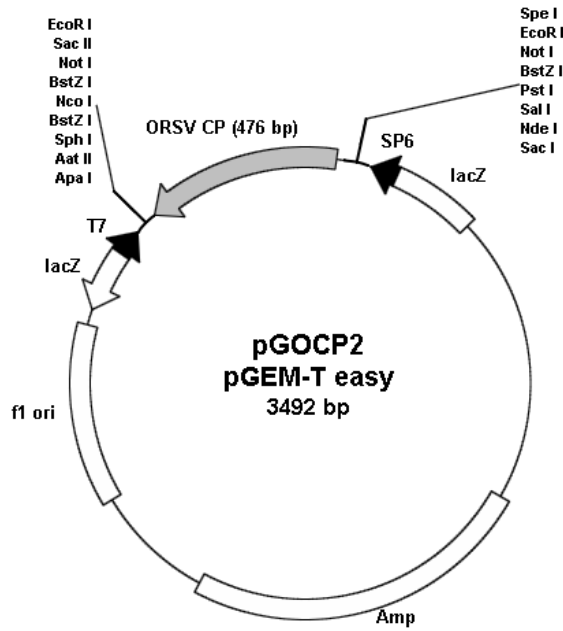


Fig. 31. Fold changes of expression levels of some miRNAs in mock-, CymMV-, or CymMV and ORSV mixedly-inoculated *Phalaenopsis* validated by stem-loop qRT-PCR. miRNA levels in Mi were arbitrarily set to 1, upward boxes indicate increased and downward boxes indicate repressed expression levels relative to Mi. Bars represent standard deviation from 3 biological replicates. Mi (Mi-2), Ci, Di: inoculated (i) tissues of mock (M)-, CymMV (C)-, and doubly (D)-inoculated plants. Mc (Mc-2), Cc, Dc, Dsi, Dsc: non-inoculated (c) tissues of mock (M)-, CymMV (C)-, and doubly (D)-inoculated plants.

(A)



(B)

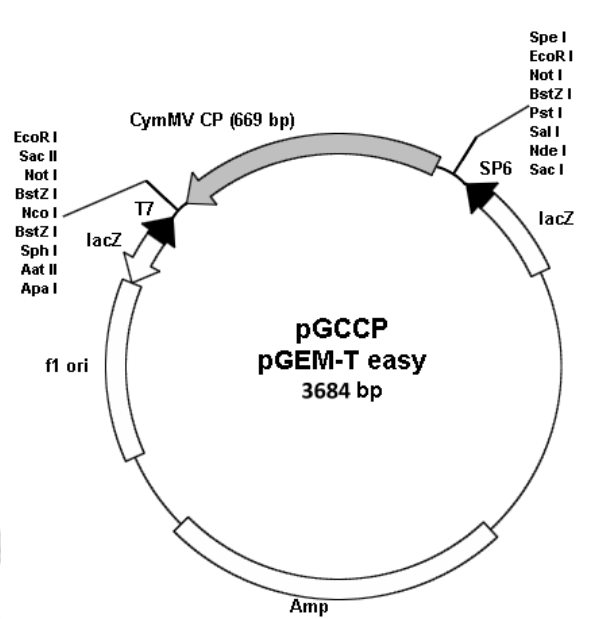
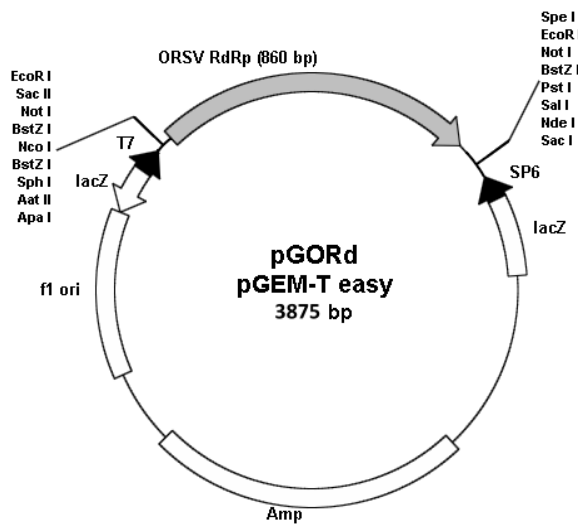


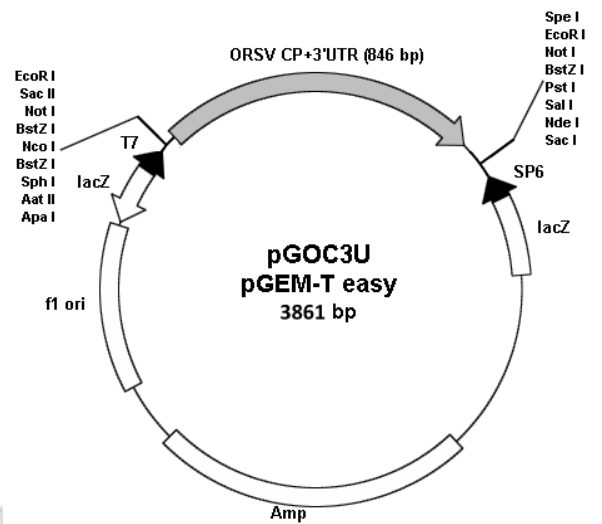
Fig. S1. Plasmids used for generating ORSV- or CymMV-specific RNA probes for detecting virus infection.

(A) pGOCP2 harboring ORSV coat protein (CP) partial sequence. (B) pGCCP harboring CymMV coat protein (CP) partial sequence.

(A)



(B)



(C)

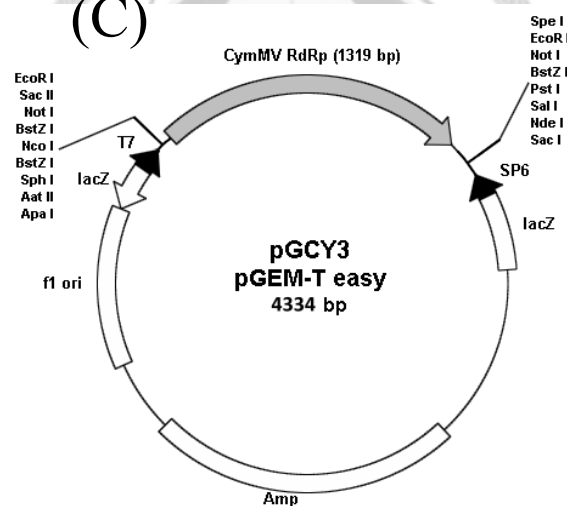


Fig. S2. Plasmids used for generating ORSV- or CymMV-specific RNA probes for detecting vsRNA accumulation.

(A) pGORD harboring ORSV RNA-dependent RNA polymerase (RdRp) partial sequence. (B) pGOC3U harboring ORSV coat protein (CP) partial sequence and 3'-untranslated region (3'UTR) full length sequence. (C) pGCY3 harboring CymMV RNA-dependent RNA polymerase (RdRp) partial sequence.

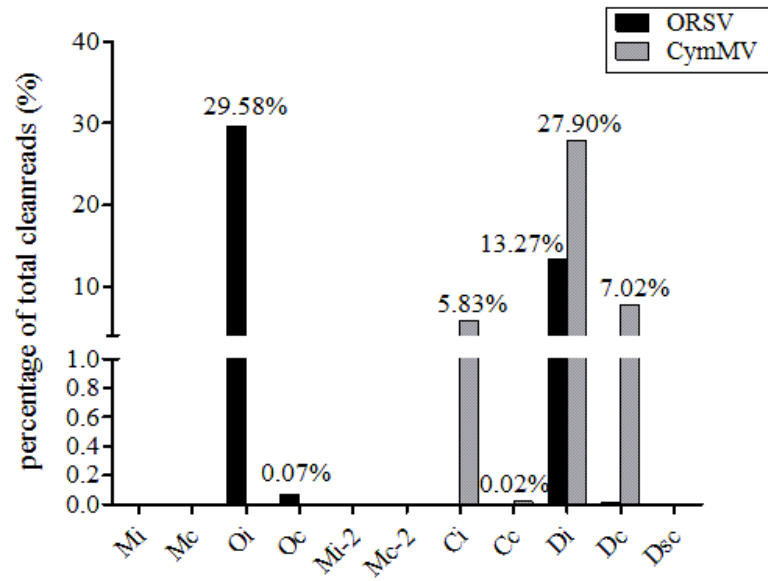


Fig. S3. Percentages of CymMV and ORSV vsRNAs of total clean reads in small RNA libraries. Mi, Mi-2, Oi, Ci, Di: inoculated (i) tissues of mock (M)-, ORSV (O)- CymMV (C)-, and doubly (D)-inoculated plants. Mc, Mc-2, Oc, Cc, Dc, Dsc: non-inoculated (c) tissues of mock (M)-, ORSV (O)-, CymMV (C)-, and doubly (D)-inoculated plants.

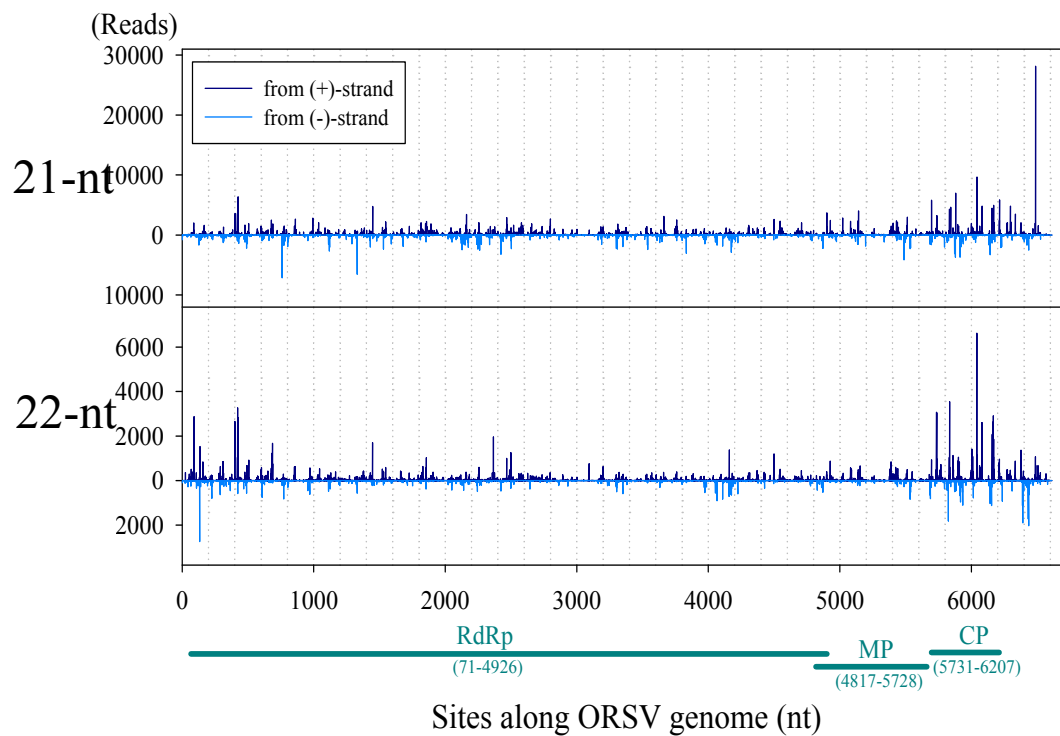


Fig. S4. Distribution of 21- and 22-nt viral siRNAs along ORSV genome corresponding to reads from Oi library. Upward dark blue lines representing reads of (+)-polarity and downward light blue lines representing (-)-polarity reads. Genomic sites of RdRp, MP, and CP gene coding regions are indicated below (numbers based on DQ139262).

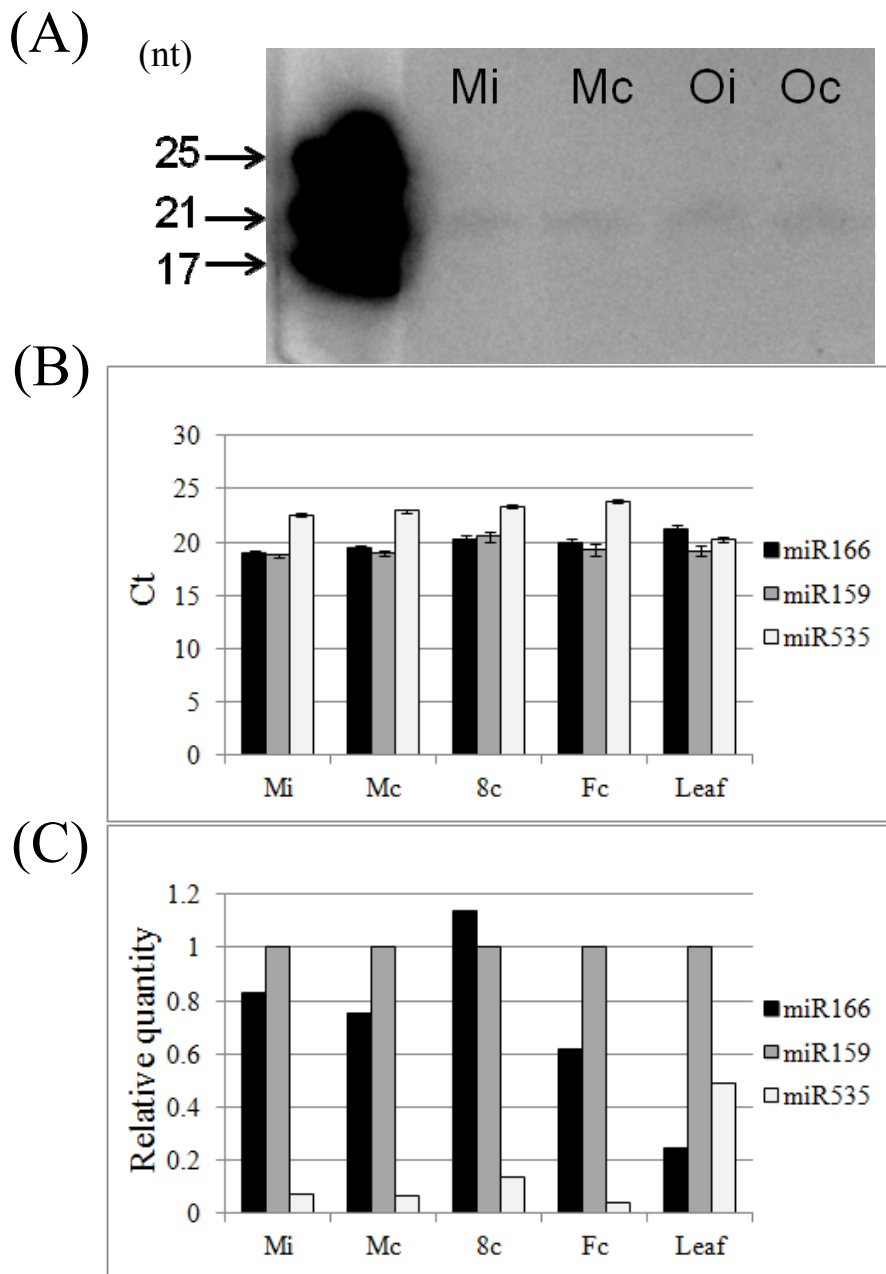


Fig. S5. Validation of miR166 abundance.

The expression level of miR166 in Mi and Mc RNA sample were validated by (A) small RNA Northern blot and (B-C) qRT-PCR. The qRT-PCR results are presented in (B) Ct value and (C) relative quantity compared to miR159 (arbitrary set to 1) and miR535. Mi, Mc: inoculated and non-inoculated tissues of mock-inoculated plants. 8c, Fc: non-inoculated *Phalaenopsis amabilis* plants maintained in the greenhouse used as comparisons. Leaf: *Phalaenopsis aphrodite* plant from another lab used as a comparison.

(A) Size distribution of total reads

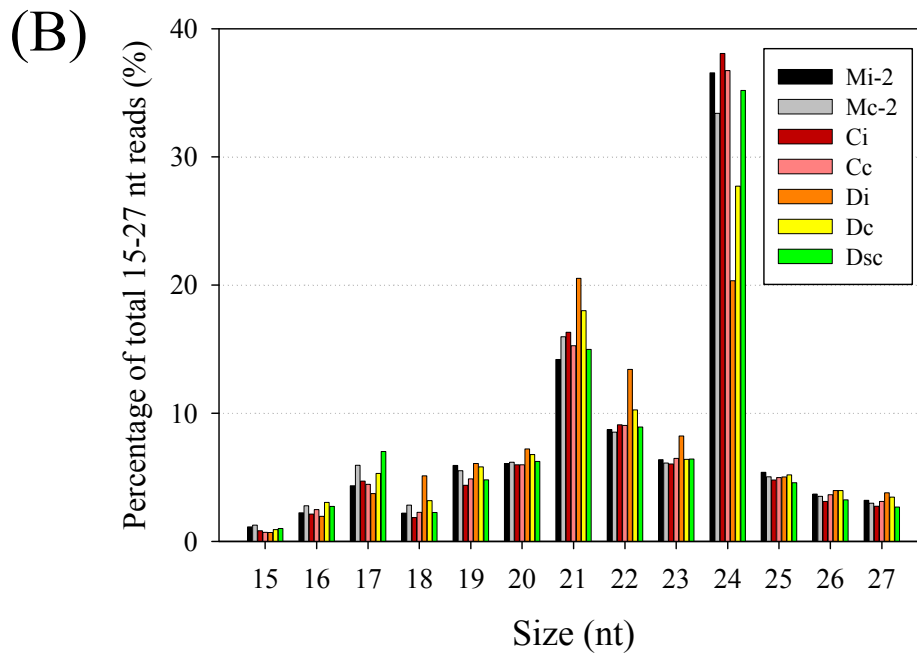
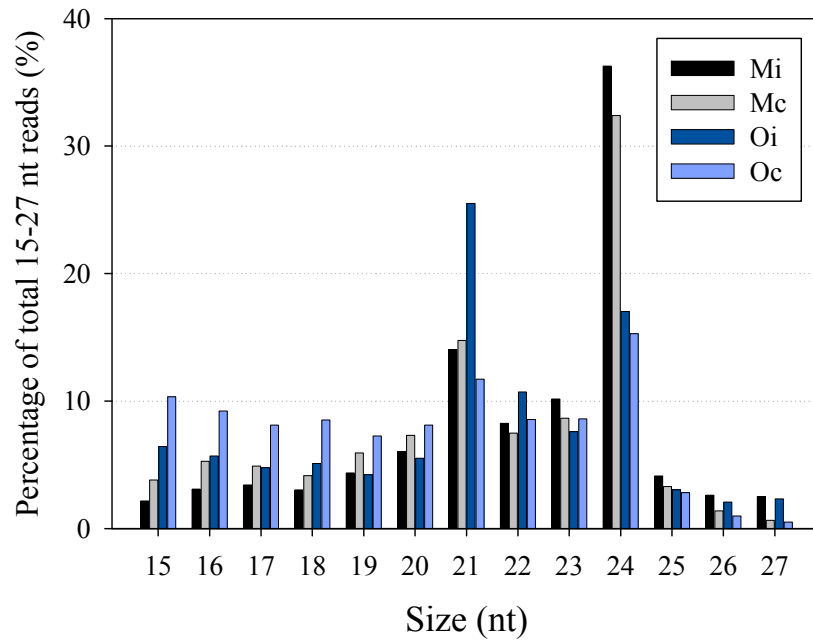


Fig. S6. Size distribution of small RNAs modified with the removal of the super-abundant miR166 tag.

Percentage and size distribution of 15-27 nt reads in libraries of (A) mock and ORSV (B) mock and CymMV or doubly infected tissues. Mi, Mi-2, Oi, Ci, Di: inoculated (i) tissues of mock (M)-, ORSV (O)-, CymMV (C)-, and doubly (D)-inoculated plants. Mc, Mc-2, Oc, Cc, Dc, Dsc: non-inoculated (c) tissues of mock (M)-, ORSV (O)-, CymMV (C)-, and doubly (D)-inoculated plants.

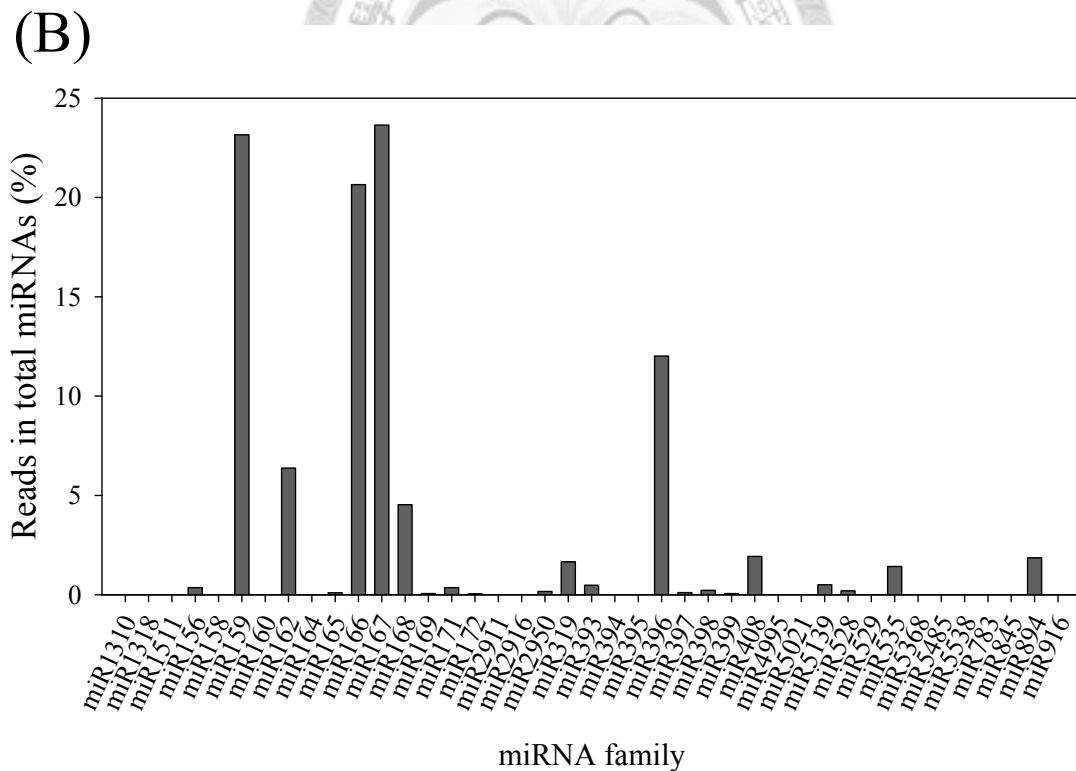
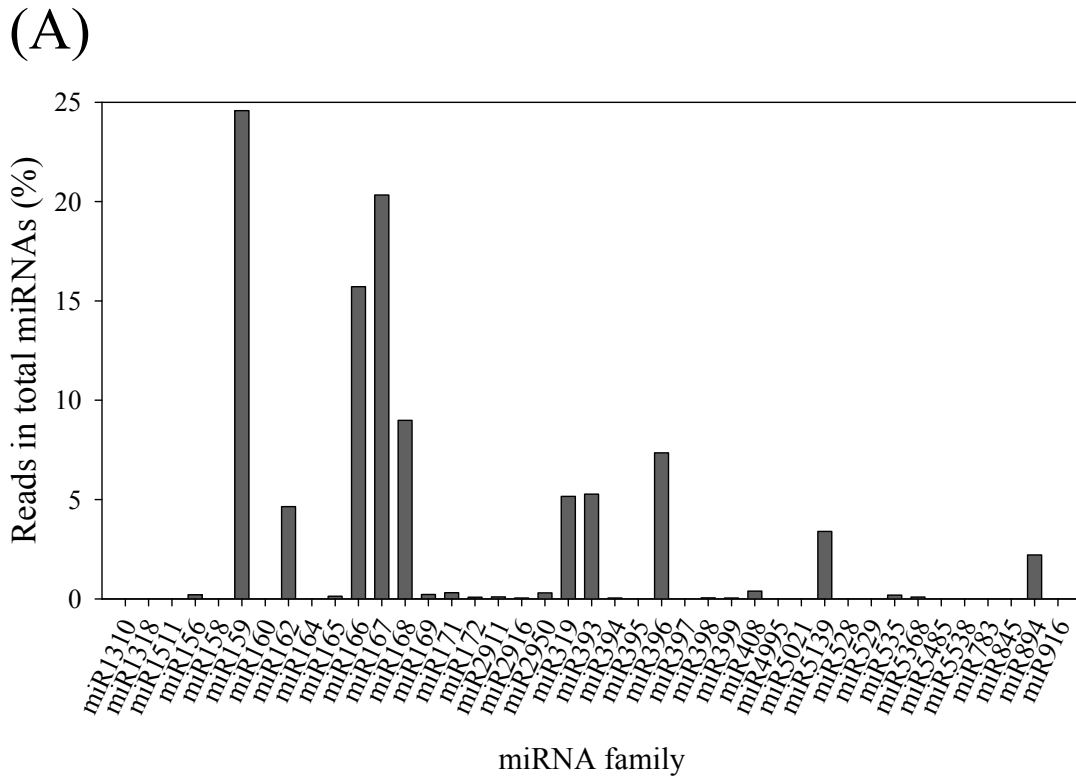


Fig. S7. Modified relative abundance of miRNA families after removal of the super-abundant miR166 tag. The percentages were calculated from sum of (A) Mi, Mc, Oi, and Oc and (B) Mi-2, Mc-2, Ci, Cc, Di, Dc and Dsc libraries.

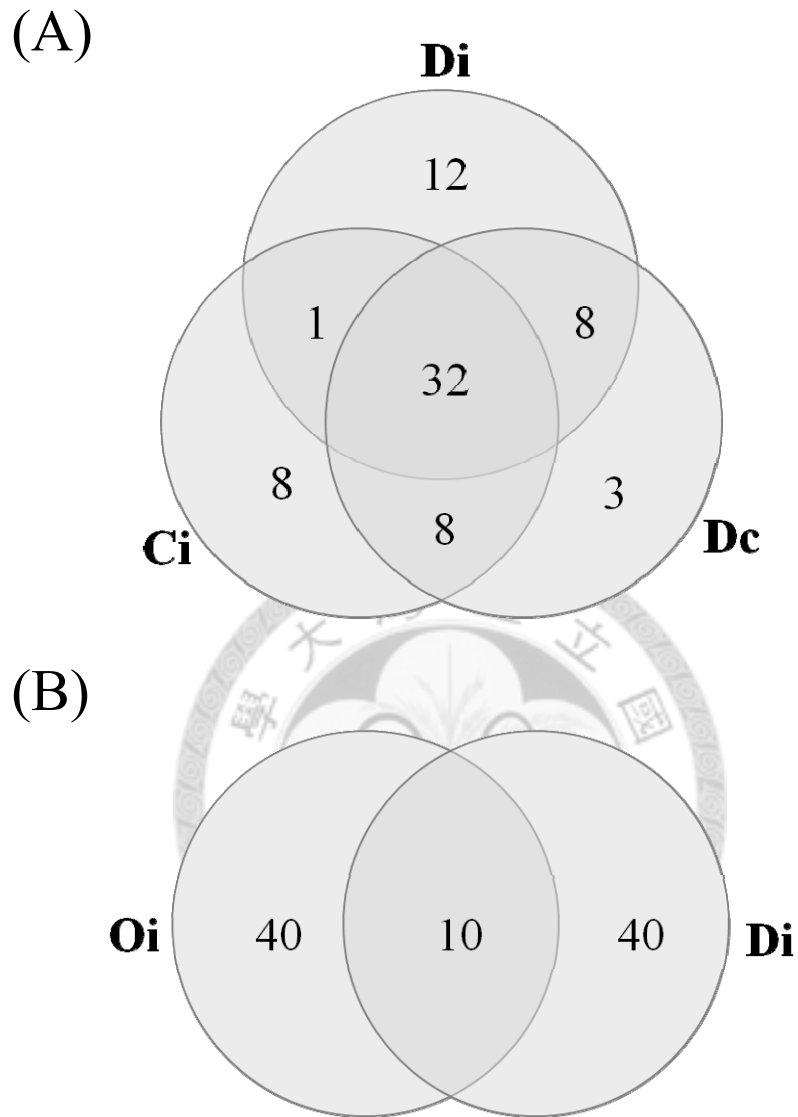


Fig. S8. The redundancy of top 50 abundant vsRNA tags in Oi, Ci, Di, and Dc libraries. The overlapped distribution of abundant (A) CymMV and (B) ORSV vsRNA tags between libraries are indicated. Oi, Ci, Di: inoculated (i) tissues of ORSV (O)-, CymMV (C)-, and doubly (D)-inoculated plants. Dc: non-inoculated (c) tissues of doubly (D)-inoculated plants with CymMV infection was detected by tissue-blotting.